

REPORT NO. MDC E0018

MARTIAN SOFT LANDER INSULATION STUDY

FINAL REPORT

BY O. J. WILBERS, J. C. CONTI,
J. V. MCGEE, J. I. MCPHERSON

PREPARED FOR JET PROPULSION LABORATORY,
PASADENA, CALIFORNIA UNDER JPL CONTRACT NO. 952327

CASE FILE
COPY

MCDONNELL DOUGLAS



REPORT NO. MDC E0018

15 SEPTEMBER 1969

COPY NO.

MARTIAN SOFT LANDER INSULATION STUDY

FINAL REPORT

BY O. J. WILBERS, J. C. CONTI,
J. V. MCGEE, J. I. MCPHERSON

PREPARED FOR JET PROPULSION LABORATORY,
PASADENA, CALIFORNIA UNDER JPL CONTRACT NO. 952327

THIS WORK WAS PERFORMED FOR THE JET PROPULSION LABORATORY,
CALIFORNIA INSTITUTE OF TECHNOLOGY AS SPONSORED BY THE
NATIONAL AERONAUTICS AND SPACE ADMINISTRATION UNDER CONTRACT
NAS 7-100

**MCDONNELL DOUGLAS ASTRONAUTICS COMPANY
EASTERN DIVISION**

Saint Louis, Missouri 63166 (314) 232-0232

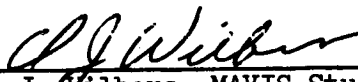
MCDONNELL DOUGLAS




FOREWORD

This report was prepared by McDonnell Douglas Astronautics Company (Eastern Division) under Contract No. 952327, for the Jet Propulsion Laboratory. The work was administered under the technical direction of the Engineering Mechanics Division of the Jet Propulsion Laboratory, with Mr. Bruce Schelden acting as Cognizant Engineer.

Submitted by:


O. J. Wilbers, MAVIS Study Manager
McDonnell Douglas Astronautics Company

Approved by:


Bruce G. Schelden, Cognizant Engineer
Jet Propulsion Laboratory

ABSTRACT

Insulation materials and their application techniques were studied for the Viking soft lander mission to Mars in 1973. Two unique environmental conditions complicated the already difficult problem of selecting materials for the mission. These were the requirement for heat sterilization, and the presence of the Martian atmospheric gas after landing. Completion of the study objective required: (1) selection of initial candidate materials, (2) definition of specific tests to simulate the Mars mission environments, (3) selection of two high value candidate materials through screening tests, (4) definition and design of applicable insulation systems which included the candidate insulations plus associated support structure, and (5) subjecting the selected materials and insulation systems to the significant Mars mission environmental conditions. Two high value materials, isocyanurate foam and silicone bonded "AA" fiberglass were identified from 26 candidates by use of a rapid transient heating technique for evaluating thermal conductivity, and compatibility tests for heat sterilization effects. In order to realistically evaluate the integrity of the two materials in the thermal and dynamic mission environments, test panels identified as Insulation System Modules (ISM's) were designed and fabricated. These ISM's, consisting of insulation and associated support structure, were exposed to heat sterilization, Titan launch venting and vibration, Mars landing shock and the Martian surface environment. The ISM panel utilizing foam material failed during a chamber pumpdown from causes which could not be identified in subsequent element testing. The panel utilizing fiberglass insulation passed all tests successfully with no indicated change in performance, thus demonstrating a lightweight, usable insulation configuration.

	Page
7.2-8	83
7.2-9	90
7.2-10	91
8.1-1	96
8.1-2	96
8.3-1	98
8.3-2	99
9.1-1	105
9.1-2	106
9.1-3	107
9.1-4	108
9.1-5	108
9.1-6	113
9.1-7	114
9.1-8	114
9.2-1	115
9.2-2	116
9.2-3	118
9.2-4	119
9.2-5	121
9.2-6	123
9.2-7	125
9.2-8	126
9.3-1	128
9.3-2	129
9.3-3	130
9.4-1	132
9.4-2	133
9.4-3	134
9.5-1	136
9.5-2	137
9.5-3	139
10.1-1	142
10.1-2	144
10.1-3	144

LIST OF ILLUSTRATIONS

	PAGE
3.1-1 Study Flow Plan	4
3.1-2 Representative Lander	5
4.1-1 Launch Ambient Pressure Levels	10
4.1-2 Launch Vibration Spectrum	11
4.1-3 Acoustic Environments	12
4.1-4 Shock Spectra of Soft Landing And Pyrotechnic Events	14
4.1-5 Martian Entry Pressure/Altitude History	16
4.1-6 Thermal Conductivity of Martian Atmospheric Gases	19
4.1-7 Carbon Dioxide Sublimation Conditions	20
4.1-8 Mars Surface Temperatures - Beginning of Post Landed Mission	21
4.1-9 Mars Surface Temperatures - End of Post Landed Mission	22
4.1-10 Free Convection Heat Transfer Coefficients	23
4.1-11 Forced Convection Heat Transfer Coefficients	25
4.1-12 Convection Effect on Insulation Heat Loss	26
5.3-1 Thermal Conductivity of Multilayer Insulations as a Function of Gas Pressure	34
5.3-2 Effect of External Compression on NRC-2 (Crinkled Aluminized Mylar) Thermal Performance	35
5.3-3 Effect of Pressure on Thermal Conductivity of Foam	38
5.3-4 Effect of Pressure on Thermal Conductivity of Fiberglass	38
6.3-1 Initial Insulation Installation Tradeoff	47
6.3-2 Applicable Insulation Attachment Methods	49
6.3-3 Applicable Insulation Packaging Methods	50
6.3-4 Comparison of Insulation Panel Edge Losses	51
6.3-5 Convection Effect on Insulation Heat Loss	52
6.4-1 ISM Design Concepts	53
7.1-1 Thermal Insulation Material Before TGA	59
7.1-2 Thermal Analysis Apparatus	60
7.1-3 Thermal Insulation Material After TGA	62
7.1-4 Thermogravimetric Analysis Results	64
7.1-5 Thermogravimetric Analysis Results	65
7.2-1 Thermal Diffusivity Test Specimen Assembly	69
7.2-2 Thermal Response of a Typical Heater In Vacuum	72
7.2-3 Thermal Diffusivity Test Setup	73
7.2-4 Thermal Diffusivity Test Instrumentation Schematic	74
7.2-5 Thermal Diffusivity Test Instrumentation	75
7.2-6 Thermal Diffusivity Test Computer Analysis Model	80
7.2-7 Comparison of Thermal Diffusivity Test and Analysis Results	81

LIST OF ILLUSTRATIONS (Cont.)

	Page
7.2-8 Thermal Diffusivity Test - Data Reduction Curves	83
7.2-9 Thermal Diffusivity Test Results Mars Atmosphere	90
7.2-10 Thermal Diffusivity Test Results $k\rho$, Mars Atmosphere	91
8.1-1 Required Insulation Thickness for Constant Heat Loss	96
8.1-2 Insulation System Module Weights for Candidate Materials	96
8.3-1 Foam ISM Design	98
8.3-2 Fiberglass ISM Design	99
9.1-1 Heat Sterilization Test Samples	105
9.1-2 Aluminum Foil Covering of Small Canister Prior to Final Assembly	106
9.1-3 Heat Sterilization Test Setup	107
9.1-4 Thermal Diffusivity Specimens in Sterilization Oven	108
9.1-5 Thermal Conductivity and ISM Materials and ISM Panels in Sterilization Oven	108
9.1-6 Temperature Profiles for Canisters 14, 7, 9 During the 384 Hour Heating Period	113
9.1-7 Temperature Profile of Reference Point Thermocouples During 6 Hour Heatup Period	114
9.1-8 Temperature Profiles of Reference Point Thermocouples During 6 Hour Cooldown Period	114
9.2-1 Thermal Performance Test Apparatus	115
9.2-2 Thermal Performance Test Apparatus	116
9.2-3 Thermal Performance Test Thermocouple Location for Test Samples, Heaters and Coldplates	118
9.2-4 Thermal Performance Test Thermocouple Locations for Guard Insulation	119
9.2-5 Vacuum Chamber Pumping Rates	121
9.2-6 Foam ISM Panel After Failure	123
9.2-7 Equilibrium Temperature Data - Thermal Performance Tests No. 1 and 2 - Vacuum Phase	125
9.2-8 Equilibrium Temperature Data - Thermal Performance Tests No. 1 and 2	126
9.3-1 Vibration Test Setup For Testing in the Vertical Axis	128
9.3-2 Power Spectral Density Analysis	129
9.3-3 Acceleration Transmissibility	130
9.4-1 Shock Test Setup	132
9.4-2 Shock Test Data	133
9.4-3 Typical Acceleration - Time Histories During Shock Testing	134
9.5-1 Thermal Conductivity Test Apparatus	136
9.5-2 Installation of Thermocouples on Silicone Bonded "AA"	137
9.5-3 Thermal Conductivity Test - Calibration Data, Test Material	139
10.1-1 Foam ISM Failure During Thermal Performance Test Pumpdown	142
10.1-2 Launch Decompression Specimen Containing a Vent Hole	144
10.1-3 Launch Decompression Specimen Containing a 1/2 X 1/2 Inch Air Pocket	144

		PAGE
10.1-4	Launch Ambient Pressure Profile for Analysis of Foam Insulation Panel Failure	145
10.2-1	Transducer Locations - Cover Plate	148
10.2-2	Transducer Locations - Plastic Laminate Casing	149
10.2-3	Acceleration Transmissibility - Center of Aluminum Cover	152
11.1-1	Test Data Comparison - Silicone Bonded "AA" Fiberglass	157

LIST OF TABLES

	PAGE
4.1-1 Significant Environmental Parameters	9
4.1-2 Mars Surface Atmospheric Conditions	17
4.2-1 Test Summary	27
5.1-1 Materials Selection Criteria	31
5.3-1 Candidate Insulation Material Selection	40
6.2-1 Insulation System Module - Design Parameters	46
6.2-2 Major Design Considerations for Lander Insulation Installation	46
6.4-1 Insulation System Module Weight Comparison for 3 Inch Thickness	55
6.4-2 ISM Component Part Weight Breakdown (Predicted)	56
7.1-1 Sterilization Screening Test Matrix	58
7.1-2 Weight Loss in the TGA Test	63
7.1-3 Materials Considered to Have Passed Sterilization Screening	63
7.2-1 Heat Sterilized Specimens for Second Phase of the Thermal Diffusivity Test	67
7.2-2 Density of Thermal Diffusivity Specimens	68
7.2-3 Heater Thermal Cycle Test	71
7.2-4 Chromel-Constantan Thermocouple Calibration	71
7.2-5 Chamber Stabilization for Vacuum Test	77
7.2-6 Chamber Stabilization for Test at Mars Atmospheric Pressure	77
7.2-7 Power Supplied to Specimens for Mars Atmosphere Test	78
7.2-8 Thermal Diffusivity Test Data Reduction Techniques	79
7.2-9 Data Reduction Assumptions for Multilayer Analysis	84
7.2-10 Parameter Values Used in Multilayer Analysis	84
7.2-11 Thermal Conductivity Calculations for Multilayer Materials	86
7.2-12 Thermal Diffusivity Test Results Before Heat Sterilization	88
7.2-13 Thermal Diffusivity Test Results After Heat Sterilization	92
7.2-14 Effects of Heat Sterilization Cycle	93
8.1-1 Insulation System Module Weight Comparison	97
8.4-1 Fabricated Weights - Insulation System Modules	101
9.1-1 Heat Sterilization Test	104
9.1-2 Oxygen Content of Purge Gas During Heat Sterilization	111
9.2-1 Thermal Performance Test Data - Test Apparatus Evaluation Phase	120

PAGE

9.2-2	Thermal Performance Test Data - ISM Evaluation	124
9.5-1	Thermal Conductivity Test Conditions	140
9.5-2	Thermal Conductivity Test Results	140
10.1-1	Foam Failure Test Specimens	143
10.1-2	Tensile Strength of Sterilized and Unsterilized HTF-200 Foam	147
10.2-1	ISM Cover Plate Static Load Test Summary	151
10.2-2	Incremental Shock Test Summary	153
11.1-1	Thermal Diffusivity Test Data Comparisons	156
11.2-1	Comparison of Minimum Weight Designs	158

1. SUMMARY

From the numerous potential insulation materials which could be considered for the Viking lander, the effort of this study resulted in identification of two high value insulation candidates, an isocyanurate foam and silicone bonded "AA" fiberglass. Selection of the two high value candidate materials was based on rapid screening tests of 26 candidates from four materials classes, foams, fibers, powders and multilayers. The material classes included those types which were known to have high performance at either one atmosphere or vacuum, and would be expected to perform adequately in the intermediate Martian atmospheric pressure (0.005 to 0.02 atm).

Because the requirements of the mission included both good thermal performance, and adequate strength for the dynamic environments of launch vibration and landing shock, an integrated insulation system approach was used for selecting and testing the insulations.

The two high value materials were integrated into Insulation System Modules (ISM's) test panels for evaluations. The ISM's included the insulation, its associated support structure and attachment provisions, with each ISM tailored for a specific insulation class. The ISM test environments then included heat sterilization, launch venting and vibration, Mars landing shock, and exposure to Mars surface temperature, pressure, and gas composition. Heat loss measurements before and after exposure to these environments were used to detect any changes. The ISM containing fiberglass exhibited no changes due to the environmental exposures. The foam ISM, which had the lowest predicted weight as installed, did not complete all tests because the ISM failed during a chamber pumpdown. The program scope did not permit reevaluation of another foam ISM, although subsequent element tests indicated that the material should survive depressurization, and several approaches to relieving the panel design problem became apparent.

In addition to the insulation system tests, steady state thermal conductivity tests of the fiberglass material were performed. These tests indicated that thermal conductivity varies significantly over the range of postulated Martian surface pressure, temperature and gas composition.

2. INTRODUCTION

Early Voyager Program studies for a Martian lander indicated that thermal performance of the lander insulation was a key uncertainty area. After exposure to the mission environments and landing in the Martian surface atmosphere, performance degradation could easily result in insulation weight increases of 100%. Since the weight required for insulation is comparable to that for the entire science payload, this uncertainty was highly significant for overall lander design.

Several unique mission constraints made the problem difficult: existence of the Martian atmosphere, and the effects of heat sterilization and landing shock. It was known that the presence of the Martian gas at 0.005 to 0.02 atmospheres would degrade insulation performance from its best value in vacuum to a value intermediate between that in vacuum and at one atmosphere. The amount of change was not known. However, between these two limiting conditions thermal conductivity changes of up to about four orders of magnitude have been demonstrated, e.g., multilayer materials. Previous test programs had also shown that heat sterilization had a severe effect on some insulation materials (organic foams and multilayers particularly), but the data was limited. There was almost complete lack of industry experience in the composite effects of the mission environments of heat sterilization, launch venting and vibration, and landing shock on insulation performance. Insulation performance also ultimately affected both heater power requirements and structure weight. These factors dictated the necessity of early lander insulation evaluation to minimize these uncertainties. The objective then of the study was to investigate insulation materials and their installation techniques for use on a Martian soft lander. The end usage was directed toward support of the Viking Program with a planned launch to Mars in 1973.

Because the presence of supporting structure increases overall heat loss from the insulation, and the dynamic characteristics of the structure affect the actual vibration and shock loads experienced by the insulation, the candidate materials required evaluation as structural systems. These systems, designated Insulation System Modules (ISM's) consisted of the insulation, associated support structure and attachment provisions. This approach assured adequate assessment of the overall insulation system behavior essentially as it would be installed on the Martian lander.

3. SCOPE OF EFFORT

This study included investigation of the insulation aspects of the thermal control design for a Martian soft lander without consideration of the remaining thermal control system. This approach was acceptable since the thermal control system will necessarily be adapted to the insulation performance obtained. A study plan was used throughout the program to assure continuous direction and give perspective to the overall study philosophy. The plan, Figure 3.1-1 included: candidate materials selection, environmental parameter and test requirement definition, investigation of insulation system designs; heat sterilization and thermal diffusivity screening tests to reduce the number of candidates to two high value materials; and environmental tests including heat sterilization, thermal performance, launch vibration, landing shock and thermal conductivity.

The study was performed as outlined in the following discussion.

- o Environmental Parameters Definition - The environmental parameters which were most significant to insulation performance included heat sterilization (275°F (135°C) for 384 hours in dry nitrogen), launch venting and vibration, landing shock, and exposure to the Martian surface environment. Test criteria for these environments were assessed and selected to best evaluate the candidate insulation materials.
- o Candidate Materials Selection, Procurement - Upon program initiation, studies were also begun to select approximately 25 materials for initial screening tests. Selection was based on results of a vendor and literature survey, use of existing in-house data, and definition of selection criteria.
- o Insulation System Design Studies - An investigation of insulation attachment/installation/fabrication techniques was made. A typical lander configuration is shown in Figure 3.1-2. Specific means of integrating each of the four classes of materials into a lander system were defined. These installation techniques were then available for comparison of materials on the basis of installed performance and weight.
- o Test Facilities, Sequence, Schedule Defined - Shortly after study initiation, final selection of test facilities was made, the test sequence reviewed and approved, and all significant milestones identified.
- o Screening Tests - Two rapid screening test series were employed:
 - A. Heat Sterilization Screening Test - Those materials which probably would not pass the actual long term heat sterilization test were identified in this rapid screening test. Three tests were considered in this series: (1) Thermogravimetric Analysis (measures weight loss during

STUDY FLOW PLAN

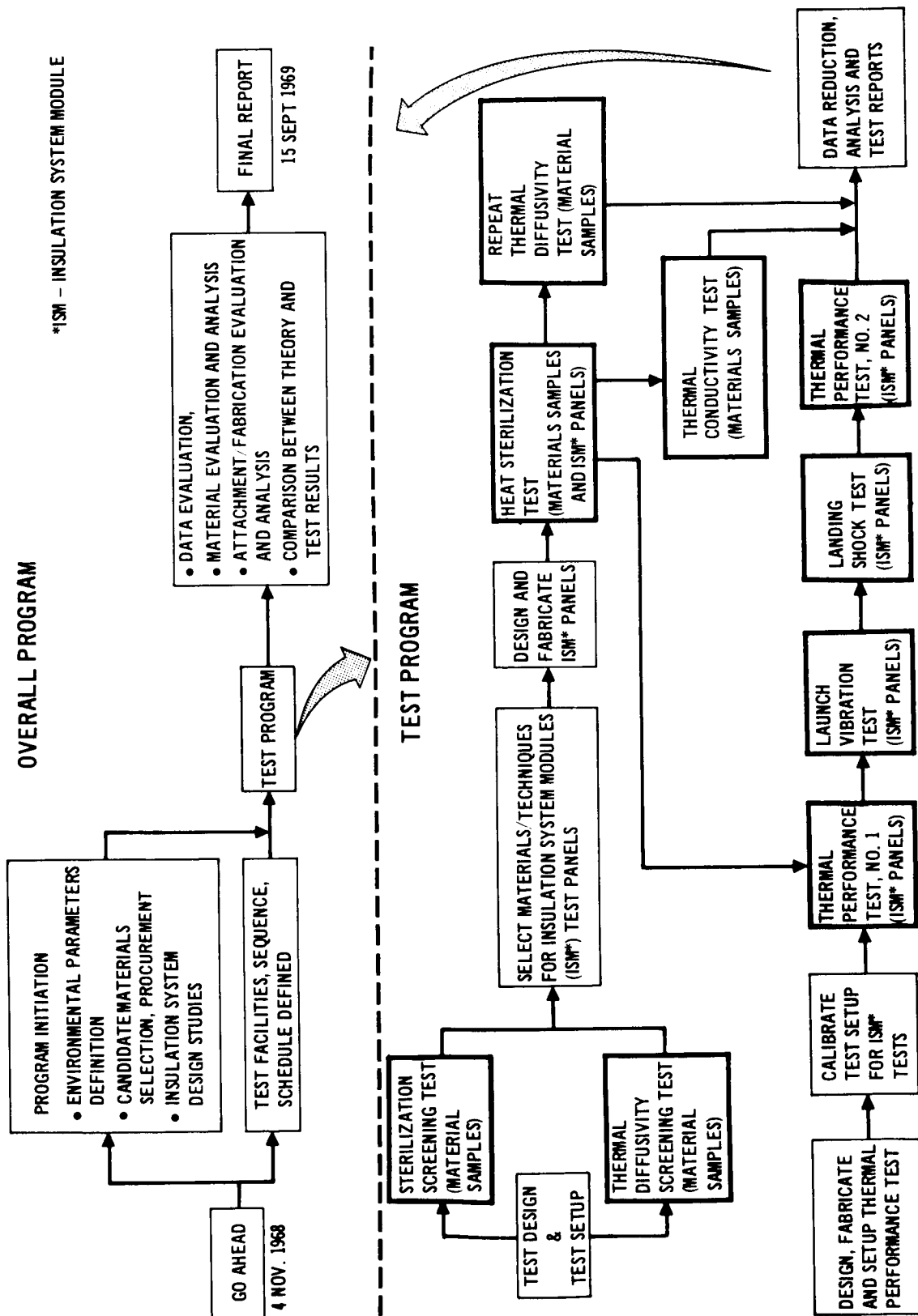


FIGURE 3.1-1

REPRESENTATIVE LANDER

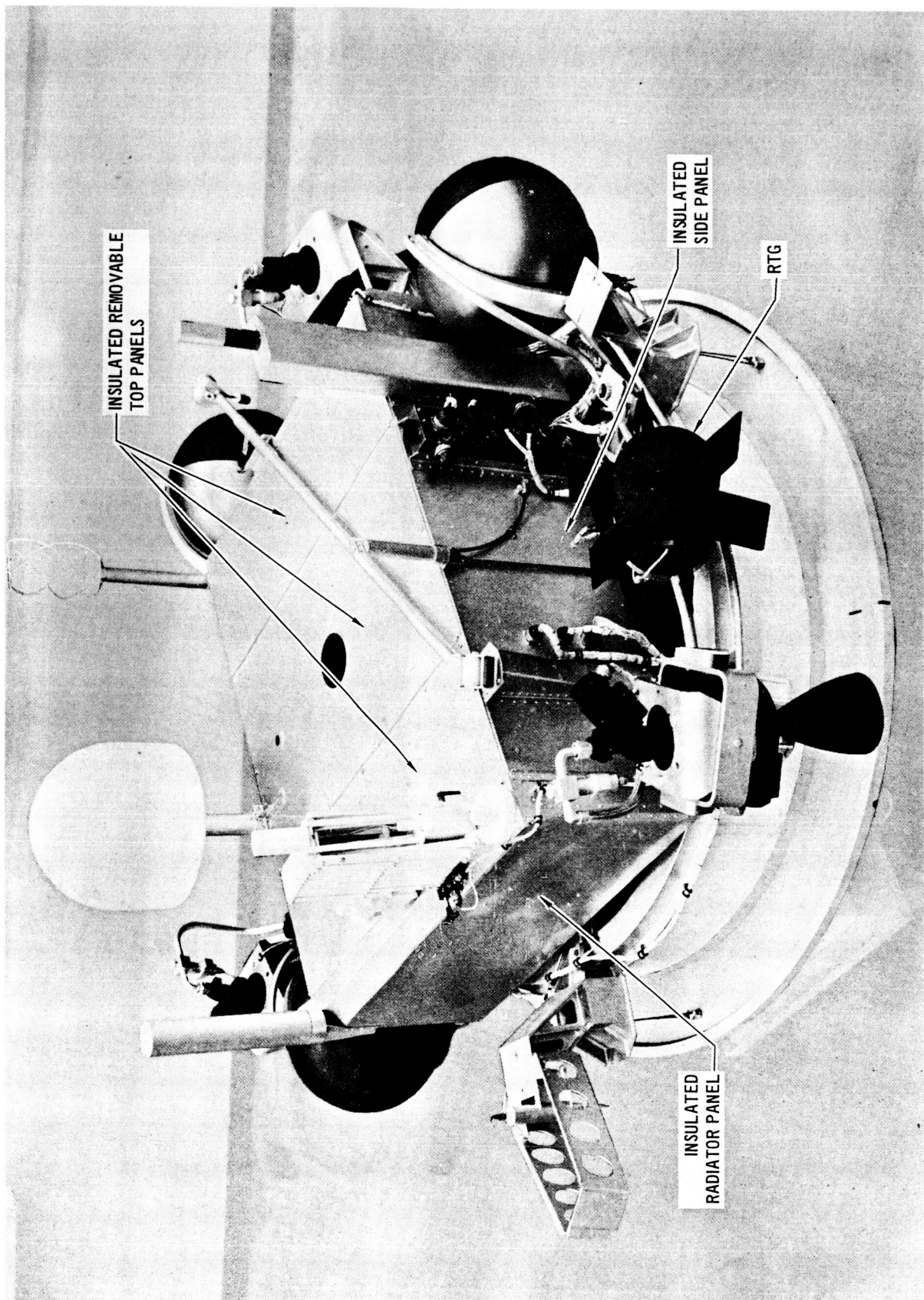


FIGURE 3.1-2

heatup of the sample); (2) Differential Thermal Analysis (detects temperature pulses during heatup indicating either a chemical reaction or a phase change); and (3) Effluent Gas Analysis (determines gas evolution during a heating reaction). Only those materials which were considered susceptible to heat sterilization damage were selected for test.

The samples were each heated to 235°C (100°C above the heat sterilization temperature) in each test to approximate the heat sterilization environment and to accelerate long term changes which would occur during the actual 384 hour heat sterilization exposure.

B. Thermal Diffusivity Screening Test - Fifty samples (26 material configurations) were evaluated simultaneously in this rapid screening test. The test involved transient heating of the materials using a milliwatt heater in the center of each 6 inch cube sample. Heater power was selected to give a heater temperature rise of about 50°F after 12 minutes. Analysis of the temperature rise per unit heat input allowed derivation of thermal conductivity. The test was performed in vacuum, at 20 mb (15 torr) pressure in the LRC maximum model Mars atmosphere, and at one atmosphere in air.

- o Materials/Techniques Selection for ISM's - Based on the results of the two screening tests and the design studies, two materials, UpJohn HTF-200 Isocyanurate foam and Johns Manville silicone bonded "AA" fiberglass were selected to be fabricated into Insulation System Modules (ISM's) for further systems tests. The foam material was bonded into a foam sandwich structure utilizing the load carrying capability of the foam to obtain structure weight half that required for the silicone bonded fiberglass. The bonded fiberglass was selected over unbonded material due to its inherent resiliency, which allowed a loose layup in an ISM design with beaded and corrugation-stiffened structure.
- o Heat Sterilization Test - Three specimen types were simultaneously exposed in this test to 275°F (135°C) dry nitrogen for 384 hours. The test samples were (a) twelve Thermal Diffusivity Test samples which included the two high value candidate insulation materials, and additional materials which were considered as back-up candidates, (b) materials samples, (two) for thermal conductivity testing, and (c) the two Insulation System Modules containing the high value insulations. Individual, nitrogen purged canisters were used to isolate each material type. After heat sterilization a repeat Thermal Diffusivity Test was performed on the same samples to determine whether any materials suffered adverse effects.
- o Thermal Performance Test - The two ISM panels were to be compared for relative heat loss in vacuum and in the Martian atmosphere, before and after exposure to the mission dynamic environments. During a preliminary pumpdown of the test chamber the foam ISM panel failed, causing the foam material to fragment. Loss of this panel comprised one objective of the thermal performance test, direct comparison of the two ISM's. Thermal performance testing of the fiberglass filled ISM panel was completed using a dummy panel to replace the failed ISM in the test apparatus.

- o Launch Vibration Test - Vibration levels consistent with a Titan III launch were imposed on the fiberglass ISM panel. The selected test level was a random vibration exposure with overall level of 16.1 grms.
- o Landing Shock Test - Following vibration testing the panel was subjected to simulated landing shock at a selected test level of 120 g pulse with a 12.8 msec. duration. The second Thermal Performance test subsequently provided ISM heat loss values at the same hot and cold face temperatures as the initial test. These data indicated no thermal degradation of the fiberglass ISM panel as a result of the launch vibration and landing shock exposures.
- o Thermal Conductivity Test - Using a MDAC designed guarded hot plate apparatus, thermal conductivity of the silicone bonded "AA" fiberglass was evaluated at 6 test conditions over the predicted range of Martian atmospheric pressure, temperature, and gas compositions. Thermal conductivity was found to be sensitive to temperature, pressure and gas composition over the range of postulated Martian atmospheric conditions.

Two tests were performed in addition to those in the initial study plan. One was an investigation of the cause of failure of the foam ISM panel; the other test included a series of incremental shock tests to determine the design margin in the fiberglass ISM structure. In the foam tests none of the samples failed during launch evacuation, even those fabricated in configurations which were expected to fail. This test indicated the basic integrity of the foam design concept, but did not explain the cause of the foam ISM failure. The incremental shock tests were performed to the 250 g level (120 g was required) indicating significant design margin with potential for weight savings in any subsequent panels.

Data reduction, analysis and test reports were completed subsequent to testing. This allowed evaluation of the materials, reassessment of the ISM designs, and comparisons between theory and test.

4. ENVIRONMENTAL PARAMETERS SELECTION

A review of the Mars mission environments was necessary to identify those environmental conditions which might significantly affect performance of the insulation on the Martian surface and those which would be used as criteria for selection of materials. Specific test conditions were then selected to insure that the insulation materials and ISM's were fully exercised throughout their required environmental ranges.

4.1 MISSION ENVIRONMENT REVIEW - The significant environmental conditions affecting insulation performance are identified in Table 4.1-1, and are discussed in the following paragraphs in the order that they are experienced in the actual mission. Selected test conditions are defined in the next section (4.2).

4.1.1 Pre-Launch Phase - The most significant environment prior to launch is the heat sterilization exposure. Several heat sterilization test levels have been identified in JPL Specification VOL-50503-ETS depending on the article to be tested, and when it is integrated in the vehicle during fabrication. For this study the "piece parts and materials" test level was selected, consisting of exposure to 275°F (135°C) for a total of 384 hours in a dry nitrogen environment.

4.1.2 Launch Phase - The significant environments during launch are the ambient pressure history, vibration, acoustic and pyrotechnic shock during separation.

Ambient Pressure - During launch the ambient pressure change imposes pressure loads on the lander insulation panels. The rate of changes of these loads will depend on the venting rates of the launch shroud and the bioshield, but should not be more than several psi above ambient throughout the launch. Thus the internal pressure changes will be similar to ambient, except displaced in time. The ambient pressure history for a Titan launch is shown in Figure 4.1-1.

Launch Vibration and Acoustic - During launch the structural resonances built up in the insulation panels can result in significant damage. Both vibration and acoustic inputs can excite these resonances, and hence are discussed together. A launch vibration spectrum for a typical Titan launch is shown in Figure 4.1-2, (data provided by JPL).

A Titan launch acoustic spectrum for design of payload compartments is shown as curve 1 in Figure 4.1-3, provided by JPL. The planetary payload will be enclosed by both the launch shroud and a sterilization canister, and hence will experience an acoustic environment significantly less than this design environment. A conservative estimate of this reduction is 10 db in all of the 1/3 octave bands. Using a 10 db reduction, the resulting launch acoustic environment which will be experienced by the lander insulation is shown as curve 2 in Figure 4.1-3.

SIGNIFICANT ENVIRONMENTAL PARAMETERS

LAUNCH PHASE

- * AMBIENT PRESSURE
- * VIBRATION
- ACOUSTIC
- PYROTECHNIC SHOCK

CRUISE & MARS ORBIT

- * AMBIENT PRESSURE

ORBITAL DESCENT & ENTRY

- SEPARATION SHOCK
- ENTRY HEATING
- AMBIENT PRESSURE

* PARAMETERS TESTED

LANDING

- ACOUSTIC
- * SHOCK LEVEL

POST LANDED

- * ATMOSPHERIC PRESSURE
- * GAS COMPOSITION
- * TEMPERATURE
- FREE CONVECTION
- FORCED CONVECTION
- SAND & DUST ABRASION

TABLE 4.1-1

LAUNCH AMBIENT PRESSURE LEVELS TITAN III C

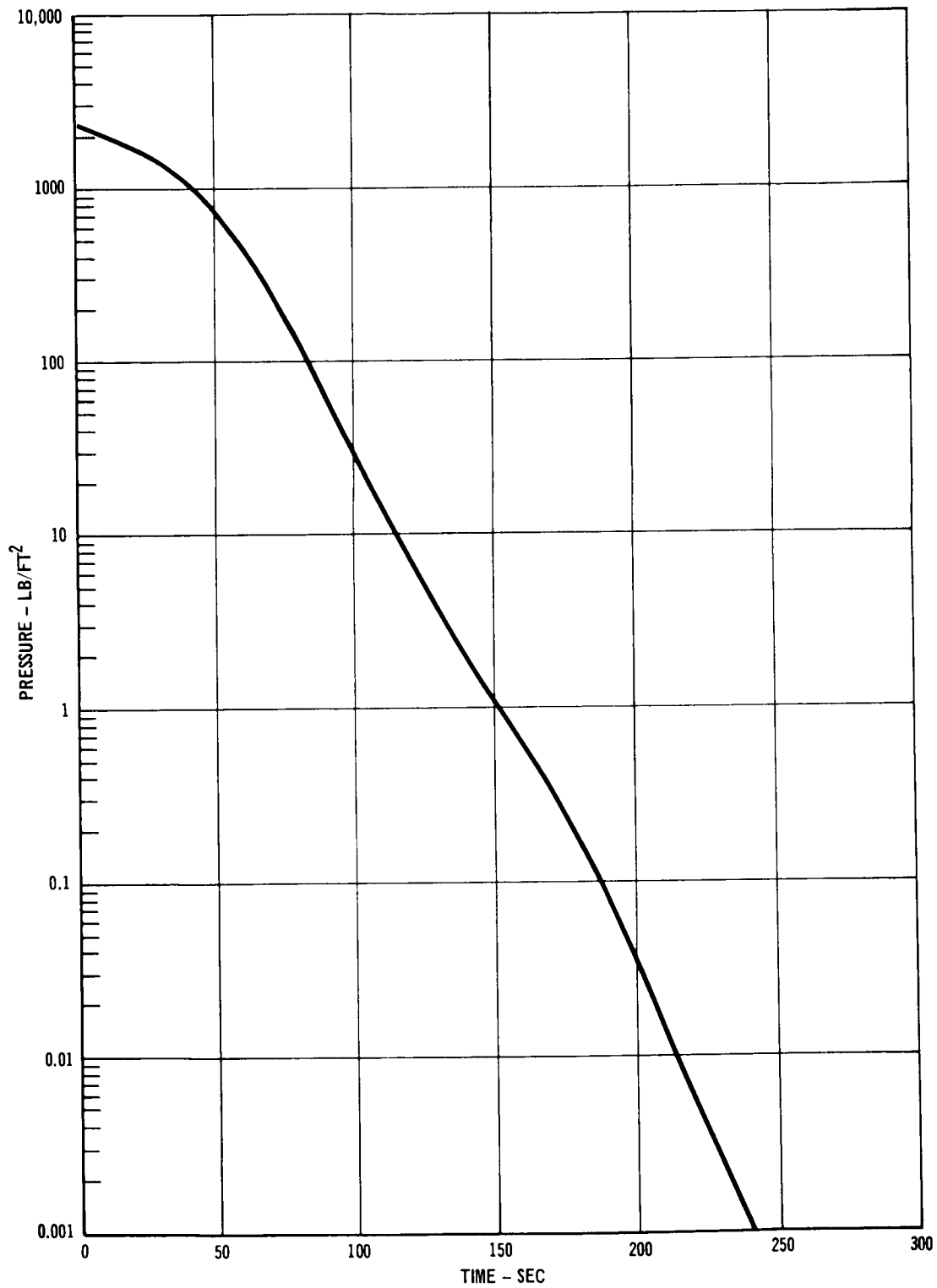


FIGURE 4.1-1

LAUNCH VIBRATION SPECTRUM

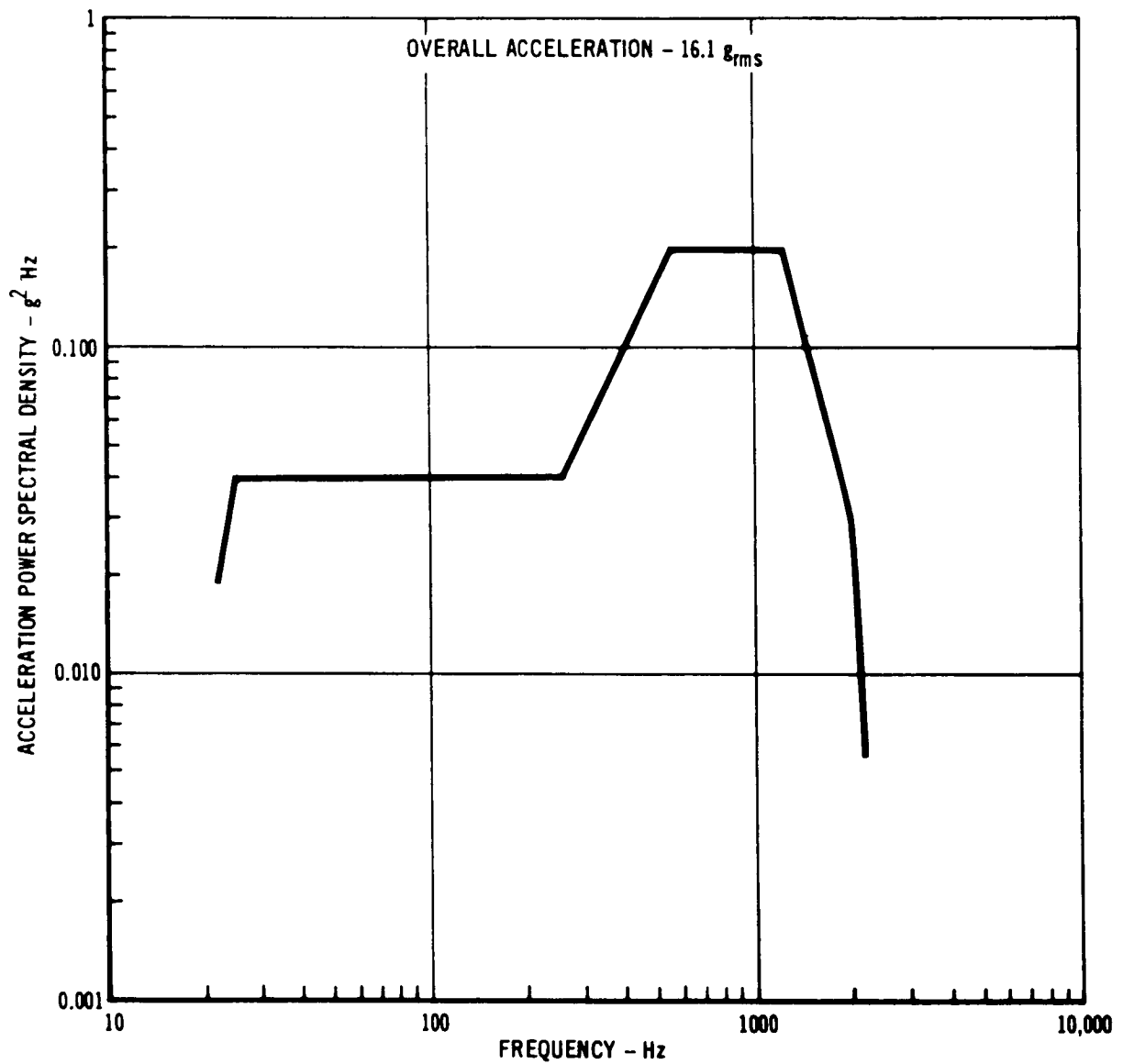


FIGURE 4.1-2

ACOUSTIC ENVIRONMENTS

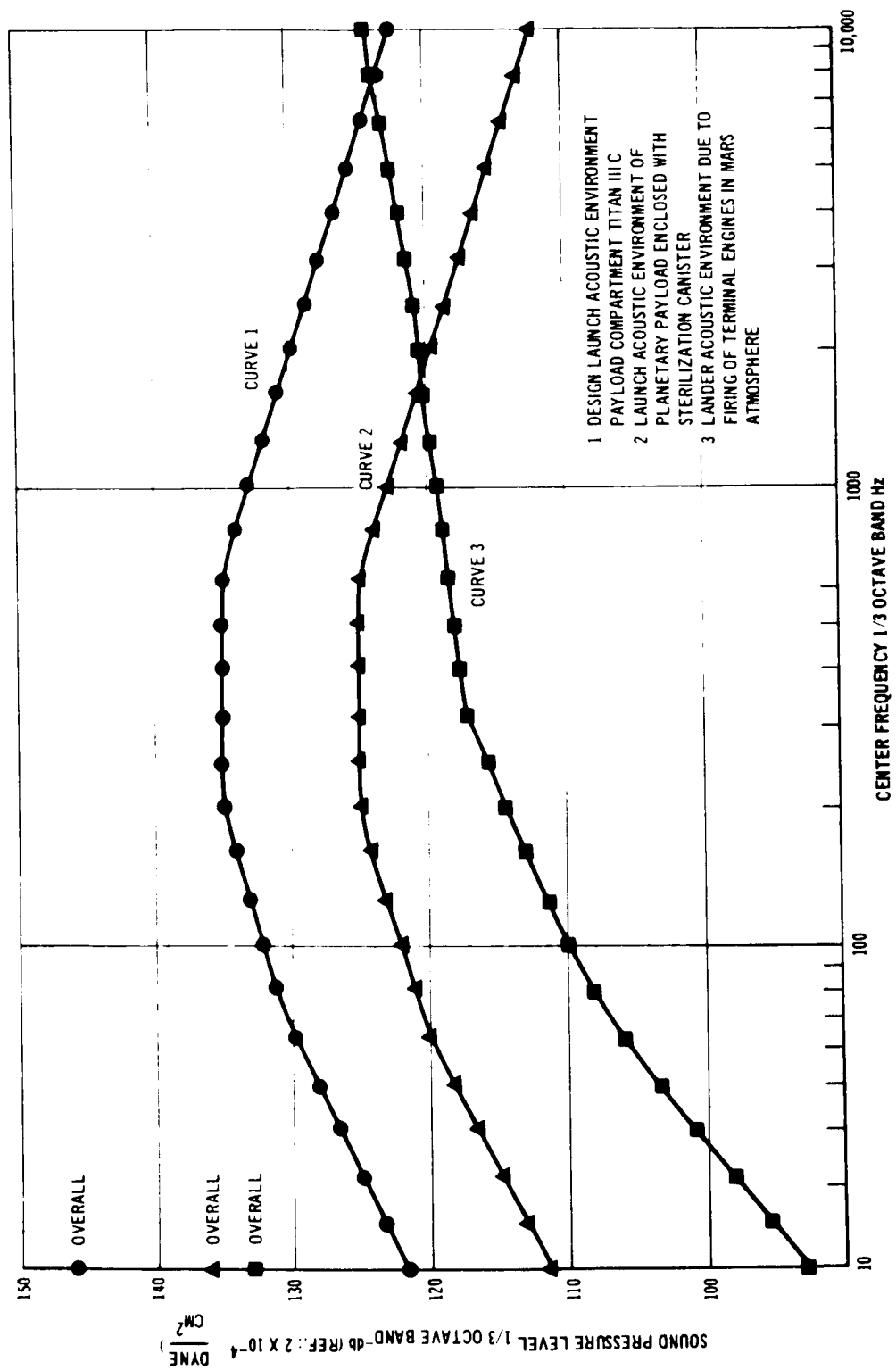


FIGURE 4.1-3

The lander will also experience a less severe acoustic environment than above during firing of the terminal descent engines in the Mars atmosphere. An estimate of acoustic environment thus produced is shown as curve 3 in Figure 4.1-3. This estimate is derived by determining the noise sources for three terminal engines, each 450 pounds thrust, in a Martian atmosphere composed of CO₂ at 20 mb pressure. This is the most severe atmospheric condition. A correction of 3 db was added to the predicted acoustic levels to account for ground effect and spacecraft reflection.

Pyrotechnic Shock - The shocks imposed on the insulation during launch separation events are not significant compared to the expected landing shocks. A typical pyrotechnic shock test spectrum is shown in Figure 4.1-4 together with the predicted envelope of shock spectra for the soft landing events. At frequencies below 150 Hz where the material may be affected by the shock environments, the spectra of Figure 4.1-4 show the landing shock to be more severe. The assumptions used in deriving the landing shock spectrum are discussed later in the section covering landing.

4.1.3 Cruise and Mars Orbit Phases - The environmental condition having most potential effect on lander insulation materials during this phase is the long term vacuum in which extensive outgassing can occur. Outgassing can have two major effects: (1) damage or contamination of nearby surfaces on which the gases recondense, and (2) physical degradation of the insulation. Many of the candidate materials can have absorbed water which will outgas. Other materials especially the organic based materials can have multiple hydrocarbon outgassing products which may be harmful.

Initial test planning included no provision for testing outgassing effects. However, if the material finally selected for lander application were suspected of outgassing, further investigation of this aspect would be recommended.

4.1.4 Orbital Descent and Entry - In addition to the initial vacuum environment during this period, three other conditions require consideration: (1) shock during separation from the orbiter, (2) transient heating during entry, and (3) repressurization of the panels with the Mars atmosphere.

Orbiter Separation Shock - The shock level during this period will depend on the separation method selected, e.g., springs, shaped charge, etc. In any event this shock is not expected to be more severe than the pyro shock at booster separation. The landing shock is more severe than either the booster separation or orbiter separation shocks.

Entry Heating - The heat shield and aft thermal curtain prevent most of the entry heating pulse from reaching the lander. However a potential lander heating problem exists, in that the heat shield backface temperature reaches 850 to 1500°F, depending on the base heating rate experienced. Preliminary transient thermal analysis indicated that the short heating time involved will prevent most of this heating from reaching the lander prior to aeroshell separation. Thus only the outer surface of the insulation panel might be affected by entry heating. Should insulation finally be selected which is

SHOCK SPECTRA OF SOFT LANDING AND PYROTECHNIC EVENTS (5% DAMPING)

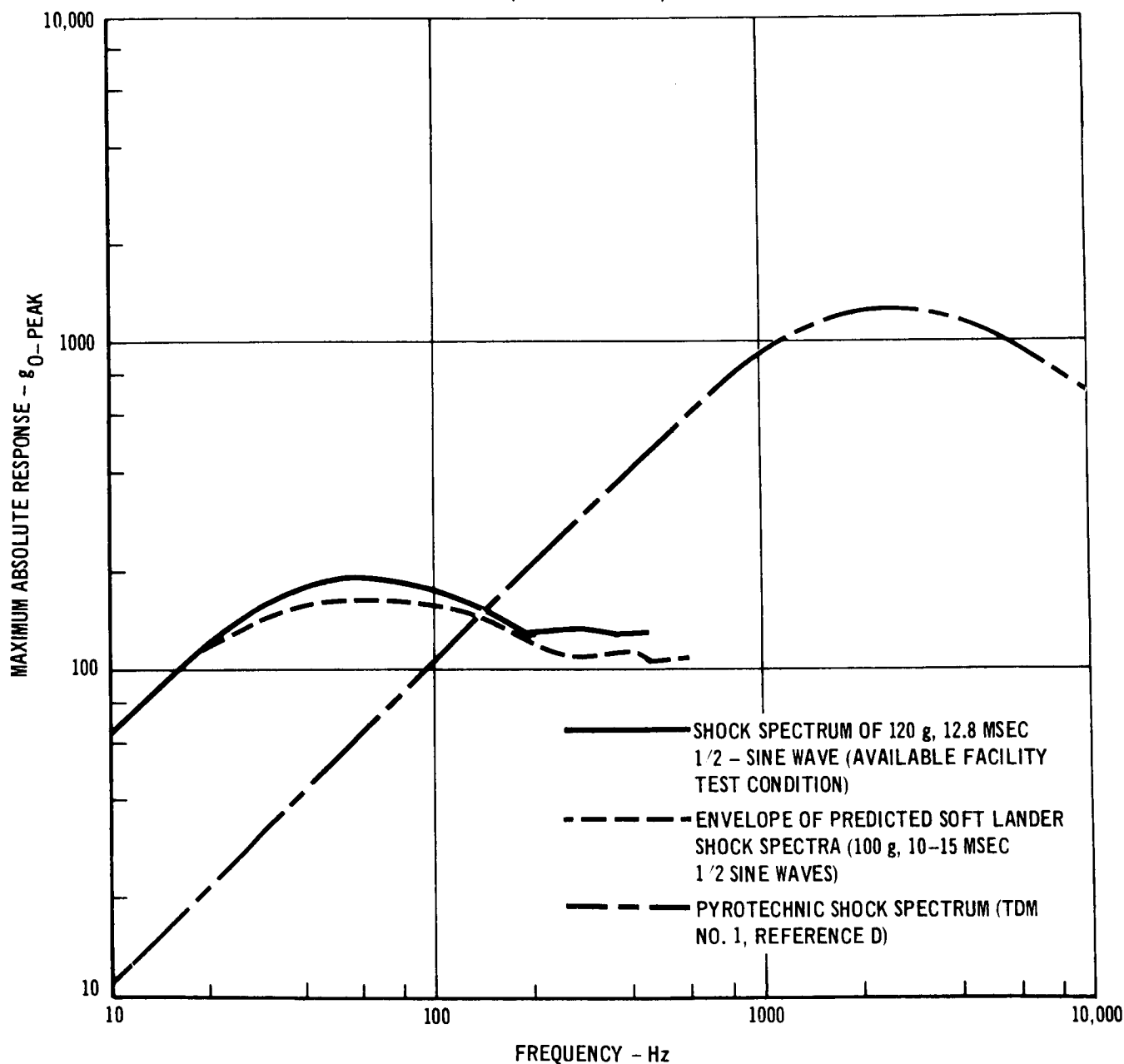


FIGURE 4.1-4

extremely temperature limited, further study of this heating period is indicated. However for materials that are not unduly temperature sensitive, such as fiberglass, further investigation did not appear necessary.

Ambient Pressure - Repressurization of the capsule interior will occur during entry and descent as shown in Figure 4.1-5. The pressure levels shown correspond to entry into the minimum and maximum atmosphere models of Reference 4-1. The resulting crushing loads imposed on the panels are smaller than those at other mission periods and are not sufficient to cause damage.

Landing - The insulation test panels will experience transient motion due to the landing shock. The envelope of predicted soft lander shock spectra is shown in Figure 4.1-4, together with an equivalent 1/2-sine wave test condition which will adequately demonstrate the capability of the insulation to withstand the dynamic motion. The predicted spectrum is an envelope of several landing conditions, including 10 fps horizontal velocity, 16 fps vertical velocity, a dynamic magnification factor of 4 and a design rigid body acceleration of 25 g. Since the time duration of landing is influenced by the attenuation material and the landing surface properties, it was estimated to vary between 10 and 15 milliseconds for a lander using the Unidisk soft landing concept (Figure 3.1-2).

Post Landing - The primary environmental characteristics of importance after landing are gas pressure, composition and temperature. Other influences are gravity and the thermodynamic properties of the gas mixture which contribute to gas conduction and free and forced convection. Sand and dust abrasion during Martian storms affects the radiative properties of exposed thermal control coatings.

Atmospheric Pressure and Gas Composition - Three model atmospheres have been defined in Reference 4-1 using analysis of the interrelated parameters of gas pressure composition and temperature, and data provided by available ground based and Mariner IV measurements. On the Martian surface the models have atmospheric pressure levels of 6, 9 and 20 mb pressure, corresponding to the minimum, mean and maximum model definitions, respectively. These pressures apply at the mean surface elevation. At higher and lower altitudes the pressure changes as shown in Table 4.1-2. According to the reference, the landing site has 99% probability of being within these altitude limits. Thus these are the most probable conditions to consider for testing.

Careful selection of test pressure levels was necessary since for many candidate materials thermal performance is sensitive to pressure. The effective insulation thermal conductivity increases with pressure, indicating that testing at the highest predicted pressure (20 mb) is the most conservative approach and will result in selection of materials and designs which will have performance in the actual Martian atmosphere which is at least as good as or better than that measured in preflight tests.

Gas composition of the test atmospheres was important because the thermal conductivity of each gas constituent affects the gaseous conduction mechanism

MARTIAN ENTRY PRESSURE/ALTITUDE HISTORY

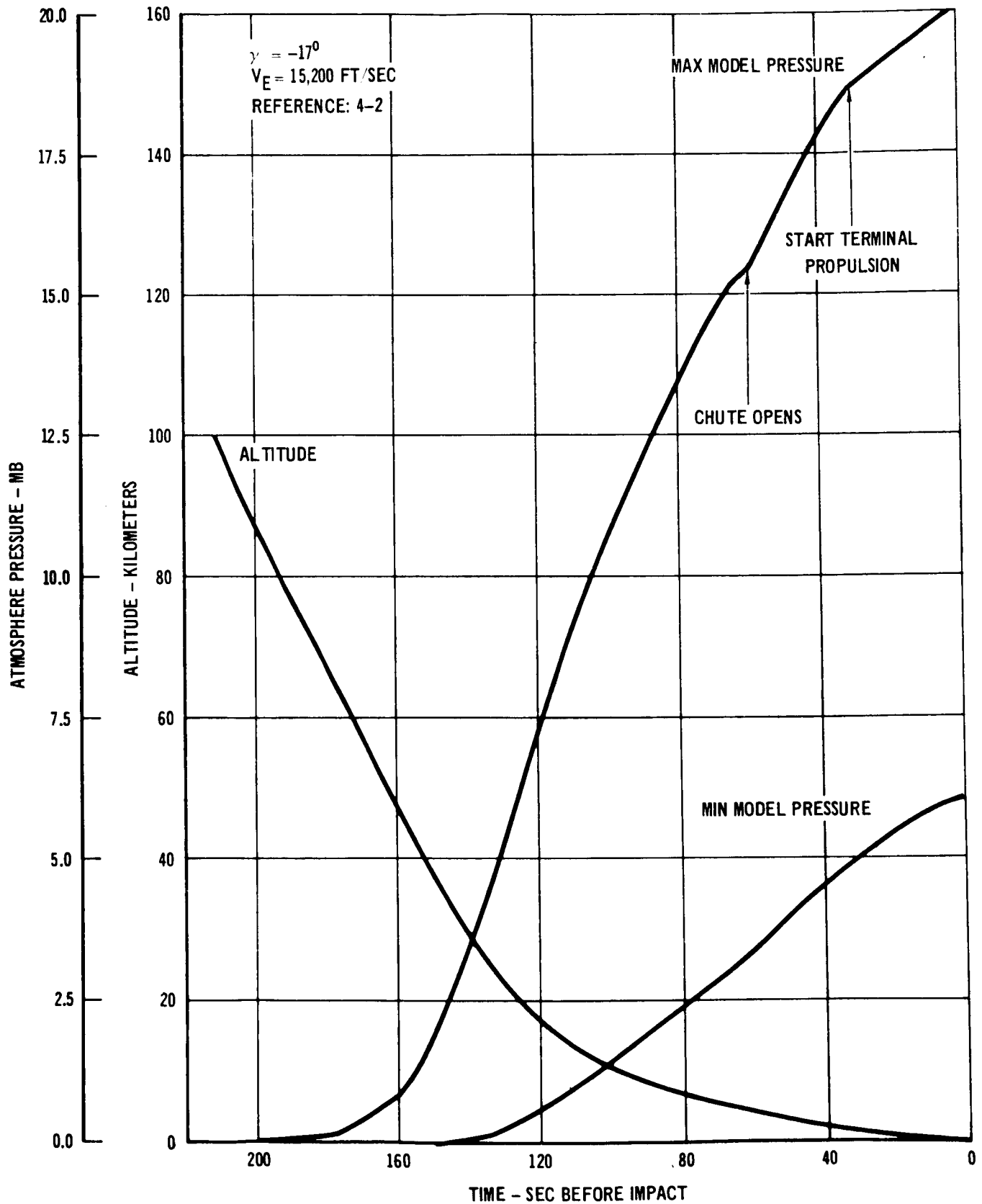


FIGURE 4.1-5

MARS SURFACE ATMOSPHERIC CONDITIONS

REFERENCE 4-1

MODEL	MINIMUM			MEAN			MAXIMUM		
ALTITUDE, KM	-5	0	+9	-5	0	+9	-5	0	+9
SURFACE PRESSURE, MB	11.6	6	1.8	13.1	9	4.2	26	20	11.9
COMPOSITION:									
BY WEIGHT, PERCENT									
CO ₂	100			74.4			25		
N ₂	0			12.8			50		
A	0			12.8			25		
BY VOLUME, PERCENT									
CO ₂	100			68.5			19		
N ₂	0			18.5			60		
A	0			13			21		
CO ₂ PARTIAL PRESSURE, MB	6			6.16			3.8		
SURFACE TEMPERATURE (MEAN)									
°K	150			230			280		
°F	-190			-46			44		

TABLE 4.1-2

within the insulation. Thermal conductivity values of the individual Mars atmosphere gases are shown in Figure 4.1-6. In the temperature region of interest, nitrogen has the highest thermal conductivity, followed by argon and carbon dioxide. Since nitrogen and argon have increasing concentrations at the higher pressures, selection of higher pressure atmosphere models would have a twofold effect on insulation performance, i.e., (1) increased pressure will increase gaseous conduction, and (2) the increased concentration of the higher conductivity nitrogen and argon will additionally increase overall conductivity.

It appeared then that the most conservative approach to selecting atmospheric conditions for test was to use the maximum model atmosphere composition, which has the highest percentage of nitrogen and argon.

Temperature - For insulation selection and sizing purposes, definition of temperature was most important for the Martian night time period. At night the greatest cooling of equipment can occur and insulation performance is the most critical for successful thermal control. The minimum surface temperature which might be considered is that which would allow carbon dioxide to begin condensing from the atmosphere. Temperatures lower than those are not probable since CO_2 would then be removed from the atmosphere over extensive areas. Figure 4.1-7 shows the vapor pressure curve for CO_2 in the temperature range of interest. Also included are the CO_2 partial pressure values for the three model atmospheres. The curve indicates CO_2 does not condense at temperatures above about -192°F for any atmosphere model, thus requiring that acceptable temperature levels for both environment definition and testing be above this value.

Other temperature measurement data, Figures 4.1-8 and 4.1-9, Reference 4-1 indicate that near the Mars Equator, minimum daily temperature is above about -155°F . Plotted on the same curves are temperature profiles taken from Reference 4-1 for other latitudes during a three month period of post landed operations for the 1973 mission. These additional data indicate that an acceptable minimum temperature for insulation evaluation is about -150°F , and that the band of temperatures defined for use at the Equator should be acceptable throughout the latitude range of at least $\pm 25^\circ$.

Free Convection Heat Transfer - In the low Martian gravity and atmospheric pressure range, free convection effects tend to be negligible, with the possible exception of within the insulation. Using conventional free convection relationships, Figure 4.1-10 shows predicted rates at Mars gravity conditions. It should be noted that for earth based testing in 1 "g", the free convection transfer rates will be higher than on Mars by a factor of $(g_{\text{Earth}}/g_{\text{Mars}})^{1/4}$ equals 1.275, or about 27%, an increase which continues to indicate the small influence of free convection on the lander heat transfer.

Forced Convection Heat Transfer - This heat transfer mode occurs as a result of the expected winds associated with storm fronts moving across the Martian surface in a manner similar to those on Earth. Variation of the forced convection coefficient for parallel flow across external surfaces is

THERMAL CONDUCTIVITY OF MARTIAN ATMOSPHERIC GASES

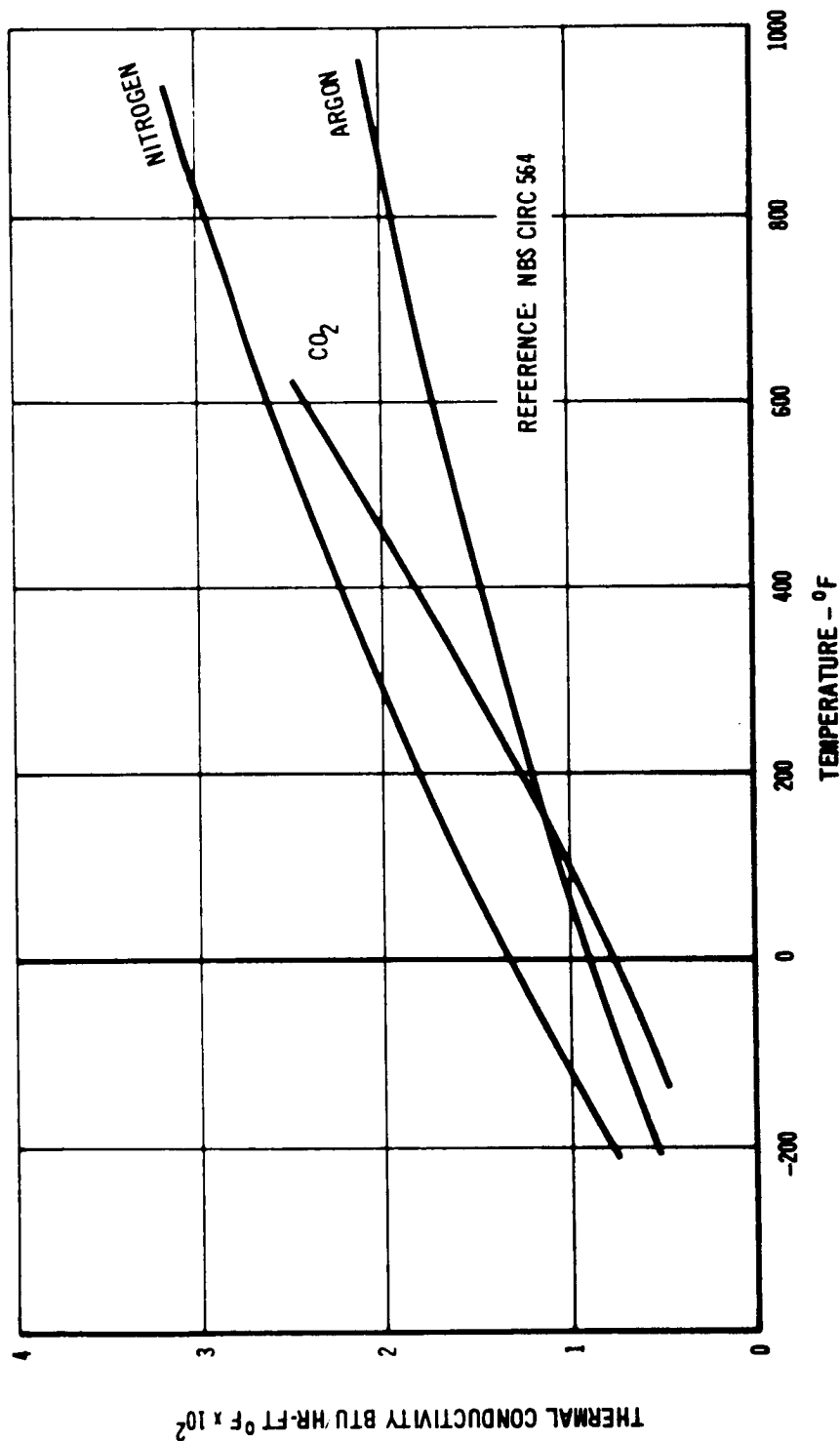


FIGURE 4.1-6

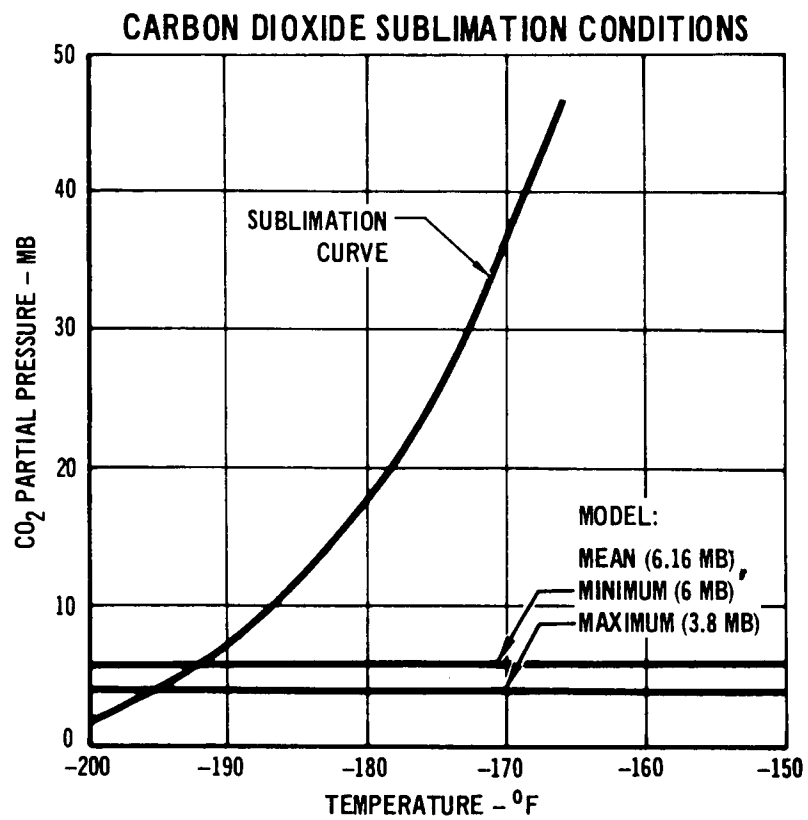


FIGURE 4.1-7

MARS SURFACE TEMPERATURES
BEGINNING OF POST LANDED MISSION
(HELIOCENTRIC ANGLE, $\eta = 83^\circ$)

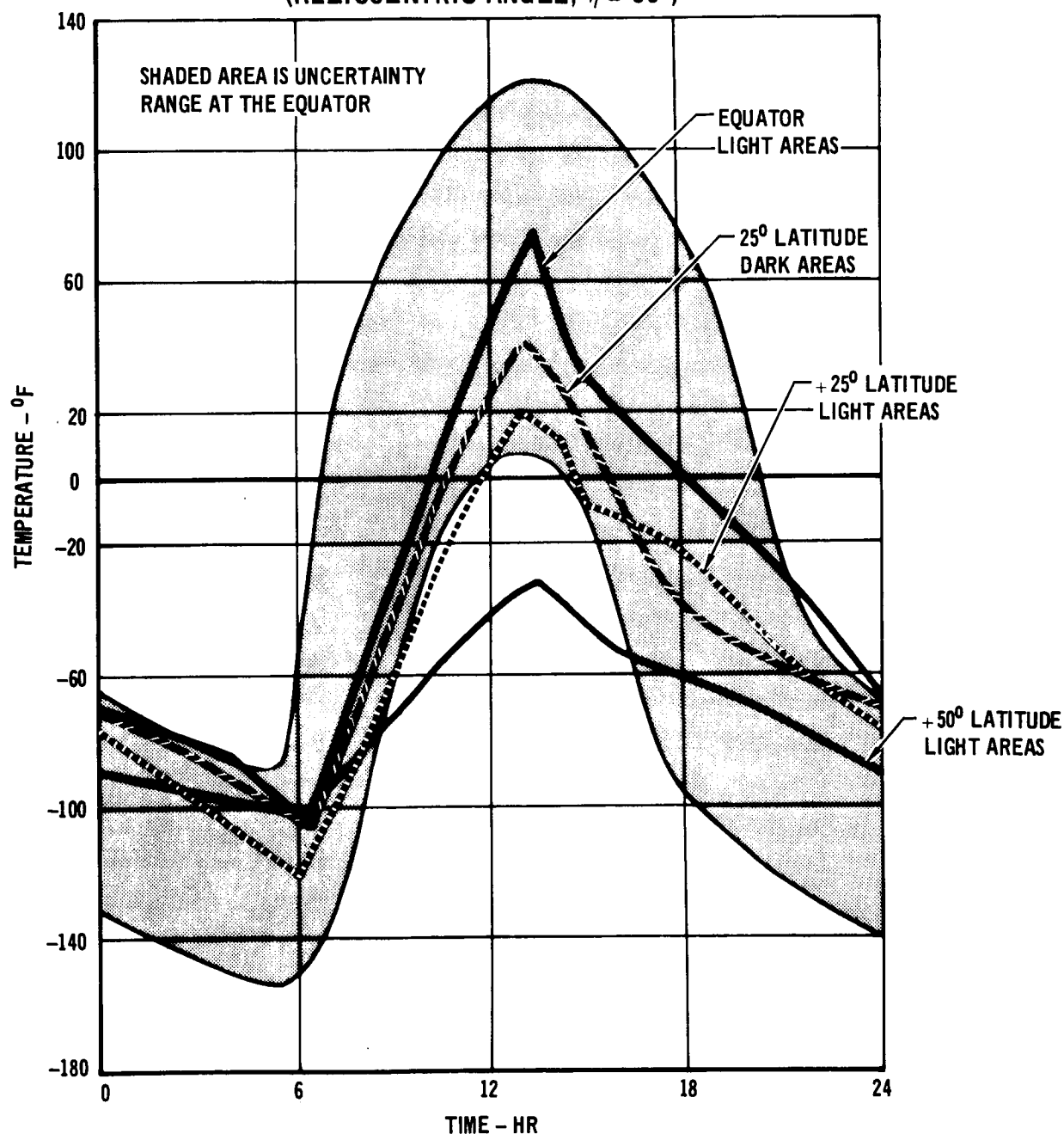


FIGURE 4.1-8

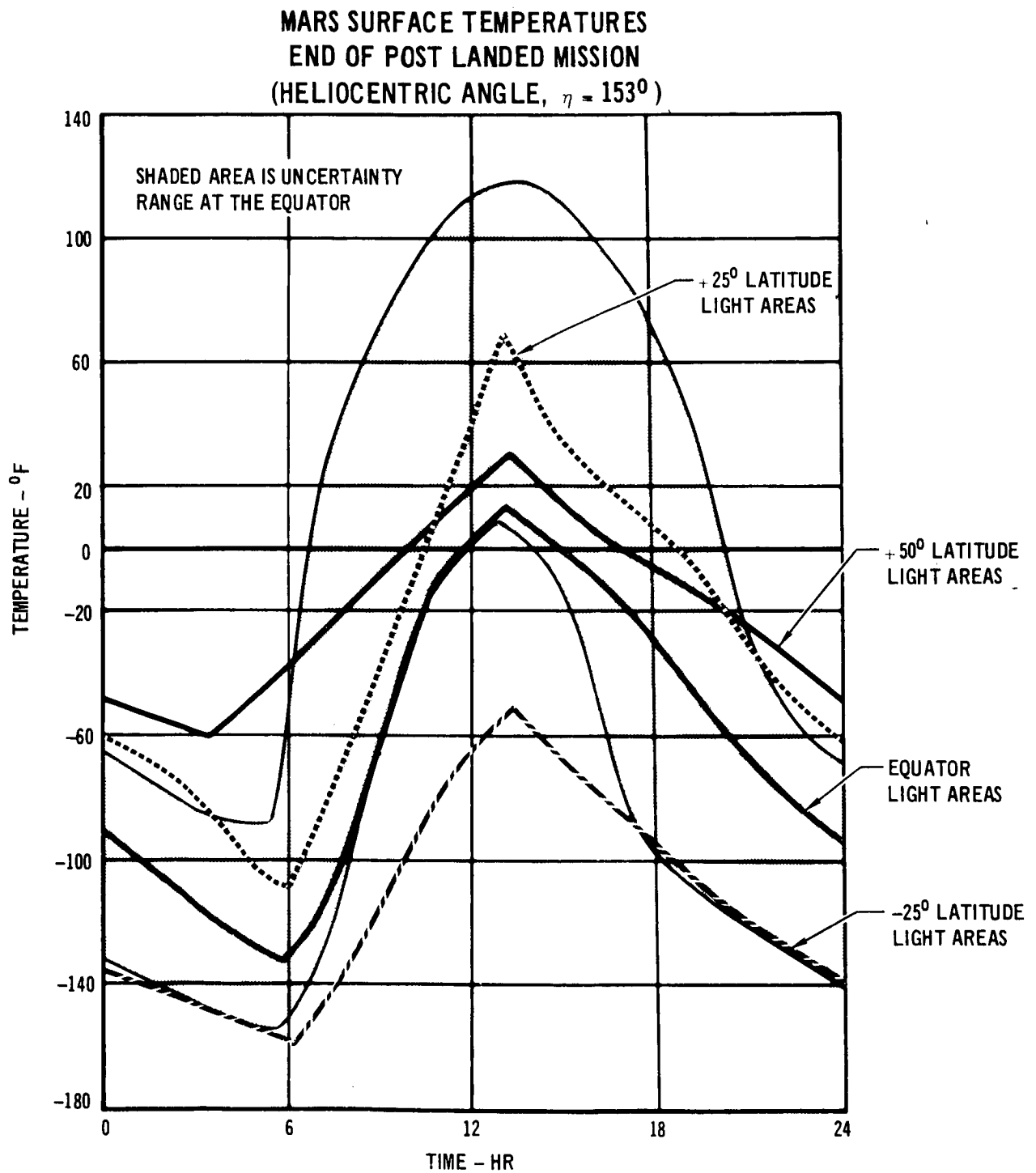


FIGURE 4.1-9

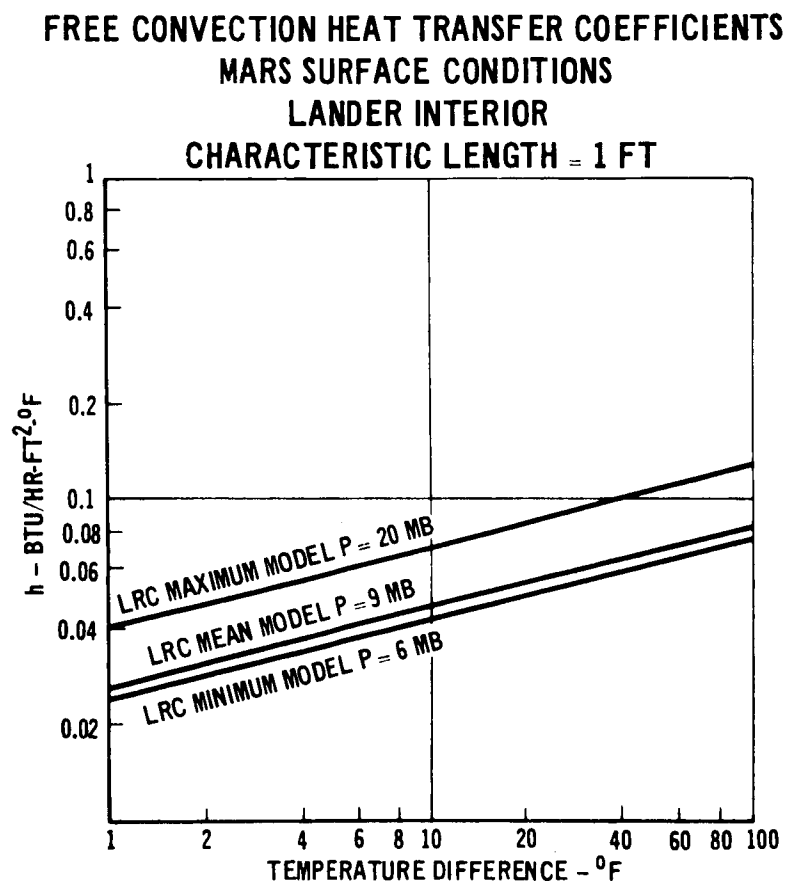


FIGURE 4.1-10

shown in Figure 4.1-11. The effect of forced convection cooling on the overall lander heat balance has been determined for a night time environmental condition of -150°F , Figure 4.1-12. The curve shows that for lower insulation conductivity values and/or thicker insulation, the variation in total heat loss becomes negligible with any appreciable wind speed and the assumed boundary conditions. However, heat loss for thin insulation with high thermal conductivity value is strongly influenced by convection cooling.

Sand and Dust Abrasion - Dust storms on the Martian surface can have a large effect on overall lander heat balance because the abrasion and erosion of thermal coatings can radically alter their radiative properties. Experimental studies of this phenomena have been conducted at MDAC-ED over the past several years. This initial work has culminated in a contracted study, NAS 18708, which will provide design data to support selection of lander thermal coatings.

4.2 SELECTED TEST PARAMETERS - The environmental parameters previously discussed were reviewed and selections identified for use in the test program. The tests together with the recommended environmental parameters are identified in Table 4.2-1, and discussed in the order of the test sequence.

- o Thermal Diffusivity (No. 1) - In this test fifty $6 \times 6 \times 6$ in. material specimens were tested at three environmental conditions, (a) vacuum ($<10^{-4}$ torr), (b) maximum model Martian atmosphere at 20 mb pressure, and (c) air at one atmosphere. All tests were performed near room temperature. These conditions were selected to determine relative insulation performance in the worst case Martian atmospheric pressure and gas composition values. The tests in vacuum and one atmosphere provided insulation performance for the flight phases of the mission, and for comparison with other available test data.
- o Sterilization Screening - This test, run in parallel with the above test, provided quantitative support and insight into the changes which would occur in materials exposed to the heat sterilization cycles. The test techniques included thermogravimetric analysis, differential thermal analysis, and effluent gas analysis. Materials which were found to degrade near the sterilization temperature were deleted from further consideration.

The test specimens were heated to a maximum temperature of 455°F (235°C) to examine ability to tolerate long term changes which might occur during the extended heat sterilization process.

- o Heat Sterilization - This test was conducted on the most promising candidates to allow later evaluation of heat sterilization effects on material samples, and to provide the initial environmental exposure of the ISM panels. The test consisted of an initial heatup from room temperature, stabilization at $275 \pm 10^{\circ}\text{F}$ for 384 hours, and a final cooldown.

FORCED CONVECTION HEAT TRANSFER COEFFICIENTS -
MARS SURFACE CONDITIONS
LANDER EXTERIOR, PARALLEL FLOW
CHARACTERISTIC LENGTH = 1 FT

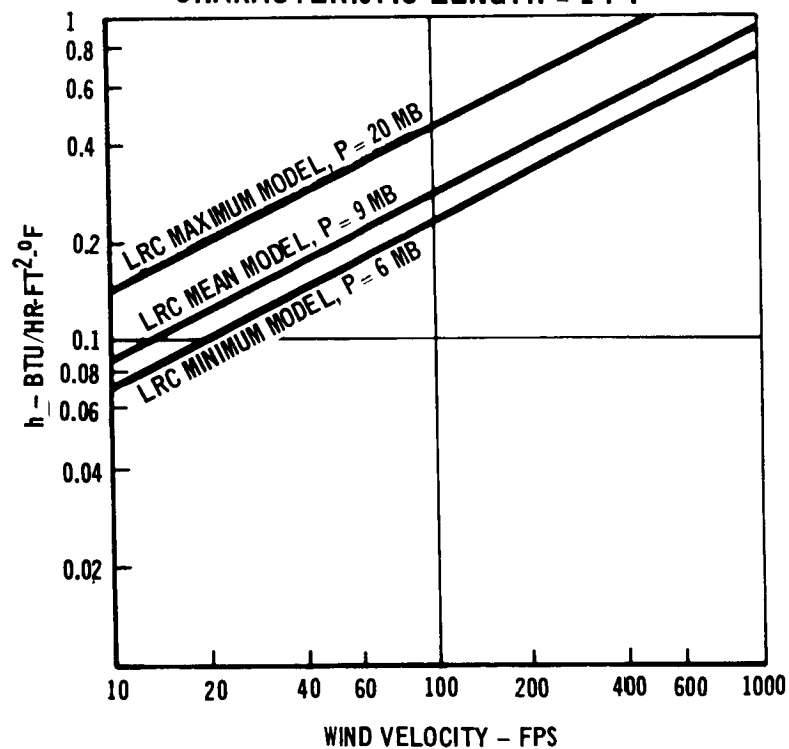


FIGURE 4.1-11

CONVECTION EFFECT ON INSULATION HEAT LOSS

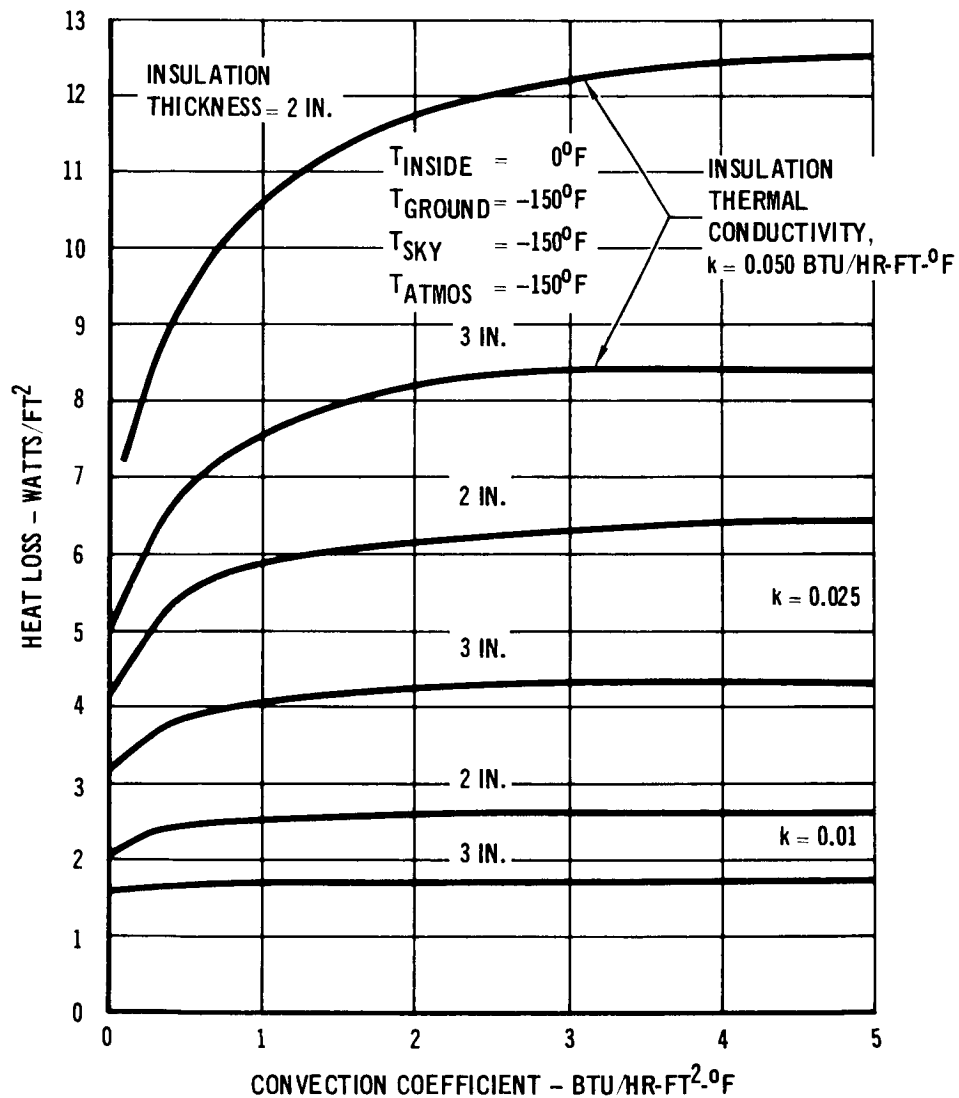


FIGURE 4.1-12

TEST SUMMARY

TEST	TEMPERATURE	PRESSURE	GAS COMPOSITION	COMMENTS
THERMAL DIFFUSIVITY NO. 1	a) AMBIENT ($75 \pm 5^{\circ}\text{F}$) b) AMBIENT ($75 \pm 5^{\circ}\text{F}$) c) AMBIENT ($75 \pm 5^{\circ}\text{F}$)	VACUUM (10^{-4} TORR) 20 MB 1 ATM	- MAXIMUM MODEL AIR	50 SAMPLES
STERILIZATION SCREENING	SEE COMMENTS	1 ATM	DRY NITROGEN	SAMPLES HEATED TO A MAXIMUM OF 235°C (100°C ABOVE HEAT STERILIZATION) FOR TGA, DTA AND EGA ANALYSIS - 7 SAMPLES IN INITIAL TEST.
HEAT STERILIZATION	275°F	SLIGHTLY ABOVE 1 ATM	DRY NITROGEN	12 THERMAL DIFFUSIVITY SAMPLES 2 ISM'S 2 THERMAL CONDUCTIVITY SAMPLES SPARE MATERIAL
THERMAL DIFFUSIVITY NO. 2	SAME AS TEST NO. 1			9 SAMPLES
THERMAL CONDUCTIVITY	HOT FACE/COLD FACE (a) $50/-150^{\circ}\text{F}$ (b) $50/-150^{\circ}\text{F}$ (c) $50/-150^{\circ}\text{F}$ (d) $70/-100^{\circ}\text{F}$ (e) $70/-100^{\circ}\text{F}$ (f) $70/-100^{\circ}\text{F}$	6 mb 9 mb 20 mb 6 mb 9 mb 20 mb	MINIMUM MODEL MEAN MODEL MAXIMUM MODEL MINIMUM MODEL MEAN MODEL MAXIMUM MODEL	SILICONE BONDED "AA" FIBERGLASS MATERIAL
THERMAL PERFORMANCE	(a) -150°F (COLD PLATE); $+50^{\circ}\text{F}$, (HOT FACE) (b) SAME AS ABOVE	VACUUM (10^{-4} TORR) 20 mb	--- MAXIMUM MODEL	CHAMBER EVACUATED ALONG LAUNCH PRESSURE PROFILE, FIGURE 4.1-1 FOR FIBERGLASS ISM PANEL
LAUNCH VIBRATION	AMBIENT	AMBIENT	AMBIENT	FIGURE 4.1-2 LEVEL FOR FIBERGLASS ISM PANEL
LANDING SHOCK	AMBIENT	AMBIENT	AMBIENT	SOFT LANDING LEVEL, FIGURE 4.1-4 FOR FIBERGLASS ISM PANEL
THERMAL PERFORMANCE NO. 2	(A) -150°F (COLD PLATE); $+50^{\circ}\text{F}$, (HOT FACE) (B) SAME AS ABOVE	VACUUM (10^{-4} TORR) 20 MB	- MAXIMUM MODEL	CHAMBER EVACUATED ALONG LAUNCH PRESSURE PROFILE, FIGURE 4.1-1; FOR FIBERGLASS ISM PANEL

TABLE 4.2-1

Samples included in the test were (a) Thermal Diffusivity test specimens, (b) (2) Insulation System Modules (ISM), 18 x 18 x 3 inches, plus spare material for (2) additional ISM's of the same material, and (c) (2) thermal conductivity test specimens, plus spare material for (2) additional specimens of the same material.

- o Thermal Diffusivity (No. 2) - Following heat sterilization the thermal diffusivity test was repeated at the same test conditions.
- o Thermal Conductivity - Thermal conductivity of the silicone bonded "AA" Fiberglass was determined at (6) test points as shown in Table 4.2-1. The test apparatus was a guarded hot plate designed and fabricated under a MDAC-ED IRAD program for use in the Martian environment studies.
- o Thermal Performance (No. 1) - Comparative heat loss measurements were planned on both ISM panels at the worse case vacuum and Mars ambient environments. Because the foam panel was destroyed, the heat loss could be determined for only the fiberglass panel. Hot and cold face temperatures were 50 and -150°F respectively, in both the vacuum and 20 mb maximum model Mars atmosphere conditions. Data from this test provided the initial temperature levels and heat loss values for comparison in the second thermal performance test, conducted after exposure of the ISM to the launch and landing environments.
- o Launch Vibration - The fiberglass ISM panel was subjected to the launch vibration levels shown in Figure 4.1-2.

It was recommended that an acoustic environment test not be performed because acoustic excitation inside the shroud acting on the ISM would produce less structural response than the vibration test. Successful completion of the launch vibration test demonstrated adequate structural capability of the insulation material for both the acoustic and vibration environments to be experienced in the mission.

- o Landing Shock - The loads imposed on the ISM panels during landing were simulated in this test. Based on the landing assumptions discussed previously, the soft landing shock level for testing is shown in Figure 4.1-4. This test demonstrated capability for withstanding not only the landing shock but also the less severe separation events occurring during launch and Mars orbit. The landing shock is more severe than these separation events at frequencies below 150 Hz where the panels would be most affected by these environments. Comparison of the landing shock and pyrotechnic separation shock spectra, Figure 4.1-4 verifies this conclusion, and resulted in the recommendation that a pyrotechnic shock level test not be performed.
- o Thermal Performance (No. 2) - After completion of the vibration and landing shock tests, the ISM panel underwent a second heat loss

test which duplicated the environmental conditions of the initial test. This second test demonstrated no change in thermal performance of the panel as a result of the above environmental exposures, verifying the basic integrity of the silicone bonded "AA" fiberglass panel design.

5. CANDIDATE MATERIAL SELECTION

Material selections for the initial screening tests were made by comparing available data with selection criteria developed for the Mars mission. Data on potential candidate materials was sought through a literature and vendor survey. The survey also helped identify those material parameters e.g. layer density, fiber diameter and pore size, which would be most significant for parametric study to identify optimum configurations. Based on these studies 26 material configurations, consisting of four classes, fibers, foams, powders and multilayers were selected for initial evaluation.

5.1 SELECTION CRITERIA - The most significant criteria used to select the candidate materials are itemized in Table 5.1-1 and discussed as follows.

- o Thermal Conductivity - Since the primary purpose of the material is to provide thermal protection, it is imperative that the insulation material selected have low thermal conductivity. Thermal conductivity is affected by many parameters including temperature, ambient gas composition and pressure. It is therefore important to make thermal conductivity comparisons under similar conditions. This objective was not entirely possible to achieve during the selection process due to lack of test data for the materials in Mars atmospheric conditions.
- o Density - Total weight and volume of insulation are important since they can effect the allowable science payload. A density difference of only one pound per cubic foot in the insulation can be translated into approximately 22 pounds of landed weight and several times this in launch weight.
- o Conductivity-Density Product - The lowest " $k\rho$ " material will provide the minimum weight of insulation for given heat loss. Use of this parameter requires some judgement since materials could be selected to provide a very lightweight package, but which had no payload volume remaining for scientific equipment. Comparisons of materials installed differently can also be misleading using only $k\rho$ considerations since insulation attachment and structure weight changes for each material must be considered.
- o Temperature Resistance - Materials used must withstand the expected mission thermal environments without degradation. Also because of planetary quarantine requirements, the materials must withstand the required heat sterilization cycle. Materials that were expected to be most affected by the extreme temperature requirements (pre-flight sterilization and landed diurnal temperature levels) were the organic types.

MATERIALS SELECTION CRITERIA

- THERMAL CONDUCTIVITY
 - TEMPERATURE
 - PRESSURE
 - GAS COMPOSITION
- DENSITY
- CONDUCTIVITY - DENSITY PRODUCT
- TEMPERATURE RESISTANCE
 - HEAT STERILIZATION COMPATIBILITY
- SPECIFIC HEAT
- VIBRATION AND SHOCK RESISTANCE
- LONG TERM VACUUM COMPATIBILITY
- HANDLING CHARACTERISTICS
 - PENETRATION EFFECTS
 - PACKAGING AND ATTACHMENT TECHNIQUES
- AVAILABILITY
- COST

TABLE 5.1-1

- o Specific Heat - This parameter is normally not considered when the design is for steady state conditions. It does affect overall thermal performance in a transient condition. Materials with high specific heats are preferred to attenuate environmental temperature extremes.
- o Vibration and Shock Resistance - The insulation material must be able to pass the expected launch vibration and Mars landing shock. This study was based upon a "soft landing" configuration which greatly reduces requirements placed upon the insulation material. Care however must be taken to assure that friable material does not "settle out" or "pack."
- o Vacuum Compatibility - The primary objective of a Martian lander is to deliver a scientific payload to the surface of Mars for obtaining useful information about its make-up. One of the more important scientific aspects is to ascertain whether or not life as known here on earth exists on Mars. To that end it is most important that the scientific instruments carried on board are not contaminated by earth's organic materials. These organics can come from the recondensation of volatile materials liberated from adjacent components upon exposure to the long term vacuum exposure (cruise period). Further, the loss of these volatiles may degrade the thermal performance of the material.
- o Fabrication Characteristics - The manner in which the insulation material can be contained and attached to the lander will affect overall thermal performance and weight. If the insulation can be incorporated into the overall design of the lander to carry some structural loads, then it usually is lighter than a non-structural installation. Use of a thicker structure to support non-load bearing insulation usually means an attendant increase in weight and heat loss.
- o Availability and Cost - Economic factors dictated that the materials employed be available in sufficient quantities to enable fabricating a useable system within cost and time constraints.

5.2 DATA SURVEY - To assure that all promising materials were included in the candidate material list, a survey was made of available literature, materials suppliers and research organizations. A copy of a vendor survey letter as well as a list of the organizations contacted is included as Appendix A of this report. The survey revealed no startling conclusions. In general developmental materials were either not available or were too costly for the current study. The survey did confirm that the materials list did include the best choices that could be made. Several interesting points resulting from the survey should be noted for possible future consideration. A synopsis of these points is also included in Appendix A.

5.3 CANDIDATE MATERIAL DISCUSSION AND SELECTION - The four generic classes of thermal insulation considered for this study were the following:

- o Multilayer
- o Foams
- o Fibers
- o Powders

Each of these materials have specific advantages at either one atmosphere or vacuum pressure conditions, and thus would be expected to be satisfactory at the intermediate pressures of the Martian atmosphere. Combinations of the above materials might also have been considered, but it was felt that any small increases in overall system performance would in general not warrant the complexities of additional evaluation parameters in an initial study such as this. Candidate materials in each class were chosen on the basis of the selection criteria just discussed. Most generic material classes were selected for testing in several forms to examine differences in vendor products and to exercise variations due to significant parameters such as density, pore size, fiber diameter, etc.

5.3.1 Discussion of Insulation Classes - Data and physical characteristics for each of the material classes are discussed to provide background for the materials selections.

- o Multilayer Insulations - This material class has the lowest thermal conductivity-density product for operation in high vacuum. The material, consisting essentially of radiation shields, sometimes separated by low conductivity spacer material, owe their low thermal conductivity to the low emittance of the shields and elimination of gaseous conduction and convection when operating in a vacuum (less than 1×10^{-4} torr). Typical radiation shield materials include aluminum foil, aluminized Mylar and Kapton films, and Mylar and Kapton films with gold coatings. Nonconducting spacers include fiberglass and fibrous silica papers or mats, thin sheets of polyurethane foam, and various forms of nylon and silk fabrics, such as woven cloth, netting, and screens.

As shown in Figure 5.3-1, the thermal performance of multilayer insulation is highly sensitive to ambient gas pressure and composition. The sensitivity of a typical multilayer insulation to installation procedures is demonstrated by the effect of compressive loads as shown in Figure 5.3-2.

THERMAL CONDUCTIVITY OF MULTILAYER INSULATIONS AS A FUNCTION OF GAS PRESSURE

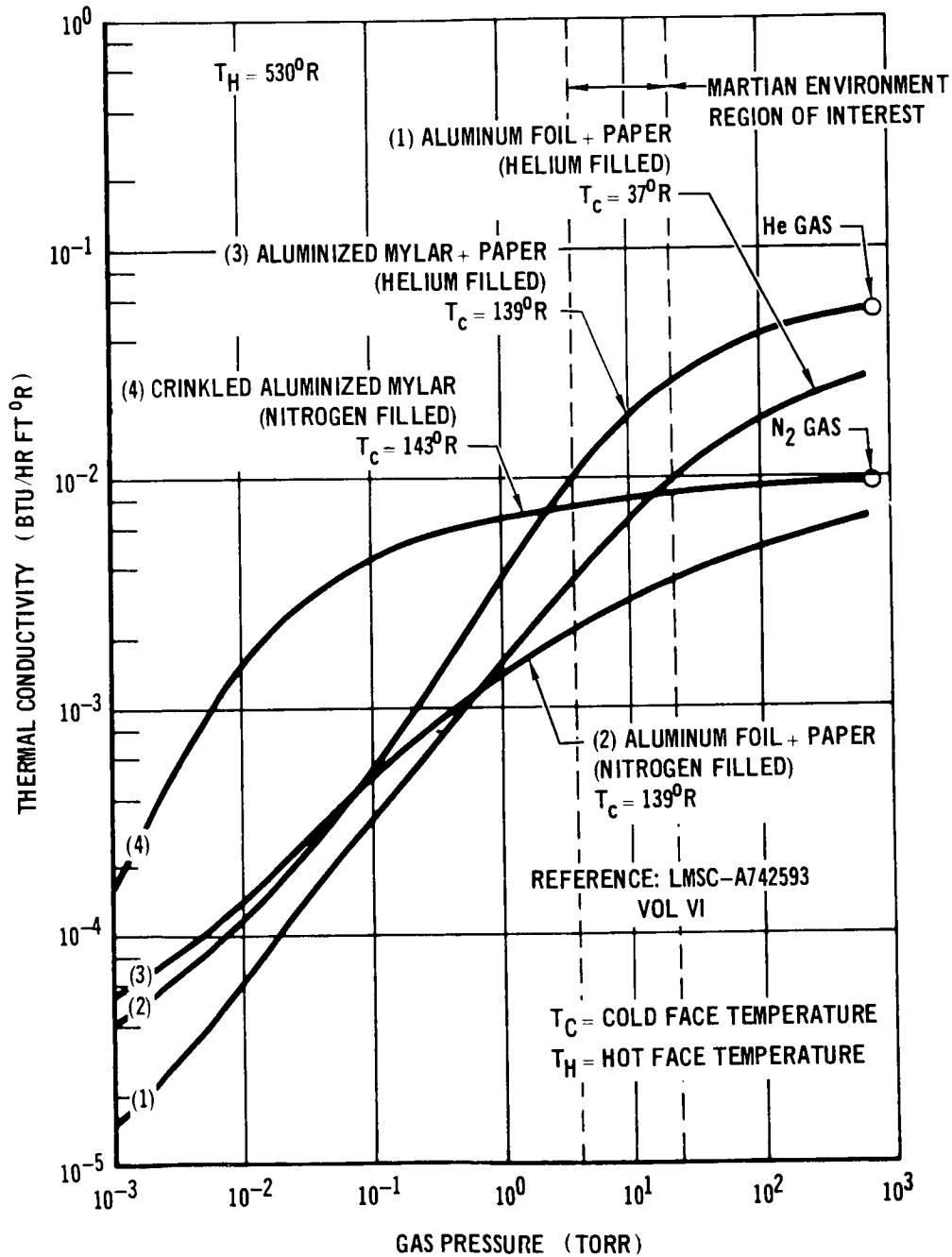


FIGURE 5.3-1

EFFECT OF EXTERNAL COMPRESSION LOADING ON NRC-2
(CRINKLED ALUMINIZED MYLAR) THERMAL PERFORMANCE

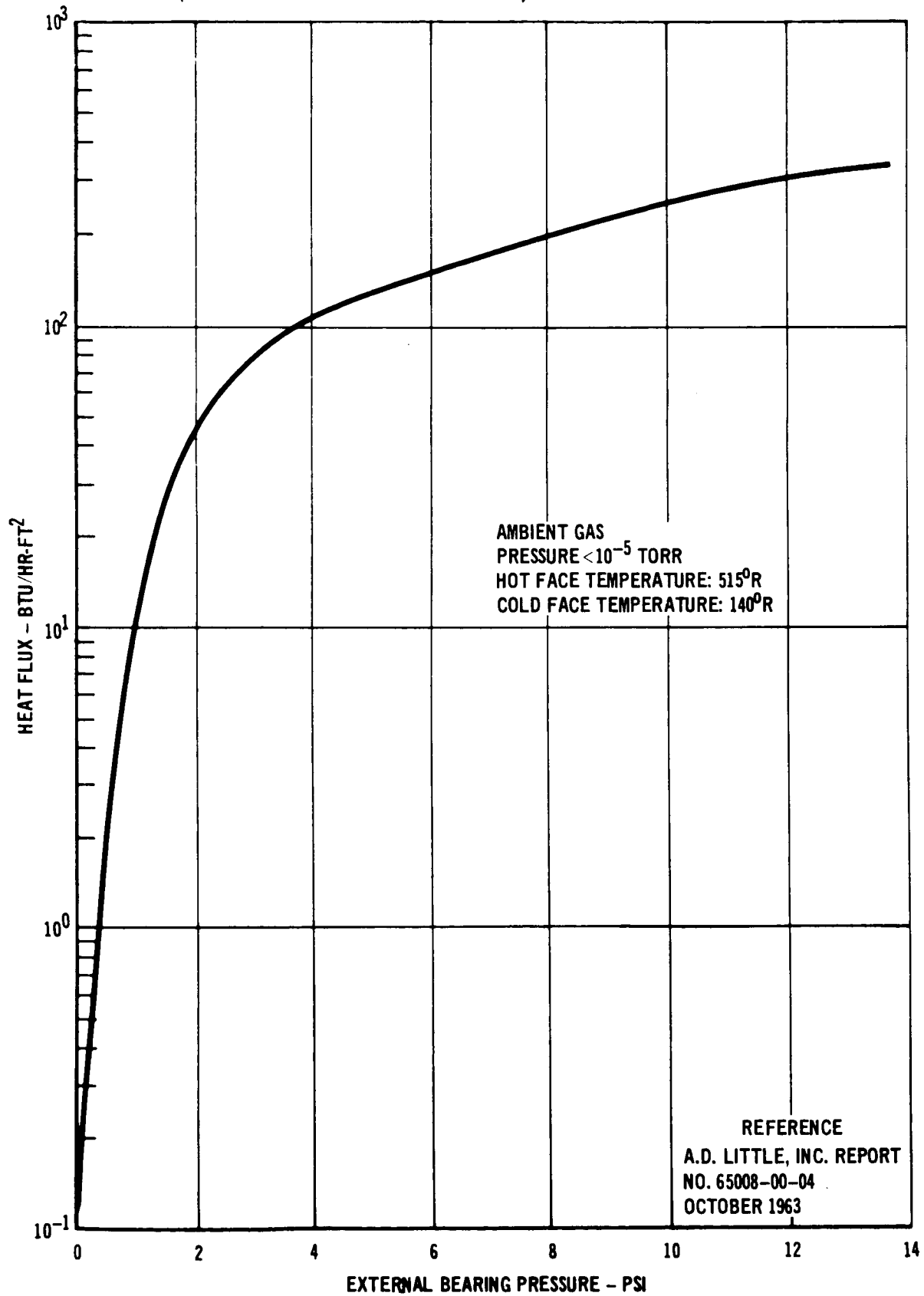


FIGURE 5.3-2

Residual gas conduction also plays a vital role in the heat transfer characteristics of these insulations. When the gas pressure is such that the mean free path of that gas is comparable to or greater than the distance between the two surfaces, the heat transfer ceases to be continuum in nature, and becomes essentially proportional to the pressure. This is illustrated by Figure 5.3-1, which shows the effect of residual gas pressure, as well as composition, on thermal performance. In the pressure region of interest for Mars (3.75 to 15 torr), the thermal conductivity of the multi-layer insulations is two orders of magnitude greater than the value at 10^{-3} torr, making them comparable to the conductivity obtainable with fibrous batting, compressed powders, and foams at these pressures.

In addition to the residual gas pressure, the conductivity of the particular gas composition is important and must be taken into consideration. Figure 4.1-6 gives the conductivity of the individual Martian atmospheric gases at 760 torr.

- o Foams - Prefoamed and foamed-in-place materials are widely used for insulation in a wide temperature range, from cryogenic temperatures up to and above room temperature. Various chemical formulations, including polyurethane resins (either polyester or polyether base); and rigid polyvinylchloride resin have been utilized.

Advantages of plastic foam include low density (2-4 lb/cu ft), low thermal conductivity, and low cost. Also, some of the foams are rigid and have load-carrying capability. These materials also can be foamed in place. Thus odd-shaped voids and cavities can be completely insulated by pouring the unreacted chemicals in place before the foaming reaction occurs.

The rigid organic foams are affected to a small degree by ambient pressure because their basic heat transport mechanism is solid conduction (Figure 5.3-3). Outgassing rates during the seven-month exposure to vacuum associated with interplanetary flight must be considered with respect to performance change as well as contamination. Repressurization effects after entering the planet atmosphere may also be important. Experience indicates that the foams can survive short term vacuum exposure without detrimental effect to their properties, but the effect of long term exposure must be considered.

- o Fibrous Insulation - Fibrous insulations have long been used in aerospace applications. They are available with various chemical compositions and fiber diameters. The borosilicate fiberglass and high-purity silica-based materials are of particular interest because they are inorganic and non-metallic, and are therefore relatively insensitive to heat sterilization and long-term vacuum

exposure. Available forms include bulk fibers or batts (unbonded or bonded with a variety of organic binders). Densities can be varied from 0.5 to 50 lb/cu ft by manufacturing methods.

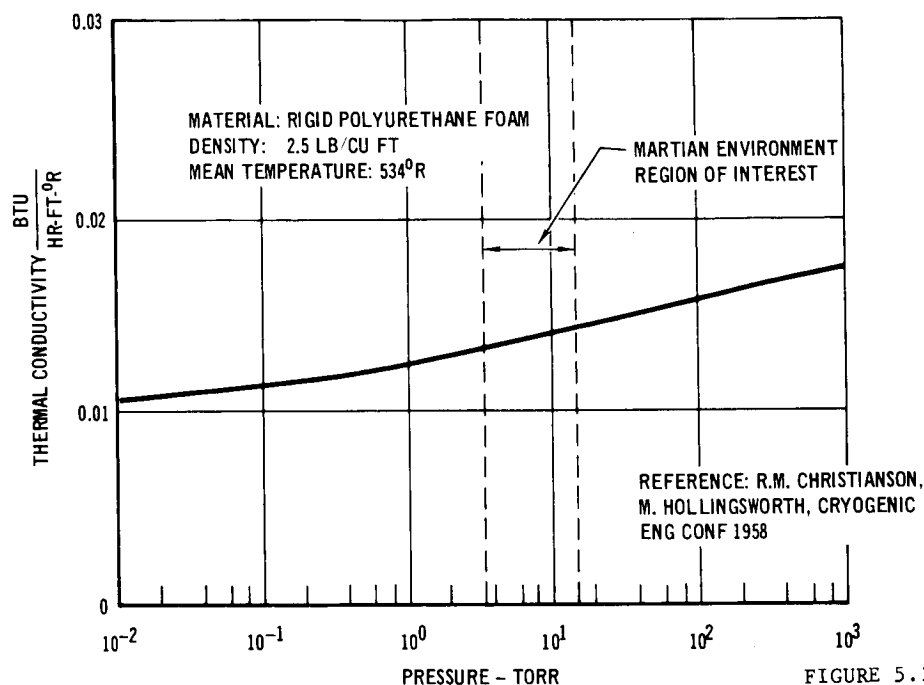
Figure 5.3-4 shows experimental thermal conductivity data for three different sizes of fiber diameter. These samples had a packed density of approximately 4 lb/cu ft and were heat felted. The curves represent the thermal conductivity as a function of pressure for typical fibrous insulation.

The effect of density on performance is an important parameter for this material. Increasing the density of a fibrous insulation batt from a very small value generally decreases its conductivity. Beyond a certain density however, the conductivity increases because of the increased contribution of solid conduction. Identification of the resulting minimum " $k\rho$ " value for Martian conditions was one of the objectives in the materials selection. Past experience has shown that fibrous batts should be contained by cloth "facings" to prevent material loss and thickness change during handling and installation. Designs that permit the insulation areas to be completely enclosed by structure can eliminate the need for facings, however, as was successfully demonstrated by the fiber-glass ISM evaluated in this study.

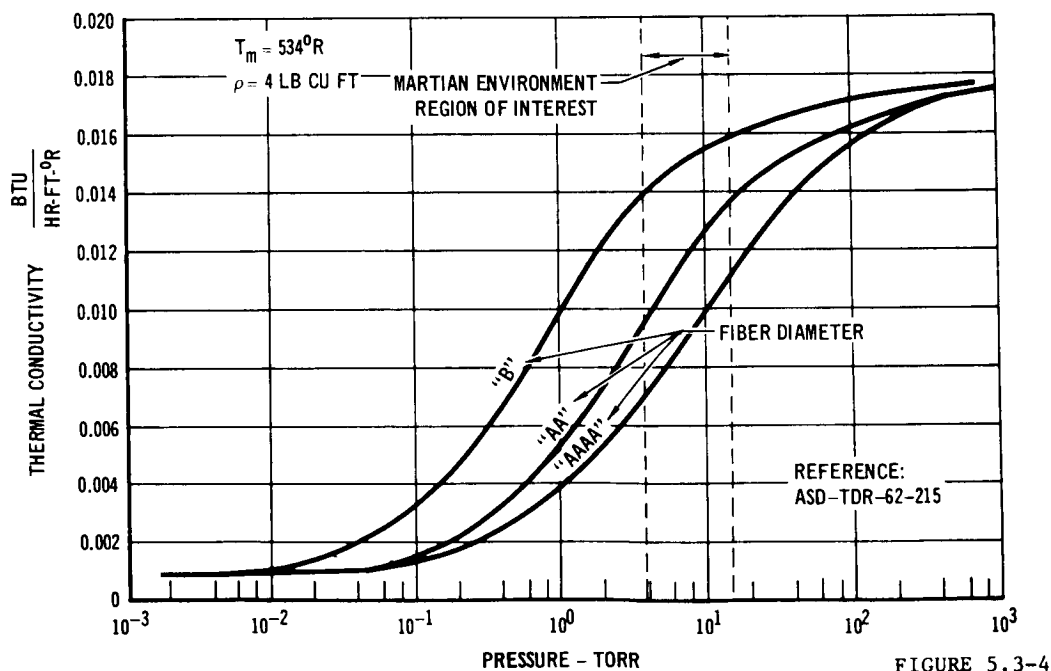
- o Powders - Powders were included as a class of materials for this program even though there are several factors which limit their use:
 - o Friability (high density compressed powders)
 - o Shifting under vibration and "g" loads
 - o Containment of fine powders necessary to prevent loss during vibration and "g" loads
 - o Weight
- o Compressed Powders - This type of insulation consists of non-metallic, inorganic particulate material, compressed into block form. Compressed powder insulations have been utilized in areas where volume was critical. They have also been used in ground storage tanks for liquid cryogenics. The low conductivity of this class of material is essentially due to the reduction of gaseous conduction and convection, since the distance between the particles is less than the mean free path of the residual gas. Opacifiers have also been used to reduce the radiant heat transfer.

In the Martian pressure region the thermal efficiency (" $k\rho$ ") of these materials appears to be comparable to that of multilayer insulation, although compressed powders such as Min K have a higher k .

EFFECT OF PRESSURE ON THERMAL CONDUCTIVITY OF FOAM



EFFECT OF PRESSURE ON THERMAL CONDUCTIVITY OF FIBERGLASS



In the block form, compressed powders (Min K specifically) have high load carrying capability (5% compression for a 195 psi load). Use of this material is definitely warranted in areas where a load bearing spacer is required. The design of such spacers, however, would account for the friability of the material, which does present some problem during manufacture and assembly. Adequate design is necessary to retain the material, including use of fine mesh screens and flexible blanket coverings.

- o Loose Powders - These materials are similar to the compressed materials, with the major distinction being reduced density. From a fabrication standpoint, they have advantages since odd shaped cavities can be easily insulated by a pouring operation. Their resistance to vibration and "g" loading is lower however, because of the lower density. Further, the containment problem is greater because of their fine particulate size. Careful installation design is necessary for these materials to provide proper venting, while insuring that the material does not "settle" or "pack."

5.3.2 Sample Selection - Table 5.3-1 lists the candidate materials selected for the overall program. The rationale for the selection of these materials is discussed in the succeeding paragraphs.

Sample Nos. 1-4 are unbonded fiberglass batt materials having a bulk density of 1.2 pcf. The variable for these samples is fiber diameter. By varying the fiber diameter, it was planned that insight would be learned as to the gaseous conduction and radiation effects. By keeping the bulk density constant and varying diameter, the total number of fibers increases (as diameter decreases) thereby reducing the effective distance between fibers and in essence reducing the mean free path for gaseous conduction. Similarly it was hoped to determine whether the fiber diameter change could affect the apparent opacity either by making the sample more homogeneous in structure (reducing the number of air gaps for radiation to pass through) or effectively increasing the number of refractive surfaces.

Fiberglass ("E" glass) was the fiber chemistry selected since previous data from numerous sources had already indicated that for the temperature region of interest, fiberglass had low conductivity and cost, and was readily available. The effects of Martian gas composition and pressure were not known.

Samples 5-7 were also unbonded fiberglass batt but they were all of the same fiber diameter (AAAA) with the variable being bulk density. The "AAAA" was picked since it had the smallest effective diameter. Density values ranged from 0.7 to 2.2 pcf. Literature data indicated that the lowest "k" material would fall in this density range. By this series of samples it was planned to confirm whether minimum "k" was in fact obtained. Increasing bulk density tends to reduce the radiation component of heat transfer as well as gaseous conduction. Increasing density also tends to increase solid conduction since the number of "point contacts" are increased.

CANDIDATE INSULATION MATERIAL SELECTION

SAMPLE NO.	NO. OF TEST SPECIMENS	MATERIAL CLASS	GENERAL TYPE	TEST DENSITY PCF	VENDOR DESIGNATION	EVALUATION PARAMETER
1	2	FIBERS	UNBONDED "A" FIBER	1.2	J-M MICRO-FIBERS WEB CODE 110 2.5 GMS/FT ²	FIBER DIAMETER
2	2		UNBONDED "AA" FIBER	1.2	J-M MICRO-FIBERS WEB CODE 108 1.5 GMS/FT ²	
3	2		UNBONDED "AAA" FIBER	1.2	J-M MICRO-FIBERS WEB CODE 106 1.8 GMS/FT ²	
4	2		UNBONDED "AAA" FIBER	1.2	J-M MICRO-FIBERS WEB CODE 104 1.6 GMS/FT ²	
5	2		UNBONDED "AAAA" FIBER	0.7	J-M MICRO-FIBERS WEB CODE 104 1.6 GMS/FT ²	DENSITY
6	2		UNBONDED "AAAA" FIBER	2.2	J-M MICRO-FIBERS WEB CODE 104 1.6 GMS/FT ²	
7	2		UNBONDED "AAAA" FIBER	1.7	J-M MICRO-FIBERS WEB CODE 104 1.6 GMS/FT ²	

CONTINUED

TABLE 5.3-1

CANDIDATE INSULATION MATERIAL SELECTION (Continued)

SAMPLE NO.	NO. OF TEST SPECIMENS	MATERIAL CLASS	GENERAL TYPE	TEST DENSITY PCF	VENDOR DESIGNATION	EVALUATION PARAMETER
8	2	FIBERS (CONT.)	SILICONE BONDED "AA"	1.2	J-M MICROLITE	VARIATIONS IN BINDER CHEMISTRY FROM VENDORS
9	2		SILICONE BONDED "AA"	1.2	HITCO TG 15000	
10	1		PHENOLIC BONDED "AA"	1.2	J-M MICROLITE	VENDOR AND BINDER VARIATIONS
11	1		PHENOLIC BONDED "AA"	1.2	HITCO TG 3000	
12	2	FOAMS	CLOSED CELL ISOCYANURATE	2.0	UPJOHN CO. HTF-200	BASIC CHEMISTRY DIFFERENCES
13	2		CLOSED CELL POLYPHENYLENE OXIDE	2.0	GE POLYPHENYLENE OXIDE FOAM	
14	2		CLOSED CELL POLYURETHANE	2.0	UPJOHN CO. CPR 385 D	
15	2		CLOSED CELL POLYURETHANE	2.0	DIAMOND SHAMROCK G 302	VENDOR CHEMISTRY FOR SAME GENERIC TYPE
16	2		CLOSED CELL POLYURETHANE	2.0	STAFOAM AA 1802	
17	1		FLEXIBLE OPEN CELL POLY-URETHANE	2.0	SCOTT FOAM 80 CELLS/IN.	
18	2		FLEXIBLE OPEN CELL POLY-URETHANE	2.0	SCOTT FOAM 60 CELLS/IN.	EFFECTIVE PORE SIZE
19	2		FLEXIBLE OPEN CELL POLY-URETHANE	2.0	SCOTT FOAM 45 CELLS/IN.	

CONTINUED

TABLE 5.3-1 CONTINUED

CANDIDATE INSULATION MATERIAL SELECTION (Continued)

SAMPLE NO.	NO. OF TEST SPECIMENS	MATERIAL CLASS	GENERAL TYPE	TEST DENSITY PCF	VENDOR DESIGNATION	EVALUATION PARAMETER
20	2	POWDERS	COLLOIDAL ALUMINA	4.0	GODFREY CABOT ALON-C .01-.04 MICRON	PARTICLE CHEMISTRY
21	2		COLLOIDAL SILICA	4.0	GODFREY CABOT CAB-0-SIL H-5 .01-.02 MICRON	
22	2	MULTI-LAYERS	GOLD ON KAPTON (CRINKLED)	2.4	JPL FURNISHED GOLD ON 1/2 MIL KAPTON 40 LAYERS/IN.	LAYER DENSITY
23	2		GOLD ON KAPTON (CRINKLED)	3.6	JPL FURNISHED GOLD ON 1/2 MIL KAPTON 60 LAYERS/IN.	
24	2		GOLD ON KAPTON (CRINKLED)	4.9	JPL FURNISHED GOLD ON 1/2 MIL KAPTON 80 LAYERS/IN.	
25	2		GOLD ON KAPTON WITH "AA" FIBER-GLASS SEPARATOR (UNCRINKLED)	1.3	JPL FURNISHED GOLD ON KAPTON AND J-M MICRO-FIBERS WEB ($\rho = 1.2$ PCF) CODE 108 (1/2 IN. THICK)	SPACER THICKNESS
26	2		GOLD ON KAPTON WITH "AA" FIBER-GLASS SEPARATOR (UNCRINKLED)	1.3	JPL FURNISHED GOLD ON KAPTON AND J-M MICRO-FIBERS WEB ($\rho = 1.2$ PCF) CODE 108 (1 IN. THICK)	
50 SPECIMENS TOTAL						

TABLE 5.3-1 CONTINUED

Samples 8 and 9 are similar to sample 2, the only difference being that samples 8 and 9 have a silicone bonding agent to hold the "AA" fibers together. AAAA fibers were not used for this variable study because they were unavailable commercially in the bonded form. Selection of a bonded fiberglass would permit determination of the ability to reduce radiation by increasing the apparent opacity. To be traded off against reduced radiation is the increased solid conduction due to the fibers now being bonded together rather than just in point contact. Silicone bonded materials from two sources were tested to determine the variation of binder chemistry as obtained from different suppliers.

The rationale for samples 10 and 11 is identical to that for 8 and 9 except the binder is phenolic instead of silicone. This series of materials would compare the effect of binder chemistry on reducing the radiation component of heat transfer.

Samples No. 12-16 were all organic foams selected to determine the effect of basic foam chemistry (samples 12 - 14) and differences that might exist for the same chemistry but with formulation variations from different sources. With the exception of the polyphenylene oxide foam, all of these foams were "Freon blown" materials. Since the conductivity of the Freon gas is lower than that of air, the effective gas conduction component should also be less.

Samples 17, 18, and 19 are also organic foam materials. They differ from the other foam materials not only in chemistry but they are flexible, whereas samples 12-16 are all rigid. Bulk density of this series of samples was essentially constant with the only variable being effective cell size. These samples were included to determine the optimum cell size for minimum overall conductivity.

Samples 20 and 21 consisted of two representative loose powders. Differences in the two were basic chemistry and particle size. It was realized that opacified powders may have lower conductivity than those tested, but rather than attempt to optimize, comparison of test data for these materials with the literature would reveal whether additional work including opacifiers was warranted.

The remainder of the samples, 22-26 were multilayer type, using goldized 1/2 mil Kapton. By concentrating on this material and then comparing to other literature values, an appraisal could be made of whether additional work with this class was warranted.

By their nature, being reflective lamina, multilayer materials very effectively reduce radiation. Reduction of the gaseous conduction mode would therefore yield a very efficient material. Samples 22-24 were therefore selected to evaluate the effect of layer density on gaseous conduction. Calculations indicated that for the expected pressure regime optimum layer densities should probably be greater than 80 layers/inch. However, these high test densities were not selected for testing since weight would become

excessive and solid conduction would begin to increase faster than gaseous conduction would be reduced.

The last two samples 25 and 26, consisted of a combination of fibrous material and the goldized Kapton multilayer. Since radiation is the largest contributor to overall heat transfer in fiberglass, it was reasoned that incorporation of radiation foils in a fibrous material would be beneficial. The fibers were AA unbonded having a bulk density of 1.2 pcf (similar to samples 2 and 8-11). Layers of goldized Kapton at two spacer thicknesses were included to determine whether the radiation component could be reduced.

6. INSULATION SYSTEM MODULE DESIGN

Methods were studied to best incorporate each of the four material classes into a suitable design which could be installed on the lander. Two basic design concepts were selected to be compatible with all candidate materials. One concept, for foam materials, used the rigidity of the foam, bonded into a structural sandwich, to stabilize the cover and casing of the ISM. The second concept had higher structure weight but allowed a loose lay-up of the other three candidate material classes, and provided controlled venting of the panel.

6.1 DESIGN OBJECTIVES - The major design objectives were to identify insulation installation methods which would provide maximum thermal protection of the lander equipment, and to assure that the insulation and surrounding structure would withstand the dynamic loads imposed during the mission. These two objectives are not necessarily compatible, i.e. selection of a minimum structure design would produce less heat losses and result in maximum thermal protection, but might not have sufficient strength to survive the shock and vibration loads. Other design objectives included minimum weight, reproducible performance, and compatibility with related systems. An overall system design approach was thus necessary to assure that the effects of all significant design implications were evaluated.

6.2 DESIGN REQUIREMENTS - The basic design parameters used for defining the ISMs are listed in Table 6.2-1. These parameters were derived from the environmental conditions selected in Section 4. To provide a design philosophy these requirements, plus the design objectives were developed into overall design implications as shown in Table 6.2-2. During the design studies, candidate ISM approaches were judged against these considerations.

6.3 DESIGN STUDIES - These studies were performed to identify means of installing the insulation on the lander. The entire lander equipment package (about 35 ft² was assumed) required insulation to protect it from the extremes of the Martian environment. The equipment package was assumed to be of sheet metal construction consisting of axial members and thin aluminum shear skins. The insulation would be attached to these aluminum shear skins.

6.3.1 Insulation Installation - One of the initial evaluations was to determine the merits of mounting the insulation either externally or internally to the structural shell, as depicted in Figure 6.3-1. The factors examined for this selection were as given in Table 6.2-2. Because of the penalties associated with the external insulation mounting, the internal mounting was deemed most practical. The poor characteristics of the external insulation approach due to lack of fastener access for panel removal was of major concern while the virtual elimination of insulation penetrations and the ease of mounting external equipment, were major considerations in selecting the internal insulation approach. Possible contamination of the lander interior due to vented gas or material particles during launch and long term vacuum outgassing dictated that a barrier be provided on the inner surface of the

INSULATION SYSTEM MODULE - DESIGN PARAMETERS

REQUIREMENT	TEMPERATURE	PRESSURE	GAS COMPOSITION	COMMENTS
HEAT STERILIZATION	275°F	SLIGHTLY ABOVE ATM.	DRY NITROGEN	-
LAUNCH VIBRATION	AMBIENT (70°F)	AMBIENT	AMBIENT	OVERALL ACCELERATION 16.1 g _{rms}
LANDING SHOCK	AMBIENT (70°F)	AMBIENT	AMBIENT	SOFT LANDING LEVEL 120G, 12.8 MSEC
VENTING	AMBIENT (70°F)	LAUNCH PROFILE	AMBIENT	STATIC (AMBIENT) TO .0001 LB/FT ² WITHIN 255 SEC
ACOUSTIC NOISE	N.A. - PROPOSED APPLICATION UNDER DOUBLE SHROUD AT LAUNCH - ENTRY AND LANDING ACOUSTIC NEGLIGIBLE COMPARED TO VIBRATION			

TABLE 6.2-1

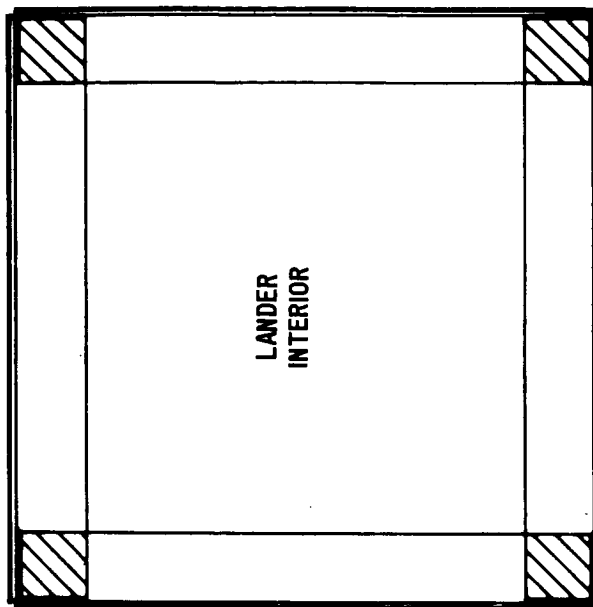
MAJOR DESIGN CONSIDERATIONS FOR LANDER INSULATION INSTALLATION

OBJECTIVES	CRITERIA	DESIGN IMPLICATIONS
MINIMIZE HEAT LOSSES	VENTING STRUCTURE PENETRATIONS	AVOID DAMAGE TO PACKAGE AND LOSS OF INSULATION COMPATIBILITY WITH ATTACHMENT DESIGN, THERMAL COATINGS, AND LOW CONDUCTIVITY MATERIALS ISOLATE COMPONENTS AND USE RADIATION BARRIERS AND LONG CONDUCTION PATHS
MINIMIZE WEIGHT	SURFACE AREA	DESIGN EQUIPMENT PACKAGE WITH MINIMUM SURFACE AREA
PROVIDE REPRO- DUCIBLE PER- FORMANCE	ATTACHMENT DYNAMIC LOADING MANUFACTUR- ING HANDLING STERILIZATION ENVIRONMENT	AVOID COMPRESSION AND PACKING OF INSULATION DURING OPERATIONAL LOADS. USE REPRODUCIBLE CONFIGURATIONS, STANDARDIZE GEOMETRY WHERE POSSIBLE MINIMIZE POTENTIAL DAMAGE AND CONTAMINATION MODES ASSURE COMPATIBILITY PROTECT INSULATION FROM WIND BLOWN SAND AND DUST
ASSURE COMPATIBILITY WITH RELATED SYSTEMS		MINIMIZE HEAT LOSS FROM WIRE BUNDLES AND SCIENCE OPENINGS. AVOID EQUIPMENT CONTAMINATION. PROVIDE EQUIPMENT ACCESS.

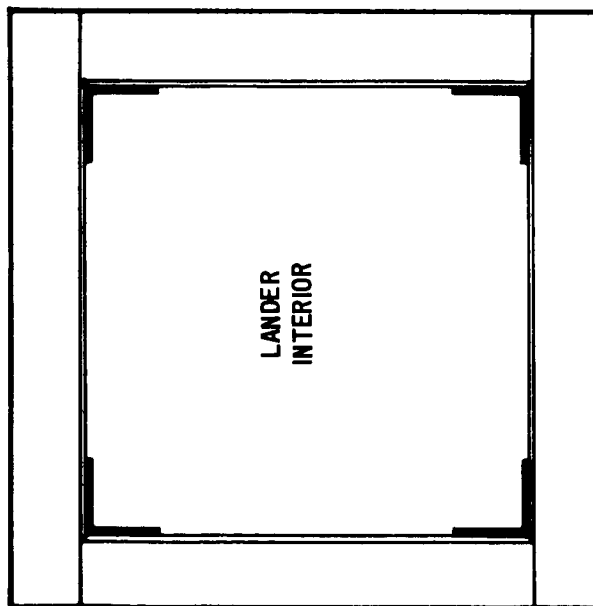
TABLE 6.2-2

INITIAL INSULATION INSTALLATION TRADE-OFF

INSULATION INSTALLED
INSIDE STRUCTURE



INSULATION INSTALLED
OUTSIDE STRUCTURE



CONCLUSIONS:

- INSULATION INSTALLED INSIDE STRUCTURE GIVES BEST ACCESS TO EQUIPMENT AND EXTERNAL HARD POINTS WITH LEAST DAMAGE POTENTIAL.
- INTERNAL COVER REQUIRED TO AVOID OUT-GASSING AND MATERIAL LOSS TO LANDER INTERIOR.

FIGURE 6.3-1

insulation. Final choice between a flexible Mylar package and a rigid fiberglass shell was made by considering loading factors. Specifically it was believed that the dynamic environments might allow a flexible package and the insulation inside, to distort, resulting in a change in thermal performance of the system. Because of this factor it was decided to use a hard backed container of locally reinforced, phenolic laminate fiberglass. The fiberglass was chosen over aluminum due to its lower thermal conductivity.

Various methods were considered for packaging and attaching the insulation to the shear panels. As shown in Figures 6.3-2 and 6.3-3, each approach has certain limitations which determine its usefulness with particular materials. Several of these approaches proved to be undesirable because they resulted in direct heat shorts or loss of material during launch venting. The investigation indicated that foams, fibers, and multilayer insulation could be installed by conventional installation methods. The powders, however, require careful attention. Because powders have a tendency to settle, they must be packaged by placing the fiberglass casing on a shaker platform and vibrating the unit until the required material density is obtained. Once the powder is installed and the assembly sealed, there is no assurance that launch vibrations will not further compress the powder to a degree that severely penalizes thermal performance. Besides settling problem, material handling and fabrication characteristics make the powders a difficult material for producing a satisfactory unit.

6.3.2 Heat Transfer Effects - Heat loss from fin effects in the fiberglass laminate have small effect on overall panel heat loss except for very low thermal conductivity insulations as shown in Figure 6.3-4. These curves are for typical convection heat transfer coefficient values of 0.5 and 0.1 BTU/hr ft²°F corresponding to Figure 4.1-11, and predicted test chamber conditions, respectively. The uncertainty range (shaded) for each panel type differs according to the fiberglass laminate thickness for each configuration and the assumed fin effectiveness for heat loss at the cold surface of the panel. The uncertainty range shown in Figure 6.3-4 is for 0 to 100% fin effectiveness on the exterior surface.

Convection effects are negligible for low conductivity, thick insulation, but become increasing important as thinner, more conductive insulation is used. If edge effects are neglected, the predicted heat loss from the panels, Figure 6.3-5, is affected by convection on the exterior surface, and insulation conductivity and thickness, for fixed boundary temperatures. In the convection coefficient range of 0 to 0.5 BTU/hr ft²°F convection can significantly affect performance of some insulation configurations.

6.4 INSULATION SYSTEM MODULE DEFINITIONS - Two basic ISM design concepts (Figure 6.4-1) were established. The first ISM design, designated 474-00-001, is for foams; the second unit, 474-00-002, can incorporate fibers, multilayer, or powders. The foam would be cut and bonded into the casing. All other candidates would be packed into their casings and the covers then bonded in

APPLICABLE INSULATION ATTACHMENT METHODS


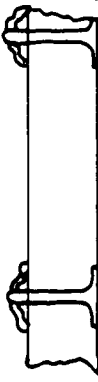
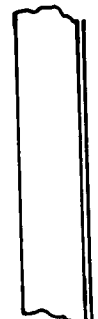


ATTACHMENT METHODS	INSULATION MATERIAL	LIMITATIONS	ATTACHMENT METHODS	INSULATION MATERIAL	LIMITATIONS
<p>A. VELCRO</p> 	<p>FIBERS FOAMS POWDERS MULTILAYER</p>	<p>DIFFICULT BLANKET REMOVAL WITHOUT INSULATION DAMAGE. REMOVAL WOULD DESTROY RIGID INSULATION. DIFFICULT BLANKET REMOVAL WITHOUT INSULATION DAMAGE. DIFFICULT BLANKET REMOVAL WITHOUT INSULATION DAMAGE</p>	<p>D. POST AND RETAINER WASHER</p> 	<p>FIBERS FOAMS POWDERS MULTILAYER</p>	<p>ALIGNMENT INCREASES POSSIBILITY OF DAMAGE DURING HANDLING, INSTALLATION, AND REMOVAL. INCREASED HEAT TRANSFER. DIFFICULT TO RETAIN INSULATION.</p>
<p>B. BONDED</p> 	<p>FIBERS FOAM POWDERS MULTILAYER</p>	<p>REMOVAL WOULD DESTROY FACING. REMOVAL WOULD DESTROY INSULATION. REMOVAL WOULD DESTROY BLANKETS. REMOVAL WOULD DESTROY FACING.</p>	<p>E. STEP STUDS - NYLON</p> 	<p>FIBERS FOAMS POWDERS MULTILAYER</p>	<p>DIFFICULTY IN ALIGNMENT. INCREASED HEAT TRANSFER. DIFFICULT TO RETAIN.</p>
<p>C. BUTTONS AND THREAD</p> 	<p>FIBERS FOAMS POWDERS MULTILAYER</p>	<p>LOAD AND VIBRATION, ENVIRONMENT LIMITATIONS. DIFFICULT TO RETAIN INSULATION.</p>			

FIGURE 6.3-2

APPLICABLE INSULATION PACKAGING METHODS


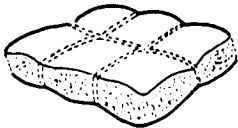


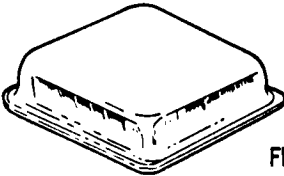
INSULATION MATERIAL	CANDIDATE PACKAGING METHODS		COMMENTS
	1. TUFTED BLANKETS	(ATTACHMENT METHOD)	CONTROL OF VENTED GASES AND LOOSE MATERIAL NOT POSSIBLE.
		VELCRO BONDED BUTTONS & THREAD POST & RETAINER WASHER STEP STUDS - NYLON	
	2. QUILTED BLANKETS	VELCRO BONDED BUTTONS & THREAD POST & RETAINER WASHER STEP STUDS - NYLON	
	3. NO COVERING	BONDED BUTTONS & THREAD POST & RETAINER WASHER STEP STUDS - NYLON	
 MYLAR FILM	4. FLEXIBLE PACKAGE	VELCRO BONDED BUTTONS & THREAD POST & RETAINER WASHER STEP STUDS - NYLON	
 FIBER GLASS	5. RIGID PACKAGE	VELCRO BONDED POST & RETAINER WASHER STEP STUDS - NYLON	POSITIVE CONTROL OF VENT GASES AND MATERIAL. ASSURED STRUCTURAL INTEGRITY FOR MISSION ENVIRONMENTS.

FIGURE 6.3-3

COMPARISON OF INSULATION PANEL EDGE LOSSES
18 x 18 x 3 IN. THICK PANELS
INSIDE TEMPERATURE: 0°F

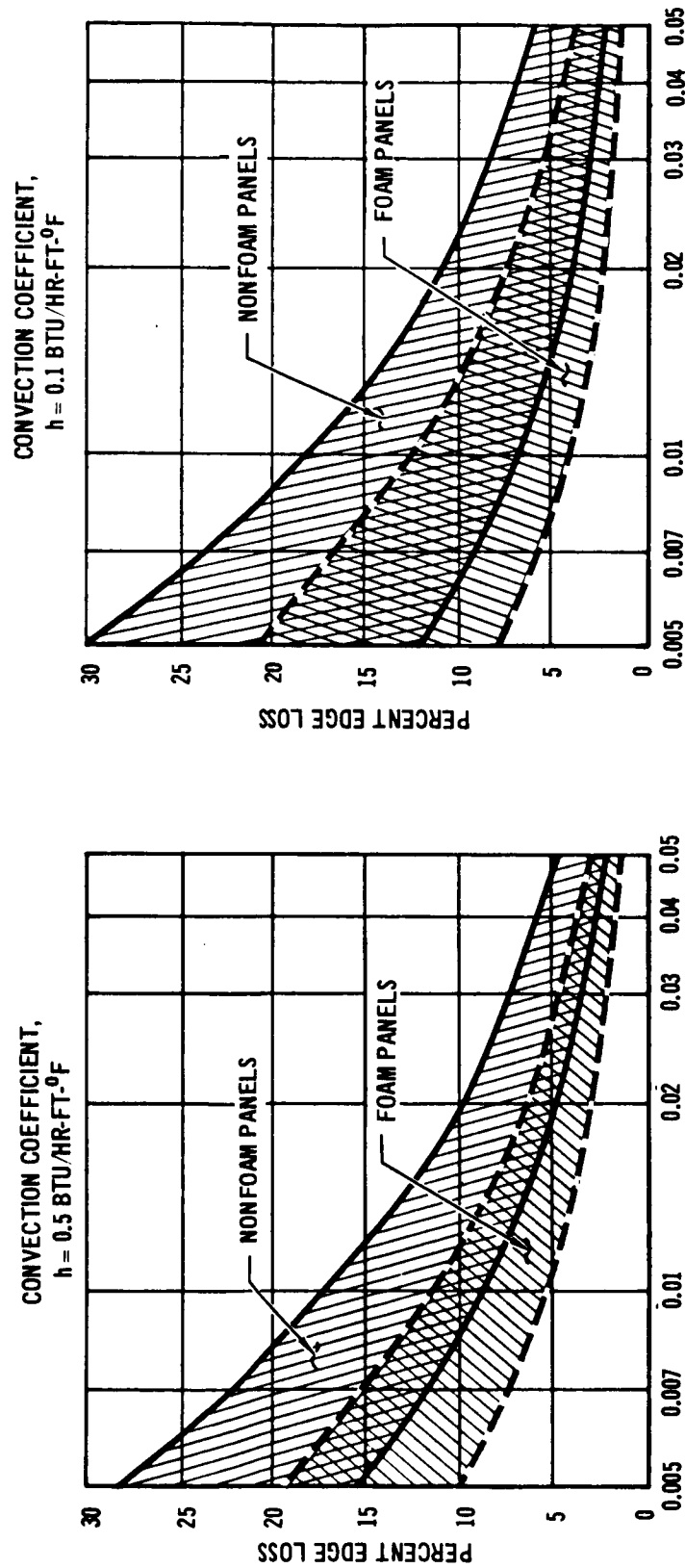


FIGURE 6.3-4

Thermal Conductivity of Insulation - BTU/HR-FT²-F

CONVECTION EFFECT ON INSULATION HEAT LOSS

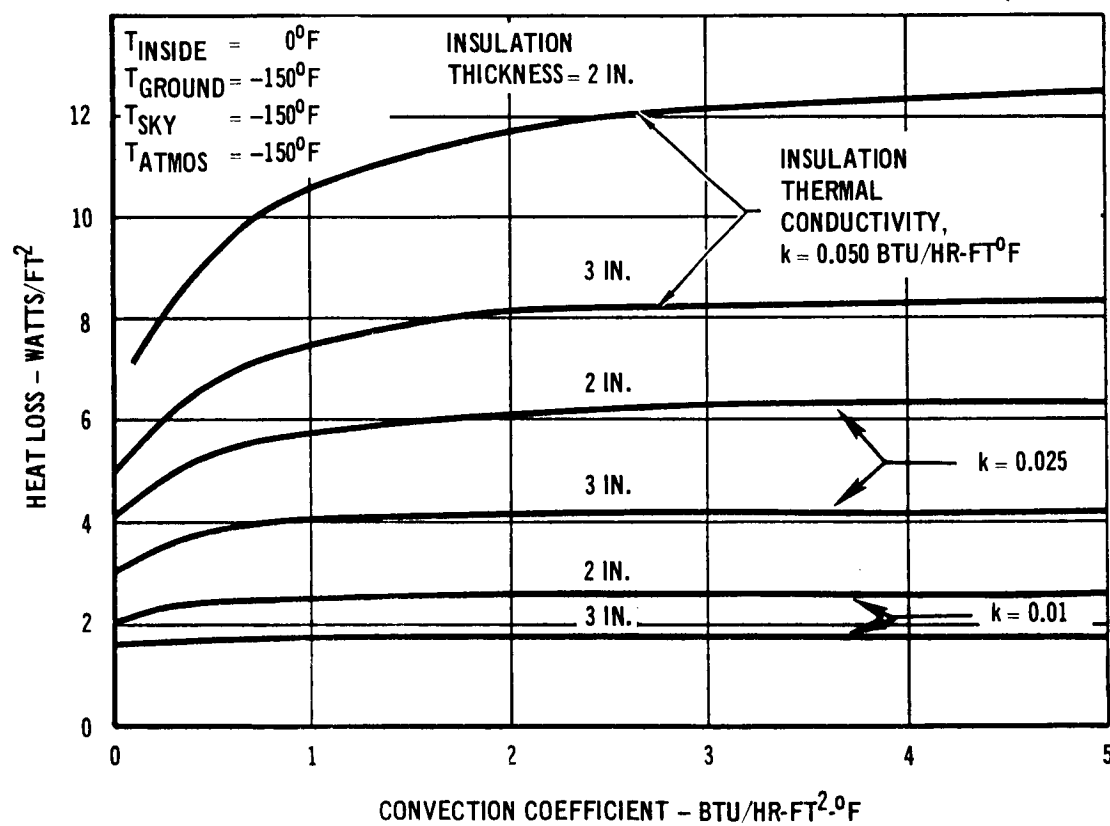


FIGURE 6.3-5

ISM DESIGN CONCEPTS

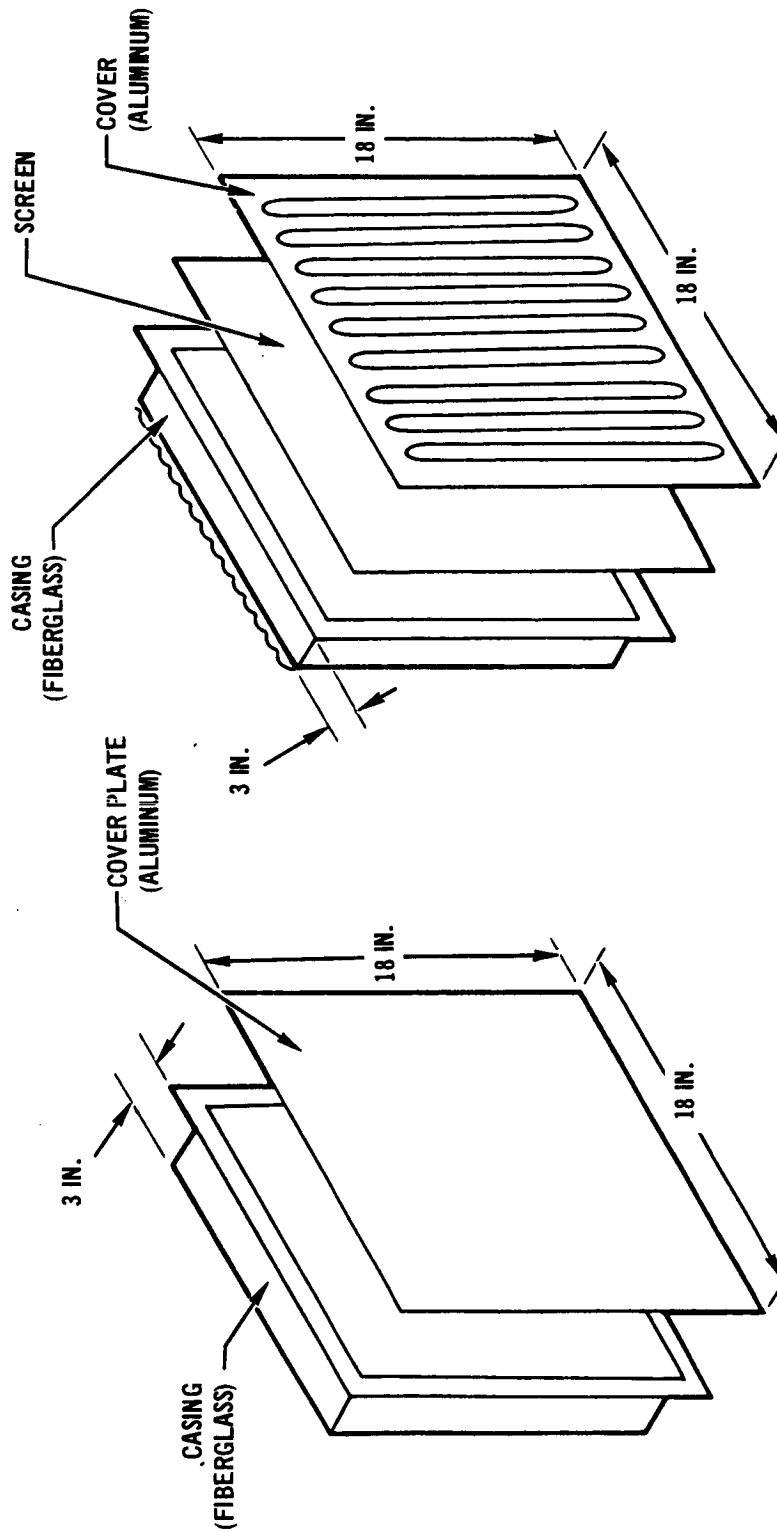


FIGURE 6.4-1

FIBER, MULTILAYER AND
COMPRESSED POWDERS CONCEPT
474-00-0002

CASING: 0.040 IN. PHENOLIC FIBERGLASS LAMINATE,
(4 PLYS)
COVER: 0.032 IN. 2024-T3 ALCLAD ALUMINUM
SCREEN: 400 MESH, 0.0010 DIA SS WIRE

FOAM CONCEPT
474-00-0001

MATERIALS

CASING: 0.012 IN. PHENOLIC FIBERGLASS LAMINATE,
(3 PLYS) REINFORCED TO 0.024 (6 PLYS) ON
EDGES AND CORNERS
COVER: 0.012 IN. 2024-T3 ALCLAD ALUMINUM

place. With the foams a smooth, thin casing and cover were employed to form a bonded sandwich structure having the lightest unit weight. The other ISM had corrugations on the casing and beads on the outer skin to provide the necessary stiffness characteristics. Installation of the ISM on the lander would be by mechanical attachment with conventional fasteners. The cover sheet for the fibers, multilayers and powders is beaded for increased rigidity, to allow use of thinner gauge material, and to permit void areas within the unit for collection of internal gases. Each bead has four 1/8 inch holes to allow for outgassing and ingassing during launch and entry phases. The hole size was established to allow sufficient area for gas passage, even with limited clogged openings, without a pressure build-up that could burst the assembly. In the second concept screens were provided to retain the insulation materials from blocking the vent holes in the cover. A 400 mesh, .0010 inch diameter stainless steel wire screen was chosen since it provided the acceptable holding action with low weight penalty.

The case of both assemblies was phenolic laminated fiberglass. Phenolic fiberglass is generally free from outgassing after adequate curing, provides good fabrication and dimensional control, and is easily procured at nominal cost. The laminated fiberglass can withstand sterilization temperatures and retains structural strength when exposed to long periods in free space. Corrugations on the back side of the second concept increase the strength while presenting no particular manufacturing problem. Fabrication details as well as design drawings for the two ISMs actually built are presented in Section 8.3.

A predicted weight comparison and breakdown of the two concepts is shown in Tables 6.4-1 and 6.4-2. The structure weight for the two panel assemblies vary greatly. For the foams structure weight is about 60% of that structure for the fibers, multilayer and compressed powders. The primary difference between the two is the thinner gauge materials allowable in the foam stiffened sandwich structure. This initial weight comparison for equal insulation thickness of 3 inches shows that two candidates, foams and fibers, are preferred for this thickness. Multilayer insulation are competitive if the lowest density material were used. The compressed powders are heavy when packed to their desired densities. It should be noted that this initial comparison does not account for differences in thermal conductivity of the materials but does allow weight comparison for fixed thickness. Final selection of materials to be fabricated into ISM panels was made after thermal conductivity data was obtained in the Thermal Diffusivity Test. The selections were then based on the weight required to obtain equal heat loss, as described in Section 8.2. Using the previously discussed constraints placed on the ISMs, these designs provided lightweight construction, simplicity of fabrication and acceptable characteristics for thermal control. The materials have low heat transfer characteristics where necessary, and can withstand heat sterilization and long periods at near vacuum condition without deterioration. The assemblies were designed for easy handling and installation, and would provide good equipment access. They are operable over large temperature extremes and pressure ranges, free from toxic and contaminate products, and are easily repaired.

INSULATION SYSTEM MODULE
WEIGHT COMPARISON FOR 3 IN. THICKNESS

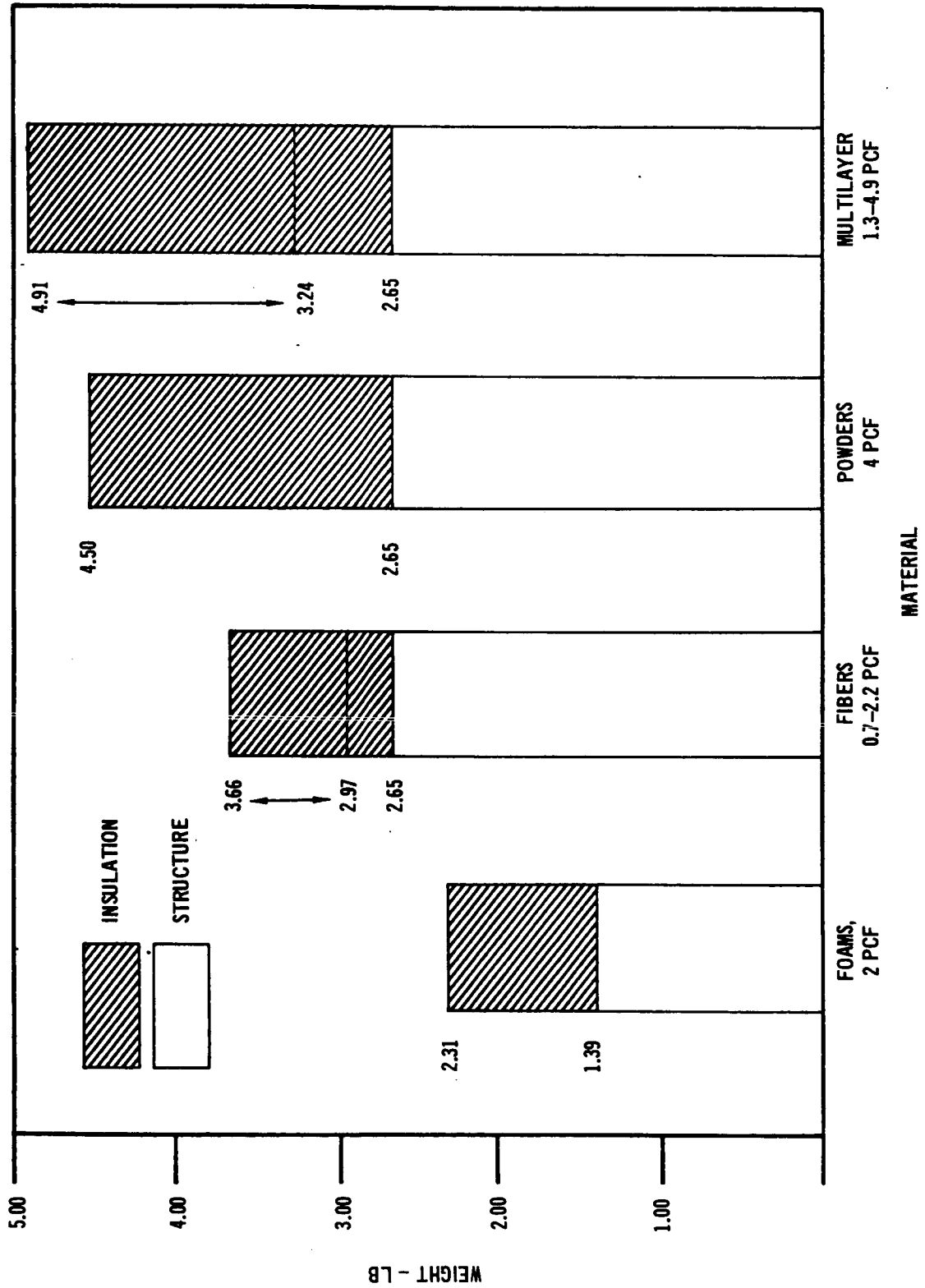


TABLE 6.4-1

ISM COMPONENT PART WEIGHT BREAKDOWN (PREDICTED)

ITEM/DRAWING NO.	WT. - LBS
<u>474-00-0001 PANEL (FOR FOAMS)</u>	
CASE	.68
COVER PLATE	.41
FILM BOND ADHESIVE	.30
TOTAL STRUCTURE	<u>1.39</u>
<u>474-00-0002 PANEL (FOR OTHER MATERIALS)</u>	
CASE	1.50
COVER PLATE	1.09
SCREEN	.06
TOTAL STRUCTURE	<u>2.65</u>
<u>INSULATION</u>	
FOAMS, $\rho = 2.0 \text{ LB/FT}^3$.92
FIBERS	
A. $\rho = .7 \text{ LB/FT}^3$.32
B. $\rho = 1.2 \text{ LB/FT}^3$.56
C. $\rho = 1.7 \text{ LB/FT}^3$.79
D. $\rho = 2.2 \text{ LB/FT}^3$	1.01
MULTI-LAYERS	
A. $\rho = 1.3 \text{ LB/FT}^3$.59
B. $\rho = 2.4 \text{ LB/FT}^3$	1.11
C. $\rho = 3.6 \text{ LB/FT}^3$	1.67
D. $\rho = 4.9 \text{ LB/FT}^3$	2.26
POWDERS, $\rho = 4.0 \text{ LB/FT}^3$	1.85

TABLE 6.4-2

7. CANDIDATE MATERIALS SCREENING TESTS

Two types of tests were conducted concurrently to rapidly identify the best two materials from the 26 candidates initially selected for consideration. Materials which probably would not pass heat sterilization were identified in the Heat Sterilization Screening Test. Thermal conductivity was derived from the Thermal Diffusivity Screening Test. This information, plus that developed in the design studies, Section 6, were integrated to identify the two best overall materials for incorporation into Insulation System Module test panels.

7.1 HEAT STERILIZATION SCREENING - The heat sterilization screening test was defined to provide a rapid means of verifying probable heat sterilization compatibility of materials. For those materials that failed the test, quantitative reasons for rejection were provided by the test data. As originally planned, three different tests were considered.

- a) Thermogravimetric Analysis (TGA), in which sample weight is continuously monitored during heatup to 235°C (455°F), at a preselected rate;
- b) Differential Thermal Analysis (DTA), in which temperature pulses denoting reactions are monitored during heatup, and
- c) Effluent Gas Analysis (EGA), in which the presence of an evolved gas is detected during heatup.

The peak temperature of 235°C was selected to identify those materials which have marginal temperature stability above the 135°C required in the actual heat sterilization. The excess temperature was also chosen to accelerate long term changes occurring during the 384 hours of actual heat sterilization.

7.1.1 Test Samples - A total of seven samples were subjected to the sterilization screening tests (Table 7.1-1). The seven materials consisted of two general types of foams and bonded fibers. Samples of either powders or multilayers were not included because their expected maximum temperature capability was well in excess of that required for heat sterilization. The samples were fabricated into small cylinders, each weighing approximately 100 mg for testing, as shown in Figure 7.1-1.

7.1.2 Test Apparatus - The primary piece of equipment employed for the sterilization screening tests was a Robert L. Stone Thermal Analysis apparatus with the following attachments:

- a) Thermogravimetric Analyzer - Model TGA-3A
- b) Differential Thermal Analyzer - Model KA-2HD
- c) Effluent Gas Analyzer - Model EG-E

Figure 7.1-2 shows the assembled apparatus.

STERILIZATION SCREENING TEST MATRIX
HEATING RATE - 5°C/MIN

MATERIAL	TGA	DTA	EGA
SILICONE BONDED "AA" FIBERS - JM	X	NO	NO
PHENOLIC BONDED "AA" FIBERS - JM	X	NO	NO
ISOCYANURATE FOAM - UPJOHN HTF-200	X	X	NO
POLYPHENYLENE OXIDE FOAM - GE PPO	X	X	NO
POLYURETHANE FOAM - UPJOHN CPR 385D	X	X	NO
POLYURETHANE FOAM - DIAMOND SHAMROCK G302	X	X	NO
POLYURETHANE FOAM - STAFORM AA 1802	X	X	NO

TABLE 7.1-1

THERMAL INSULATION MATERIAL BEFORE TGA

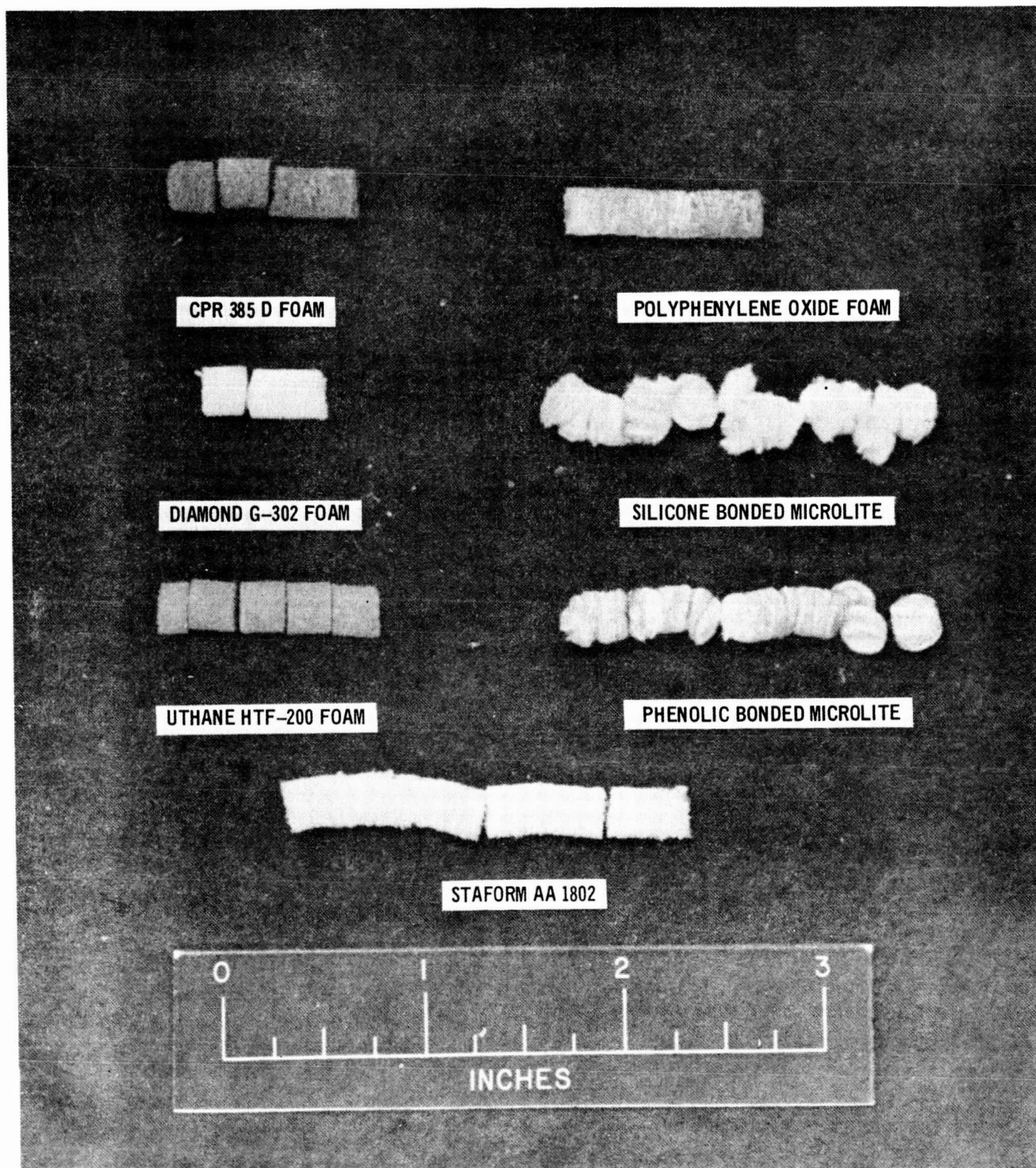


FIGURE 7.1-1

THERMAL ANALYSIS APPARATUS

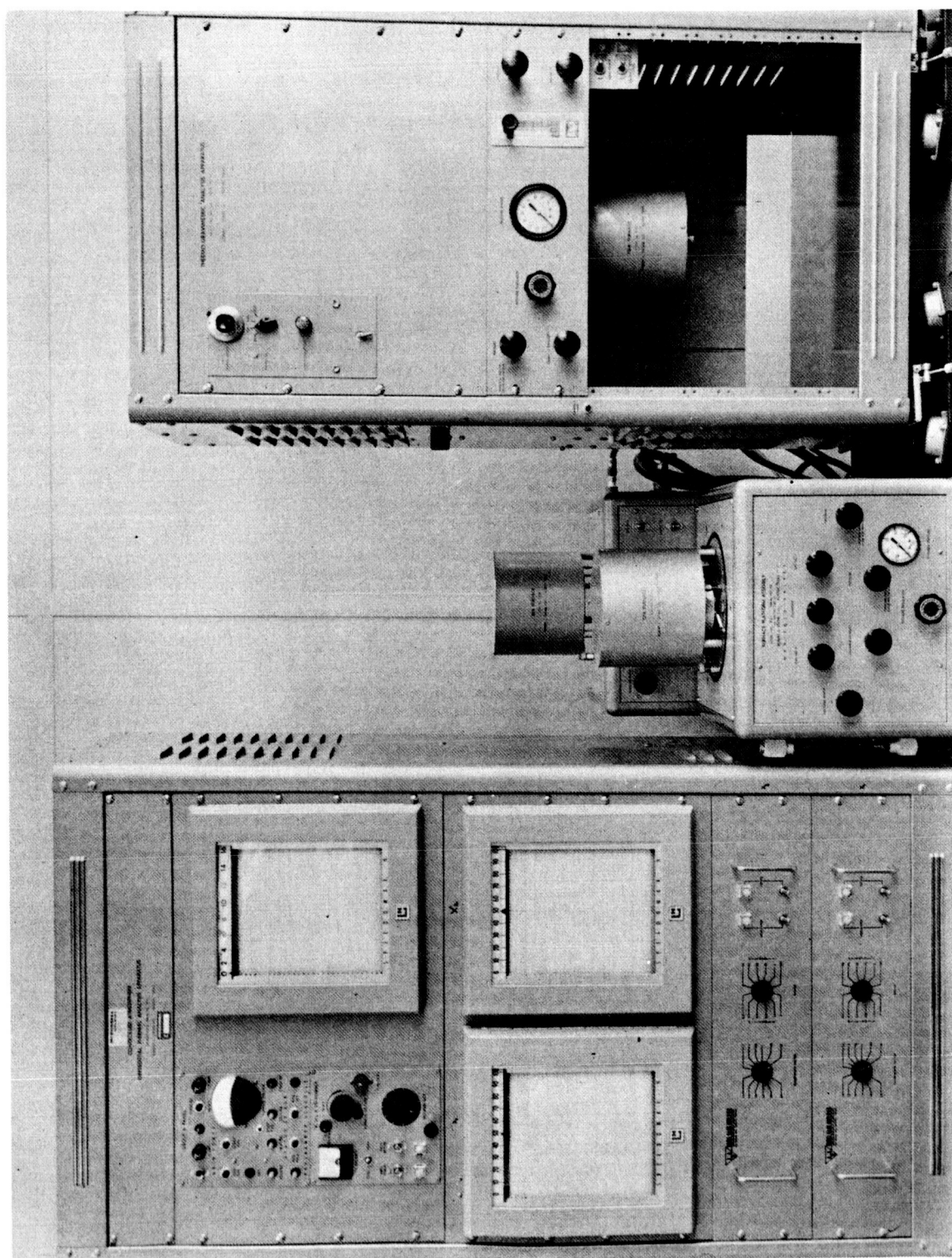


FIGURE 7.1-2

7.1.3 Test Description - Thermogravimetric Analysis (TGA) of the seven candidate materials was performed at a heating rate of 5°C/min. to a maximum temperature of 235°C. All tests were conducted in dry nitrogen atmosphere at ambient pressure. Three materials, Upjohn HTF-200 foam, Polyphenylene Oxide foam, and G 302 polyurethane foam were chosen to undergo Differential Thermal Analysis (DTA). The same heating sequence was used as with the TGA testing. No EGA (Effluent Gas Analysis) was performed since the DTA test detected no reactions during the heating period.

7.1.4 Test Results and Discussion - The samples are shown after TGA testing in Figure 7.1-3. Two materials - CPR 385 D foam and Stafoam AA 1802 - underwent weight loss in the TGA prior to reaching the specified heat sterilization temperature as shown in Table 7.1-2, Figures 7.1-4 and 7.1-5. In both cases, the weight loss was greater than 10% at 235°C. The Upjohn HTF-200 foam underwent initial weight loss at the sterilization temperature and this loss increased to 4.9% at 235°C. The other materials did not exhibit weight loss until 160°C or higher and their total weight loss was considerably lower than that of the three materials previously mentioned. The silicone bonded Microlite experienced the least amount of weight loss (0.3%) to 235°C and showed no visual signs of degradation. No shrinkage was observed with either the phenolic bonded Microlite or the silicone bonded Microlite. Some shrinkage was observed in all of the foam insulations. Of the foams, the G 302 polyurethane shrank the least amount.

The phenolic bonded fiberglass was deleted from further evaluation after the TGA test because it had higher weight loss during the test than the silicone bonded fiberglass. Although it had lower weight loss than the HTF-200 (refer to Table 7.1-2) it was not as acceptable as the silicone bonded material. Since the two bonded materials are similar in their thermal performance, the slight increase in cost for the silicone material would be more than offset by the increased confidence in its passing the heat sterilization cycle. The DTA test results indicated no reactions over the temperature range of interest.

7.1.5 Conclusions - Based on the testing completed under this phase, the materials listed in Table 7.1-3 were judged to be acceptable for further consideration. It should be emphasized that this testing was used strictly as a screening tool and did not verify that either the actual materials tested or the class of materials that they represented would pass the actual heat sterilization cycle.

7.2 THERMAL DIFFUSIVITY SCREENING TESTS - The purpose of this test was to rapidly obtain comparative thermal performance data on candidate insulation materials. The most accurate method of comparing materials would have been to determine the absolute thermal conductivity by one of the standard steady state techniques. To do so for each of the 26 candidate materials would have been both time consuming and expensive. Thus a transient heating technique was selected to reduce the number of candidate materials to a more manageable number yet allow confident selection of those materials which best fulfill the planetary mission objectives.

THERMAL INSULATION MATERIAL AFTER TGA

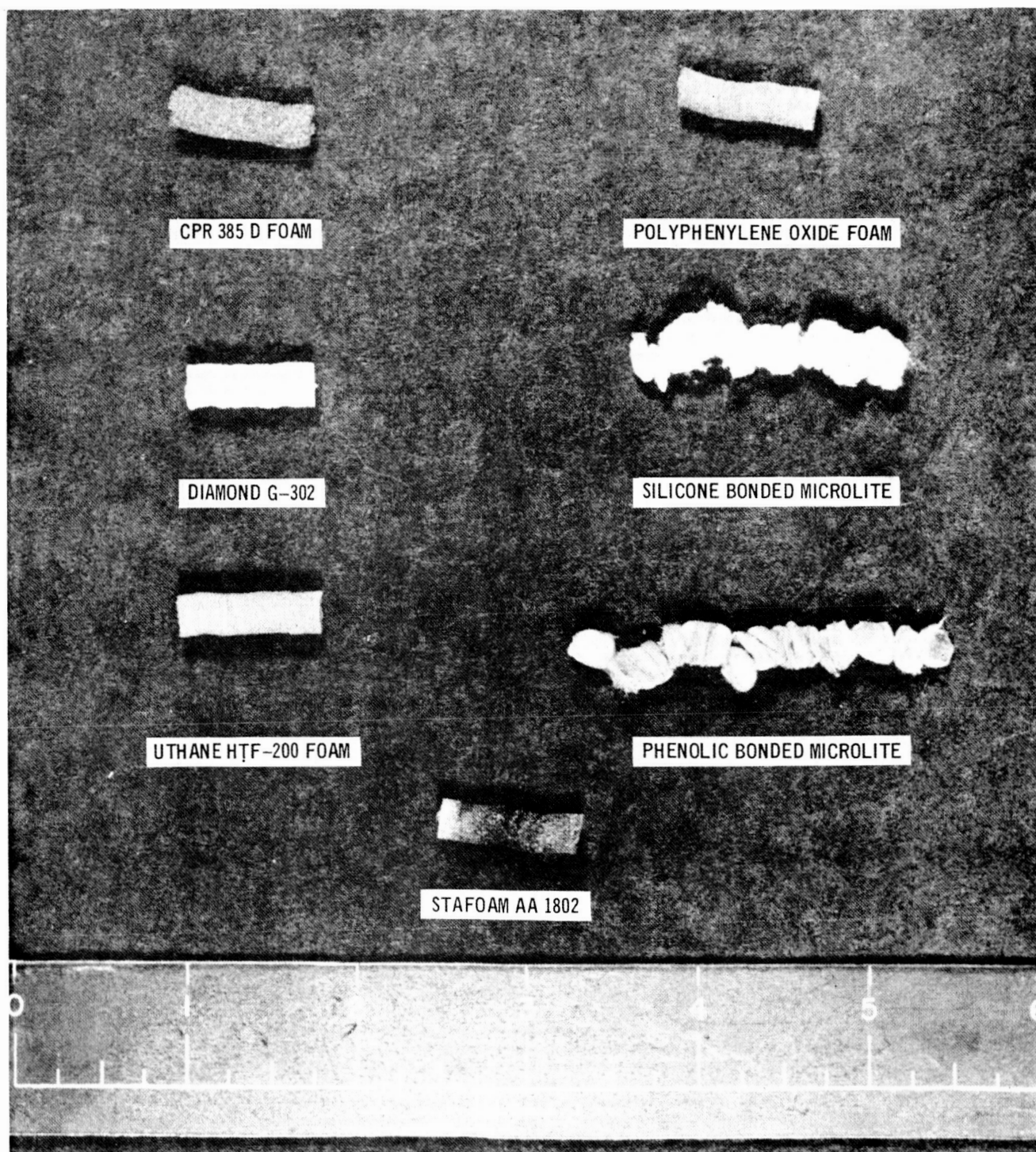


FIGURE 7.1-3

WEIGHT LOSS IN THE TGA TEST

MATERIAL	CUMULATIVE WEIGHT LOSS - %	
	135°C	235°C
1. SILICONE BONDED MICROLITE	0.0%	0.3%
2. PHENOLIC BONDED MICROLITE	0.0	2.2
3. UTHANE HTF-200 FOAM	0.0	4.9
4. POLYPHENYLENE OXIDE FOAM	0.0	1.2
5. CPR 385 D POLYURETHANE FOAM	0.4	10.8
6. G 302 POLYURETHANE FOAM	0.0	1.2
7. STAFOAM AA 1802	0.7	10.4

TABLE 7.1-2

MATERIALS CONSIDERED TO HAVE PASSED STERILIZATION SCREENING

MATERIAL	VENDOR
MICROLITE, SILICONE BONDED "AA" FIBERGLASS FIBERS	JOHNS -MANVILLE SALES CORP.
ISOCYANURATE FOAM UTHANE HTF-200, CLOSED CELL	THE UPJOHN COMPANY
POLYPHENYLENE OXIDE FOAM, CLOSED CELL	GENERAL ELECTRIC COMPANY
POLYURETHANE FOAM, G302, CLOSED CELL	DIAMOND SHAMROCK CHEMICAL COMPANY

TABLE 7.1-3

THERMOGRAVIMETRIC ANALYSIS RESULTS

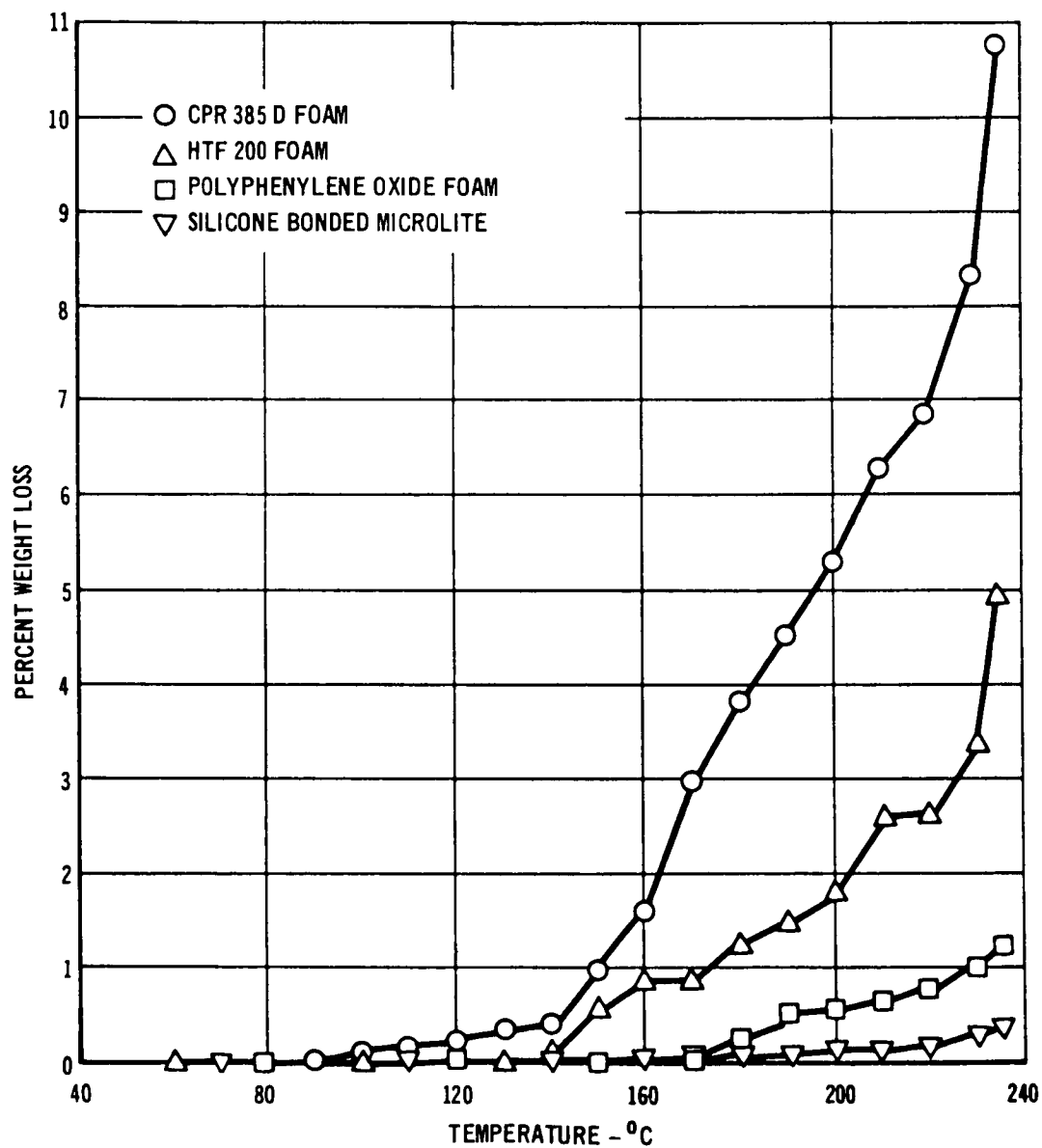


FIGURE 7.1-4

THERMOGRAVIMETRIC ANALYSIS RESULTS

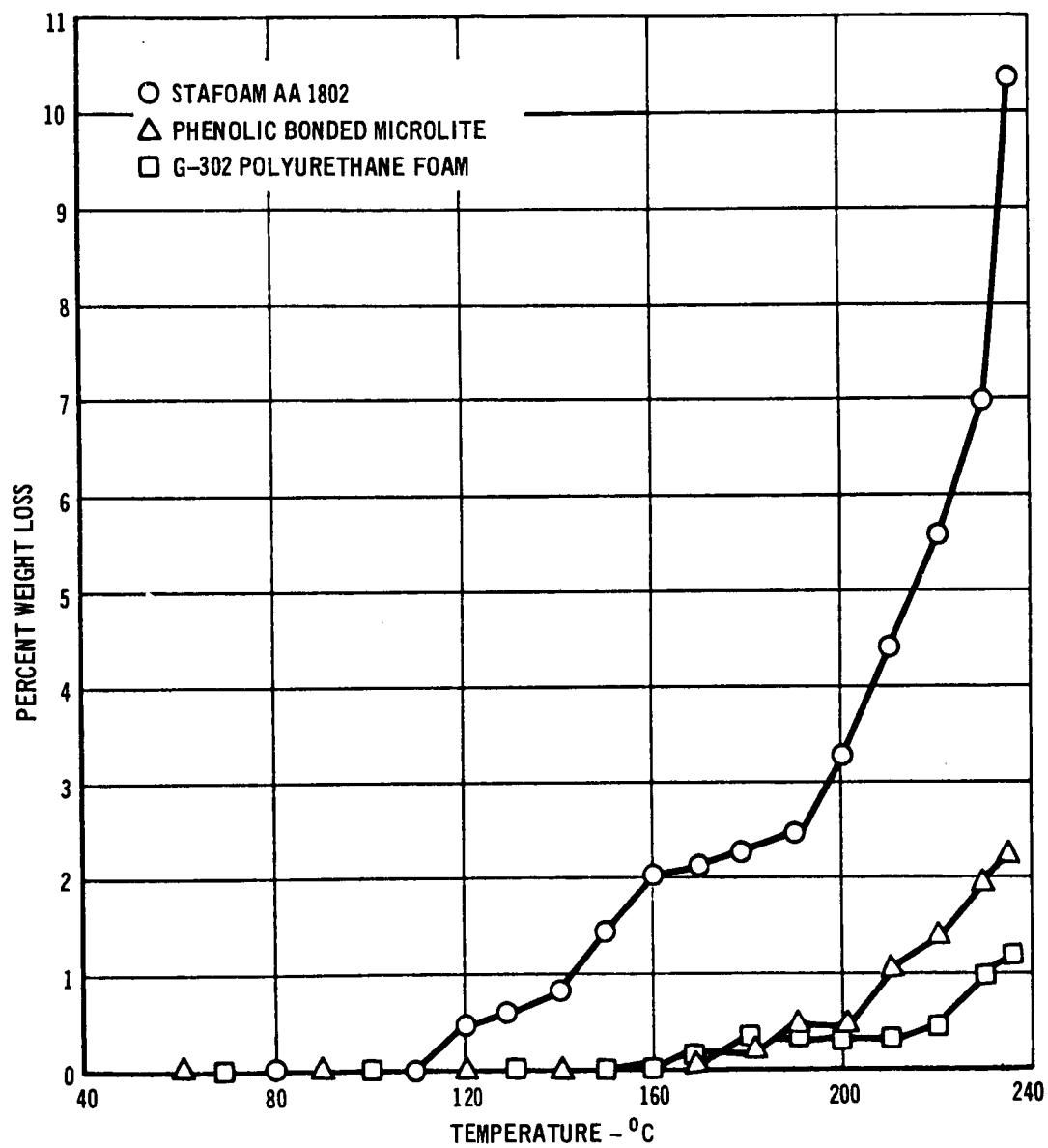


FIGURE 7.1-5

The test specimen size was determined such that the energy dissipated by a central heater was retained within the insulation during the heating period. Desired temperature rise of the heaters was selected to be 40-70°F. The basic objective of the test was to measure the temperature rise per unit heat input of a heater in the center of each specimen. From this data thermal conductivity could be derived.

Based on analysis which indicated that essentially all the heater energy would be contained within the samples, and that initial transients associated with heater mass would be damped out, a heating time of 12 minutes was selected for all samples.

This test was repeated to determine the effect of the heat sterilization cycle on both the primary and backup insulation materials. Since the same samples and apparatus were used for both diffusivity tests (before and after heat sterilization exposure), there was a high degree of confidence that this test would enable detection of possible heat sterilization effects.

7.2.1 Test Samples - The materials subjected to this test are delineated in Table 5.3-1. A total of 50 specimens from 26 different materials were tested in the first phase of the test. As shown in Table 5.3-1, only the bonded "AA" fiberglass samples were not tested in duplicate samples. Nine of the 12 materials subjected to heat sterilization, Table 7.2-1, were evaluated in the second test phase. Initial test densities of each thermal diffusivity sample are given in Table 7.2-2. Specimen size for the fibers, foam and multilayer material was a cube measuring 6" along each edge. The powder materials were placed in a standard one gallon can (diameter 6.45 inches). Each thermal diffusivity specimen, Figure 7.2-1, contained a centrally located thermofoil heater, 1 inch in diameter by 0.008 inch thick. Each heater was painted black and instrumented with a 40-gage chromel-constantan thermocouple. The specimens of fibers, foams, and multilayer material were covered with plastic film at the top and bottom to minimize convection during heating. A wire mesh box retained the specimens in a cube configuration for handling protection and density control.

The weight of each heater and the individual heater assembly components was determined to a) assure that the final mass was sufficiently low to exclude it from data reduction calculations and b) as a check for specimen assembly completeness.

Typical heater assembly weights were as follows:

<u>Item</u>	<u>Weight (mg)</u>
Heater	161.0
Thermocouple	53.5
Power Lead	330.0
Solder	8.5
High emittance paint	16.0
Total Assembly	569.0

HEAT STERILIZED SPECIMENS FOR REPEAT
THERMAL DIFFUSIVITY TEST

SAMPLE NUMBER	GENERAL DESCRIPTION
3A	JOHNS-MANVILLE UNBONDED "AAA", CODE 106
4B	JOHNS-MANVILLE UNBONDED "AAAA", CODE 104
8A	JOHNS-MANVILLE SILICONE BONDED "AA"
9A	HITCO SILICONE BONDED "AA" TG 15000
10A	JOHNS-MANVILLE PHENOLIC BONDED "AA"
12A	UPJOHN CO. HTF-200 FOAM
12B	UPJOHN CO. HTF-200 FOAM
13A	GE POLYPHENYLENE OXIDE FOAM
21A	GODFREY CABOT CAB-O-SIL H-5 COLLOIDAL SILICA POWDER

TABLE 7.2-1

DENSITY OF THERMAL DIFFUSIVITY SPECIMENS

SAMPLE NUMBER	DENSITY LB/FT ³	SAMPLE NUMBER	DENSITY LB/FT ³
1A	1.20	15A	2.41
1B	1.20	15B	2.28
2A	1.20	16A	2.13
2B	1.20	16B	2.14
3A	1.20	17A	1.90
3B	1.20	17B	1.88
4A	1.20	18A	1.80
4B	1.20	18B	1.83
5A	0.70	19A	1.83
5B	0.70	19B	1.81
6A	2.20	20A	3.74
6B	2.20	20B	3.54
7A	1.70	21A	3.15
7B	1.70	21B	3.14
8A	1.10	22A	2.12
8B	1.05	22B	2.13
9A	1.35	23A	3.18
9B	1.34	23B	3.19
10A	1.12	24A	4.25
11A	1.42	24B	4.26
12A	2.03	25A	1.30
12B	2.05	25B	1.30
13A	2.27	26A	1.26
13B	2.63	26B	1.25
14A	3.21		
14B	3.29		

TABLE 7.2-2

THERMAL DIFFUSIVITY TEST SPECIMEN ASSEMBLY
SILICONE BONDED "AA" FIBERS

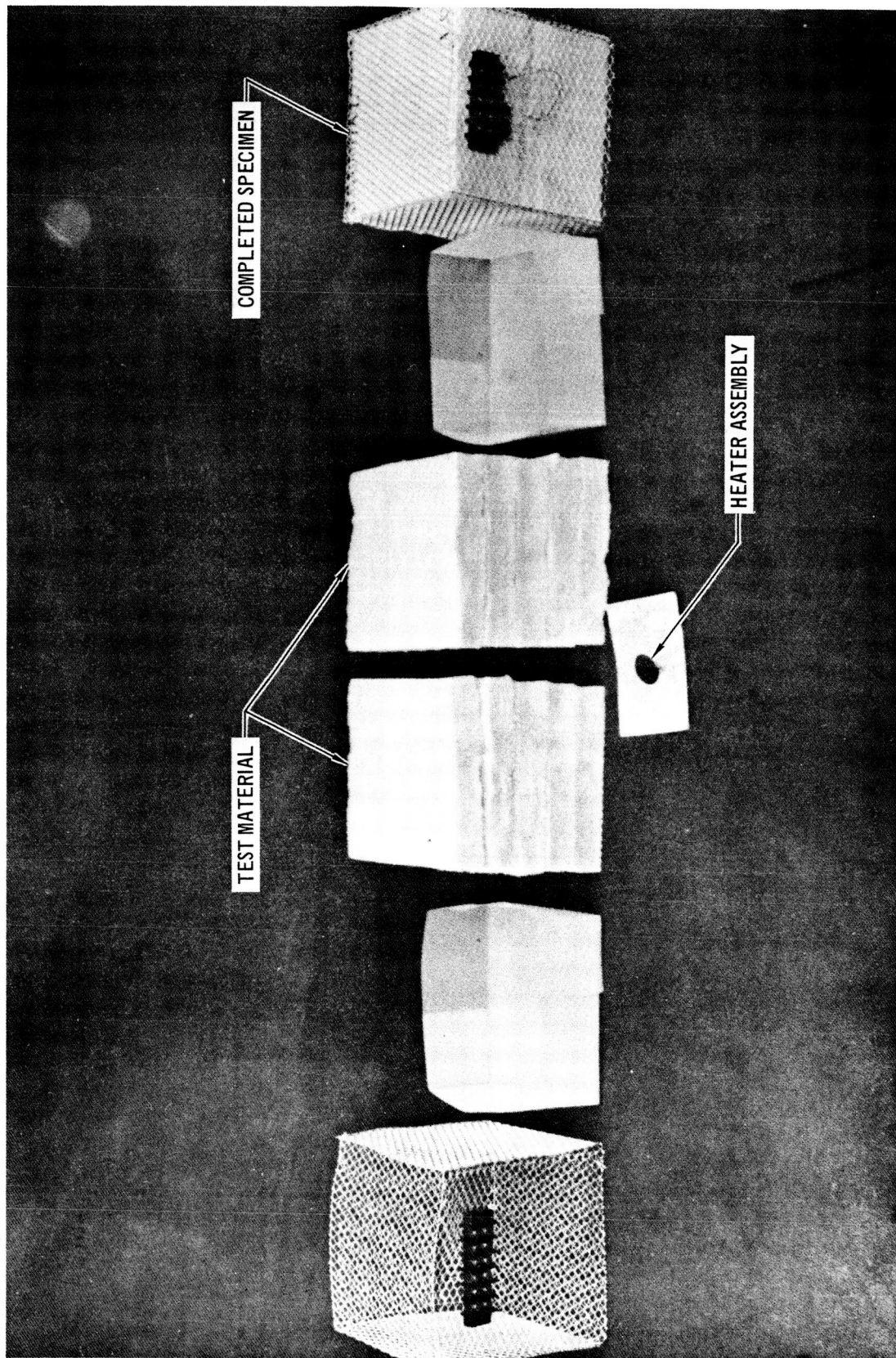


FIGURE 7.2-1

The lowest actual total assembly weight and the highest were 551.3 and 592.1 mg respectively. This amounts to approximately 1.5% of the total specimen weight for the lowest density material (0.7 pcf fiberglass).

The resistance of each heater and power lead was measured and recorded for use in determining specimen power input. To determine the effects that heat sterilization may have on the heaters, five heaters were cycled five times from ambient to 275°F. The resistance before and after each of the temperature cycles is presented in Table 7.2-3. No hysteresis was observed.

Since each batch of thermocouple wire can produce a thermocouple emf slightly different from the published tables, a typical thermocouple was calibrated against a platinum resistance thermometer. The thermocouple calibration results are presented in Table 7.2-4. After the thermocouples were installed on the heaters, the output of thirty thermocouple assemblies were spot-checked at ambient temperature against the platinum resistance thermometer. Agreement was excellent between the calibration curve made from the typical thermocouple and the one-point calibration of the thermocouple as installed on a typical heater.

Thermal response of a typical heater assembly was evaluated in vacuum to determine the transient characteristics of the assembly, and to provide input should the heat capacity of the heater be needed to accurately reduce the test data. The heater response data is shown in Figure 7.2-2. Because the final heater assembly mass was very low, and the selected heating time was rather long, the heat capacity of the heater was not necessary for data reduction.

7.2.2 Test Apparatus - The 50 test samples are shown in Figure 7.2-3 mounted on the 8 ft. chamber door prior to chamber closure. The instrumentation schematic is presented in Figure 7.2-4. The required voltage drop across each heater assembly was determined using the measured heater and lead resistance and the calculated power level which would provide the desired temperature rise of 40 to 70°F. Since this voltage was set by the variable resistor in one leg of each heater circuit, the required power was applied simultaneously to each specimen heater.

Temperatures were continuously monitored during each test by the Central Data Acquisition System. This system recorded the test data on magnetic tape for later reduction to corrected temperature histories. Figure 7.2-5 shows the test instrumentation set up mounted on the back side of the chamber door.

7.2.3 Test Description - A total of 6 thermal diffusivity test runs were made as shown below:

<u>Test Conditions</u>	<u>1st Test</u>	<u>2nd Test</u>
	<u>Before Sterilization</u>	<u>After Sterilization</u>
Ambient Air	X	X
Vacuum ($<5 \times 10^{-6}$ torr)	X	X
20 mb Simulated Mars atmosphere*	X	X

* 19% CO₂, 60% N₂ and 21% A by volume

HEATER THERMAL CYCLE TEST

HEATER NUMBER	INITIAL	RESISTANCE (OHMS)				
		CYCLE 1	CYCLE 2	CYCLE 3	CYCLE 4	CYCLE 5
1	324.5	324.6	324.6	324.4	324.5	324.5
2	317.5	317.4	317.4	317.4	317.4	317.4
3	309.8	309.8	309.8	309.7	309.7	309.7
4	312.8	312.7	312.8	312.7	312.6	312.7
5	319.4	319.3	319.3	319.3	319.3	319.3

TABLE 7.2-3

CHROMEL - CONSTANTAN THERMOCOUPLE CALIBRATION

TEMPERATURE °F	HANDBOOK STANDARD THERMOCOUPLE OUTPUT MILLVOLTS	MEASURED THERMOCOUPLE OUTPUT MILLVOLTS
71.99	1.33	1.333
100.00	2.27	2.298
124.98	3.15	3.178
150.00	4.04	4.077

TABLE 7.2-4

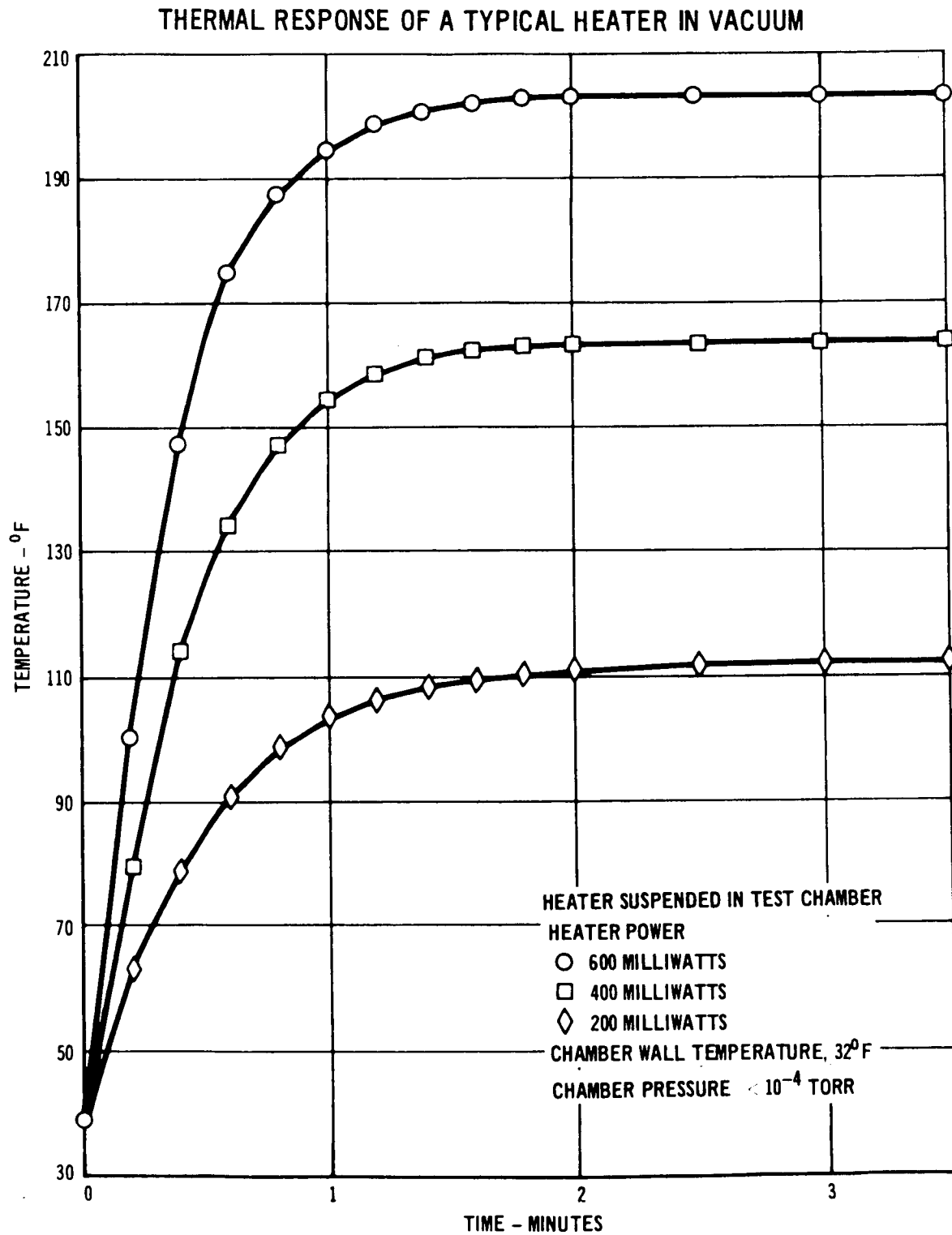


FIGURE 7.2-2

THERMAL DIFFUSIVITY TEST SETUP

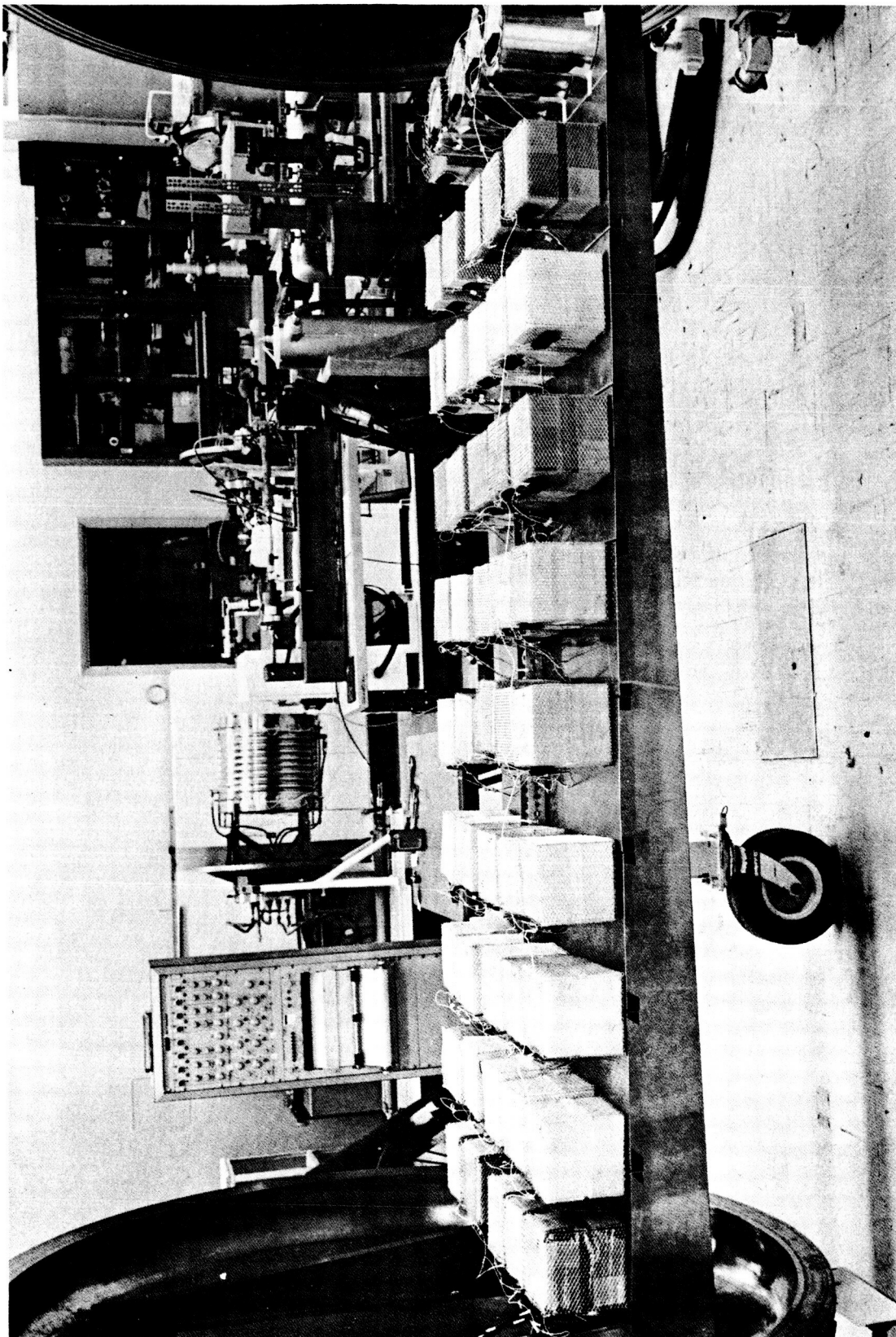


FIGURE 7.2-3

THERMAL DIFFUSIVITY TEST INSTRUMENTATION SCHEMATIC

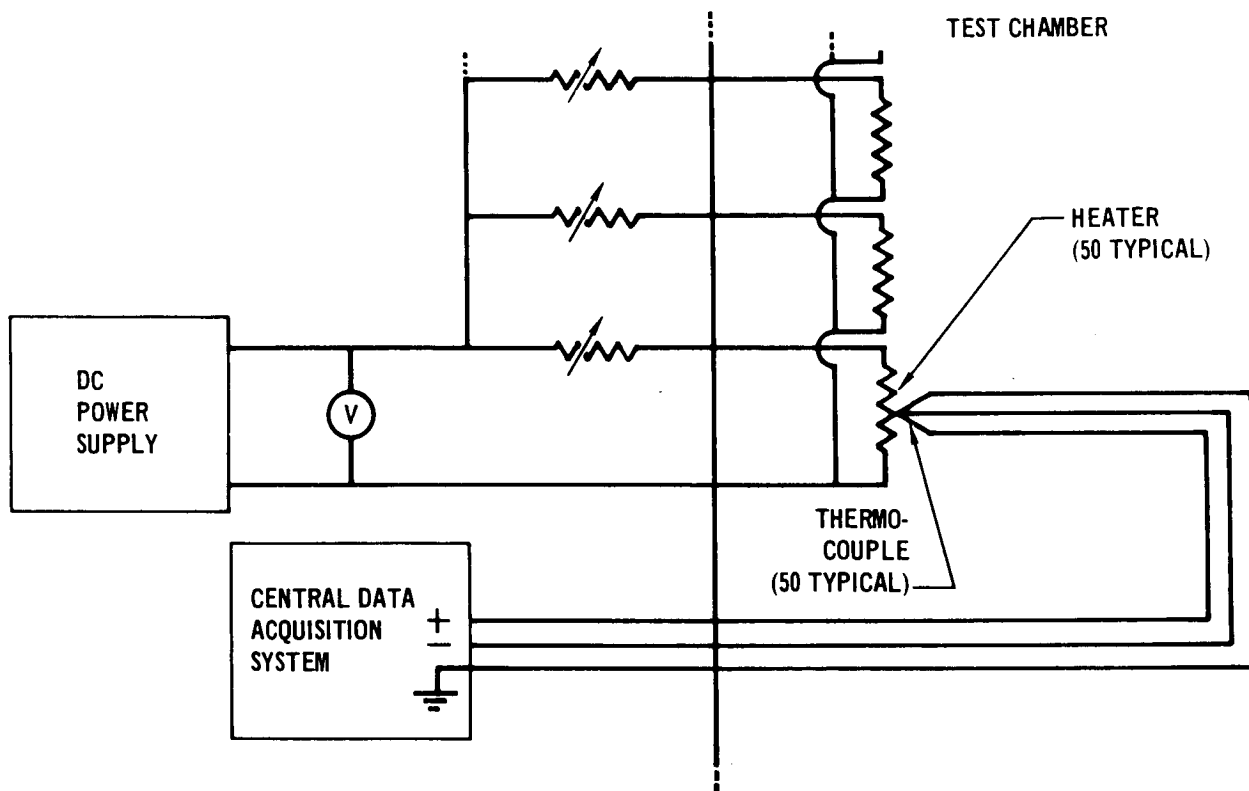


FIGURE 7.2-4

THERMAL DIFFUSIVITY TEST INSTRUMENTATION

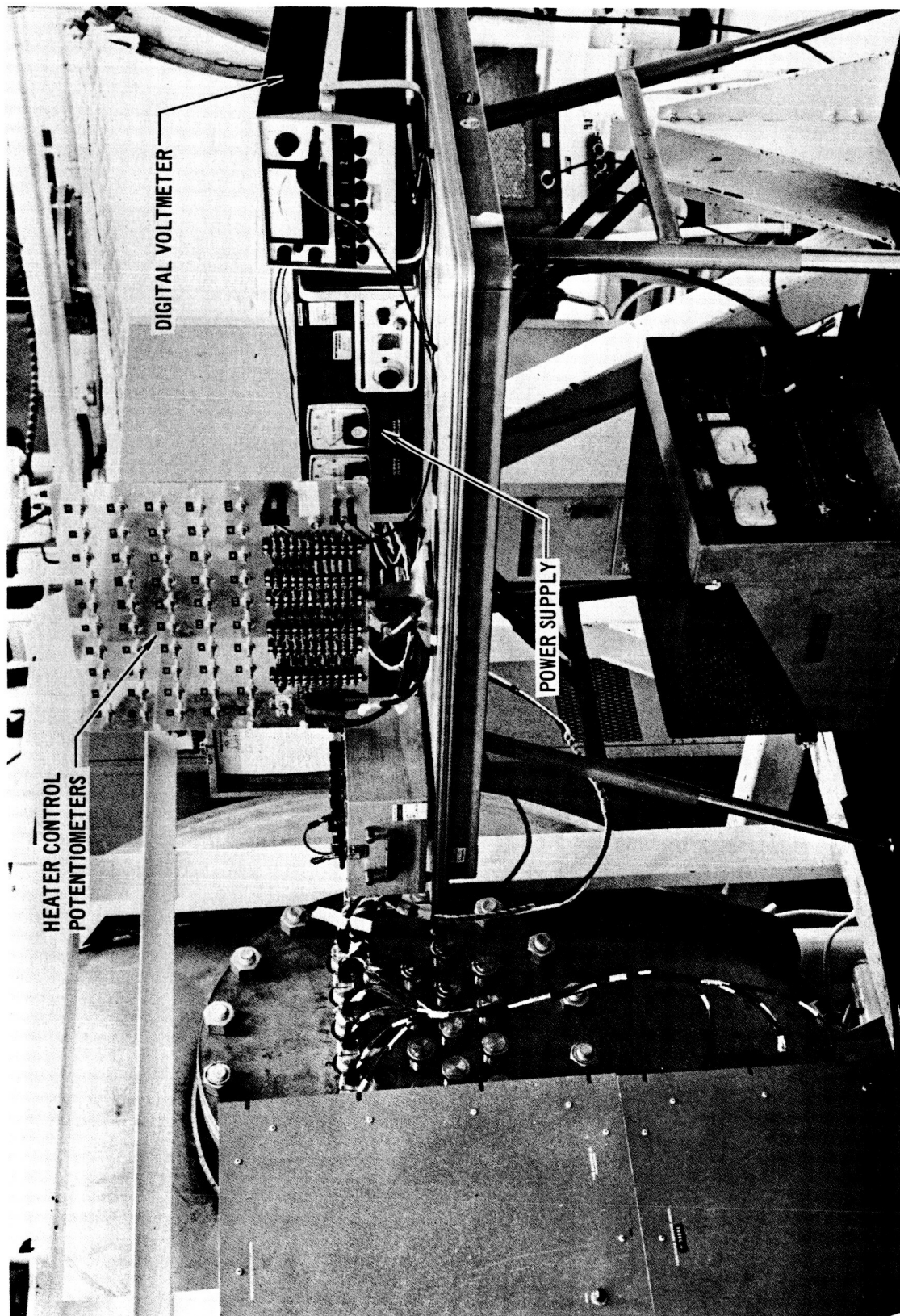


FIGURE 7.2-5

All 50 samples were subjected to the 3 test conditions before heat sterilization. Only the nine materials that successfully passed the heat sterilization cycle were subjected to the three conditions for the second test. After stabilizing the chamber at ambient temperature and the desired pressure, the resistance of each heater was adjusted using the variable in-line resistor. Table 7.2-5 gives the temperature and pressure of the chamber for approximately 24 hours prior to the first vacuum test. Table 7.2-6 presents the same data for the first simulated Mars atmosphere test. Both tables are typical of the results obtained during the second diffusivity test (after heat sterilization). The ambient air tests were run after stabilization for approximately 24 hours.

A typical comparison of the desired heater power versus the actual power supplied to each specimen is shown in Table 7.2-7 for the initial simulated Mars condition test. This data indicates that close heater control was maintained.

7.2.4 Data Reduction - Development of a data reduction technique was required to calculate the thermal conductivity from the test data. Two techniques were selected, a closed form analytical solution and a finite difference computer model. The analytical solution was used for all isotropic materials (fibers, foams, and powders) and the computer model for the multi-layer materials. The analytical solution (Table 7.2-8) was used for the isotropic materials because of its convenience and good agreement with both data from a checkout test as well as the computer model solution. The analytical solution was a closed form expression derived by Carslaw and Jaeger (Reference 7-1). It predicts the temperature rise of a uniformly heated disk in a semi-infinite solid, neglecting the thermal mass of the heater.

The finite difference computer model (Figure 7.2-6) was developed to assure that a variety of test and insulation variables could be analyzed. Insulation properties such as density, specific heat, thermal conductivity (radial and axial) and physical dimensions could be varied. Also, the heater characteristics and effects of gaps between the heater and the insulation could be examined. The insulation, heater and leads were accurately modeled. By investigating a range of gap sizes, a gap of 0.001 inch, with both radiation and gas conduction across the gap was found to be most realistic.

Prior to the actual thermal diffusivity test, these two data reduction techniques were compared with a checkout test using fiberglass insulation. The checkout test was performed in air at one atmosphere. The test sample was J-M "AAA" Microlite fibers (1.2 pcf), fabricated identical to the thermal diffusivity test samples. The purpose of the test was to compare the closed form analytical solution with the computer model. Heater power during checkout was maintained at 80 milliwatts throughout the test duration of 12 minutes. The temperature histories are shown in Figure 7.2-7. As shown on the curve, the two calculated histories and the measured test history all indicated a temperature rise of 44 to 46°F at the end of heating. Comparing the data

CHAMBER STABILIZATION FOR VACUUM TEST

(TASK 3)

TIME (HOURS)	PRESSURE (TORR)	TEMPERATURE (°F)
0	760	-
0.50	2×10^{-1}	-
1.50	3×10^{-5}	-
10.17	2.9×10^{-6}	53
11.00	2.4×10^{-6}	53
14.00	2.0×10^{-6}	53
15.25	1.9×10^{-6}	53
18.33	1.6×10^{-6}	55
21.13	1.5×10^{-6}	55
21.33	1.5×10^{-6}	55

TABLE 7.2-5

CHAMBER STABILIZATION FOR TEST AT MARS ATMOSPHERIC PRESSURE

TIME (HOURS)	(TASK 3) PRESSURE (MB)	TEMPERATURE (°F)
0	20.0	-
9.67	20.1	75
10.67	20.1	75
11.67	20.1	75
12.67	20.1	75
12.87	20.1	75

TABLE 7.2-6

POWER SUPPLIED TO SPECIMENS FOR MARS ATMOSPHERE TEST

SAMPLE NUMBER	COMPUTED POWER REQUIRED (WATTS)	ACTUAL POWER DELIVERED (WATTS)	SAMPLE NUMBER	COMPUTED POWER REQUIRED (WATTS)	ACTUAL POWER DELIVERED (WATTS)
1A	6.00×10^{-2}	6.00×10^{-2}	14A	6.00×10^{-2}	5.99×10^{-2}
1B	6.00×10^{-2}	5.98×10^{-2}	14B	6.00×10^{-2}	5.99×10^{-2}
2A	6.00×10^{-2}	6.02×10^{-2}	15A	6.00×10^{-2}	6.01×10^{-2}
2B	6.00×10^{-2}	6.00×10^{-2}	15B	6.00×10^{-2}	6.01×10^{-2}
3A	6.00×10^{-2}	6.02×10^{-2}	16A	6.00×10^{-2}	6.00×10^{-2}
3B	6.00×10^{-2}	6.00×10^{-2}	16B	6.00×10^{-2}	5.99×10^{-2}
4A	6.00×10^{-2}	5.99×10^{-2}	17A	6.00×10^{-2}	6.00×10^{-2}
4B	6.00×10^{-2}	6.01×10^{-2}	17B	6.00×10^{-2}	5.92×10^{-2}
5A	6.00×10^{-2}	6.01×10^{-2}	18A	6.00×10^{-2}	6.00×10^{-2}
5B	6.00×10^{-2}	6.00×10^{-2}	18B	6.00×10^{-2}	5.92×10^{-2}
6A	6.00×10^{-2}	5.99×10^{-2}	19A	6.00×10^{-2}	6.00×10^{-2}
6B	6.00×10^{-2}	6.02×10^{-2}	19B	6.00×10^{-2}	6.02×10^{-2}
7A	6.00×10^{-2}	6.01×10^{-2}	20A	1.00×10^{-1}	1.00×10^{-1}
7B	6.00×10^{-2}	6.01×10^{-2}	20B	1.00×10^{-1}	1.00×10^{-1}
8A	6.00×10^{-2}	6.02×10^{-2}	21A	1.00×10^{-1}	9.74×10^{-2}
8B	6.00×10^{-2}	5.98×10^{-2}	21B	1.00×10^{-1}	9.97×10^{-2}
9A	6.00×10^{-2}	5.97×10^{-2}	22A	6.00×10^{-2}	6.01×10^{-2}
9B	6.00×10^{-2}	5.99×10^{-2}	22B	6.00×10^{-2}	5.99×10^{-2}
10A	6.00×10^{-2}	6.00×10^{-2}	23A	6.00×10^{-2}	6.00×10^{-2}
			23B	6.00×10^{-2}	6.02×10^{-2}
11A	6.00×10^{-2}	5.99×10^{-2}			
12A	6.00×10^{-2}	5.98×10^{-2}	24A	6.00×10^{-2}	6.01×10^{-2}
12B	6.00×10^{-2}	6.03×10^{-2}	24B	6.00×10^{-2}	6.00×10^{-2}
13A	6.00×10^{-2}	6.02×10^{-2}	25A	6.00×10^{-2}	6.00×10^{-2}
13B	6.00×10^{-2}	6.02×10^{-2}	25B	6.00×10^{-2}	5.97×10^{-2}
			26A	6.00×10^{-2}	6.00×10^{-2}
			26B	6.00×10^{-2}	5.92×10^{-2}

TABLE 7.2-7

THERMAL DIFFUSIVITY TEST - DATA REDUCTION TECHNIQUES

METHOD USED FOR MULTILAYER MATERIAL

- FINITE DIFFERENCE COMPUTER MODEL

METHOD USED FOR FIBERS, FOAMS AND POWDERS

- CLOSED FORM ANALYTICAL SOLUTION, CARSLAW AND JAEGER-PREDICTS TEMPERATURE RISE OF A UNIFORMLY HEATED, CIRCULAR DISK IN A SEMI-INFINITE SOLID

$$\Delta T = \frac{Q (kt)^{1/2}}{K} \left[\operatorname{ierfc} \frac{Z}{2 (kt)^{1/2}} - \operatorname{ierfc} \frac{(Z^2 + A^2)^{1/2}}{2 (kt)^{1/2}} \right]$$

WHERE: ΔT - TEMPERATURE RISE ON THE HEATER SURFACE $k = \frac{K}{\rho C_p}$ - THERMAL DIFFUSIVITY

Q - HEATER POWER

ρ - DENSITY

K - THERMAL CONDUCTIVITY

C_p - SPECIFIC HEAT

Z - AXIAL DISTANCE FROM HEATER

A - RADIUS OF HEATER

t - HEATING TIME

TABLE 7.2-8

THERMAL DIFFUSIVITY TEST COMPUTER ANALYSIS MODEL

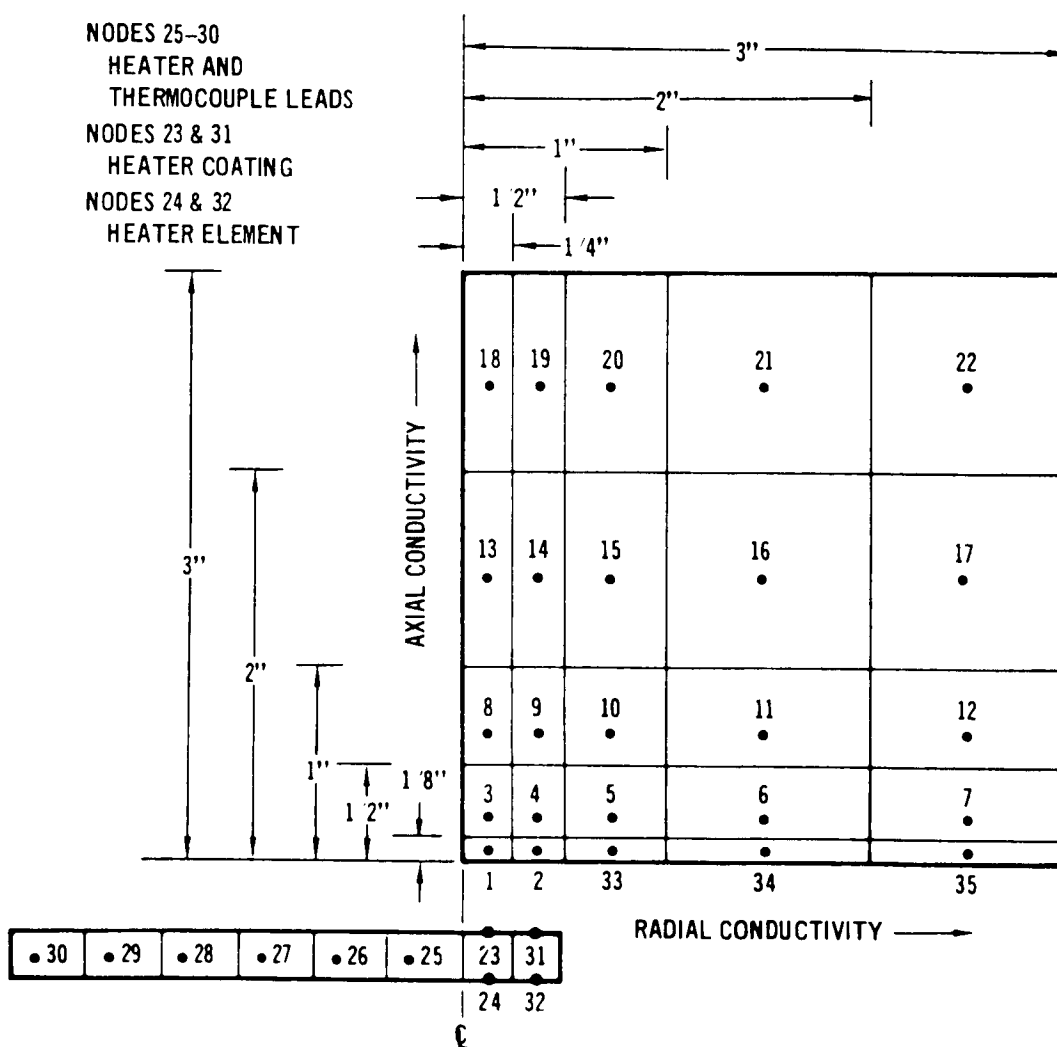


FIGURE 7.2-6

COMPARISON OF THERMAL DIFFUSIVITY TEST AND ANALYSIS RESULTS

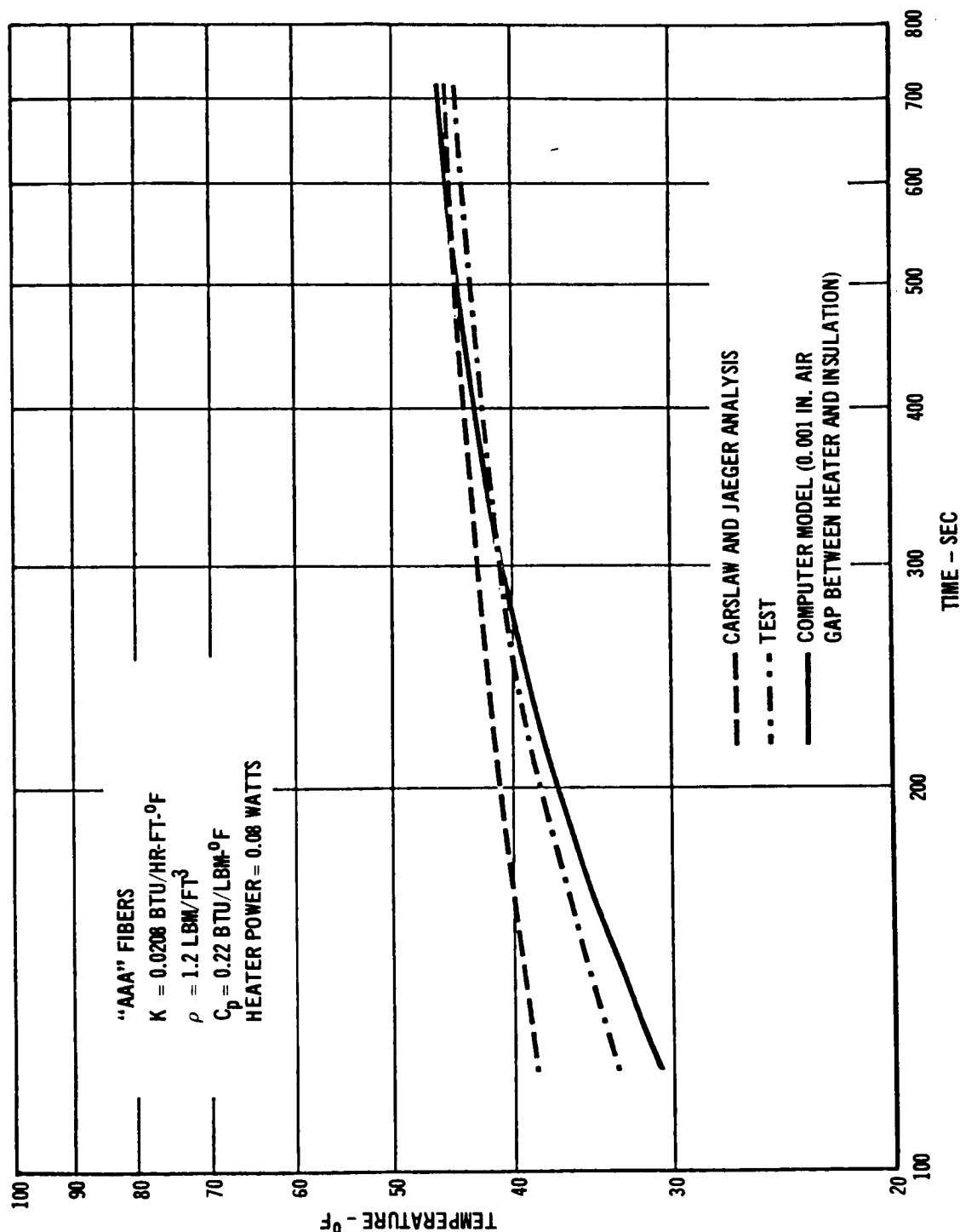


FIGURE 7.2-7

during the early portion of the heating, the analytical prediction is less accurate because the heater mass is neglected. These comparisons were sufficient to show that the two calculation methods compared well with test data for an isotropic material, and substantiated that a test time of 12 minutes was acceptable.

Based on the good agreement during the checkout test, the closed form analytical solution was selected to reduce the thermal diffusivity test data for fibers, foams, and powders. This solution was used because it was faster and less costly than the computer model. The computer model was used to reduce the data for the multilayer materials, because it could assume different thermal conductivity values in two directions to simulate heat transfer both parallel and perpendicular to the film layers. These data reduction techniques use the temperature rise and heater power from the test, along with the insulation properties of density and specific heat, to determine the insulation thermal conductivity.

- o Analysis for Non-Multilayer Materials - The closed form analytical solution was used to generate data reduction curves for fibers, foams, and powders as shown in Figure 7.2-8. The curves were used as follows: Temperature rise of the heater (ΔT) was measured at the end of 12 minutes of heating. Use of the heater power (Q) gave the ratio $\Delta T/Q$. Density of each sample (ρ) was measured. Specific heat (C_p) was determined from the literature to give (ρC_p). The curve was then entered with known ($\Delta T/Q$) and (ρC_p) to read the ($k\rho C_p$). The thermal conductivity (k) was then computed from this parameter.
- o Analysis for Multilayer Data - The computer model was employed to generate a second series of curves for multilayer insulations. Three sets of curves (one set for each layer density) were used, with each set having several curves for different thermal conductivities in the radial direction; i.e. along the layers. Only one set (40 layers/inch) is shown in Figure 7.2-8. In the area on the curve where the radial and axial thermal conductivities are approximately equal, the results agree as they should, with the predictions for the isotropic materials. The radial thermal conductivity is the sum of conductivity contributions from the gas, the Kapton film, the gold layer, and radiation (Table 7.2-9). The thermal conductivity due to the gas, Kapton, and the gold layer is available from the literature. However, the heat loss due to radiation tunneling had to be estimated. A method from Coston (Reference 7-2) based on analysis by Sparrow (Reference 7-3) uses a radiation shape factor to obtain an effective thermal conductivity for diffusely reflecting and emitting surfaces:

THERMAL DIFFUSIVITY TEST - DATA REDUCTION CURVES

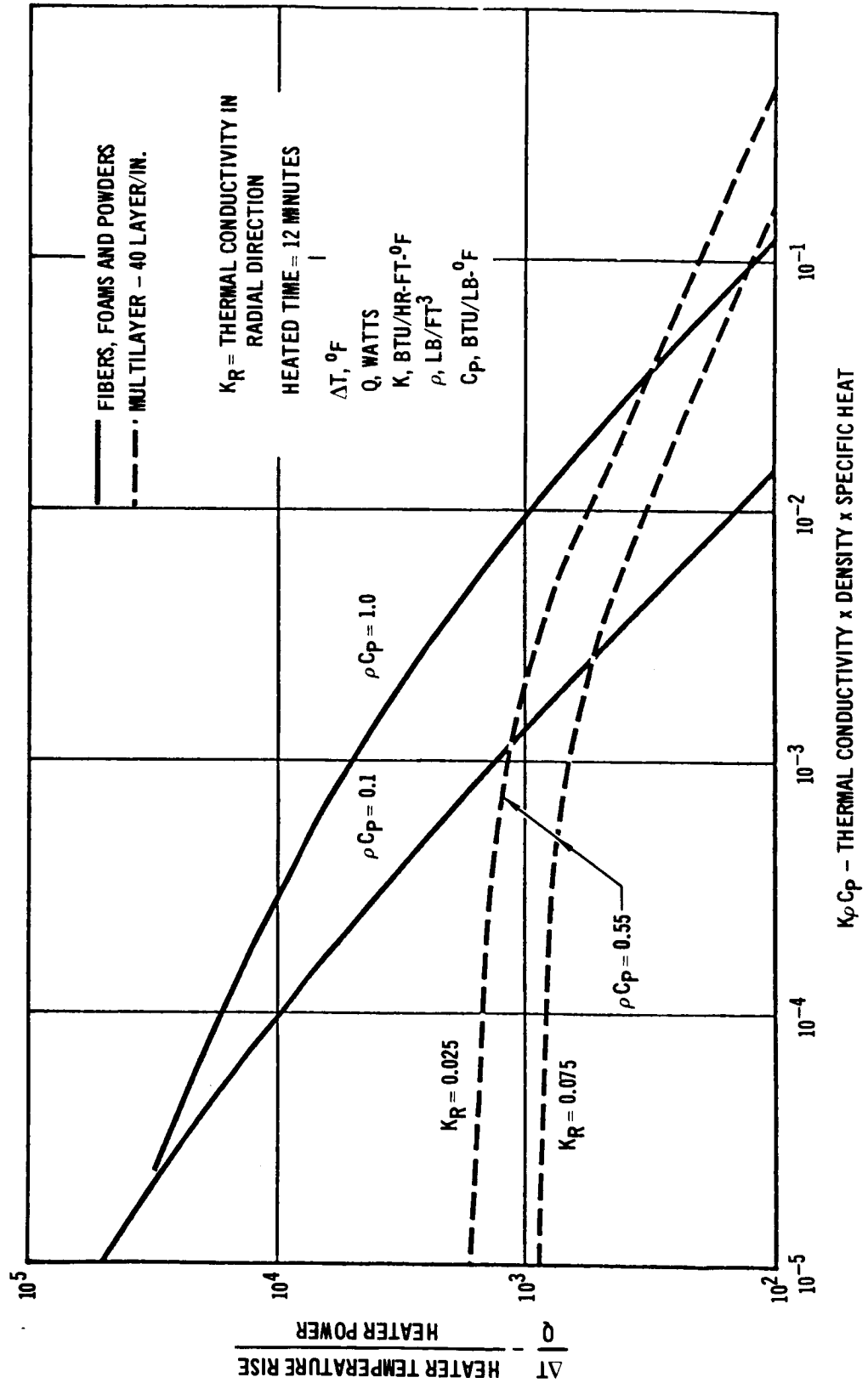


FIGURE 7.2-8

DATA REDUCTION ASSUMPTIONS FOR MULTILAYER INSULATION

LET: K_A = THERMAL CONDUCTIVITY ACROSS LAYERS

K_R = THERMAL CONDUCTIVITY ALONG LAYERS

THEN: $K_R = K_{GAS} + K_{KAPTON\ FILM} + K_{GOLD\ LAYER} + K_{RADIATION}$

K_{GAS} , K_{KAPTON} , K_{GOLD} WERE COMPUTED FROM LITERATURE DATA

$K_{RADIATION}$ WAS COMPUTED WITH ASSUMED GEOMETRY

TABLE 7.2-9

PARAMETER VALUES USED IN MULTILAYER ANALYSIS

PARAMETER	SYMBOL	VALUE	UNCERTAINTY	REFERENCE
LAYER DENSITY	N	40/IN. 60/IN. 80/IN.	$\pm 5\%$	TEST VARIABLE
FILM THICKNESS	t_f	0.0005 IN.	+0.0001 IN. -0.0002	VENDOR
GOLD THICKNESS	t_g	350 \AA	$\pm 50 \text{\AA}$	VENDOR
GAS CONDUCTIVITY	k_g	0.013 BTU/HR FT ⁰ F	$\pm 4\%$	MIXTURE VALUE COMPUTED
KAPTON CONDUCTIVITY	k_f	0.09 BTU/HR FT ⁰ F	$\pm 3\%$	VENDOR
GOLD CONDUCTIVITY	k_{Au}	170 BTU/HR FT ⁰ F	$\pm 3\%$	LITERATURE
TUNNEL LENGTH	L_s	3 IN.	$\pm 5\%$	

TABLE 7.2-10

$$K_{\text{RAD}} = (eF) \sigma L_s (T_H^2 + T_C^2) (T_H + T_C)$$

where:

$$(eF) = \frac{2 \ln \left(\frac{2L_s}{\tau} \right) - 1}{2 \frac{L_s}{\tau}}$$

σ , Stefan-Boltzmann constant

T_H, T_C , Surface temperatures at each end of radiation path

L_s , Tunnel length

τ , Layer spacing

The expression is simplified if T_H and T_C are not greatly different. Then taking an average temperature value, \bar{T} ,

$$K_{\text{RAD}} = 4 (eF) \sigma L_s \bar{T}^3$$

This expression was used to compute the radiation tunneling contribution to radial conductivity. It is approximate for the following reasons:

- a) The shape factor was derived for diffuse surfaces while the test configuration had one diffuse (Kapton) and one specular (gold) surface.
- b) Because of crinkling, the radiation is blocked from direct transfer from the heater to outside the sample.
- c) The central heating source causes the radiation to spread radially, whereas the expression is derived for parallel radiation.
- d) Because the heating is applied centrally, some of the radiation absorbed on the layers is transferred across the layers rather than reemitted. This effectively reduces the radiant heat loss from a given "tunnel".

Point (a) above probably results in radiation somewhat higher than predicted by the expression, while points (b), (c) and (d), result in reduced radiation. Thus, the radiation term used in the total radial thermal conductivity expression gives the highest expected K_R , and the lowest predicted values for the axial conductivity, K_A for the multilayer materials.

The parameter values used for the analysis, together with their estimated uncertainty are given in Table 7.2-10. Using the nominal values of these parameters, the resulting K_R and K_A values (Table 7.2-11) were computed.

THERMAL CONDUCTIVITY CALCULATIONS FOR MULTILAYER MATERIALS

SAMPLE NO.	LAYER DENSITY	$\Delta T/Q$	ρC_p	k_{GAS}	k_{KAPTON}	k_{GOLD}	$k_{RADIATION}$	ΣK_R	$K_A \rho C_p$	K_A
22	40	452	.55	0.013	0.0018	0.0094	0.012	0.036	0.011	0.020
A										
B	40	431	.55	0.013	0.0018	0.0094	0.012	0.036	0.012	0.022
23										
A	60	426	.83	0.013	0.0027	0.014	0.0088	0.039	0.015	0.018
B	60	388	.83	0.013	0.0027	0.014	0.0088	0.039	0.019	0.023
24										
A	80	377	1.11	0.013	0.0036	0.019	0.0069	0.042	0.022	0.020
B	80	380	1.13	0.013	0.0036	0.019	0.0069	0.042	0.022	0.020

GOLD THICKNESS = 350 Å

ΔT HEATER TEMPERATURE RISE, °F

Q HEATER POWER, WATTS

ρ MATERIAL DENSITY, LBM/FT³

C_p MATERIAL SPECIFIC HEAT, BTU/LBM-°F

K_R THERMAL CONDUCTIVITY ALONG LAYERS, BTU/HR-FT-°F

K_A THERMAL CONDUCTIVITY ACROSS LAYERS, BTU/HR-FT-°F

TABLE 7.2-11

- o Uncertainty Evaluation - Of all the materials evaluated in the Thermal Diffusivity test, the multilayer insulations had the highest uncertainty. This conclusion is apparent because the heat loss along the layers must be estimated. The uncertainty for foams, fibers and powders was less than 6.8%. The test uncertainty for the multilayer materials was evaluated as follows:

The range of uncertainty was initially computed for K_R using the uncertainty values shown in Table 7.2-10. The resulting uncertainty range for K_A was then determined to be 6.8%, (least square error). The overall uncertainty has two additional contributions, that due to inherent inaccuracy of the test apparatus and procedure, and that due to the uncertainty in radiation tunnelling. The inherent test accuracy has not been evaluated, but the limiting effects of radiation tunnelling were identified, by neglecting it, i.e. assuming that effectively all radiation along the layers was either blocked by the crinkles and/or absorbed by the layers. The resulting range of K_A was +20.9% to -6.8% including both the uncertainty in radiation tunnelling and the parameters of Table 7.2-10.

7.2.5 Data and Computed Values - The thermal conductivity values from the first diffusivity test (before heat sterilization) are given in Table 7.2-12. Included in the table are the measured $\Delta T/Q$ values. They are included because they are large numbers, giving a better indication of the relative sensitivity of the technique. The thermal conductivity values for the Mars test condition are plotted in Figure 7.2-9. Similarly Figure 7.2-10 is a plot of the " $k\rho$ " product versus bulk density for the Mars test condition.

Table 7.2-13 delineates the thermal conductivity obtained after the second diffusivity test. A comparison of these results with those presented in Table 7.2-12 indicate the change in conductivity due to the heat sterilization cycle. The actual differences detected in terms of $\Delta T/Q$ are presented in Table 7.2-14. The material exhibiting the largest change was the HTF-200 foam. In sample 12A conductivity increased 8.8%; sample 12B increased 10.4% at the Mars test condition.

7.2.6 Conclusions - The test technique employed for rapid thermal diffusivity screening purposes yielded data that permitted material comparisons. The accuracy of the technique for the simulated Martian condition was sufficient within the scope of this program. However, the accuracy for multilayers at vacuum conditions is poor but this was expected.

Examination of the data enables the following conclusions to be made:


- o Minimum conductivity for fiberglass batt is at about 1.7 pcf density.
- o At the mean temperature and test density tested, the effect of fiber diameter for the fiberglass materials is negligible. Literal interpretation of the test data reveals that the "AAA" material has a lower " k " than the "AAAA", a conclusion not borne out by theory.

THERMAL DIFFUSIVITY TEST RESULTS BEFORE HEAT STERILIZATION

SAMPLE NO.	MATERIAL DESIGNATION	TEST DENSITY PCF	AMBIENT 760 Torr (AIR)		VACUUM <1.5 10 ⁻⁶ Torr		SIMULATED MARS 20 mb (15 Torr) (19% CO ₂ , 60% N ₂ 21%A)	
			$\Delta T/Q$ °F/WATT	k BTU/HR FT ² °F	$\Delta T/Q$ °F/WATT	k BTU/HR FT ² °F	$\Delta T/Q$ °F/WATT	k BTU/HR FT ² °F
1A	FIBERS: JM UNBONDED "A"	1.20	520	.023	1895	.005	630	.018
1B		1.20	515	.023	1832	.006	605	.019
2A	JM UNBONDED "AA"	1.20	543	.022	2060	.005	655	.018
2B		1.20	573	.020	2060	.005	647	.018
3A	JM UNBONDED "AAA"	1.20	568	.021	2080	.005	661	.017
3B		1.20	546	.025	2080	.005	655	.018
4A	JM UNBONDED "AAAA"	1.20	541	.022	2020	.005	656	.018
4B		1.20	579	.020	1972	.005	647	.018
5A	JM UNBONDED "AAAA"	0.70	495	.024	1330	.014	545	.022
5B		0.70	521	.023	1540	.012	578	.020
6A	JM UNBONDED "AAAA"	2.20	558	.020	2210	.005	679	.017
6B		2.20	579	.020	2265	.005	692	.017
7A	JM UNBONDED "AAAA"	1.70	565	.020	2130	.005	677	.017
7B		1.70	596	.019	2205	.005	687	.016
8A	JM SILICONE BONDED "AA"	1.10	545	.021	2005	.005	640	.018
8B		1.05	562	.020	2070	.005	640	.018
9A	HITCO SILICONE BONDED "AA"	1.35	588	.019	2125	.005	659	.017
9B		1.34	561	.020	2090	.005	645	.018
10	JM PHENOLIC BONDED "AA"	1.12	565	.020	2090	.004	644	.018
11	HITCO PHENOLIC BONDED "AA"	1.42	564	.020	2205	.005	640	.018
12A	FOAMS: UPJOHN HTF-200	2.03	654	.017	985	.010	732	.015
12B		2.05	656	.017	1020	.010	742	.014
13A	GE PPO	2.27	413	.026	995	.010	460	.024
13B		2.63	410	.025	967	.010	463	.022
14A	UPJOHN CPR 385D	3.21	502	.019	980	.011	586	.018
14B		3.29	503	.019	1002	.010	588	.018

TABLE 7.2-12

THERMAL DIFFUSIVITY TEST RESULTS BEFORE HEAT STERILIZATION (Continued)

SAMPLE NO.	MATERIAL DESIGNATION	TEST DENSITY PCF	AMBIENT 760 Torr (AIR)		VACUUM <1.5 10 ⁻⁶ Torr		SIMULATED MARS 20 mb (15 Torr) (19% CO ₂ , 60% N ₂ 21% A)	
			ΔT/q °F/WATT	k BTU/HR FT°F	ΔT/q °F/WATT	k BTU/HR FT°F	ΔT/q °F/WATT	k BTU/HR FT°F
15A	DIAMOND SHAMROCK G-302	2.41	530	.020	859	.011	569	.018
15B		2.28	521	.020	803	.012	553	.019
16A	STAFOAM AA-1802	2.13	622	.017	939	.011	686	.015
16B		2.14	605	.018	918	.011	670	.016
17A	SCOTTFOAM 80 CELL/IN.	1.90	450	.024	1195	.008	515	.021
17B		1.88	453	.024	1182	.009	518	.021
18A	SCOTT FOAM 60 CELL/IN.	1.80	419	.027	1010	.010	466	.023
18B		1.83	420	.027	1002	.010	470	.024
19A	SCOTT FOAM 45 CELL/IN.	1.83	407	.028	962	.011	450	.025
19B		1.81	405	.028	977	.011	453	.025
POWDERS:								
20A	COLLOIDAL ALUMINA	3.74	511	.022	1400	.007	756	.014
20B		3.54	492	.023	1422	.007	784	.014
21A	COLLOIDAL SILICA	3.15	534	.021	1640	.006	884	.012
21B		3.14	530	.022	1582	.007	868	.013
MULTILAYER:								
22A	GOLDIZED KAPTON 40 LAYERS/IN.	2.12	445	.020	2508	- 	452	.020
22B		2.13	391	.027	2530	-	431	.022
23A	GOLDIZED KAPTON 60 LAYERS/IN.	3.18	360	.027	2340	-	426	.018
23B		3.19	374	.024	2450	-	388	.023
24A	GOLDIZED KAPTON 80 LAYERS/IN.	4.25	335	.035	2390	-	377	.020
24B		4.26	343	.039	2340	-	388	.020
25A	GOLDIZED KAPTON WITH 1/2" "AA" SPACERS	1.30	566	.020	2330	.005	630	.019
25B		1.30	562	.020	2430	.004	605	.019
26A	GOLDIZED KAPTON WITH 1" "AA" SPACERS	1.26	562	.020	2310	.005	649	.019
26B		1.25	546	.021	2245	.005	615	.020

Δ THE MULTILAYERS WERE NOT CALCULATED BECAUSE THE TECHNIQUE IS INSENSITIVE IN VACUUM FOR ANISOTROPIC MATERIALS.

TABLE 7.2-12 CONTINUED

THERMAL DIFFUSIVITY TEST RESULTS MARS ATMOSPHERE

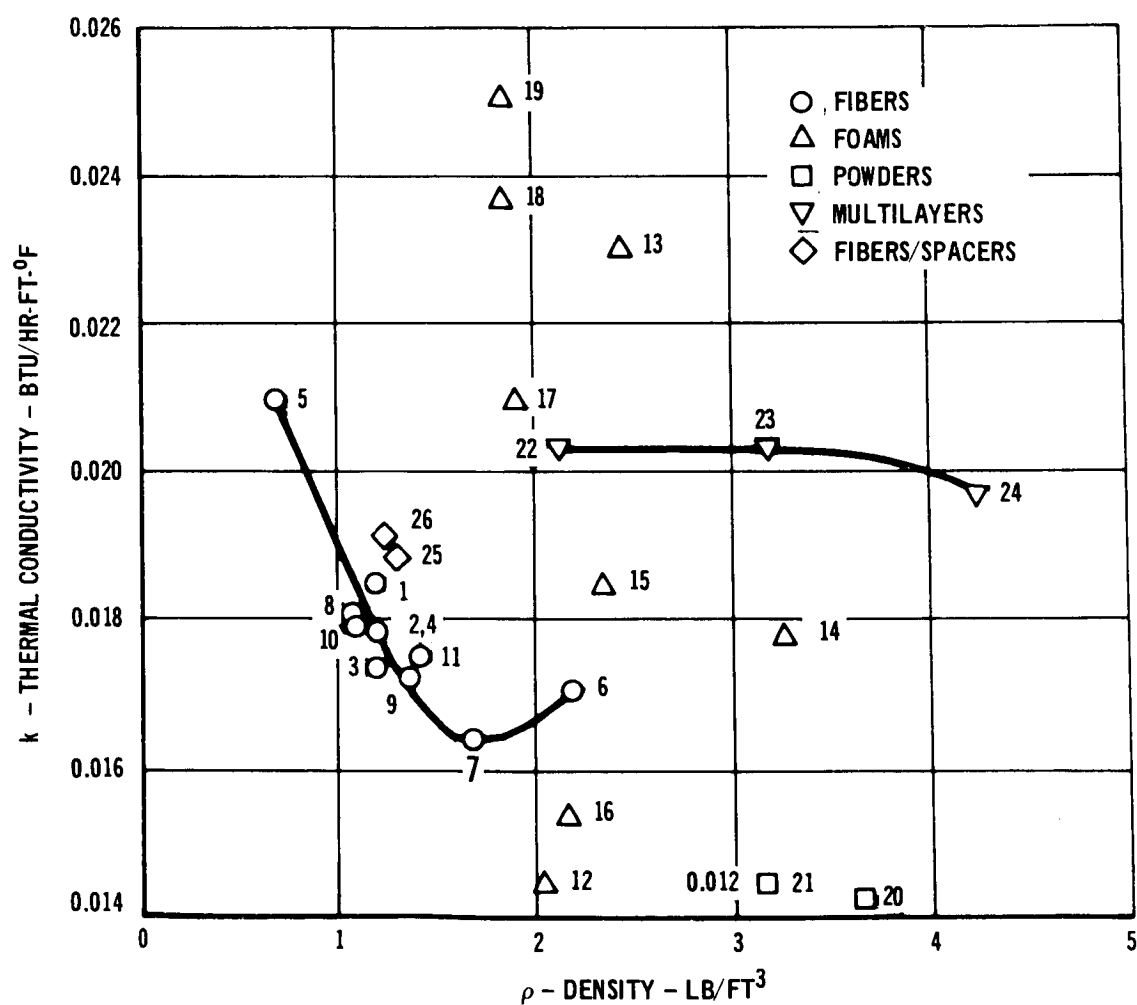


FIGURE 7.2-9

THERMAL DIFFUSIVITY TEST RESULTS ρk , MARS ATMOSPHERE

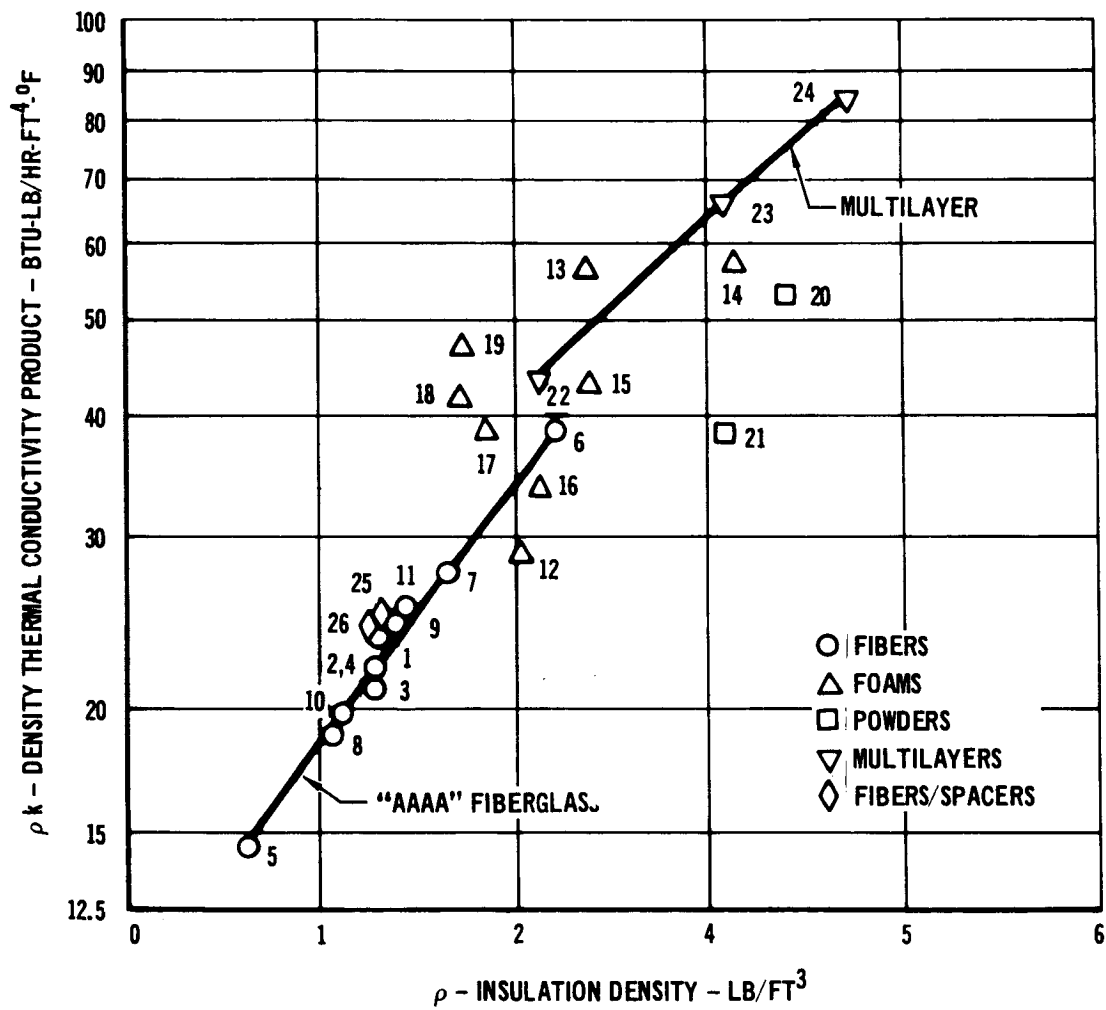


FIGURE 7.2-10

THERMAL DIFFUSIVITY TEST RESULTS AFTER HEAT STERILIZATION

SAMPLE NO.	MATERIAL DESIGNATION	TEST DENSITY PCF	AMBIENT 760 Torr (AIR)		VACUUM $<1.5 \times 10^{-6}$ Torr		SIMULATED MARS 20 mb(15 Torr) (19% CO ₂ , 60% N ₂ , 21% A)	
			$\Delta T/Q$	k	$\Delta T/Q$	k	$\Delta T/Q$	k
3A	JM UNBONDED "AA"	1.20	560	.021	2060	.005	663	.018
4B	JM UNBONDED "AAAA"	1.20	554	.021	1940	.006	660	.018
8A	JM SILICONE BONDED "AA"	1.10	560	.021	2000	.005	632	.018
9A	HITCO SILICONE BONDED "AA"	1.35	570	.019	2100	.005	656	.017
10	JM PHENOLIC BONDED "AA"	1.12	536	.021	2045	.005	650	.018
12A	UPJOHN HTF-200 (PRE-CONDITIONED)	2.03	615	.018	912	.011	678	.016
12B	UPJOHN HTF-200	2.05	614	.017	938	.011	680	.016
13A	GE - PPO	2.27	415	.026	1000	.010	462	.023
21A	COLLOIDAL SILICA	3.15	520	.022	1578	.007	883	.012

TABLE 7.2-13

EFFECTS OF HEAT STERILIZATION CYCLE

SAMPLE NO.	MATERIAL	BEFORE STERILIZATION MEASURED $\Delta T/Q$			AFTER HEAT STERILIZATION CHANGE IN $\Delta T/Q$		
		ATMOSPHERIC	MARS	VACUUM	ATMOSPHERIC	MARS	VACUUM
3A	UNBONDED "AAA"	568	661	2080	-8	+2	-20
4A	UNBONDED "AAAA"	579	647	1972	-25	+13	-32
8A	SILICONE "AA" (JM)	545	640	2005	+15	-8	-5
9A	SILICONE "AA" (HITCO)	588	659	2125	-18	-3	-25
10	PHENOLIC "AA" (JM)	565	644	2090	-29	+6	-45
12A	HTF-200 (CONDITIONED)	654	732	985	-39	-54	-73
12B	HTF-200	656	742	1020	-42	-62	-82
13A	POLYPHENYLENE OXIDE	413	460	995	+ 2	+ 2	+ 5
15A	G-302 (CONDITIONED)	530	569	859	NOT TESTED		
15B	G-302	521	553	803	NOT TESTED		
21A	COLLOIDAL SILICA	534	884	1640	-14	-1	-62
22A	GOLD ON KAPTON	445	452	2508	NOT TESTED		

TABLE 7.2-14

- o Binder content or chemistry does not influence insulation performance for these test conditions.
- o For the same density, urethane foams have a lower "kp" than fiberglass batts.
- o Isocyanurate foam belongs to the same family of "kp" values as the polyurethane foam.
- o At simulated Martian condition, the multilayer materials have the family of highest "kp" values.
- o Powders had the lowest thermal conductivities and belong to the family of lowest "kp" curves.
- o Use of radiation foils as separators in fiberglass batt reduce effectiveness rather than increase it.

Based upon the results obtained several additional materials might be considered for test e.g., powder material with a density in the 1-2 pcf range might be highly effective. An opacified low density powder also shows promise.

8. INSULATION SYSTEM MODULE SELECTION AND FABRICATION.

Selection of the two materials to be incorporated into the ISM's (Insulation System Module) test panels was based on the results of the Thermal Diffusivity and Heat Sterilization Screening Tests and the design studies. When integrated into the design approaches on the basis of weight required for equal heat loss, the HTF-200 foam showed a distinct weight advantage over the other materials. Silicone bonded "AA" fiberglass was chosen as the backup material.

8.1 PREDICTED WEIGHT COMPARISON - Comparisons of the candidate materials were made on the basis of installed weight required for equal heat loss. Installed weight was determined using the ISM design approaches of Section 6. Equal heat loss was assured if the thermal conductivity/thickness ratio of the insulation was constant for each candidate material. The required thickness for constant heat loss was determined from Figure 8.1-1, using thermal conductivity data from the Thermal Diffusivity Test. From Figure 8.1-2 the comparable ISM weights, were computed, and are presented in Table 8.1-1. These data were normalized such that the lowest weight configuration has a thickness of 3 inches, and other materials have the thickness required for equal heat loss. Predicted edge effects were not included in this comparison since they would not alter the materials selection, i.e., edge losses for non-foam materials are higher than for foam because the fiberglass structure is thicker (0.040 in. vs 0.024 in. for the foam).

8.2 ISM INSULATION MATERIAL SELECTION - Based on the evaluation results, two materials were selected to be incorporated into the ISM test panels:

- 1) UpJohn Company HTF-200 foam
- 2) J-M Microlite, silicone bonded "AA" fiberglass

The foam material was selected, based on its low weight as installed. A fibrous material was selected to avoid committing the remaining portion of the study to foam materials only (the G 302 foam was nearly as light as the HTF-200 material). The bonded fiberglass was selected in the belief that it would withstand the vibration and shock environments better than the equally light unbonded material. Powder and multilayer materials were removed from consideration due to their high weight, fabrication cost, and expected uncertainties in performance as installed.

8.3 ISM FABRICATION - The actual ISM designs used for the foam and fiber concepts are shown in Figure 8.3-1 and 8.3-2 respectively. The majority of the ISM fabrication took place in the Advanced Manufacturing Facilities of McDonnell Douglas Astronautics - Eastern Division.

8.3.1 Foam ISM Fabrication - Layup and curing procedures employed for the fiberglass laminate casings were in accordance with normally accepted aerospace techniques. Details of the procedures are given in MDAC-ED Specification PS 14034, Type I, Class D, Grade I. Thickness of the base was .012 inches. The sides were .024 inches.

WEIGHT REQUIREMENTS FOR EQUAL HEAT LOSS

REQUIRED INSULATION THICKNESS
FOR CONSTANT HEAT LOSS

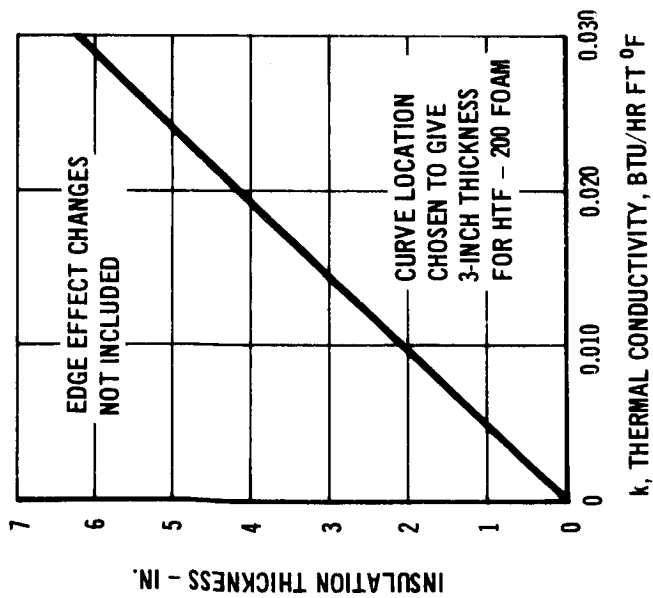


FIGURE 8.1-1

INSULATION SYSTEM MODULE WEIGHTS
FOR CANDIDATE MATERIALS

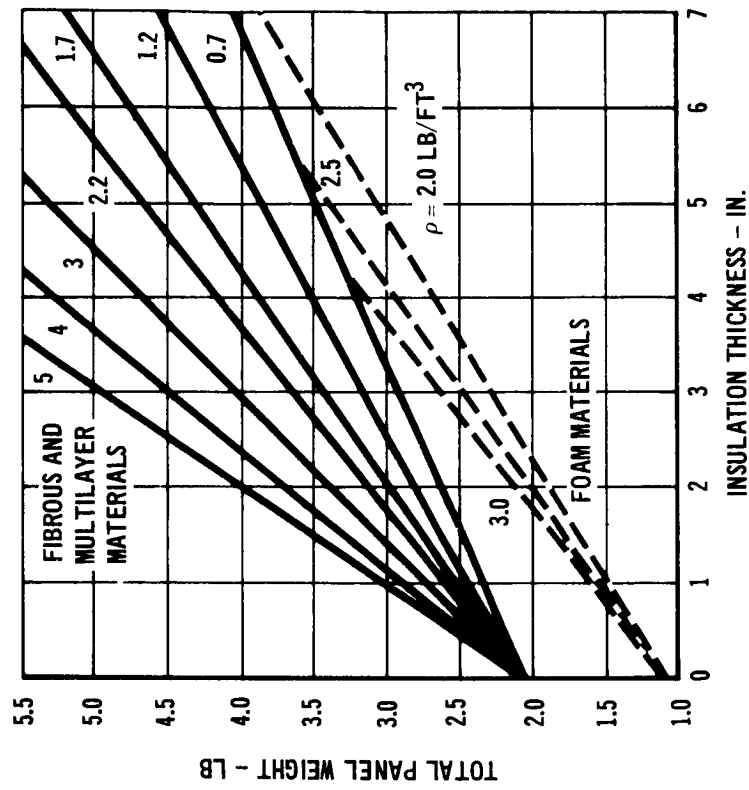


FIGURE 8.1-2

INSULATION SYSTEM MODULE WEIGHT COMPARISON

INSULATION MATERIAL	THERMAL CONDUCTIVITY BTU/HR FT °F	DENSITY LB/FT ³	*NORMALIZED THICKNESS INCH	INSULATION SYSTEM MODULE WEIGHT	
				LB	% INCREMENT
FOAM HTF-200	0.015	2.03	3.00	2.31***	0
FOAM G302	0.019	2.35	3.80	2.64	14
FIBROUS-UNBONDED "AAAA"					
$\rho = 0.7$	0.021	0.7	4.2	3.34	45
$\rho = 1.2$	0.018	1.2	3.6	3.44	49
$\rho = 1.7$	0.016	1.7	3.37	3.59	56
$\rho = 2.2$	0.017	2.2	3.49	3.91	69
FIBROUS-UNBONDED "AAA"	0.017	1.2	3.58	3.41	48
FIBROUS-SILICONE					
BONDED "AA" (JM)	0.018	1.08	3.72	3.34***	45
(HITCO)	0.017	1.35	3.58	3.50	52
FIBROUS-PHENOLIC (JM)	0.018	1.12	3.68	3.40	47
BONDED "AA" (HITCO)	0.018	1.42	3.60	3.53	53
POWER-COLLOIDAL SILICA	0.012	3.15	2.55	3.78	64
MULTILAYER-GOLD ON KAPTON					
40 LAYERS/IN.	**0.021	2.12	4.28	4.25	84
60 LAYERS/IN.	**0.021	3.18	4.27	4.95	114
80 LAYERS/IN.	**0.020	4.29	4.04	5.5	138

* THICKNESS FOR HTF-200 FOAM SELECTED AT 3.00 INCHES - ALL OTHERS ARE FOR EQUAL HEAT LOSS (NEGLECTING EDGE EFFECTS).

** ASSUMES GOLD THICKNESS OF 350 Å

*** SELECTED MATERIALS FOR ISM'S

TABLE 8.1-1

FOAM ISM DESIGN

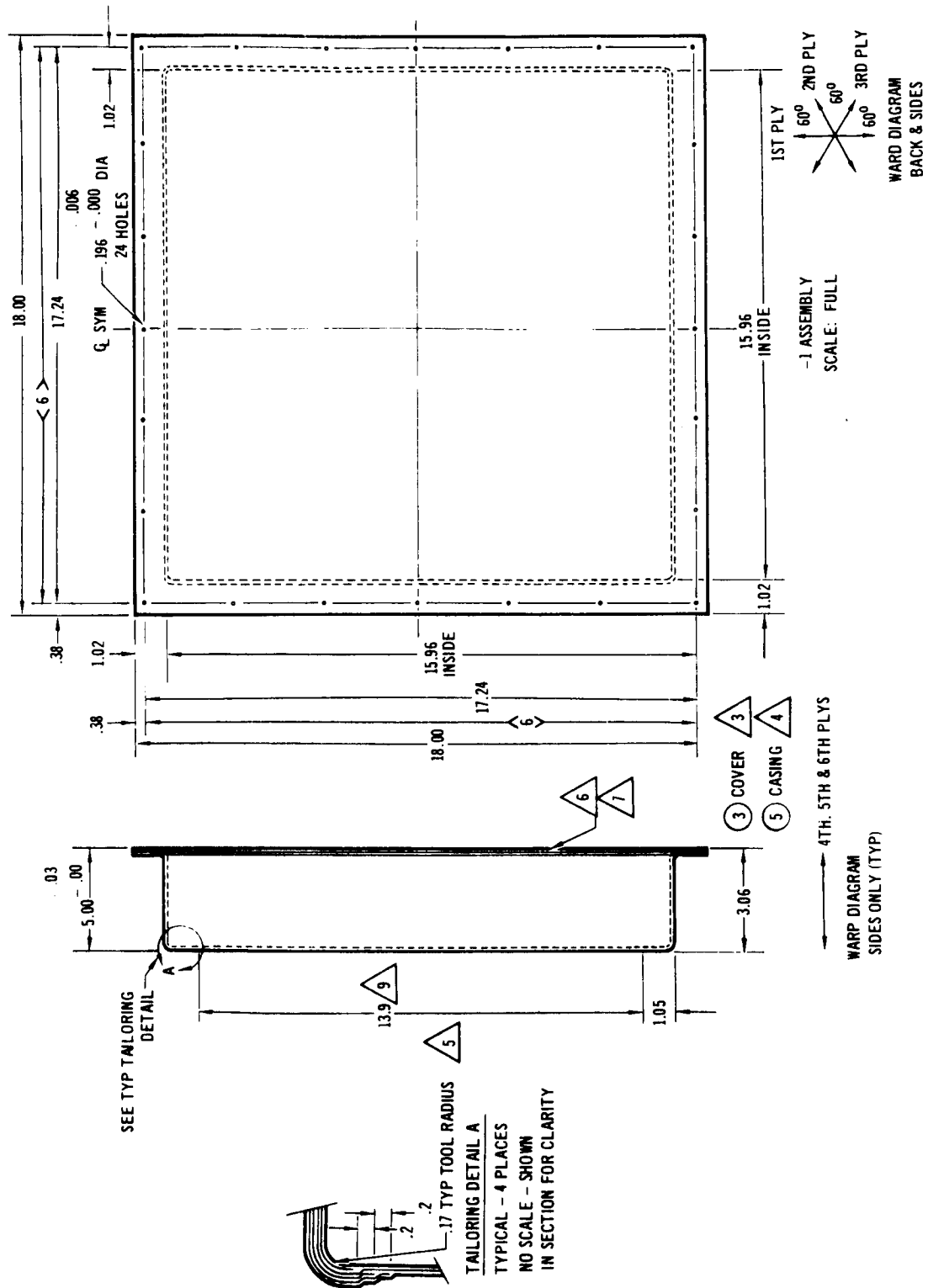


FIGURE 8.3-1

FIBERGLASS I SM DESIGN

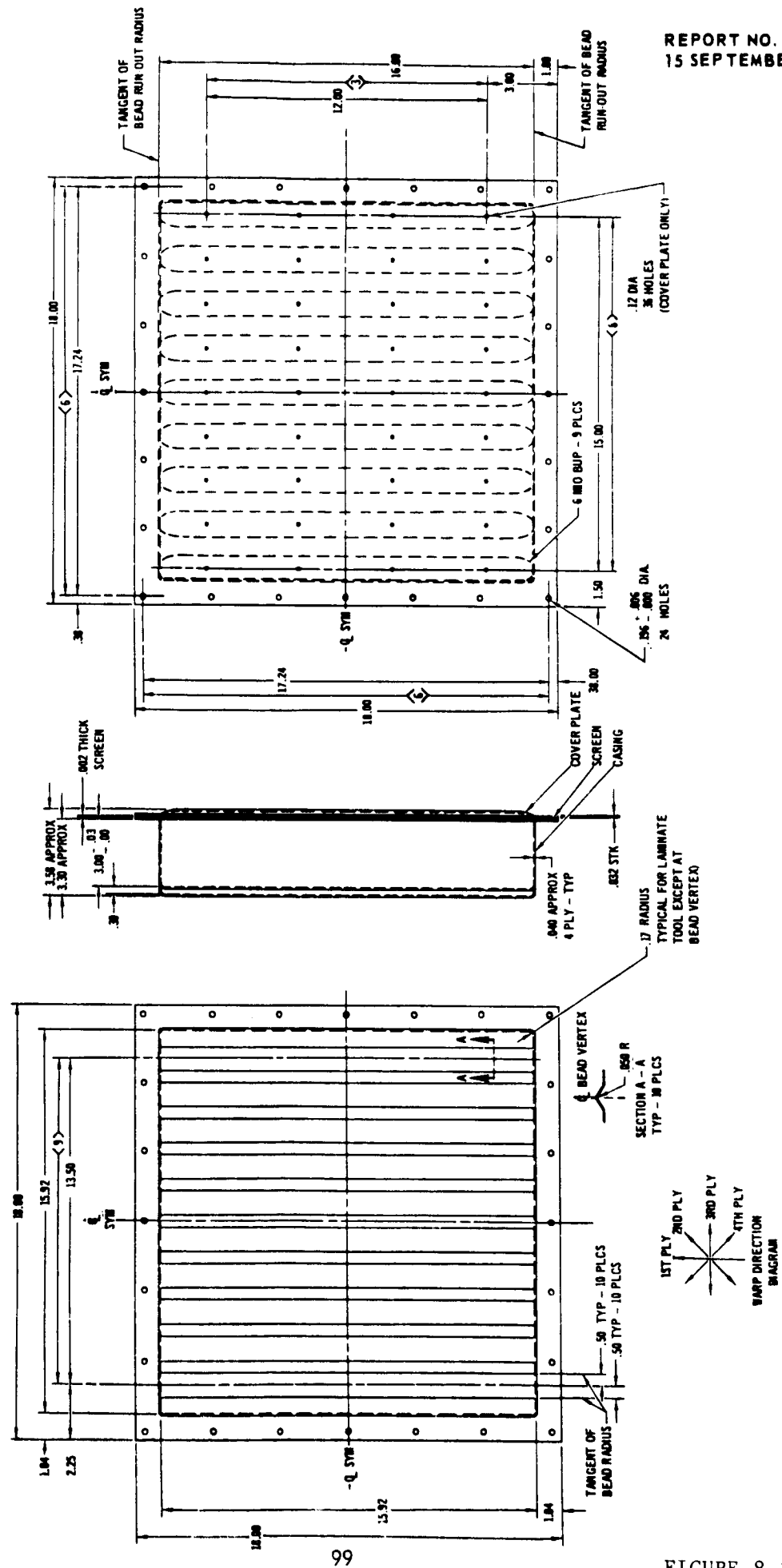


FIGURE 8.3-2

The cover was .012 inch thick 2024-T3 aluminum. Reinforcing beads similar to those used on the fiberglass ISM were unnecessary for the foam-stiffened sandwich structure.

A single homogeneous 3 inch thick foam core was preferred, but the delivery time needed to obtain three inch thick material could not be tolerated in the study schedule. Therefore, the foam sandwich was fabricated by bonding together three one inch thick pieces of the HTF-200 material. The adhesive employed to bond the sandwich was an epoxy-nylon consisting of 7 parts Epon 828, and 3 parts Versamid 125. The foam core was allowed to cure initially at room temperature under slight contact pressure, with a final cure of 8 hours at 150°F.

After bonding the core sandwich together it was sanded approximately 30 mils undersize from the inside bottom casing dimensions. The casing interior surfaces were also sanded and then solvent wiped for surface preparation. All faying surfaces were then given a coating of the same adhesive mixture used to bond the foam core sections together. After assembly the ISM was covered with bleed cloth, placed in a vacuum bag and cured while under a pressure of approximately 28 inches of mercury. The cure time for the ISM was similar to that used for the foam core.

After curing, the panel was cleaned by removing excess adhesive that had bled out and given 2 spray coats of 3M Co. Black Velvet paint to provide the high emittance coating needed for thermal performance testing.

8.3.2 Fiberglass ISM Fabrication - Layup and curing of the fiberglass casing were identical to that used for the foam ISM. The only differences in actual casing configurations were the greater wall thickness for the fiberglass ISM and the use of reinforcing beads.

The cover of the fiberglass ISM was .032 inch thick 2024-0 aluminum sheet. Nine reinforcing beads were placed in the cover per McDonnell Process Spec. 20006. Along the center line of each bead, 4 equally spaced holes 0.12 dia. were drilled for launch venting. The holes were at least 3 inches from either edge of the cover.

The Johns-Manville silicone bonded "AA" fiberglass Microlite was cut to fit into the casing. After the insulation was installed the 400 mesh screen and cover were bonded at the edges using clamps to hold the edges together until final cure. The adhesive and cure cycle was the same as that used for the foam ISM. After panel cleanup this ISM was also given three spray coats of 3M Co. Black Velvet. Shields were placed over the vent holes during spraying to prevent blockage of the fine wire screen.

8.4 FABRICATED WEIGHT COMPARISON - A comparison of actual and predicted component weight for the two ISM's is given in Table 8.4-1. The major weight differences for the foam panel were for bonding. The weight required to bond the three 1 inch sections was not included in the predictions. The remaining bonding weight was higher than expected due to bleeding into the fiberglass

FABRICATED WEIGHTS - INSULATION SYSTEM MODULES

TEST PANEL	*PREDICTED WEIGHT LB	FABRICATED WEIGHT LB	COMMENTS
FOAM INSULATION (DWG 474-00-0001)			
CASE (FIBERGLASS)	.64	.59	MFG VAR WITHIN EXPECTED TOLERANCE
COVER (ALUMINUM)	.39	.38	
FILM ADHESIVE	.29	.66	LOW VISCOSITY MASTIC TYPE EPOXY ADHESIVE USED
FOAM INSULATION (2.0 PCF)	.88	1.31	INCLUDES APPROX 0.43 LB OF ADHESIVE USED TO BOND ONE INCH LAYERS INTO THREE INCH THICKNESS
	<u>2.20</u>	<u>2.94</u>	
FIBROUS INSULATION (DWG 474-00-0002)			
CASE (FIBERGLASS)	1.42	1.28	MFG VAR WITHIN EXPECTED TOLERANCE
COVER (ALUMINUM)	1.04	1.05	
SCREEN (STAINLESS)	.06	.07 EST	
BONDING	-	.03 EST	COVER BONDED FOR HANDLING PROTECTION
FIBROUS INSULATION (1.2 PCF)	.53	.50	
	<u>3.05</u>	<u>2.93</u>	

*INCLUDES 5 PERCENT FABRICATION UNCERTAINTY

TABLE 8.4-1

laminate and possibly excessive clearance between the foam and the structure. These bonding weights would be eliminated in future panels by use of foam-in-place techniques.

For the fiberglass ISM all weight values were within expected manufacturing tolerance.

9. ENVIRONMENTAL TESTS

The tests discussed in this section were heat sterilization, thermal performance, launch depressurization, launch vibration, landing shock and thermal conductivity. The samples tested included the foam and fiberglass ISMs, material samples of these two insulations, and selected material samples which were considered to be back up candidates. With the exception of the Thermal Conductivity Test, the objective was to demonstrate the applicability of the two ISM materials for the Martian lander mission, and to identify which ISM had the better characteristics. The fiberglass ISM successfully passed all tests with no change in thermal performance. The foam ISM was destroyed when it failed during a test chamber pumpdown, thus eliminating the possibility of comparing the two ISM materials.

The results of the Thermal Conductivity Test provided the first reported data for fiberglass in the Martian atmospheric conditions, and indicated an appreciable change of thermal conductivity occurs over the postulated range of Martian conditions.

9.1 HEAT STERILIZATION TEST - The purpose of this test was to evaluate the effects of dry heat sterilization on the candidate thermal insulation materials. In addition to the foam and fiberglass ISMs two foam specimens which had been preconditioned for 20 hours at 275°F were included. Preconditioning was used to provide a basis for determining how rapidly changes occur during heat sterilization, and to evaluate whether preconditioning was an effective means of limiting change.

9.1.1 Test Samples - The samples evaluated are identified in Table 9.1-1. Included in the test were twelve Thermal Diffusivity Test specimens (6" x 6" x 6"), the two Insulation System Modules (18" x 18" x 3"), two Thermal Conductivity Test specimens and spare materials for both the ISM's and the thermal conductivity test. Selection of the Thermal Diffusivity test samples for heat sterilization is discussed in Section 7.2. Sealed canisters were used to isolate samples of each material to prevent cross contamination during the test. The canisters, Figure 9.1-1, were provided with inlet and outlet T-connectors to allow continuous nitrogen purging plus a means of installing thermocouples to measure the purge gas temperature. The volume of each canister was at least twice that of the specimen(s) in it. Aluminum foil was used as a gasket material on each canister, as shown in Figure 9.1-2 to prevent leakage of purge gas through the screw holes. After installation of the canister lid, 3MY9050 aluminized tape was wrapped around the lid edges to ensure no leak points.

9.1.2 Test Apparatus - An overall view of the heat sterilization system is shown in Figure 9.1-3. Five ovens were used for the test, four for specimens, and one for preheating the nitrogen purge gas. Two of the ovens were gravity convection-type without blowers. They were used as the test chambers for heating the twelve canisters with Thermal Diffusivity Test specimens, Figure 9.1-4. Four canisters were placed in one oven and eight canisters in

HEAT STERILIZATION TEST

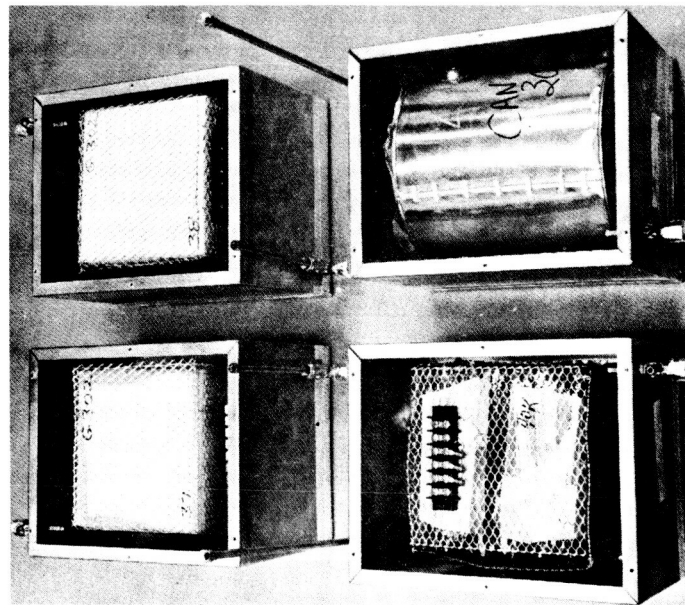
MATERIAL CLASS	DESIGNATION	VISUAL CHANGE	AVERAGE TEMPERATURE °F	WEIGHT CHANGE %
MULTILAYER	GOLD-ON-KAPTON	DECRINKLED LAYERS COLLAPSED	275	-0.58
POWDER	COLLOIDAL SILICA	NONE	276	-0.98
FIBROUS	UNBONDED "AAAA", J-M	NONE	270	-0.77
	UNBONDED "AAA", J-M	NONE	270	-0.67
	PHENOLIC BONDED "AA", J-M	DARKENED	293	-1.88
	SILICONE BONDED "AA", HITCO	NONE	257	-0.80
	SILICONE BONDED "AA", J-M	NONE	269	-0.95
	SILICONE BONDED "AA", J-M THERM. COND. & SPARE SAMPLES	NONE	274	-0.02
FIBROUS ISM*	SILICONE BONDED "AA", J-M	NONE	274	-3.74
FOAM	POLYPHENYLENE OXIDE (PPO)	NONE	261	-1.58
	POLYURETHANE G-302	SHRANK	281	-0.85
	POLYURETHANE G-302, PRECONDITIONED	SLIGHT SHRINKAGE	283	0.0
	ISOCYANURATE HTF-200	DISCOLORED	273	-2.52
	ISOCYANURATE HTF-200, PRECONDITIONED	DISCOLORED	276	0.0
	ISOCYANURATE, HTF-200 THERM COND & SPARE SAMPLES	DISCOLORED	280	-3.96
FOAM ISM*	ISOCYANURATE, HTF-200	PEELED AT BOND FLANGE	280	-3.10

* SEALED IN A LARGE CANISTER, ALL OTHERS IN INDIVIDUAL SMALL CANISTERS

TABLE 9.1-1

HEAT STERILIZATION TEST SAMPLES

THERMAL DIFFUSIVITY SPECIMENS
IN ISOLATION CANISTERS



THERMAL CONDUCTIVITY & ISM MATERIALS
& ISM PANEL IN CANISTER

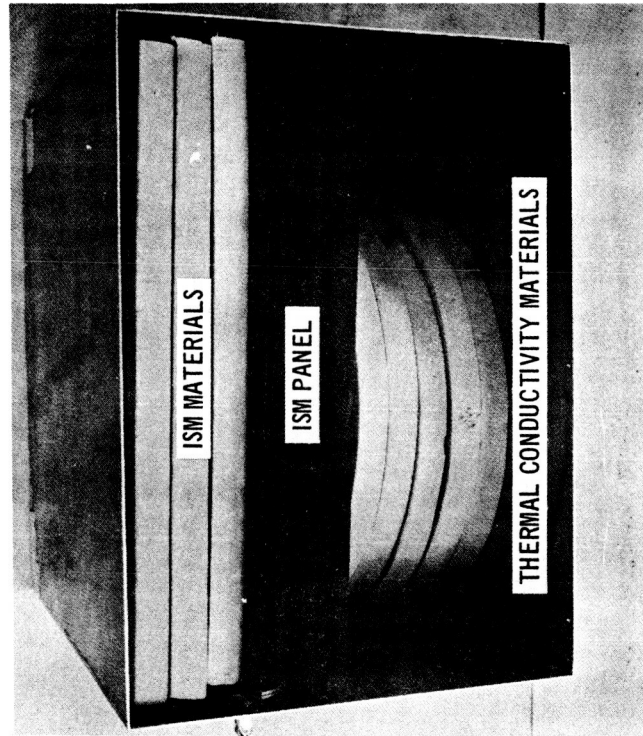


FIGURE 9.1-1

ALUMINUM FOIL COVERING OF SMALL CANISTER PRIOR TO FINAL ASSEMBLY

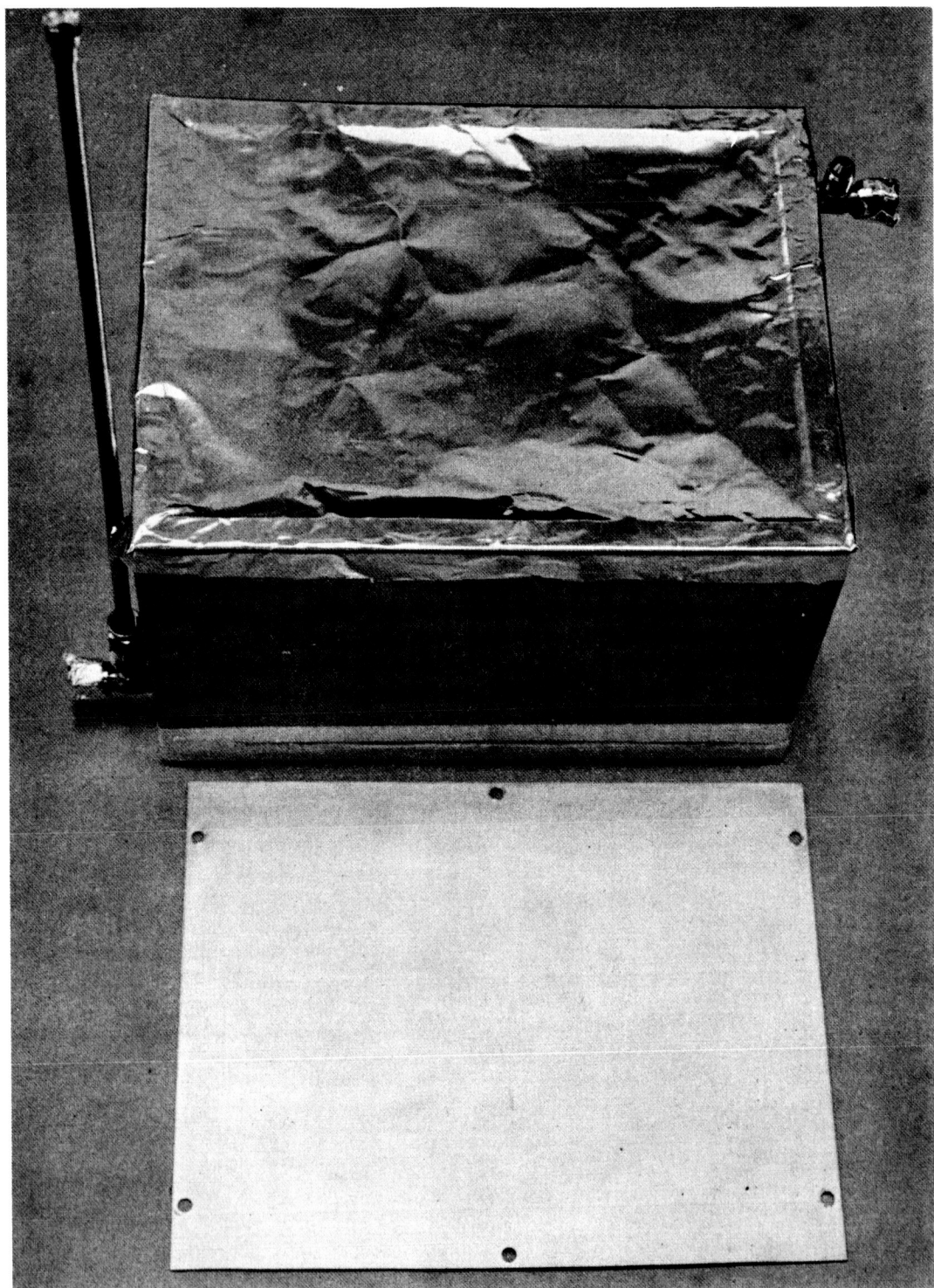


FIGURE 9.1-2

HEAT STERILIZATION TEST SETUP

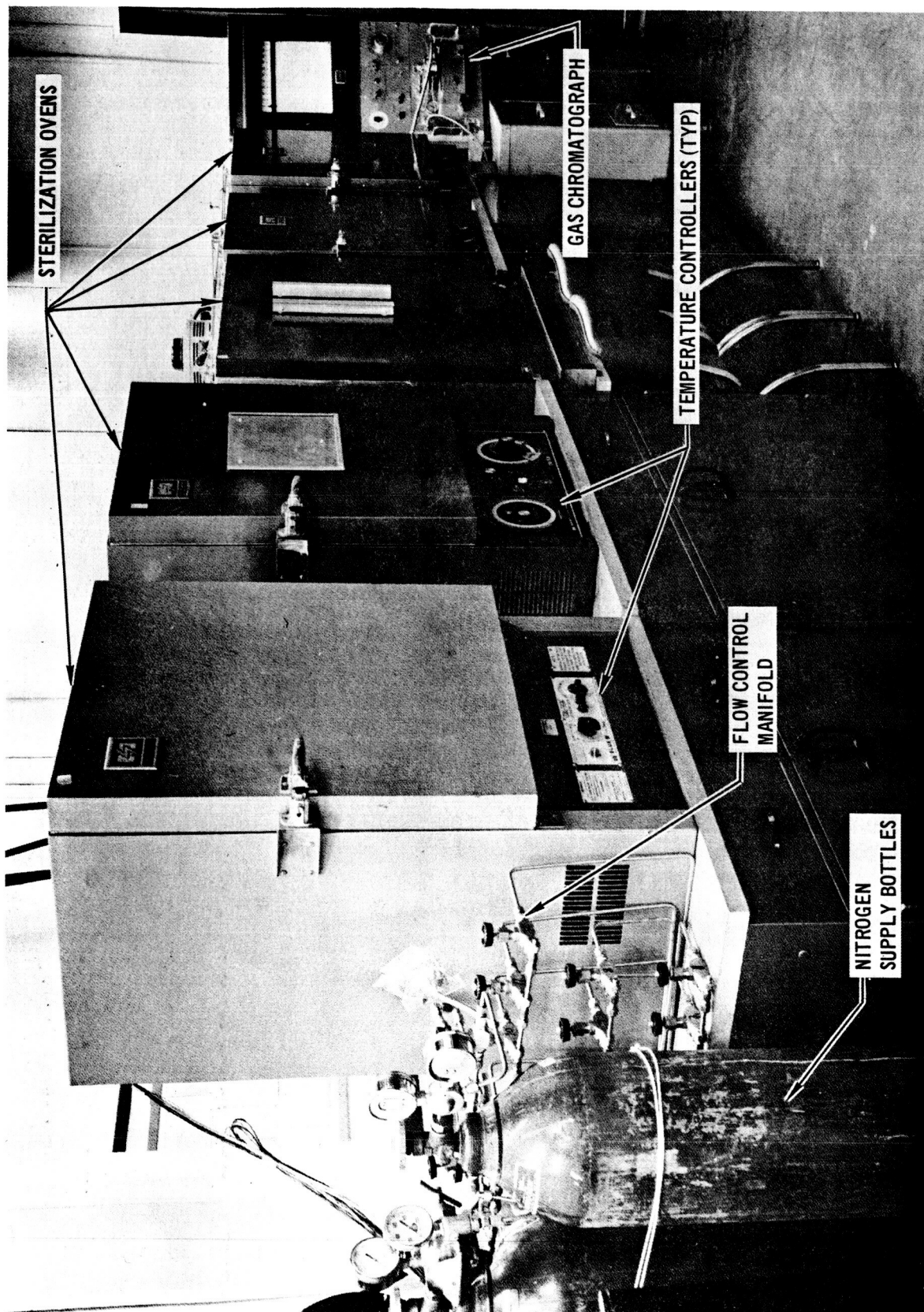


FIGURE 9.1-3

HEAT STERILIZATION TEST SETUP

THERMAL DIFFUSIVITY SPECIMENS
IN STERILIZATION OVEN

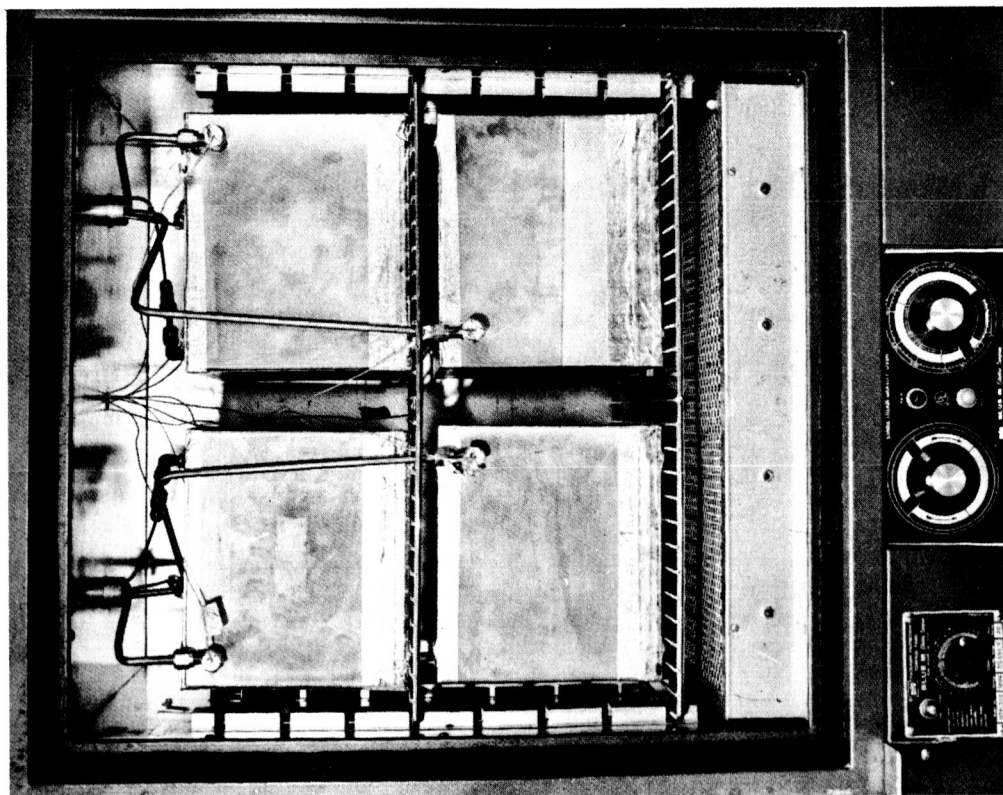


FIGURE 9.1-4

THERMAL CONDUCTIVITY & ISM MATERIALS
& ISM PANELS IN STERILIZATION OVEN

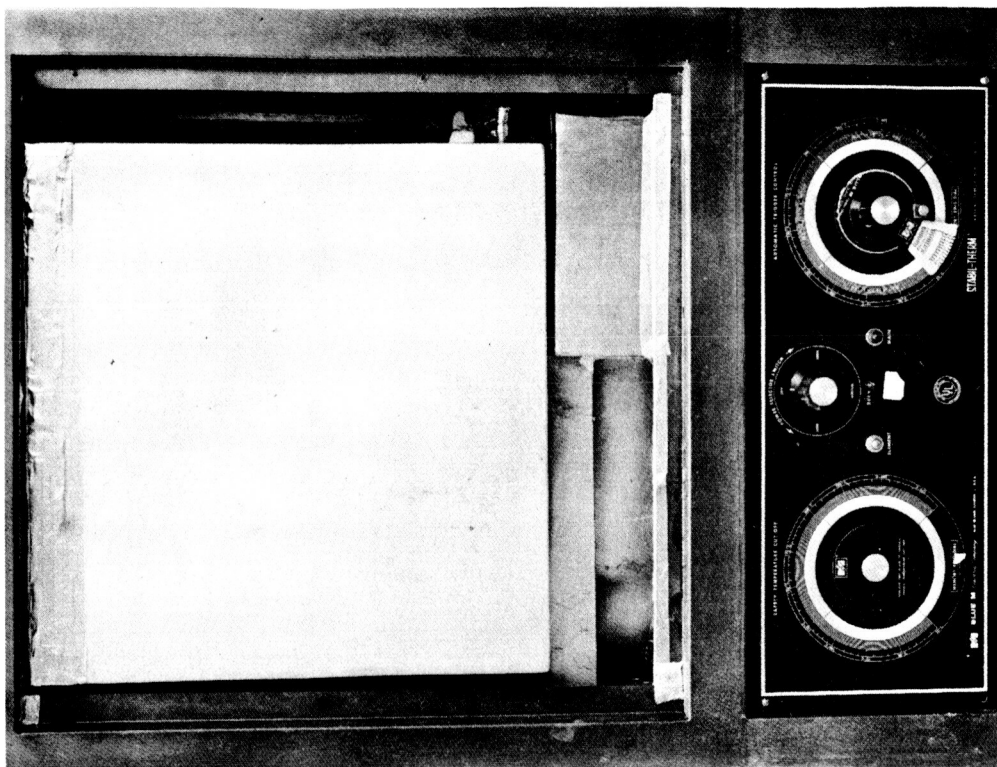


FIGURE 9.1-5

the other oven. Each canister had a separate valve-controlled nitrogen purge system and a preheater coil arrangement for controlling the flow and for heating the nitrogen purge gas before it entered the canister.

The two large canisters (18 1/8" x 18 1/8" x 13 1/8") each containing the high value candidate materials of one type were installed in two mechanical convection-type ovens with blowers, Figure 9.1-5. In addition to the T-connections for purging and monitoring the gas temperature, a thermocouple for monitoring the internal canister temperature was inserted through a small hole in the top of each large canister.

A 0 to 500°F, 24-channel Bristol temperature recorder and a Minneapolis Honeywell 0 to 300°F, 12-channel temperature recorder, both calibrated to an accuracy of $\pm 2.0^\circ\text{F}$, were employed to monitor the purge gas temperature. Each recorder had a cycle time of less than two minutes for recording all test points.

Twenty-four iron-constantan thermocouples (28 gage), all cut to the same length and from the same spool, were employed for use with the Bristol 24-channel temperature recorder. Nine copper-constantan thermocouples (28 gage), also cut to the same length and from the same spool were employed with the other recorder.

The twenty-four iron-constantan thermocouples were employed as follows: (a) one each in the inlet and outlet ports of the eight Thermal Diffusivity sample canisters in one oven, (b) one for measuring the oven reference temperature, (c) one as a reference point temperature in the oven containing the preheater coils, (d) one each as the reference point temperature in the two canisters containing the ISM's and thermal conductivity specimens, and (e) one each in the inlet and outlet ports of these two canisters to monitor the purge gas temperature.

The nine copper-constantan thermocouples were used separately to monitor the inlet and outlet purge gas temperature of the four Thermal Diffusivity sample canisters heated in the second oven, and to record a reference point temperature of this oven.

The first and last cut of each kind of thermocouple wire were certified by McDonnell Bureau of Standards as meeting the vendor's specifications, and then each was calibrated at three points (250°F, 275°F, and 300°F) to an accuracy of $\pm 1^\circ\text{F}$ for the iron constantan wire and $\pm 0.5^\circ\text{F}$ for the copper constantan wire.

A Fisher Gulf gas chromatograph, Model 300, was used to analyze for oxygen in the purge gas effluent from each canister.

9.1.3 Test Description - Each test specimen was weighed prior to and following the heat sterilization cycle. The canisters were then installed in the ovens, Figures 9.1-4 and 9.1-5. Figure 9.1-4 also shows the thermocouples installed in the inlet and outlet T-connector and taped in place with aluminized tape.

To start the test, the specimen canisters were flushed with nitrogen gas at 68 to 77°F until the concentration of oxygen in the exhaust gas from each canister was less than 0.25 percent. The nitrogen was certified to meet specification MIL-P-2740113, and was filtered through a 0.45 micron filter.

Heat-up for all ovens was started at a rate of 35°F per hour so that the 275°F stabilized condition was reached within a period of 360 ± 18 minutes. Nitrogen purge was continued during the heat-up period and throughout the test with continuous venting and preheating when necessary to maintain the required temperature. The heat soak period was begun when the oven reference temperature reached $275 \pm 10^\circ\text{F}$. Heat soaking continued for a total of 384 hours. This duration simulated exposure to 6 heat cycles of 64 hours each. A 6 hour cool down to room temperature concluded the test exposure.

9.1.4 Test Results - Weight and appearance changes of the candidate materials are noted in Table 9.1-1. All but two of the specimens experienced a weight loss after the 384 hours heating. Four of the twelve thermal diffusivity specimens exhibited visual changes. One specimen, the multilayer crinkled gold-on-Kapton material, decrinkled, causing the layers to collapse; another specimen of closed-cell polyurethane foam showed appreciable shrinkage. The closed-cell isocyanurate foam specimen showed slight warpage and discoloration, and the phenolic-bonded fiberglass specimen darkened. One sample each of two foam materials, HTF-200 and G-302 had been preconditioned for heat sterilization by exposing them to 20 hours at 275°F with continuous nitrogen purging. The weight loss during preconditioning was 1.6% for the HTF-200, and 1.0% for the G-302. These samples lost no additional weight during the 384 hours exposure, indicating that weight loss in these materials occurs during the first 20 hours of exposure, and that preconditioning can be used effectively to drive off volatiles.

The isocyanurate foam materials in one large canister showed effects from the heat. The foam ISM peeled at three of the four corners along the bond between the fiberglass laminate and the aluminum cover. The foam thermal conductivity specimens and the spares were slightly discolored.

The silicone bonded "AA" fiberglass materials in the other large canister showed no visible changes. Weight loss in this ISM was attributed to the fiberglass laminate casing since the bare Thermal Diffusivity and Thermal Conductivity samples exhibited negligible weight loss.

The results of the gas chromatographic analyses for oxygen content in each canister are shown in Table 9.1-2. Oxygen content was never in excess of 0.16% by volume of the purge gas during the entire test, and was well within the specified limit of 0.25%.

Average temperatures for the nitrogen purge gas during the 384 hour heat-soak period are also shown in Table 9.1-1. These values were based on 32 random readings (two a day) for the thermocouples located in the inlet and outlet ports of each canister during the 16 day heat-soak period. Eleven of the fourteen canisters were within the specified $275 \pm 10^\circ\text{F}$ range.

OXYGEN CONTENT OF PURGE GAS DURING HEAT STERILIZATION

CANISTER NO.	SPECIMEN		OXYGEN LEVEL (PPM)		
	GENERAL TYPE	DESIGNATION	START	MID-WAY	FINAL
1	CLOSED CELL ISOCYANURATE	HTF-200-31	1610	548	214
2	GOLD-ON-KAPTON (CRINKLED)	40 LAYERS/IN.	1020	274	171
3	CLOSED CELL POLYURETHANE	G302-38	1050	137	393
4	CLOSED CELL POLYURETHANE	G302-37	555	137	159
5	UNBONDED "AAAA" FIBER	104-14	128	684	171
6	COLLOIDAL SILICA	3093-49	128	376	214
7	SILICONE BONDED "AA" (HITCO)	T G 15000-23	128	308	171
8	CLOSED CELL POLY- PHENOLENE OXIDE	PPO-33	128	367	285
9	PHENOLIC BONDED "AA" (JM)	MICROLITE-25	64	327	357
10	SILICONE BONDED "AA" (JM)	MICROLITE-21	64	329	371
11	CLOSED CELL ISOCYANURATE	HTF-200-32	64	230	267
12	UNBONDED "AAA" FIBER	106-11	64	198	228
13	CLOSED CELL ISOCYANURATE	FOAM ISM, HTF-200 SAMPLES	1111	258	668
14	SILICONE BONDED "AA"	FIBROUS ISM, MICROLITE SAMPLES	900	288	482

TABLE 9.1-2

The averaged temperature readings for the three canisters outside of these limits were 257°F, 261°F, 293°F for canister No's 7, 8, and 9 respectively. Materials contained in each canister are identified in Table 9.1-2. Figure 9.1-6 shows the temperature profile of canisters 14, 7, and 9 that ran normal, lower and higher respectively than $275 \pm 10^\circ\text{F}$ during the 384 hour heat-soak period. Figures 9.1-7 and 9.1-8 show the reference points during the heat up and cool down periods. Variation in temperature within the test oven partly accounts for Canister 9 showing an average temperature of 293°F. This canister was located in a hot spot in the oven.

9.1.5 Conclusions - The test conclusions were as follows:

- o Multilayer gold-on-Kapton, G-302 closed-cell polyurethane foam, phenolic-bonded fiberglass, and HTF-200 closed-cell isocyanurate foam materials were affected by prolonged heating at 275°F.
- o The multilayer and G-302 foam materials were sufficiently affected to preclude their further consideration as candidate materials.
- o Further consideration of the phenolic-bonded fiberglass and HTF-200 foam, which were somewhat affected, should be based on additional post sterilization test results.
- o Preconditioning of the two foam materials indicated that weight changes in these materials occur within the first 20 hours of heating, and that preconditioning of materials before fabrication can be used to limit further changes during heat sterilization.

9.2 THERMAL PERFORMANCE TESTS (1 & 2) - The thermal performance tests were planned to provide a comparison of the heat loss characteristics of heat sterilized Insulation System Modules (ISM) panels before and after exposure to the launch pressure profile and to the mission vibration and landing shock loads. This test was performed in vacuum and in the 20 mb maximum model Mars atmosphere conditions.

9.2.1 Test Samples - In the initial test, prior to vibration and shock, the two ISM panels, one incorporating closed-cell isocyanurate foam (Upjohn HTF-200) and the other silicone-bonded "AA" fiberglass (J. M. Microlite) were to be evaluated. ISM instrumentation varied and is discussed in the test descriptions. The foam panel failed during the initial chamber pump down, and a mock ISM panel made from HTF-200 foam was substituted. The second test, following vibration and shock, utilized the same mock ISM and the original fiberglass ISM.

9.2.2 Test Apparatus - The apparatus developed to evaluate the thermal performance of these panels, Figure 9.2-1 was a guarded assembly comprised of a central heater, core heaters for each ISM panel, closed cell foam guard insulation, and cold panels. The apparatus was installed in a 5.5-foot diameter vacuum chamber as shown in Figure 9.2-2. The three heaters were 16 x 16 inch, consisting of nichrome wire interwoven in fiberglass cloth and impregnated with silicone rubber. Thickness for each heater was 0.055

TEMPERATURE PROFILES FOR CANISTERS 14,7,9 DURING THE 384-HOUR HEATING PERIOD

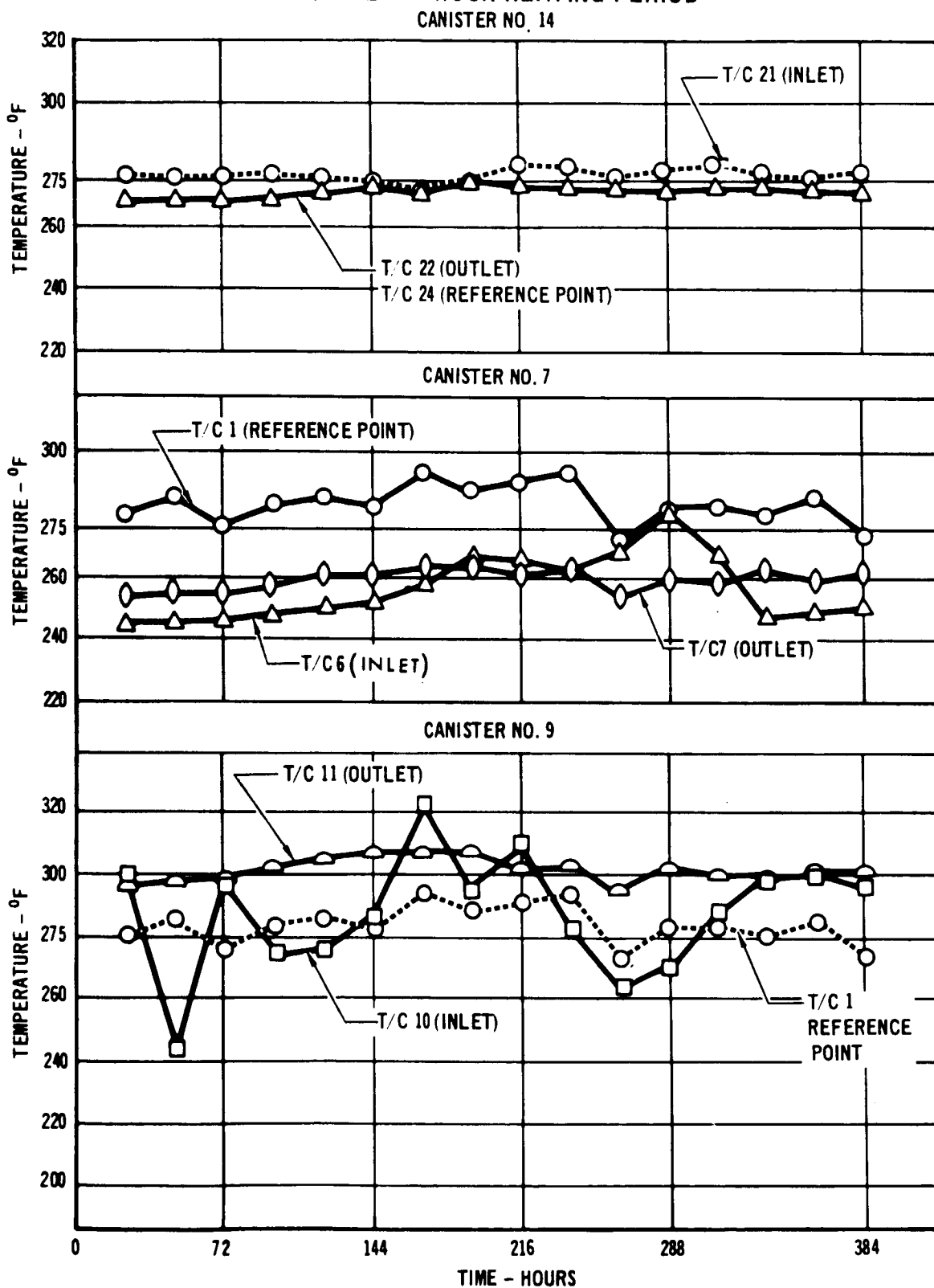


FIGURE 9.1-6

TEMPERATURE PROFILE OF REFERENCE POINT THERMOCOUPLES DURING 6-HOUR HEAT UP PERIOD

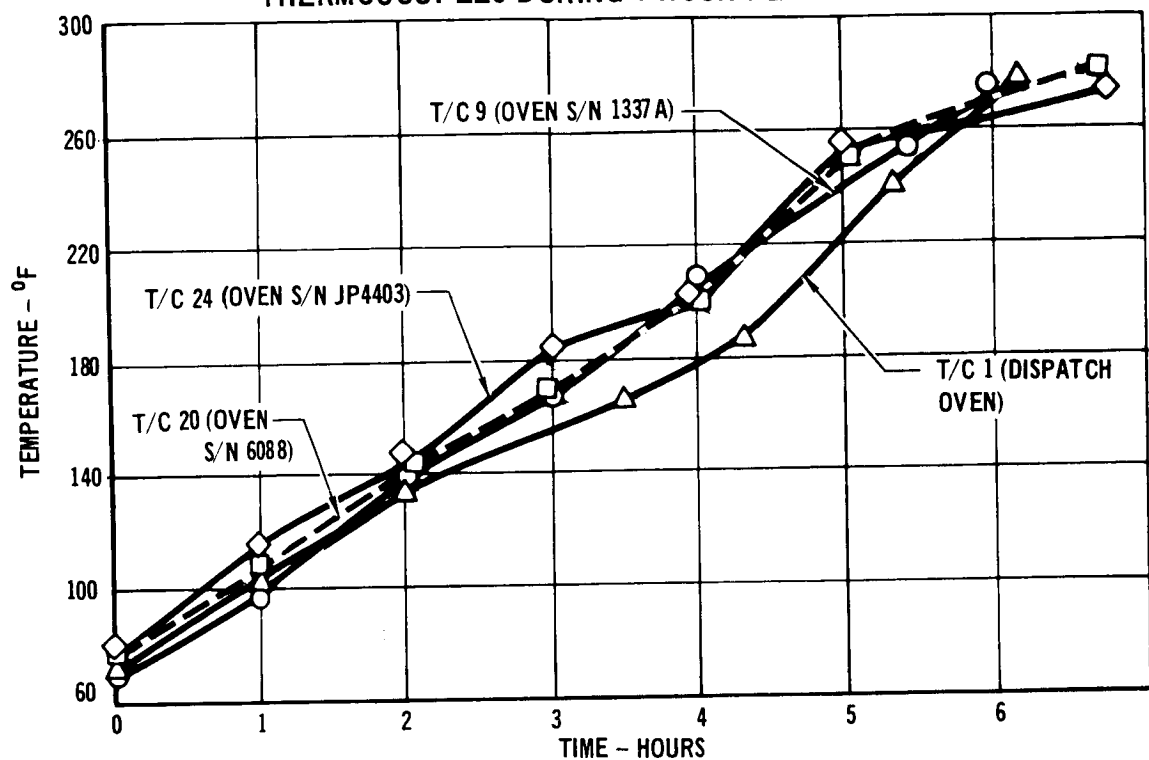


FIGURE 9.1-7

TEMPERATURE PROFILES OF REFERENCE POINT THERMOCOUPLES DURING 6-HOUR COOL DOWN PERIOD

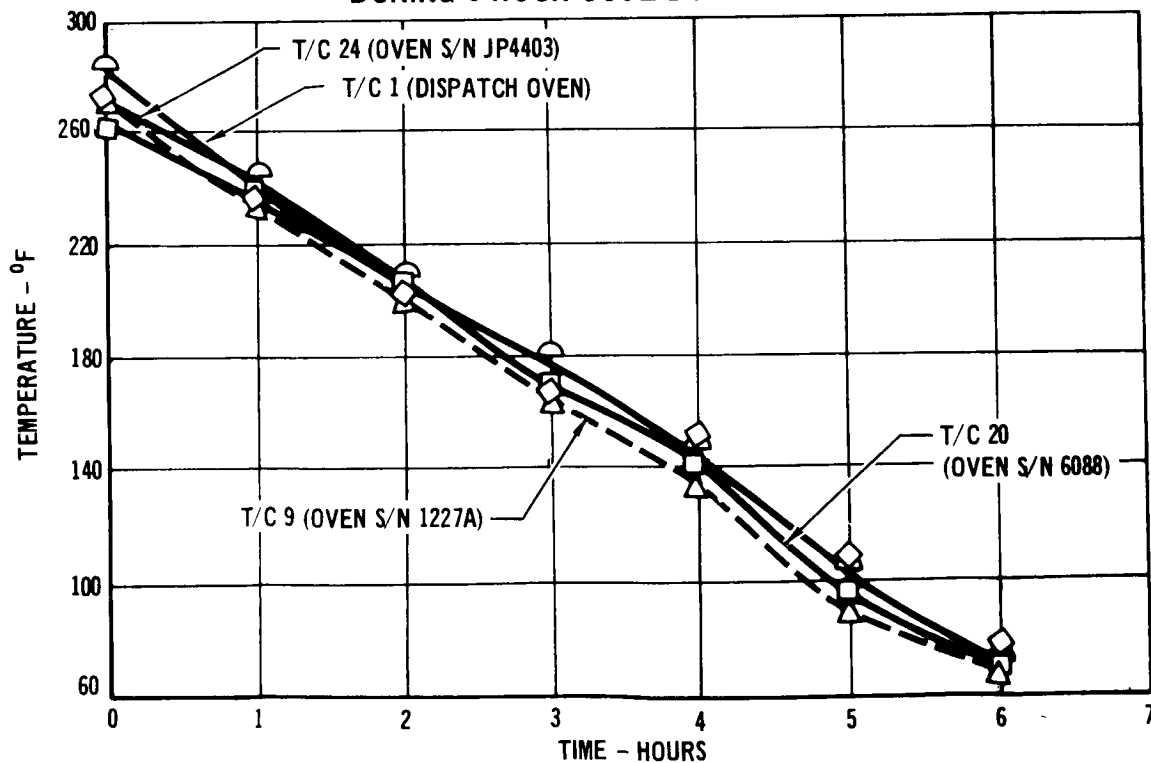
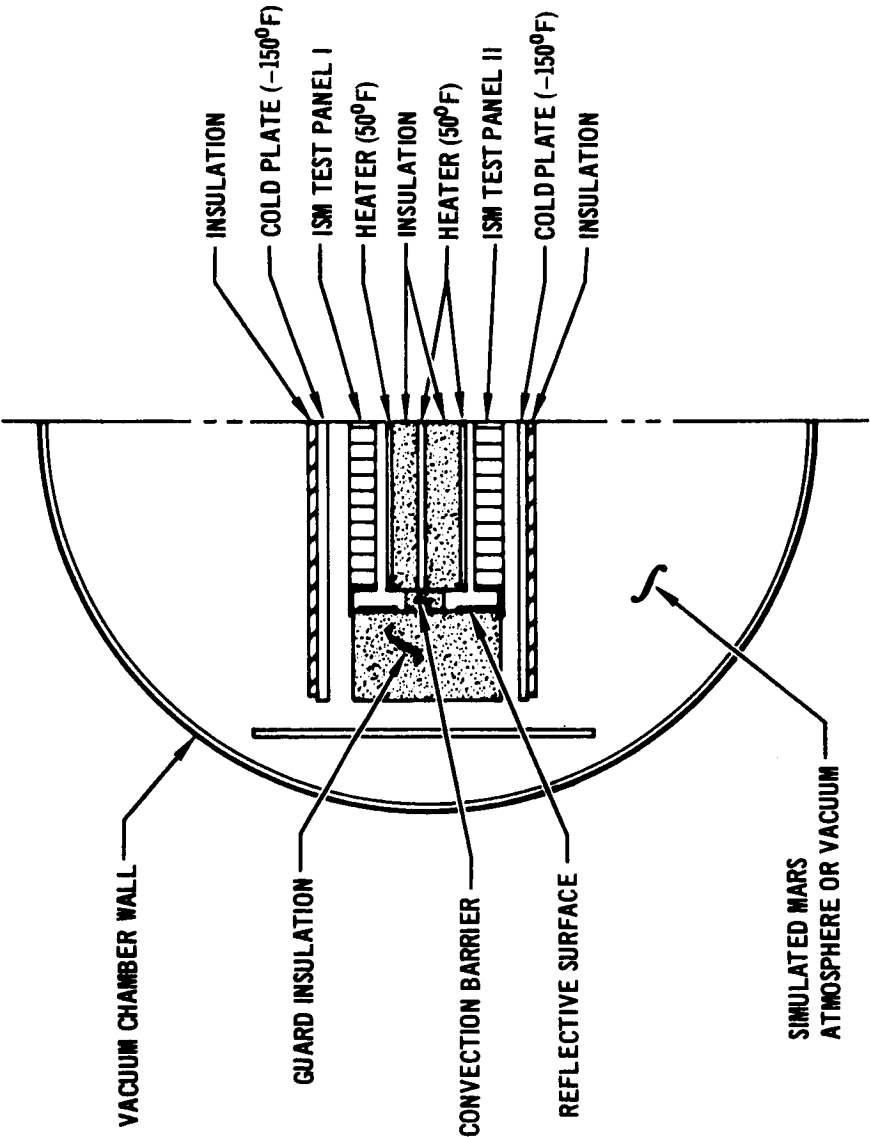


FIGURE 9.1-8

THERMAL PERFORMANCE TEST APPARATUS



NOTE: ALL TEST SURFACES BLACKENED TO APPROACH A TOTAL NORMAL EMISSIVITY OF 1.

FIGURE 9.2-1

THERMAL PERFORMANCE TEST APPARATUS
(UPPER COLD PANEL RAISED, AND GUARD
INSULATION REMOVED TO SHOW CONFIGURATION)

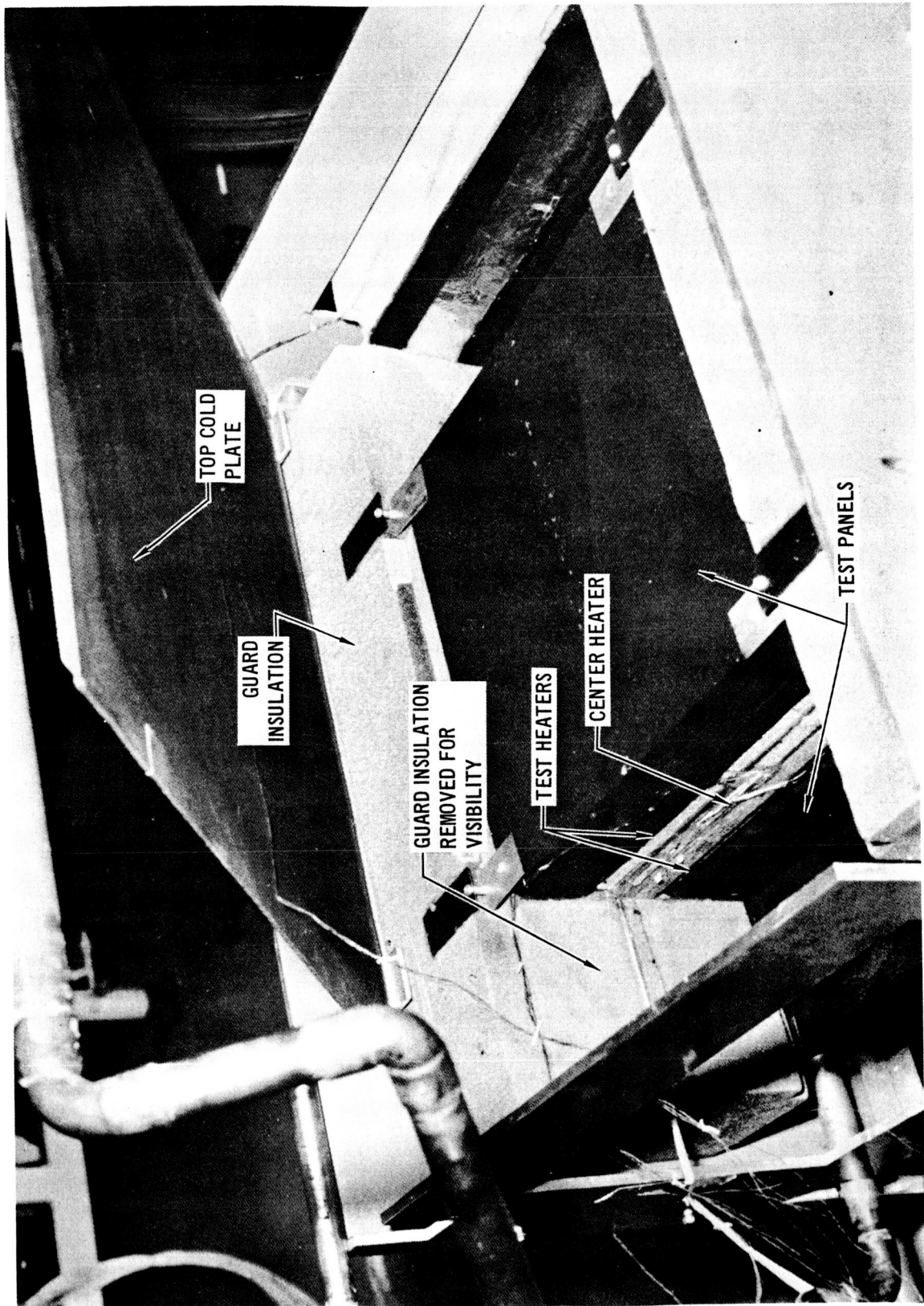


FIGURE 9.2-2

inch. The cold plates were of 16 gage 304 ELC stainless steel fabricated into a single embossed panel with parallel flow paths. Overall panel size was 29 x 29 in. with 0.31 in.² cooling channels. Panel cooling was provided by a continuously controlled gaseous nitrogen supply. Temperature was measured with premium grade copper-constantan thermocouples (30 gage), and displayed on two, twenty-four channel strip chart recorders. System pressures were measured with Bayard-Alpert ionization gages, and aneroid manometers.

9.2.3 Test Description - The experimental program included an overall test system evaluation, an initial ISM panel thermal performance evaluation before exposure to vibration and landing shock loads, and a final test at the same conditions to examine the panel for any changes in heat loss. The initial vacuum test condition was achieved by evacuating the system at a rate simulating the pressure profile anticipated during launch.

During testing the heaters were maintained at an average temperature of $50^{\circ} \pm 5^{\circ}\text{F}$ and the cold panels were chilled to $-150^{\circ} \pm 10^{\circ}\text{F}$. Thermal equilibrium was established for the system during each test under conditions of (a) vacuum, and (b) simulated Mars atmosphere. The criteria for thermal equilibrium was that system temperature changes be less than 2°F per hour.

- o Test System Evaluation - System evaluation and checkout were performed, using mock ISM panels as substitutes for the actual test articles. These mock panels were sandwiches made from Upjohn Company HTTF-200 foam blocks. Three foam blocks, each 16-inches square and 1-inch thick, were bonded together with Dow Corning Silastic 140 to form each 3 inch thick mock panel. Each panel was instrumented with six copper-constantan thermocouples and then sprayed with 3M Nextrel brand Black Velvet coating. Thermocouple locations for the interior of the apparatus and the guard insulation are identified in Figures 9.2-3 and -4.

Testing was accomplished under conditions of vacuum (6.5×10^{-7} Torr) and simulated Mars atmosphere (20 mb, 19% CO₂, 60% N₂, 21% A). Equilibrium temperatures and the electrical heater power required to maintain these levels are given in Table 9.2-1. Good agreement was obtained between data for the top and bottom test panel, particularly when it is noted that the higher heat losses in the upper panel corresponded with greater temperature drop. This indicated comparable thermal conductivity in the two identical panels.

- o Thermal Performance Test Number 1 - The two ISM test panels were placed in the test apparatus with the fiberglass panel in the upper test zone and the foam panel in the lower test zone. During pretest checks, the vacuum chamber was evacuated at the normal pumpdown rate shown in Figure 9.2-5. This rate is less than that required to simulate the launch pressure profile. When observation through the

THERMAL PERFORMANCE TEST THERMOCOUPLE LOCATIONS FOR TEST SAMPLES, HEATERS AND COLDPLATES

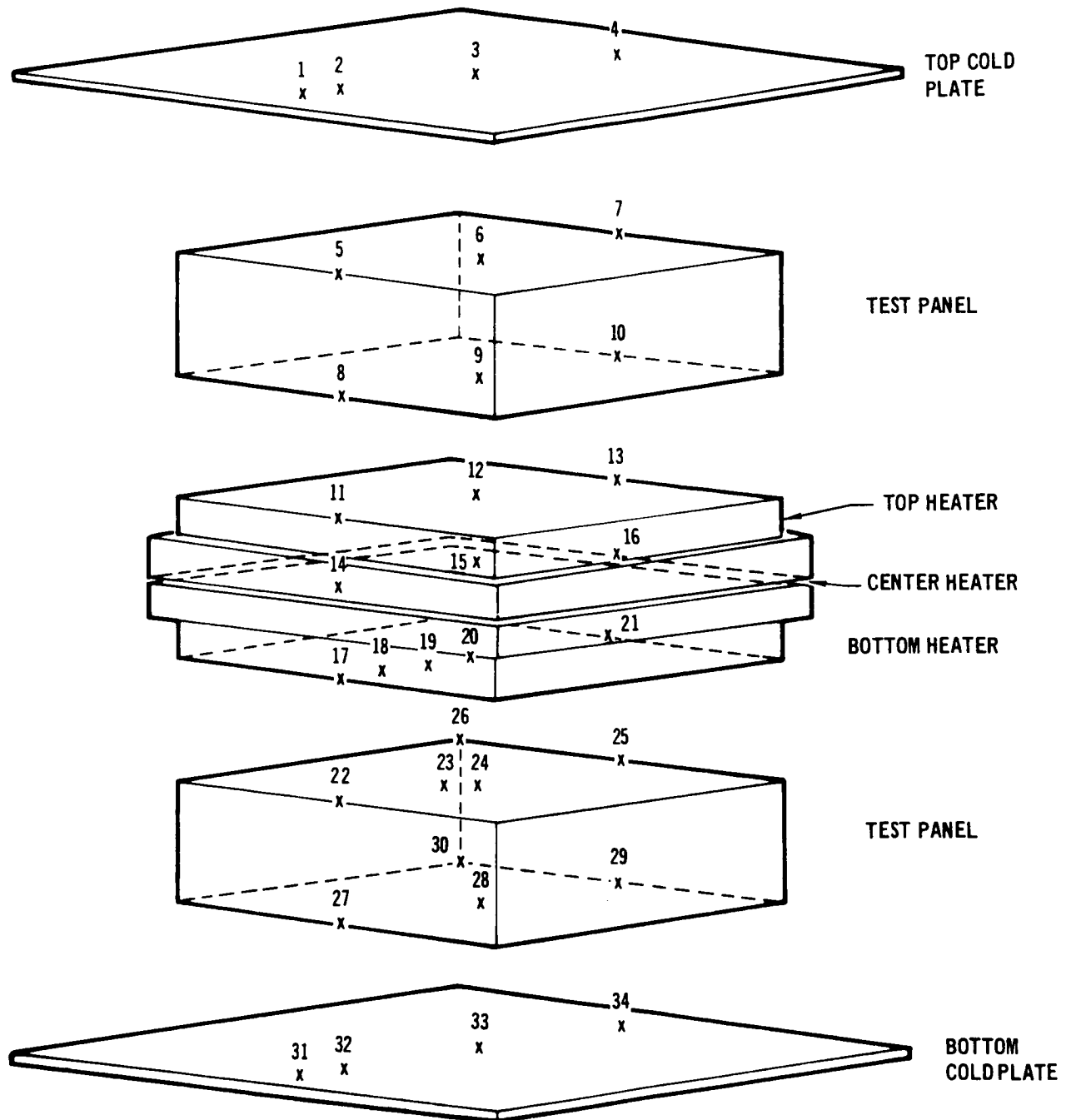


FIGURE 9.2-3

THERMAL PERFORMANCE TEST THERMOCOUPLE LOCATIONS FOR GUARD INSULATION

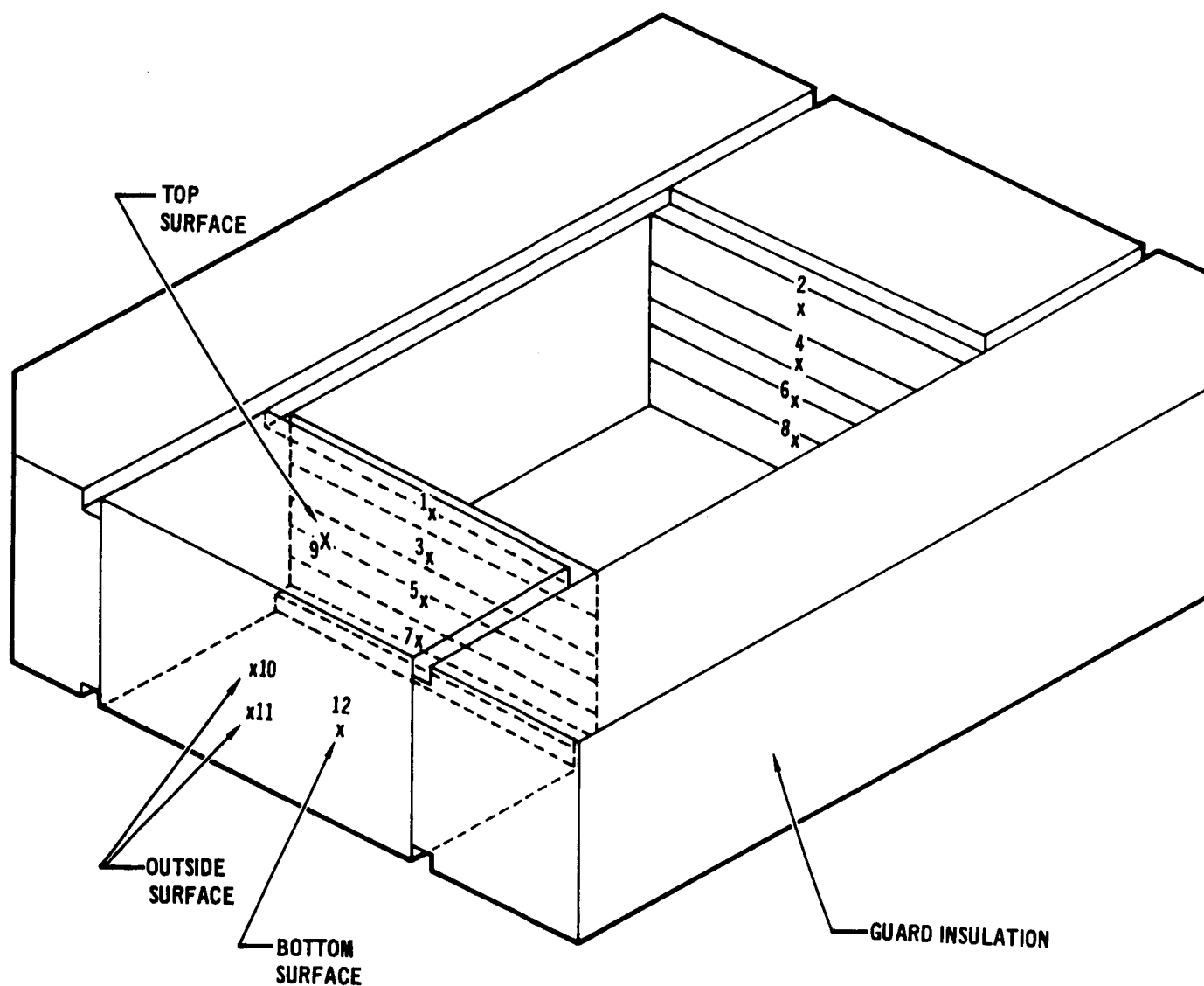


FIGURE 9.2-4

THERMAL PERFORMANCE TEST DATA
TEST APPARATUS EVALUATION PHASE

THERMO COUPLE NO.	VACCUUM		MARS ATM	
	INTERNAL °F	GUARD °F	INTERNAL °F	GUARD °F
1	-158	- 66	-177	- 81
2	-154	- 75	-170	- 81
3	-144	0	-149	7
4	-140	- 5	-141	11
5	-100	3*	-118	17*
6	-102	- 10	-115	8
7	-102	- 87	-109	- 99
8	26	- 68	23	- 75
9	61	-100	60	-138
10	44	-	39	-
11	47	4	38	16
12	66	-106	61	-134
13	53		42	
14	50		48	
15	52		50	
16	52		52	
17	50		41	
18	-		-	
19	-		-	
20	61		59	
21	48		40	
22	30		27	
23	-		-	
24	50		53	
25	40		37	
26	-		-	
27	-106		-116	
28	-103		-102	
29	-109		-119	
30	-		-	
31	-		-145	
32	-149		-160	
33	-140		-145	
34	-144		-150	

HEATER POWER:

	VACUUM	MARS ATM
TOP:	6.54 WATTS	7.07 WATTS
CENTER:	2.98	5.00
BOTTOM:	5.83	6.60

PRESSURE:

VACUUM: 6.5×10^{-7} TORR
MARS ATM: 15 TORR (20 MB),
19% CO₂, 60% N₂,
21% A BY VOLUME

* VALUE MAY BE INACCURATE
DUE TO MALFUNCTIONING
SENSOR.

TABLE 9.2-1

VACUUM CHAMBER PUMPING RATES

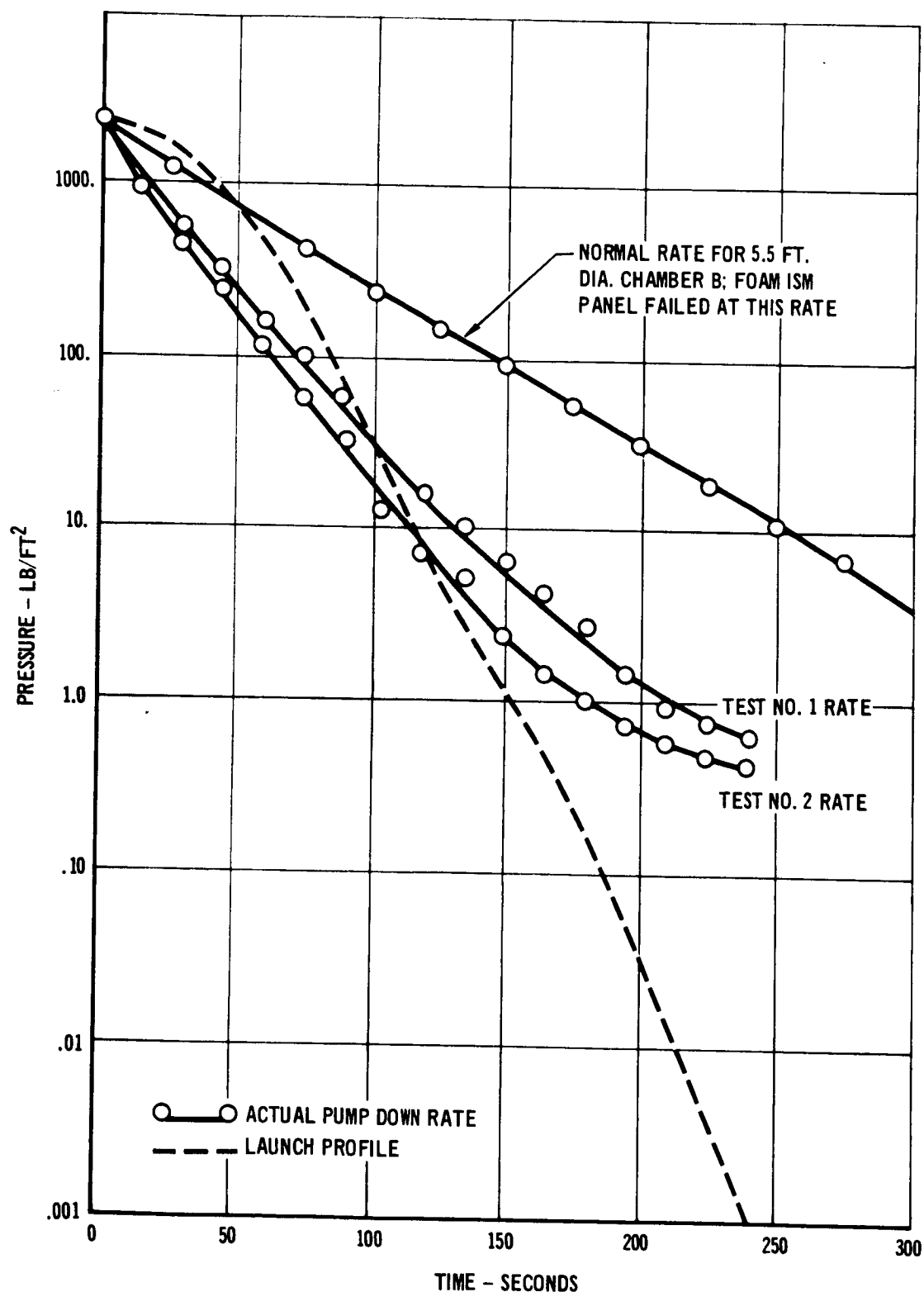


FIGURE 9.2-5

chamber view port revealed a change in alignment of the test apparatus components, the chamber was back-filled and opened. As shown in Figure 9.2-6, the sealed, foam panel had failed to withstand the pressure differential experienced during chamber evacuation by forcefully breaking open along the cover plate edge bond area. The foam within broke into many small fragments which were dispersed throughout the chamber volume.

Rather than delay testing pending the fabrication of a new foam panel, it was decided to continue testing with only the fiberglass insulated ISM. One of the mock panels was substituted for the foam ISM, and was installed in the apparatus in the upper test zone. The fibrous ISM panel was placed in the lower test zone, and thermal performance testing continued.

The chamber was evacuated at the rate shown in Figure 9.2-5. Equilibrium temperatures were then attained for both vacuum and simulated Mars atmosphere conditions. These temperatures and the associated data are given in Table 9.2-2 and Figures 9.2-7 and -8. At the completion of this test the ISM panel was removed from the apparatus and subjected to vibration and shock testing.

- o Thermal Performance Test Number 2 - The ISM panel was replaced in the thermal performance evaluation apparatus after completion of vibration and shock testing. Pressure and temperature environments of the first thermal performance test were repeated. The ISM panel and heater temperature profiles were better established for this second test by installing two additional thermocouples on each surface. Data from this phase are compared with test No. 1 in Table 9.2-2 and Figures 9.2-7 and -8.

9.2.4 Test Results - The results of these tests as shown by Figure 9.2-7 and -8 indicate that the thermal performance of the ISM panel remained unchanged after exposure to the mission vibration and landing shock environments. The sealed foam ISM panel experienced structural failure when exposed to a chamber pumpdown rate that was less severe than the anticipated launch pressure profile.

9.2.5 Conclusions - The silicone bonded fiberglass ISM successfully survived the Mars mission requirements to which it was exposed with no change in thermal performance or loss of structural integrity. The foam panel failed from unknown causes during a normal chamber pumpdown. Element tests which were designed to help develop the cause of panel failure are discussed in Section 10.1.

9.3 LAUNCH VIBRATION TEST - The purpose of this test was to expose the Insulation System Module (ISM) to the expected launch vibration environment. Subsequent testing determined whether the launch vibration environment and landing shock environment affected the thermal performance of the ISM.

FOAM ISM PANEL AFTER FAILURE

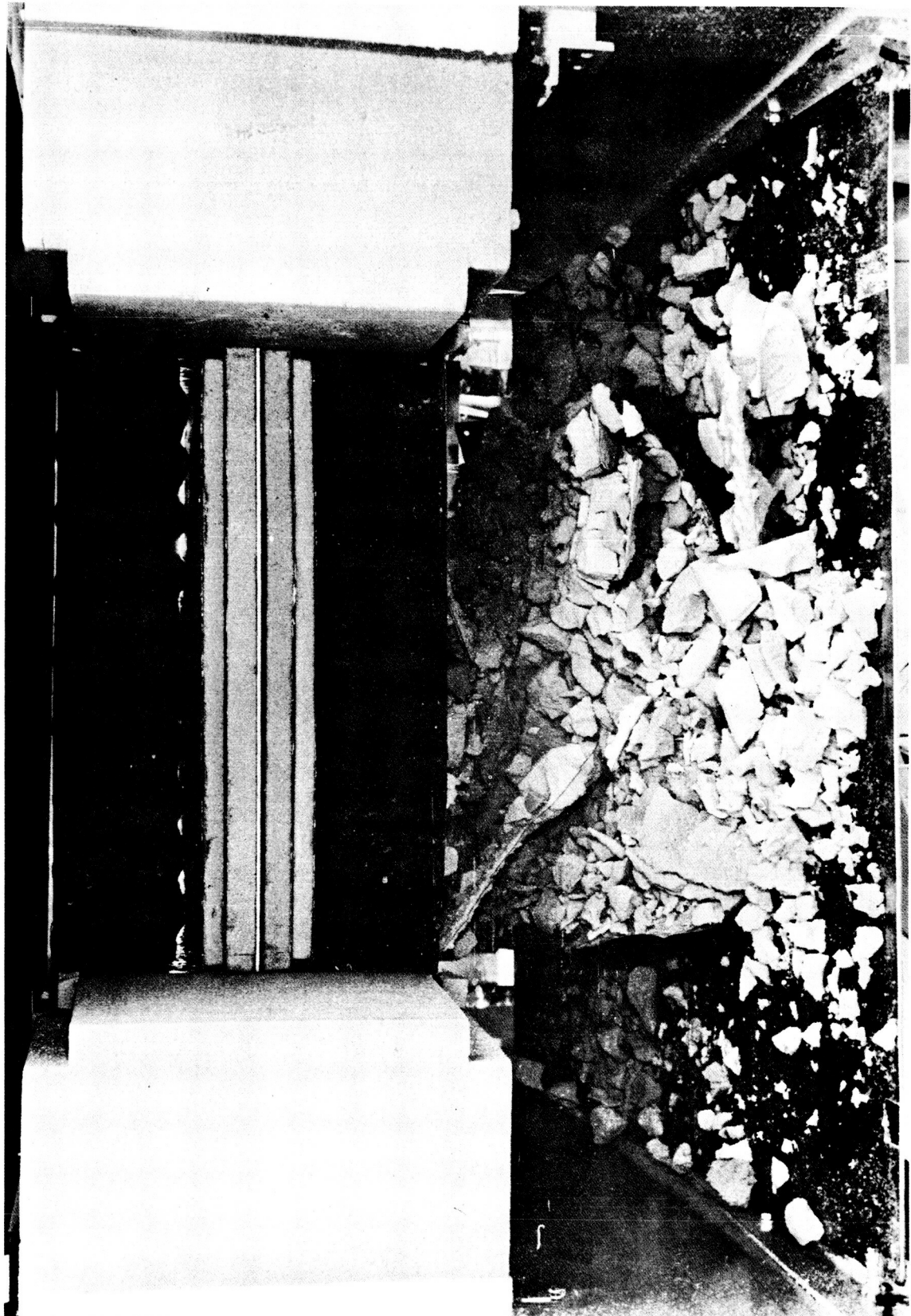


FIGURE 9.2-6

THERMAL PERFORMANCE TEST DATA
ISM EVALUATION

THERMO COUPLE NO.	VACUUM				MARS ATM			
	INTERNAL		GUARD		INTERNAL		GUARD	
	TEST 1 °F	TEST 2 °F	TEST 1 °F	TEST 2 °F	TEST 1 °F	TEST 2 °F	TEST 1 °F	TEST 2 °F
1	-158	-158	- 95	- 99	-160	-161	- 95	- 99
2	-155	-153	- 68	- 73	-153	-156	- 66	- 71
3	-144	-146	- 5	- 5	-135	-136	5	3
4	-140	-142	3	- 7	-128	-129	19	12
5	-100	-99	6*	5*	-101	-100	-	22*
6	-104	-104	- 9	- 7	-104	-104	10	13
7	-102	-101	- 70	- 64	-100	-100	- 71	- 66
8	22	17	- 53	- 52	25	22	- 59	- 55
9	52	52	-114	-112	57	59	-138	-136
10	37	35	0	0	41	41	17	17
11	43	43	1	2	39	40	18	17
12	59	59	-110	-112	59	61	-121	-121
13	44	41			41	41		
14	48	47			47	46		
15	49	50			49	49		
16	50	50			51	50		
17	40	41			40	40		
18	-	48			-	48		
19	-	58				57		
20	61	61			62	61		
21	41	41			40	40		
22	20	22			26	25		
23	-	56			-	54		
24	59	59			57	55		
25	36	37			33	32		
26	14	13			14	13		
27	-129	-128			-111	-111		
28	-129	-131			-110	-111		
29	-125	-131			-109	-112		
30	-125	-128			-108	-110		
31	-157	-157			-158	-158		
32	-151	-153			-144	-146		
33	-146	-148			-132	-134		
34	-150	-153			-140	-144		

*VALUE MAY BE INACCURATE DUE TO MALFUNCTIONING SENSOR.

TABLE 9.2-2

EQUILIBRIUM TEMPERATURE DATA THERMAL PERFORMANCE TESTS NO. 1 AND 2 VACUUM PHASE

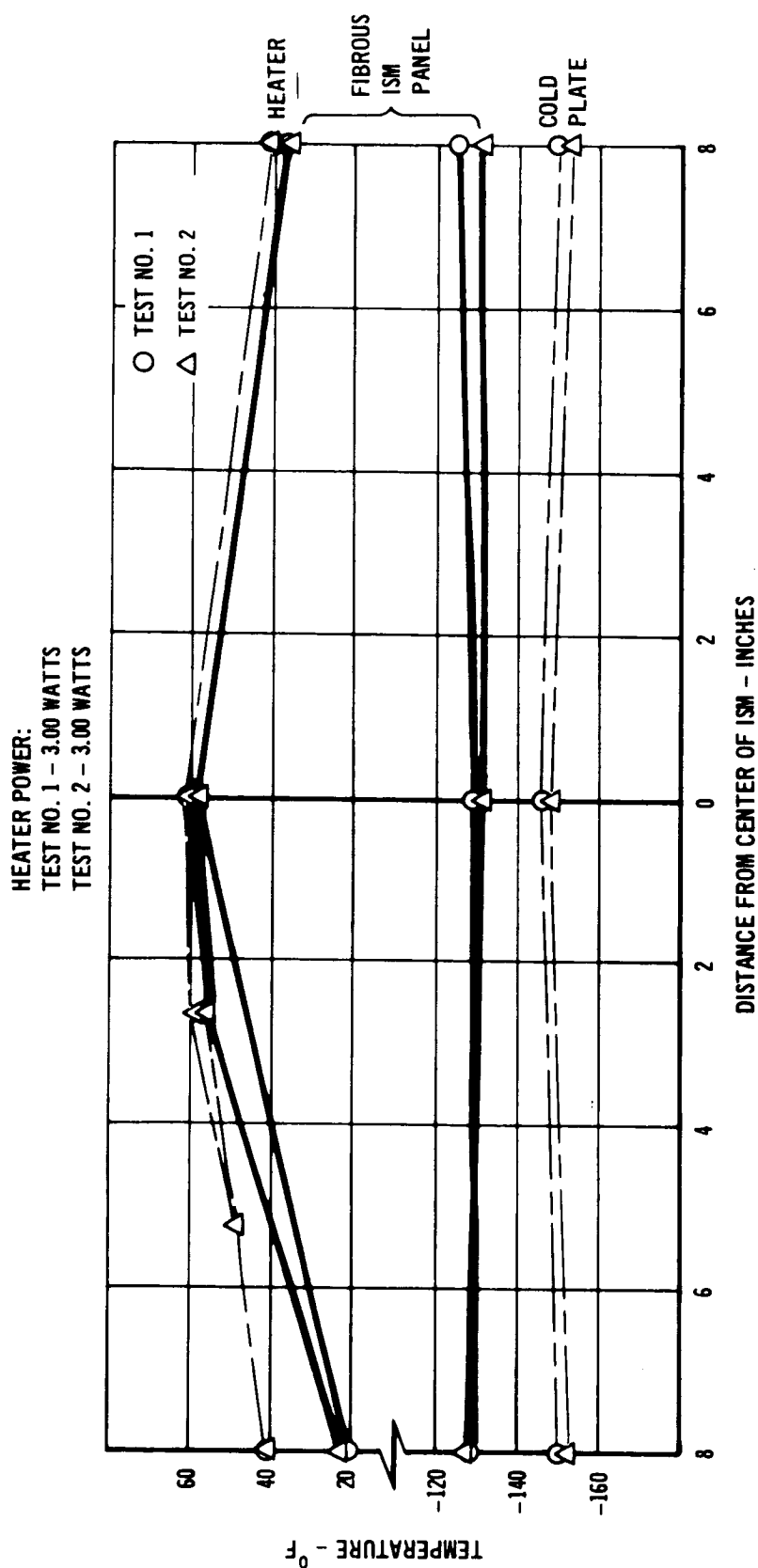


FIGURE 9.2-7

EQUILIBRIUM TEMPERATURE DATA
THERMAL PERFORMANCE TESTS NO. 1 & NO. 2
MARS ATMOSPHERE PHASE

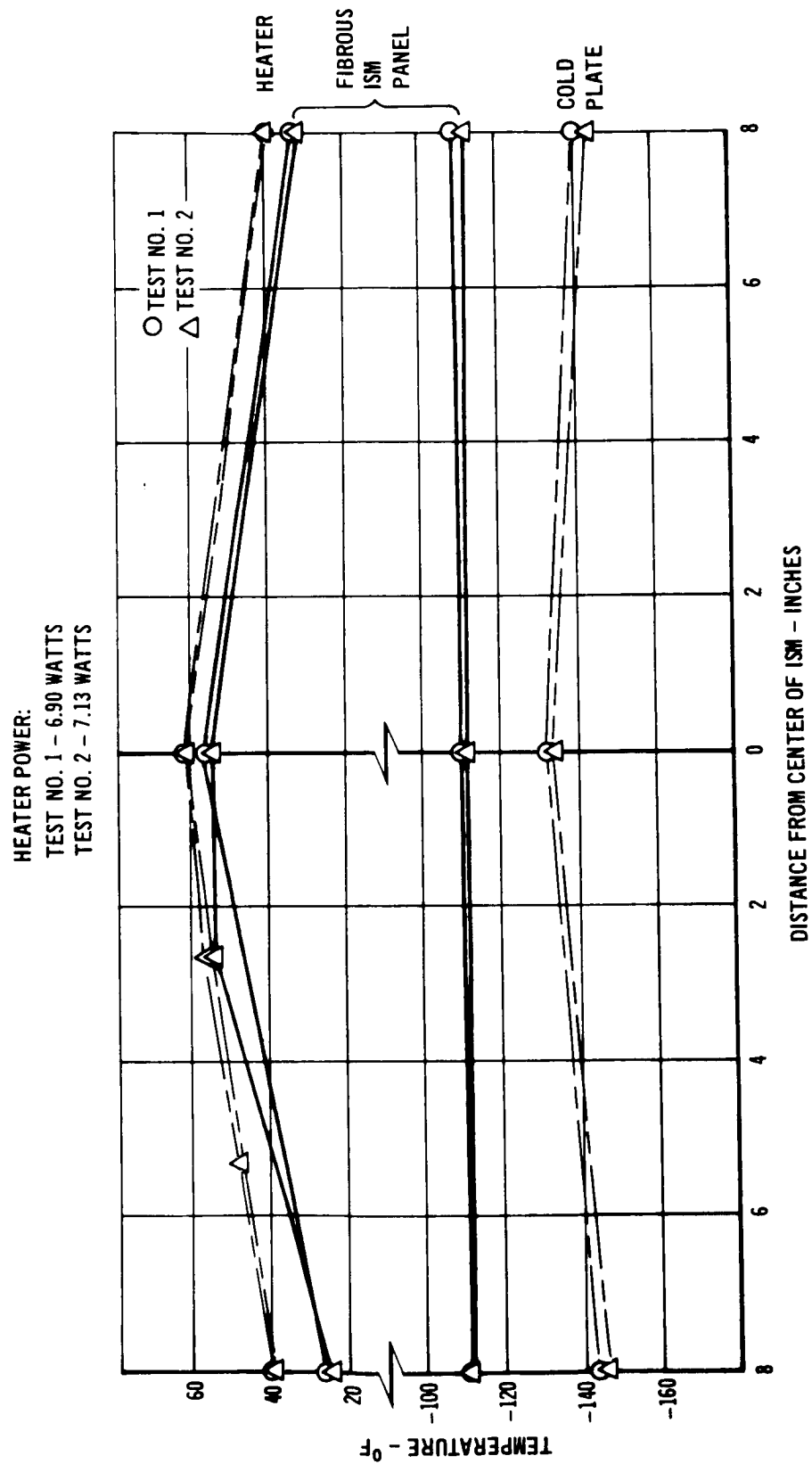


FIGURE 9.2-8

9.3.1 Test Sample - The test specimen was the 474-00-0002 fiberglass ISM panel described in Section 8.0. The specimen had previously undergone heat sterilization and initial thermal performance testing.

9.3.2 Test Apparatus - The ISM was mounted in a vibration test fixture to simulate a typical spacecraft installation. This assembly was then fastened to an electromagnetic exciter. Figure 9.3-1 shows the setup for testing in the vertical axis. A vibration pickup and two piezoelectric accelerometers (three piezoelectric accelerometers for testing in the vertical axis), located at the mounting edge of the specimen, were used to monitor the vibration environment applied to the panel. Structural response acceleration levels were also monitored by piezoelectric accelerometers mounted on the cover plate of the ISM.

9.3.3 Test Description - A frequency response survey was conducted on the ISM, consisting of one 10-minute sweep cycle during which the frequency was varied logarithmically from 5-2000 Hz. The vibration levels were 0.2 inch double amplitude for frequencies of 5 to 10 Hz, and 1g for frequencies of 10 to 2000 Hz. Following the frequency response survey, random vibration testing was conducted. Before testing, the exciter system, with the test fixture installed was equalized so the desired random excitation would be reproduced at the location of the input accelerometer. The ISM was then mounted on the fixture and subjected to 4.5 minutes of vibration testing. Any changes from the desired random excitation caused by the addition of the test specimen were automatically compensated for by the equalizer/analyzer. The specified launch vibration environment for all axes tested is presented in the spectrum curve 1 on Figure 9.3-2. The same procedure was followed for testing in each of two test axes (lateral and vertical). For testing in the vertical axis, the input control accelerometer was located near the fixture on the shaker head. The input control accelerometer for testing in the lateral axis was input accelerometer 1, located on the area shown in Figure 9.3-1, but oriented with the sensitive axis along the lateral axis.

The ISM was inspected for external structural damage before and after each phase of vibration.

9.3.4 Test Results - The frequency response of the test specimen and the fixture is presented as acceleration transmissibility plots, Figure 9.3-3. These curves present the transmissibility (ratio of the specimen response acceleration to the input control acceleration) plotted versus the applied excitation frequency. Curve 1 is the vertical response of the fixture at input 1 location, and Curve 2 is the vertical response of the center of the cover plate to a vertical acceleration input. Analyses of the applied, random-vibration environments are presented as power spectral density (PSD), Figure 9.3-2. These curves are plots of power spectral density (g^2/Hz) versus frequency (Hz), and indicate the energy distribution of the vibration environment applied to the specimen. The required PSD is shown in Figure 9.3-2 as Curve 1 and test results at input 1 accelerometer location as Curves 2 and 3,

VIBRATION TEST SETUP FOR TESTING IN THE VERTICAL AXIS

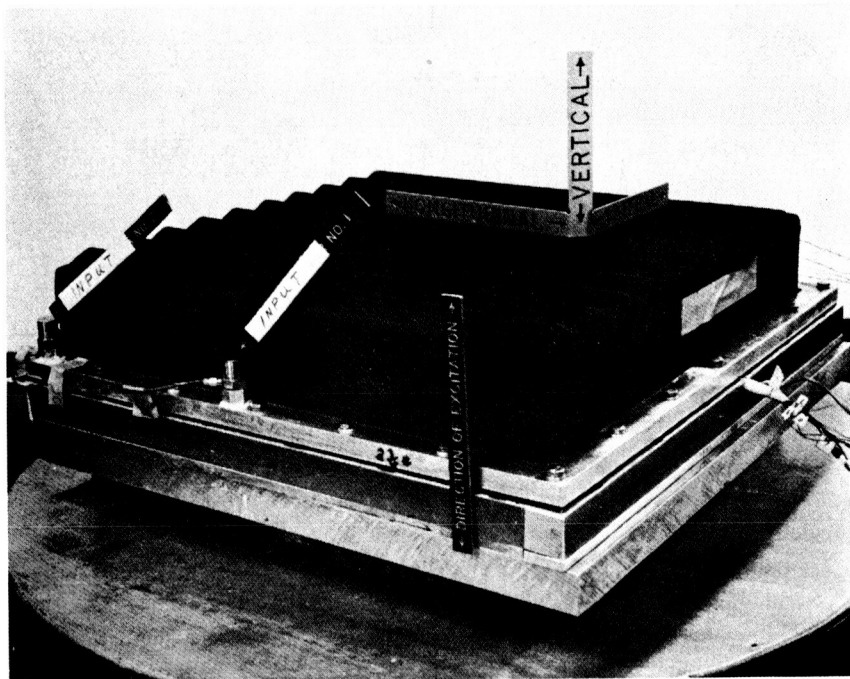


FIGURE 9.3-1

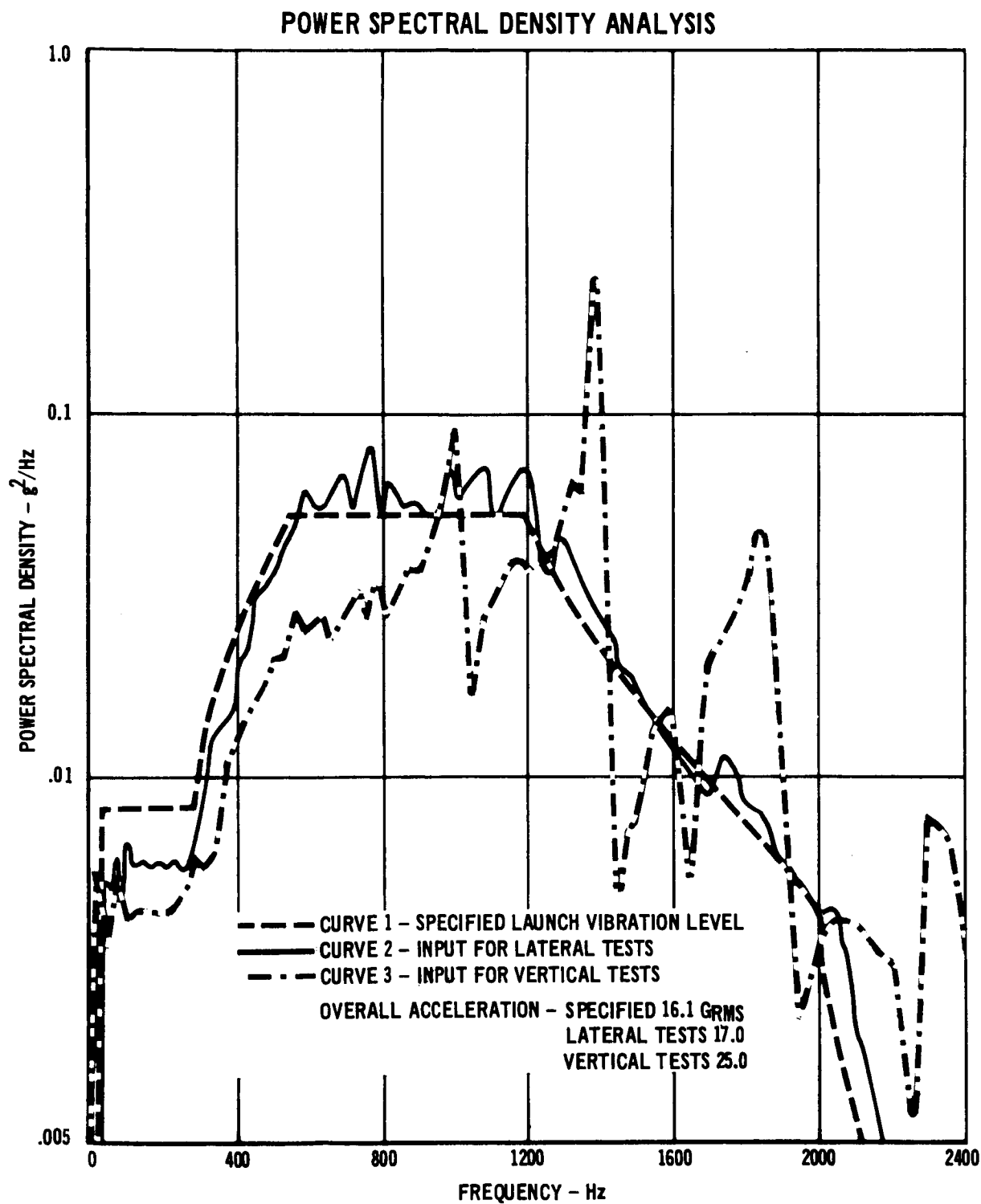


FIGURE 9.3-2

ACCELERATION TRANSMISSIBILITY

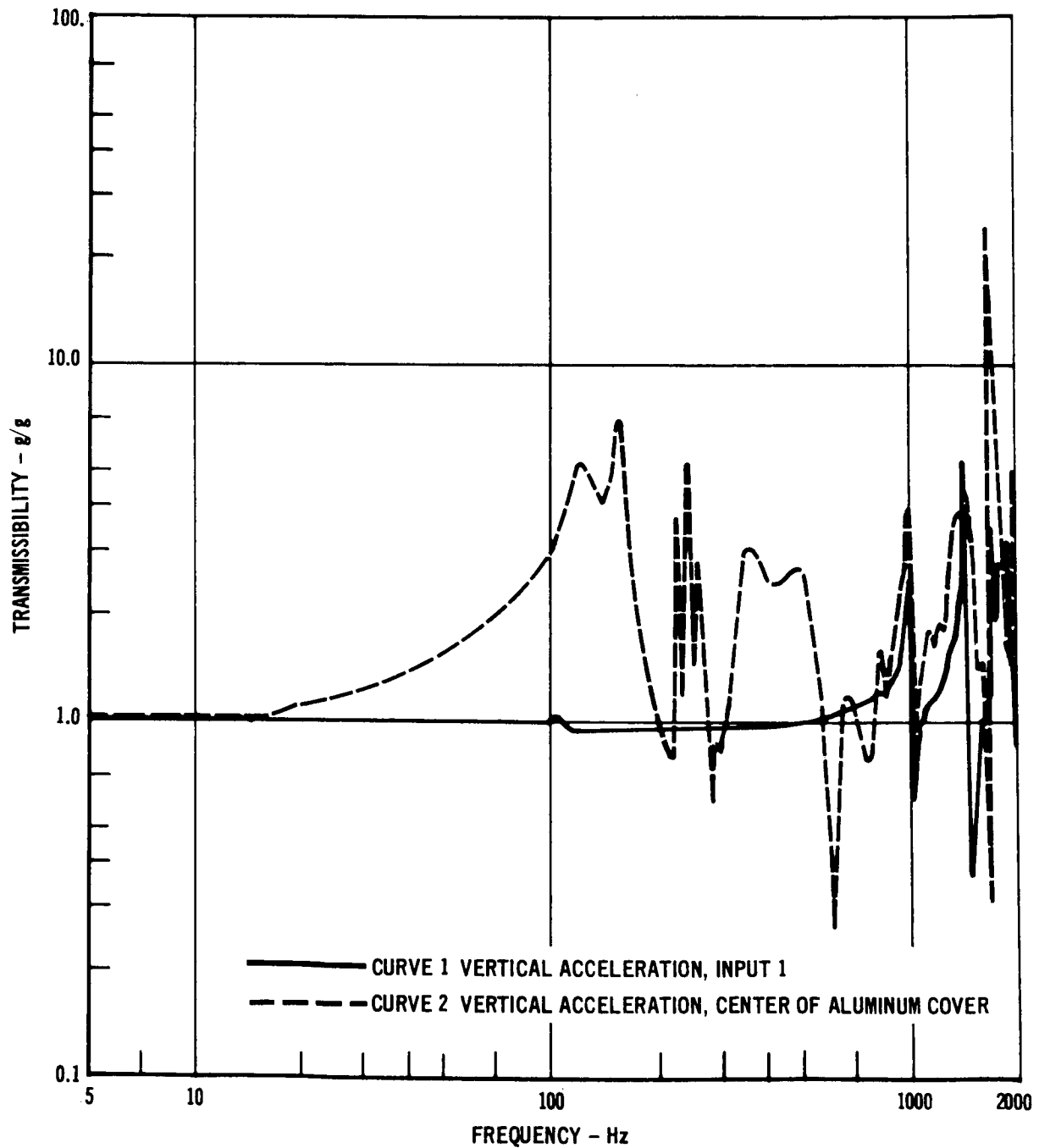


FIGURE 9.3-3

for the lateral and vertical tests, respectively. The analyses indicated that these tests were conducted within the tolerances specified in MIL-STD-810B: plus 15 percent - minus 0 percent for rms acceleration level and ± 1.5 dB (50 to 1000 Hz) and ± 3 dB (1000 to 2000 Hz) for power spectral density (over standard, 1/3 octave frequency bands).

No structural damage was observed during or after the vibration test.

9.3.5 Conclusions - Based on the visual examination and subsequent thermal performance test data, the ISM panel will satisfactorily sustain the launch vibration environment applied during this test.

9.4 LANDING SHOCK TEST - The purpose of this test was to expose the Insulation System Module to an expected Mars soft landing shock environment. Subsequent testing determined whether the landing shock environment and the launch vibration environment affected the thermal performance of the ISM.

9.4.1 Test Sample - The test specimen was the 474-00-0002 fiberglass filled ISM Panel described in Section 8.0. The panel had previously undergone heat sterilization, thermal performance and launch vibration testing.

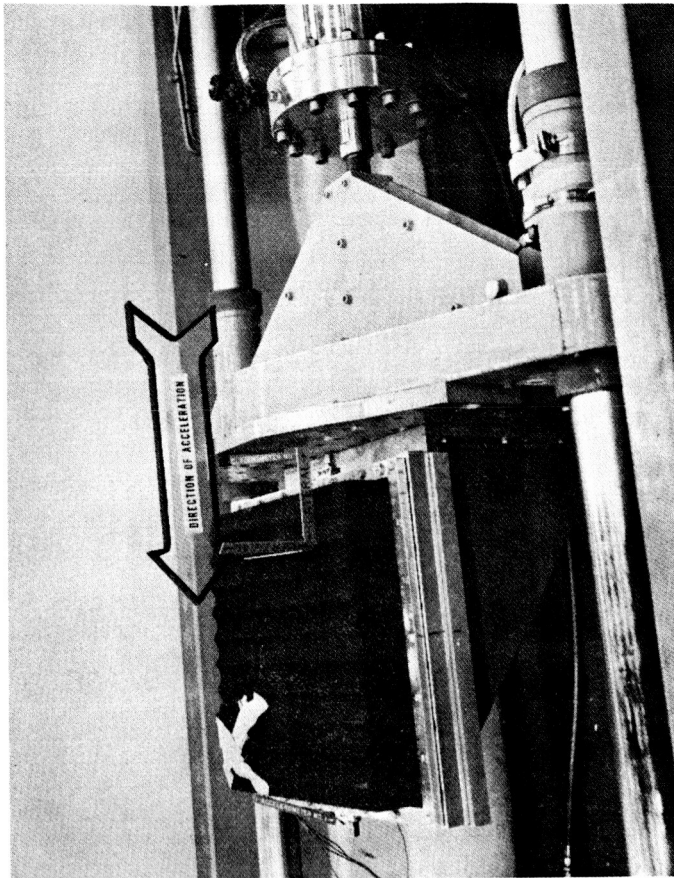
9.4.2 Test Apparatus - During shock testing, the cover plate of the ISM was instrumented with three piezoelectric accelerometers, as shown in Figure 9.4-1, to monitor the structural response of the ISM to the applied environment. The ISM was mounted in the test fixture previously used for vibration testing, in a manner representing a typical spacecraft installation. The fixture/ISM assembly was mounted on a Hyge shock tester, for shocks in both directions of the vertical and lateral axes of the ISM. Two piezoelectric accelerometers were bonded to the test fixture to monitor the applied shock environment. Two typical test setups are shown in Figure 9.4-1. During testing, an analog tape recorder was used to record the acceleration signals and a direct-write oscillograph was used for immediate accelerometer data evaluation.

9.4.3 Test Description - The specified input shock environment was the shock spectrum shown in Figure 9.4-2. This shock spectrum is represented by an idealized 120g, 12.8 msec half sine wave pulse. Three shock pulses were applied in each direction of the lateral and vertical axes of the ISM. A visual inspection for external structural damage of the ISM was made after each shock. After shock testing the ISM was retested for thermal performance changes.

9.4.4 Test Results - Typical input and specimen response acceleration-time histories are compared in Figure 9.4-3. The maximum response of the center of the aluminum cover to the applied shock is tabulated in Figure 9.4-2, indicating appreciable magnification of the input shock level. The acceleration-time history data shown in Figure 9.4-3 for input accelerometer 1 was converted by computer analysis into the shock spectrum presented in Figure 9.4-2. No structural damage was observed.

SHOCK TEST SETUP

TYPICAL TEST SETUP FOR
SHOCKS IN LATERAL DIRECTION



TYPICAL SETUP FOR SHOCKS
IN VERTICAL DIRECTION

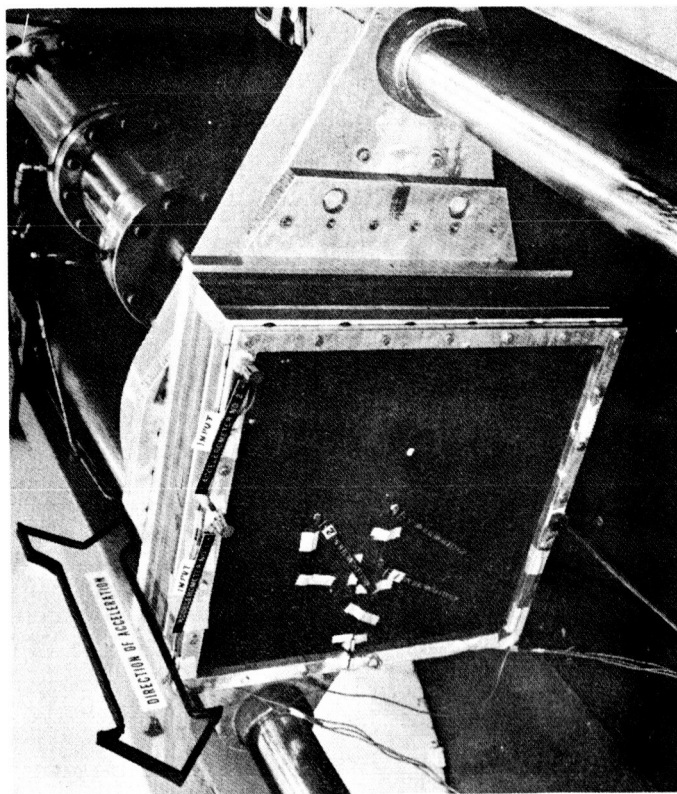
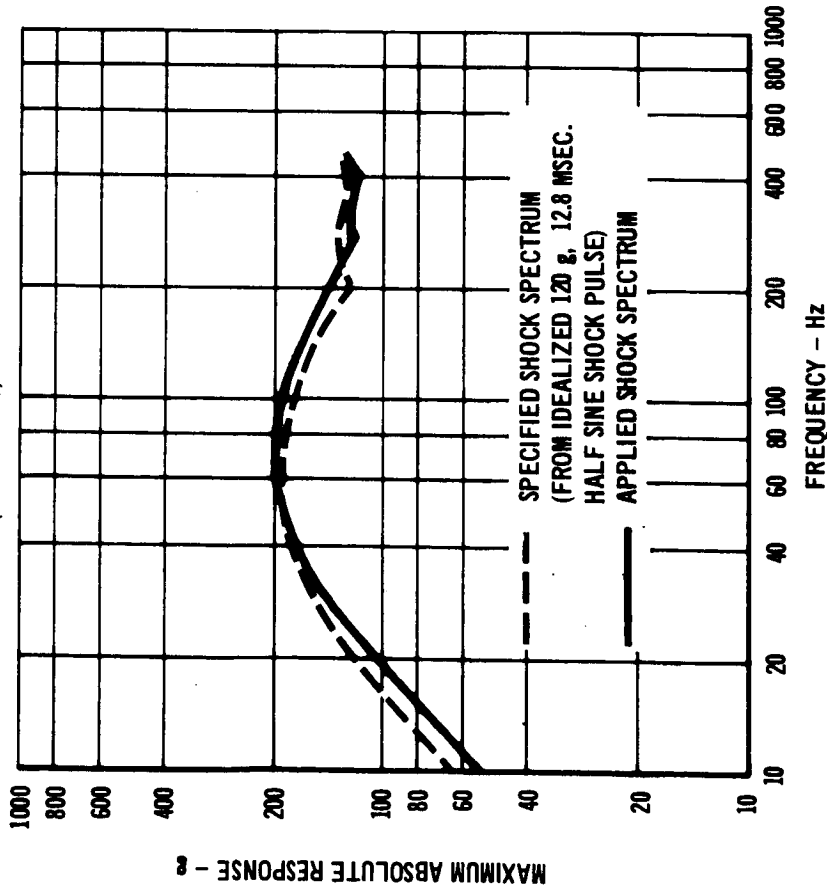


FIGURE 9.4-1

SHOCK TEST DATA

SHOCK SPECTRUM ANALYSIS OF TYPICAL INPUT
SHOCK PULSE - APPLIED IN ALL DIRECTIONS
(5% DAMPING)

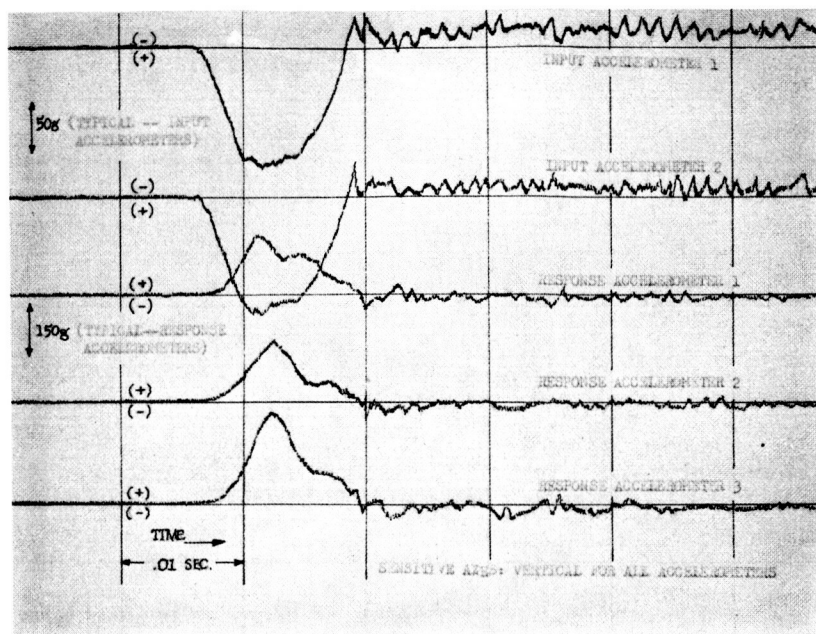


PANEL RESPONSE TO INPUT SHOCK PULSE	
DIRECTION OF APPLIED SHOCK PULSE	MAXIMUM ACCELERATION AT CENTER OF PANEL ALUMINUM FACE
+ LATERAL	30g
- LATERAL	40g
+ VERTICAL	282g
- VERTICAL	470g

FIGURE 9.4-2

TYPICAL ACCELERATION-TIME HISTORIES DURING SHOCK TESTING

SHOCKS APPLIED ALONG ISM VERTICAL AXIS (+ DIRECTION)



SHOCKS APPLIED ISM LATERAL AXIS (+ DIRECTION)

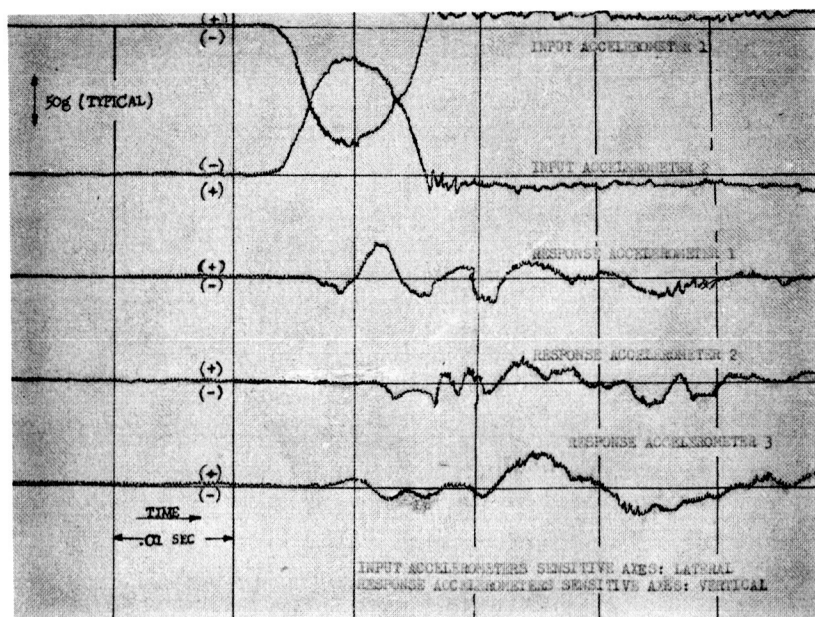


FIGURE 9.4-3

9.4.5 Conclusions - Based on visual examination and the subsequent Thermal Performance Test results, the ISM panel will satisfactorily sustain the Martian soft landing shock environment applied during this test.

9.5 THERMAL CONDUCTIVITY TEST - The purpose of this test was to measure the absolute thermal conductivity of dry heat sterilized insulation material under six stabilized conditions of temperature, pressure and gas composition representing the range of Martian atmospheric parameters. Thermal conductivity measurements were made on the pure insulation material used in the fiberglass ISM. This test supported possible future analysis of designs other than that tested, and provided data for comparison with the Thermal Diffusivity test results.

9.5.1 Test Samples - The insulation material for the thermal conductivity evaluation (Silicone-Bonded "AA" Microlite, manufactured by Johns-Manville) was assembled into a final configuration 14" in diameter and 4" thick. It consisted of two .008" flat thermofoil heaters sandwiched between eight layers of 1" thick Microlite compressed to a total specimen height of 4". The sample density was 1.29 lb/ft³, compared with 1.2 lb/ft³ used in the Thermal Diffusivity test.

9.5.2 Test Apparatus - The specimen was mounted in the guarded hot-plate type apparatus shown schematically in Figure 9.5-1. The apparatus was designed and fabricated for this study. It permits pressure variations from vacuum to one atmosphere for different gas compositions and provides for cold face temperature variations from below -150°F to +32°F. The heaters for the insulation hot face consist of a 6-inch diameter thermofoil heater for the central test section completely surrounded by a 4 inch wide thermofoil guard heater. Both heaters are 0.008 inches thick and consist of a vapor plated nichrome grid insulated by mylar. These heaters have a very small heat capacity providing for essentially immediate dissipation of the power into the insulation and for quick response to power changes. Insulation was placed around the test specimen from the outer diameter out to the inner cylinder wall to reduce the temperature drop across the guard insulation. Chromel-constantan thermocouples were installed on the insulation hot face and cold face, guard heater, central heater, and cold plate. A typical installation of Silicone Bonded "AA" in the apparatus is shown in Figure 9.5-2.

The temperature of the guard heater and central heaters were automatically controlled by matched thermistor detectors attached to the guard heater/central heater interface. The control thermistors, used in a bridge circuit, maintained an interface temperature difference within $\pm 1^\circ\text{F}$. Power was supplied to the center heater from a stabilized DC power supply.

The cold face heaters, a 22 gage nichrome grid type, were embedded in a phenolic prepreg, and bonded to the aluminum end plates. The cold temperature was monitored by a reference thermocouple attached to the inner surface of the end plate. Cold face heater power was adjusted to produce the desired cold face temperature.

THERMAL CONDUCTIVITY TEST APPARATUS

SCHEMATIC OF CALORIMETER

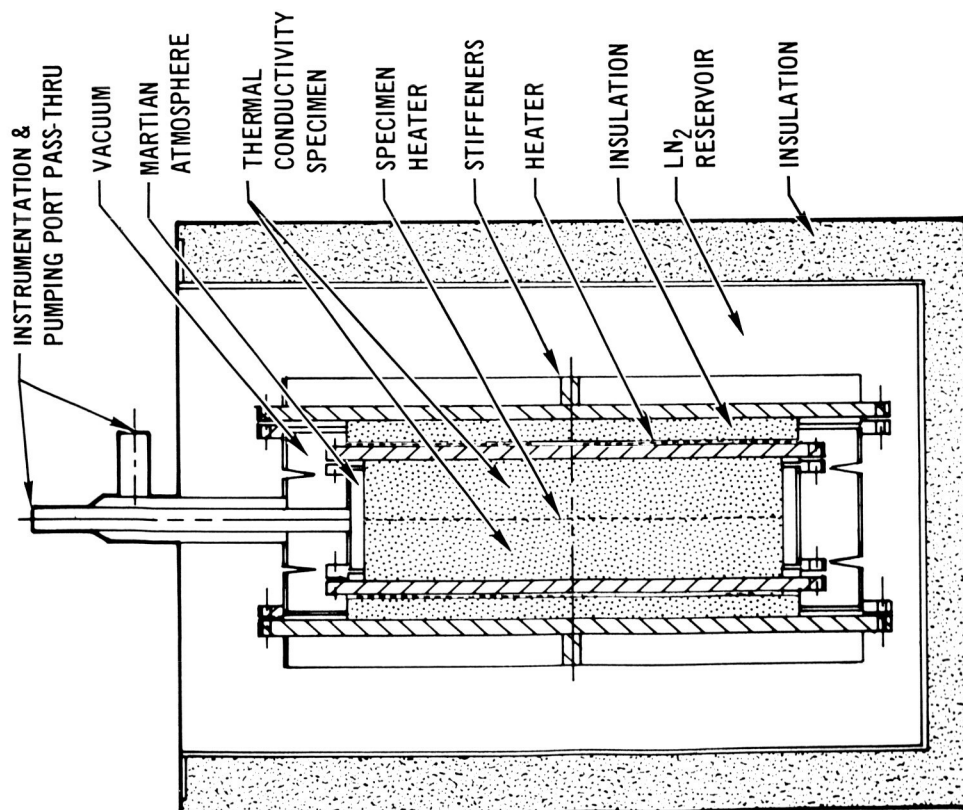
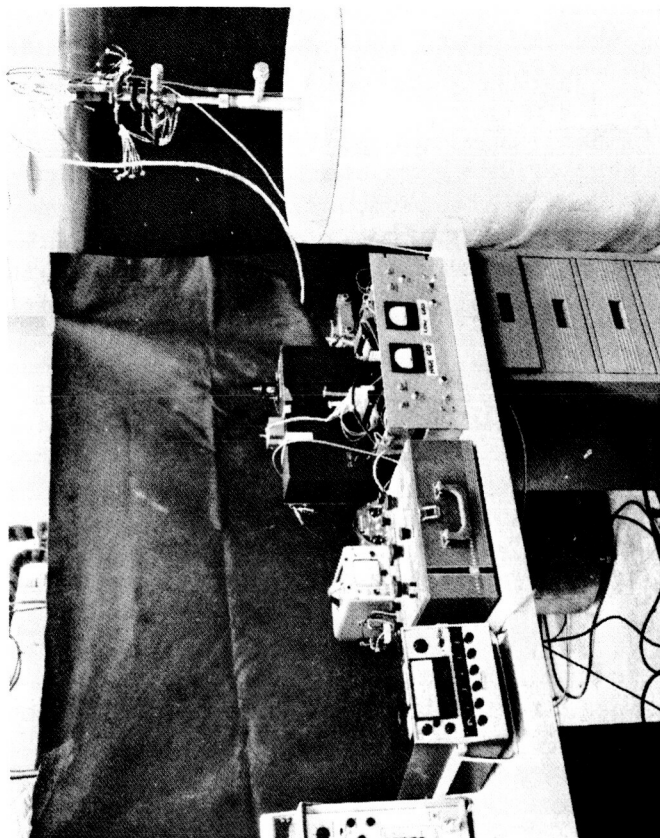


FIGURE 9.5-1

TEST SETUP



INSTALLATION OF THERMOCOUPLES ON SILICONE BONDED "AA"

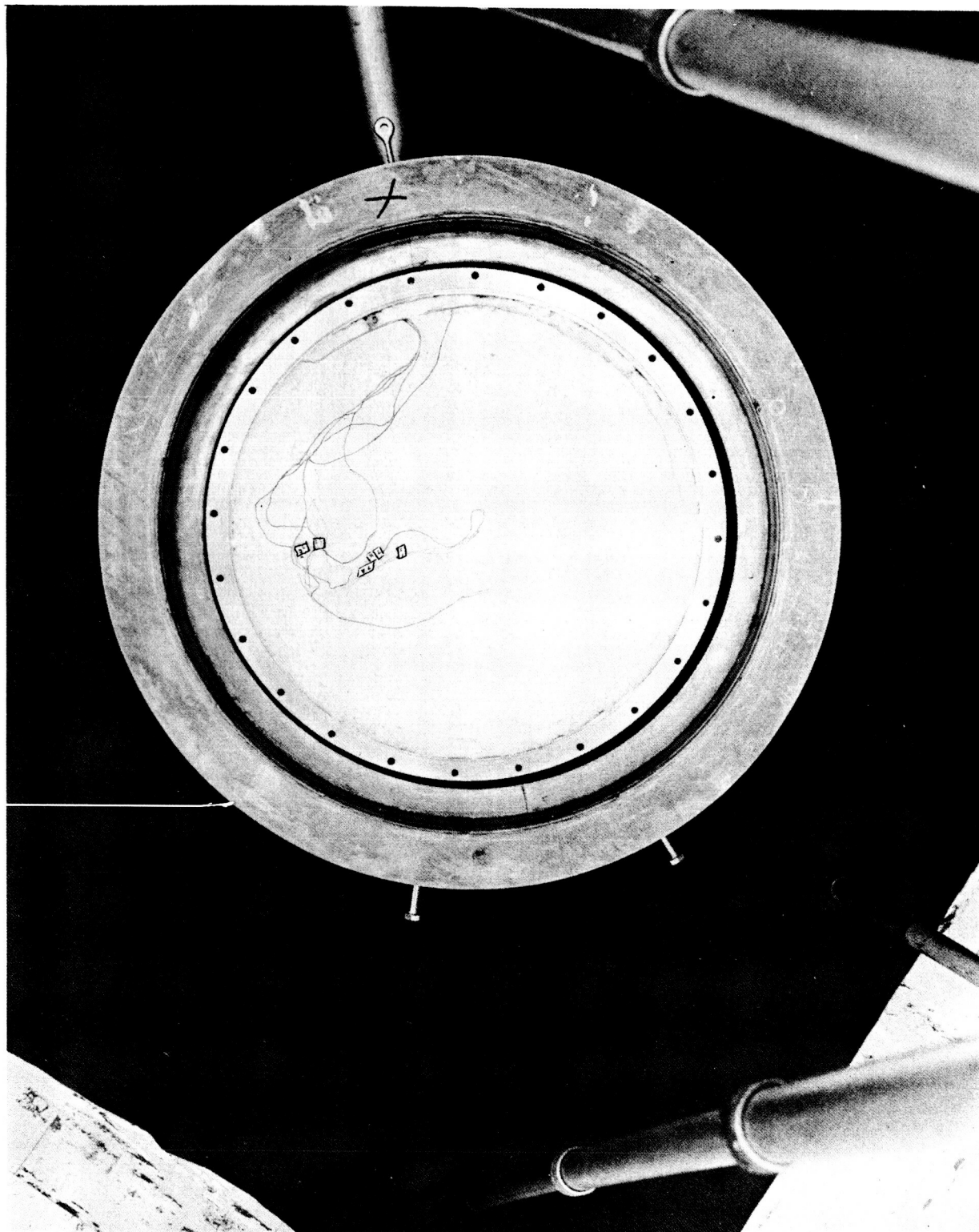


FIGURE 9.5-2

9.5.3 Test Description - The apparatus was evaluated with two layers of one inch thick fiberglass insulation supplied by Johns-Manville. The density of the insulation was 1.44 pcf at 1.00 inch spacer thickness. Figure 9.5-3 shows the excellent agreement between the thermal conductivity determined by Johns-Manville in accordance with ASTM C177, and the comparable data obtained with the new apparatus.

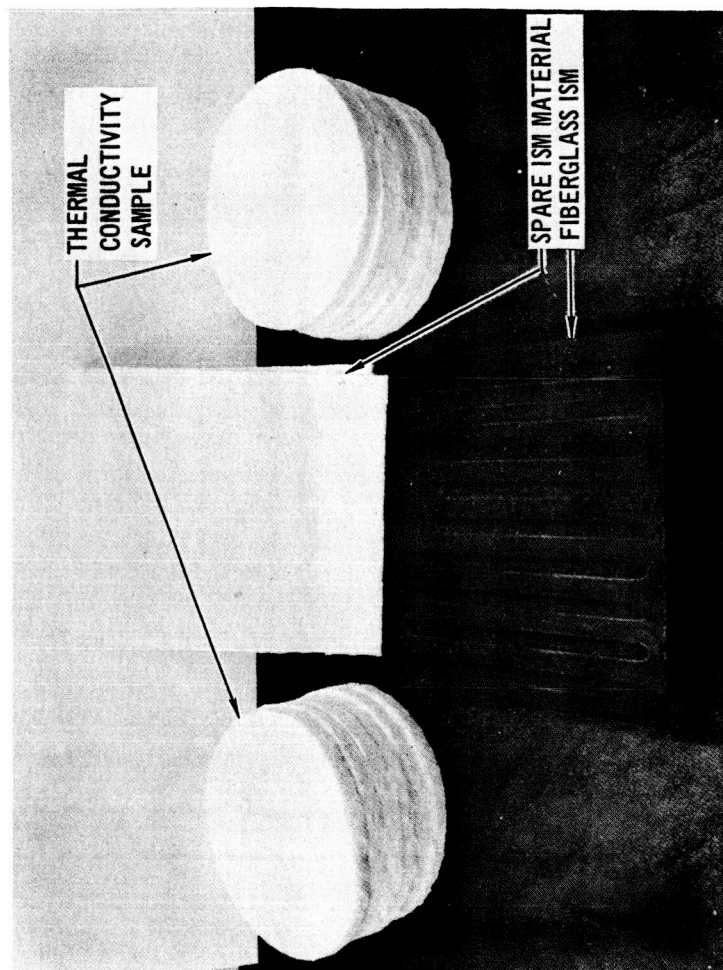
Test data was obtained as follows: The hot and cold face temperatures of the specimen were stabilized for a minimum of two hours before recording the temperatures or the heater power. Steady state conditions were then assumed to exist when a temperature change of less than 1.5°F per hour occurred. In the Mars condition tests, Table 9.5-1, changes of less than 0.6°F per hour were observed for conditions 1 through 5. In test condition number 6, a change of 1.2°F per hour was observed. After temperature equilibrium was established, the data for computing power dissipated by the central heater was recorded. Power was determined by measuring the heater voltage and the voltage drop across a 1 ohm precision resistor connected in series with the heater. Corrections were made for lead losses.

9.5.4 Test Results - The power input to the central heater, temperature difference across the insulation, pressure, and the thermal conductivity of the insulation are given in Table 9.5-2 for each of the six test conditions at steady state. The thermal conductivity was calculated using the temperatures of the heater and cold plates respectively. Thermal conductivity versus mean temperature for each of the three gas models is plotted in Figure 11.1-1, together with comparisons of other test data. As shown in Figure 11.1-1 at -50°F mean temperature, thermal conductivity increases 50% from 6 mb in the minimum model atmosphere composition, to 20 mb pressure in the maximum model. This change is a combined effect of pressure change, and change in gas composition from the pure CO₂ to the higher conductivity nitrogen, CO₂, Argon mixture. Temperature also affects thermal conductivity, but to a lesser extent over the range tested.

9.5.5 Conclusions - These results, the first detailed measurements reported, show the sensitivity of this material to the Martian surface environment range. The test uncertainty has been estimated at $\pm 6\%$, including an accounting for the small edge losses to the guard heater. The measured variation of thermal conductivity would require flexibility in the lander thermal control system to accommodate the entire range of surface environment conditions.

THERMAL CONDUCTIVITY TEST

TEST MATERIAL



CALIBRATION DATA

CALIBRATION MATERIAL:
J-M FIBERGLAS INSULATION
DENSITY - 1.44 PCF

CALIBRATION RESULTS		THERMAL CONDUCTIVITY BTU/HR-FT °F
MEAN TEMP °F		
J.M. 98.8		0.022
275.8		0.027
MDAC 118.0		0.023

FIGURE 9.5-3

THERMAL CONDUCTIVITY TEST CONDITIONS

NUMBER	HOT FACE/COLD FACE TEMPERATURE (°F)	PRESSURE (mb)	GAS COMPOSITION CO ₂ N ₂ A _r (% BY WEIGHT)		
1	50/-150	6	100	0	0
2	50/-150	9	74.4	12.8	12.8
3	50/-150	20	25.0	50.0	25.0
4	70/-100	6	100	0	0
5	70/-100	9	74.4	12.8	12.8
6	70/-100	20	25.0	50.0	25.0

TABLE 9.5-1

THERMAL CONDUCTIVITY TEST RESULTS

NUMBER	HEATER HOT FACE (°F)	INSULATION HOT FACE (°F)	COLD PLATE (°F)	INSULATION COLD FACE (°F)	PRESSURE (mb)	POWER (WATTS)	THERMAL CONDUCTIVITY ($\frac{\text{BTU}}{\text{HR-FT} \cdot ^\circ\text{F}}$)
1	50.0	46.2	-150.0	-147.6	6.0	1.09627	0.0078
		48.0	-150.0	-149.1			
2	49.2	45.5	-151.0	-148.0	8.9	1.31270	0.0093
		47.4	-151.5	-151.0			
3	49.2	46.0	-148.9	-151.1	19.6	1.65061	0.0118
		47.3	-150.4	-151.1			
4	69.6	66.3	-100.6	- 98.6	6.3	1.05400	0.0088
		67.8	-100.6	-100.0			
5	72.0	68.6	-100.1	- 98.3	9.1	1.20825	0.0100
		70.0	- 99.7	- 99.1			
6	71.3	67.4	-100.0	- 98.4	19.7	1.50624	0.0126
		69.5	- 99.4	- 99.0			

TABLE 9.5-2

10. RELATED INVESTIGATIONS

Two additional investigations, conducted as part of MDAC-ED supporting IRAD studies related to the contracted effort are reported here. The first study was an investigation of the causes of failure of the foam filled Insulation System Module during chamber evacuation. In these tests the tensile strength of sterilized and unsterilized material was evaluated, and an attempt was made to duplicate possible failure modes using small foam element samples. The tests indicated that the foam should have sufficient strength to survive the pressure differential experienced during launch. The second test was a preliminary vibration and shock test conducted on a fiberglass filled ISM fabricated using the selected design of this study (Figure 8.3-2). The test panel was subjected to incremental shock levels up to 250 g, with no visible damage. A description and results of these tests are presented in the following.

10.1 INVESTIGATION OF FOAM FAILURE - The foam insulation panel failed during chamber evacuation for the thermal performance testing (Figure 10.1-1). Several possible reasons for the failure can be postulated, including a tension failure, poor or incomplete bonding and residual internal gas pressure resulting from outgassing during heat sterilization.

The purpose of this investigation was to determine the effect of heat sterilization on the tensile properties of the foam and the reaction of several foam configurations to the launch pressure profile.

10.1.1 Test Samples - Thirty test specimens were fabricated from sterilized and unsterilized HTF-200 foam. The physical size and configuration for each specimen are given in Table 10.1-1. The coating applied to the foam blocks was an epoxy-nylon adhesive consisting of 7 parts Epon 828 and 3 parts Versamide 125. This coating was used previously to bond the foam ISM. One specimen, 1 x 2 x 2 in, containing a vent hole, is shown in Figure 10.1-2. Two of the 2 x 2 x 2 inch test specimens contained an entrapped air pocket and are shown in Figure 10.1-3.

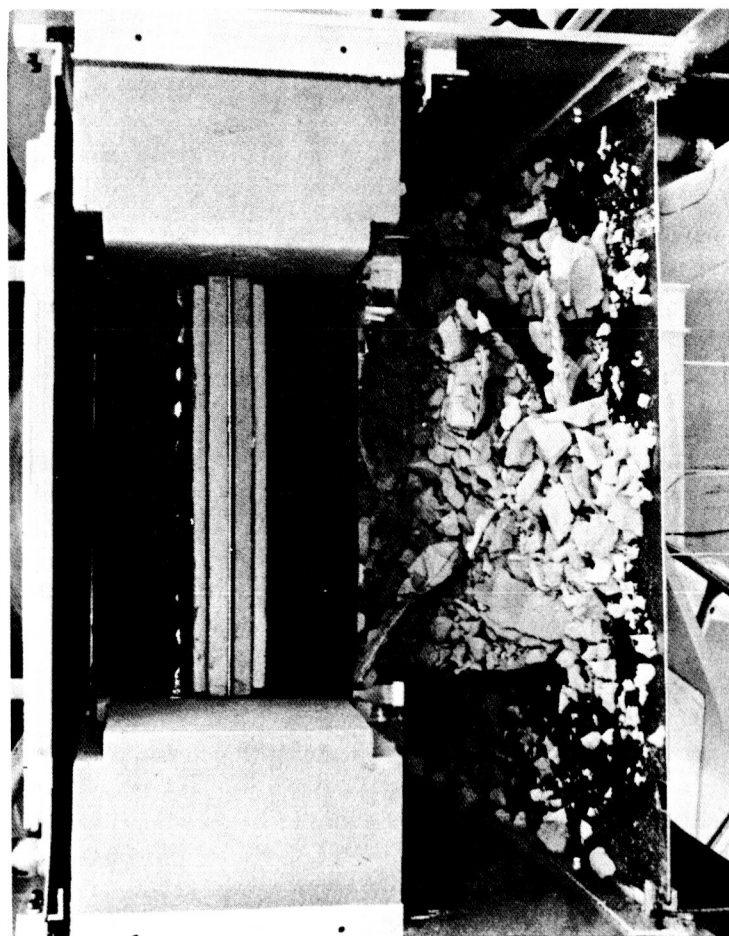
10.1.2 Test Apparatus - Tensile tests were performed in a Universal tensile test machine. The same 5.5-ft diameter vacuum chamber in which the original sealed foam panel failed was used to perform the launch pressure profile test.

10.1.3 Test Description - Tensile test specimens were mounted in the Universal test machine and uniformly loaded in tension until failure occurred. The failing load was recorded.

In the second test, all of the variously configured foam blocks described in Table 10.1-1 were placed on a flat platform in the vacuum chamber. They were viewed through a port in the chamber as it was evacuated at the rate shown in Figure 10.1-4. This evacuation profile coincides with the launch pressure profile followed in the Thermal Performance Test.

FOAM ISM FAILURE DURING THERMAL PERFORMANCE TEST PUMPDOWN

ISM IN TEST SETUP AFTER FAILURE
(LOWER COLD PLATE REMOVED)



ISM AFTER FAILURE WITH COVER REMOVED

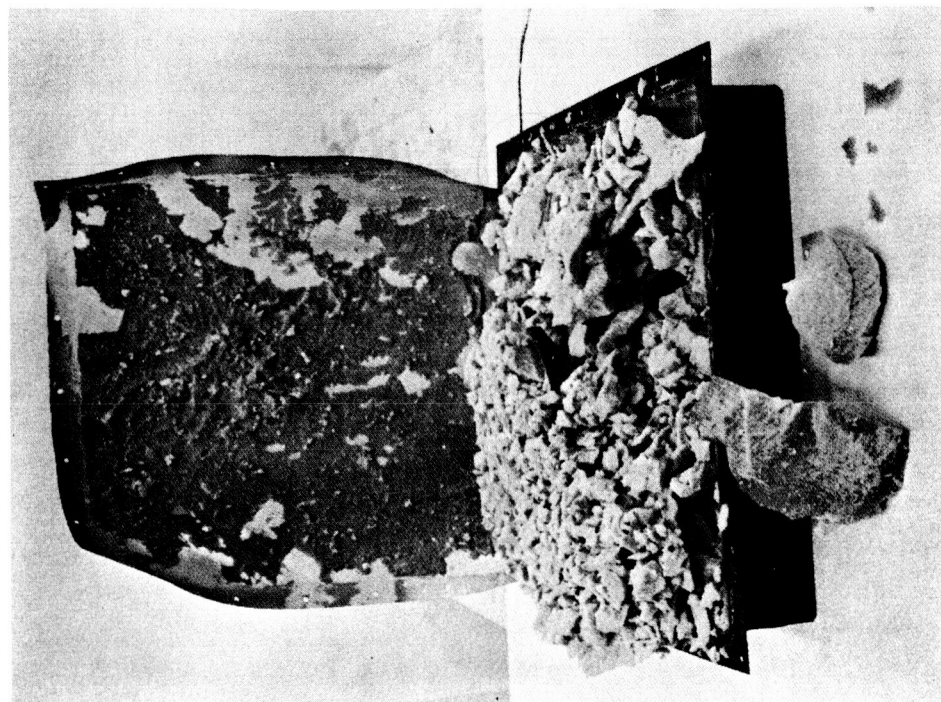


FIGURE 10.1-1

FOAM FAILURE TEST SPECIMENS

TESTS	NUMBER OF SPECIMENS		COMMENTS
	STERILIZED MATERIAL	UNSTERILIZED MATERIAL	
A. TENSILE STRENGTH 1" X 2" X 2" SAMPLES	(3)	(3)	MEASURE EFFECTS OF HEAT STERILIZATION IN THE 1 INCH DIRECTION OF THE SAMPLE.
TOTAL	3	3	
B. LAUNCH DEPRESSURIZATION CAPABILITY 1" X 2" X 2" SAMPLES			CONTROL SPECIMENS SIMULATES POSSIBLE FOAM INSTALLATIONS IN ISM TEST PANEL - WILL DEMONSTRATE VACUUM COMPATIBILITY AND/OR APPROACHES TO RELIEVE INTERNAL PRESSURE
1) BARE	(3)	(3)	
2) COATED WITH BONDING MATERIAL	(3)	(3)	
3) COATED WITH BONDING MATERIAL VENT HOLES (1/8" DIA.)	(3)	(3)	
4) TWO 1" X 2" X 2" PIECES COATED WITH BONDING MATERIAL, BONDED TOGETHER WITH AN AIR-POCKET IN THE FAYING SURFACE (2" CUBE)	(3)	(3)	
TOTAL	12	12	

TABLE 10.1-1

LAUNCH DECOMPRESSION SPECIMEN
CONTAINING A VENT HOLE

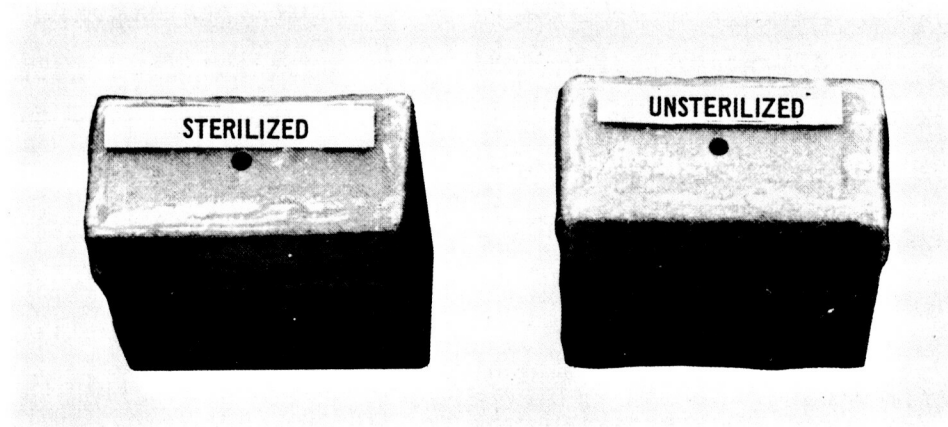


FIGURE 10.1-2

LAUNCH DECOMPRESSION SPECIMEN
CONTAINING A 1/2 x 1/2 INCH AIR POCKET

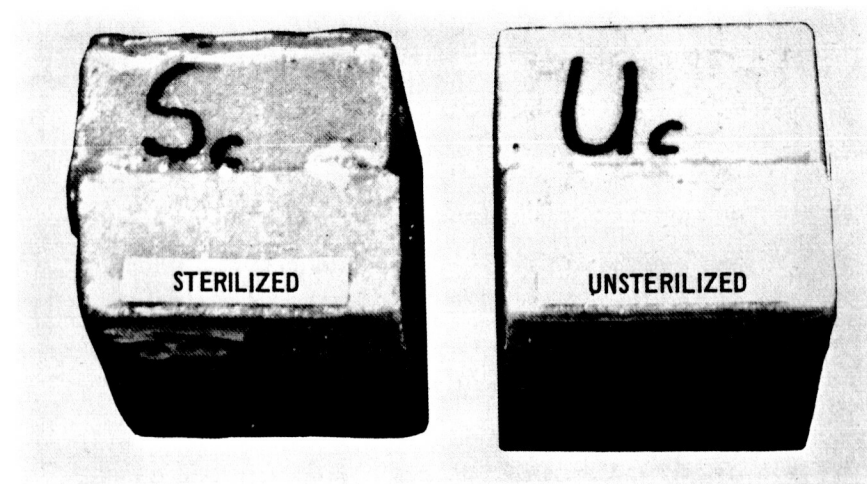


FIGURE 10.1-3

LAUNCH AMBIENT PRESSURE PROFILE FOR ANALYSIS OF FOAM INSULATION PANEL FAILURE

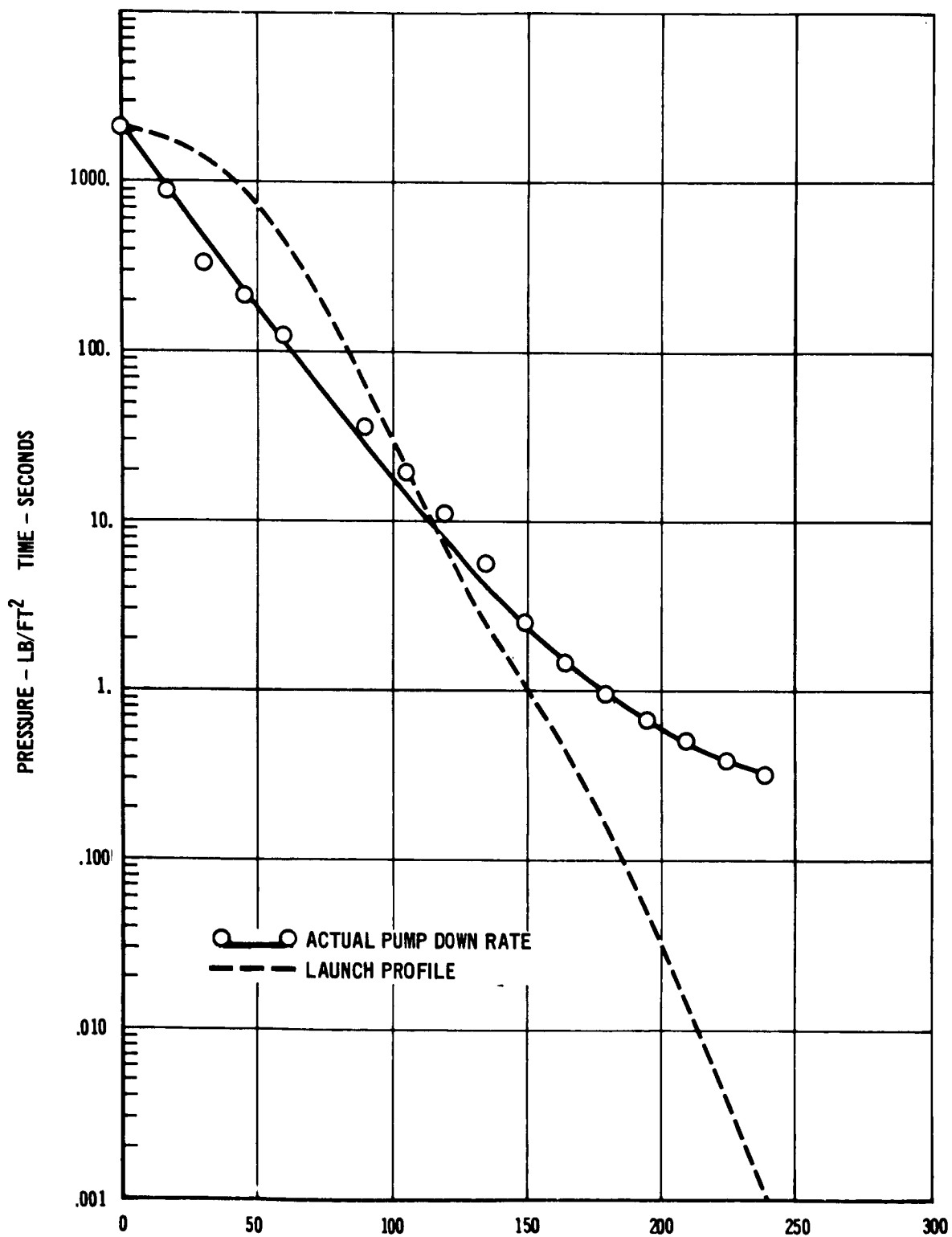


FIGURE 10.1-4

10.1.4 Test Results - The tensile strength of each sterilized and unsterilized HTF-200 foam specimen is given in Table 10.1-2. A significant reduction in strength (30%) due to heat sterilization was detected. However, even the degraded value should have been sufficient to avoid failure of the foam ISM during launch since only 14.7 psi is needed to react the pressure loads on the ISM casing and cover. After the launch venting test, the only change traceable to vacuum exposure was an increase in the number of surface pin holes where the thin skin of bubbles in the bonding material had broken at the surface. These pin holes occurred randomly in all the blocks without preference for any particular group.

10.1.5 Conclusions - Although the tensile strength of the foam decreased 30 percent during heat sterilization, the value was still in agreement with the vendor data and sufficient to prevent failure of the ISM.

These specimens did not demonstrate structural instability when subjected to a vacuum environment under controlled conditions more severe than the original test panel had experienced.

The failure mechanism is presently unknown and cannot be determined adequately without further investigation.

10.2 INITIAL SHOCK TEST OF A FIBERGLASS ISM - The purpose of this test was to investigate the effect of shock loads on a fiberglass ISM and to demonstrate that the structural design was more than adequate for the expected landing shock environment.

10.2.1 Test Sample - The ISM tested was a separate prototype panel similar to the fiberglass ISM discussed previously in this report. The prototype ISM was fabricated according to drawing No. 474-00-0002, Figure 8.3-2. It was filled with silicone bonded "AA" fiberglass insulation (Hitco TG 15000). The ISM prototype was not heat sterilized. Instrumentation on the ISM consisted of five strain gauges, three accelerometers on the aluminum cover plate, and three accelerometers on the back plastic laminate casing as shown in Figures 10.2-1 and -2 to monitor the structural response to the applied shock loads.

10.2.2 Test Apparatus - The test setup for shock testing was the same as that described in Section 9.4. Static calibration of the strain gauges was performed using a Baldwin Universal Testing Machine with the ISM installed in the vibration fixture.

10.2.3 Test Description - The strain gauges on the aluminum cover plate were statically calibrated as follows: Incremental loads were applied, using a yoke assembly, to the area shown in Figure 10.2-1. The deflection at each strain gauge location was recorded using dial indicators. The loads were applied until the deflection at the strain location reached 0.25 inches. Output of the strain gauges was recorded throughout the loading. A frequency response survey was conducted, consisting of one sweep during which the

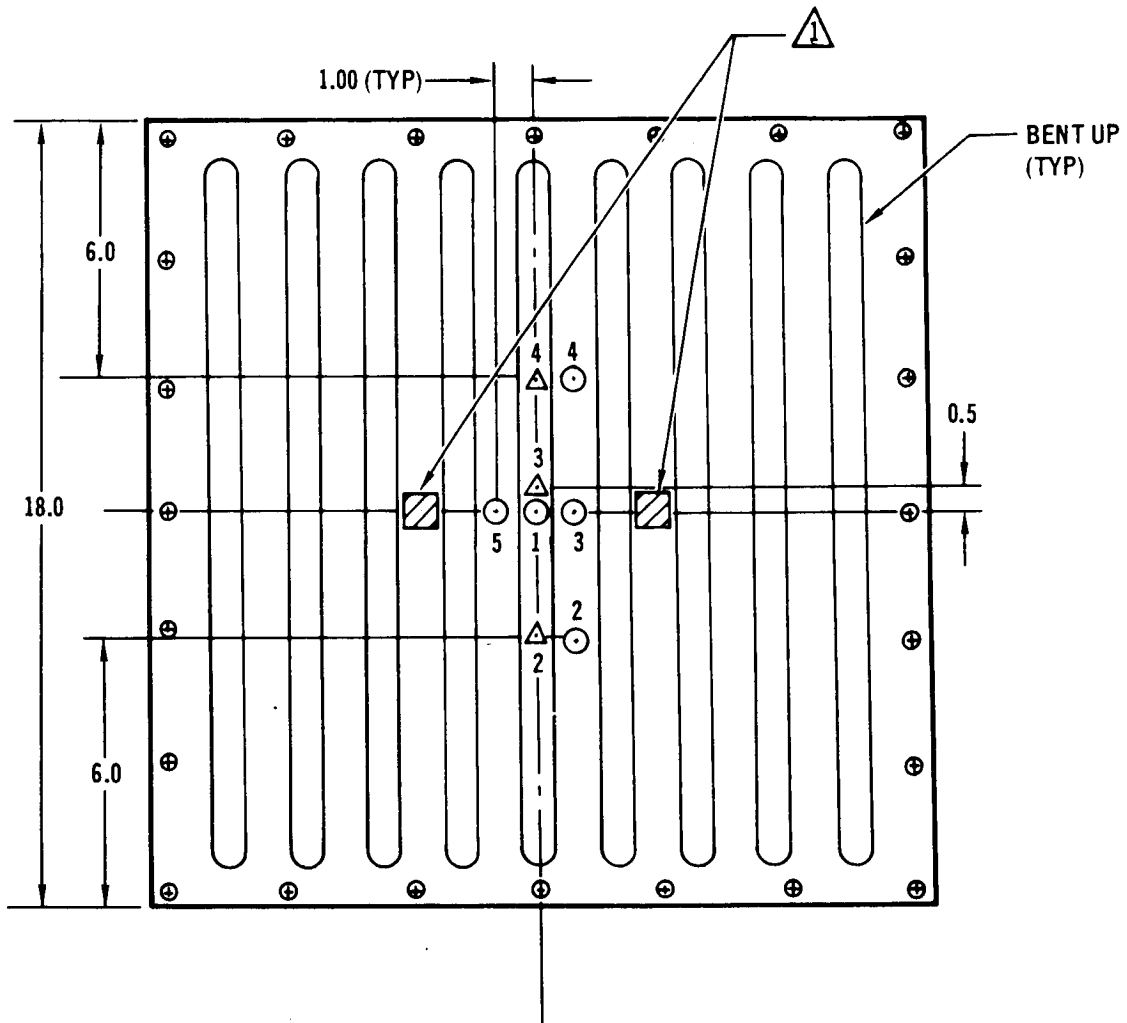
**TENSILE STRENGTH OF STERILIZED
AND UNSTERILIZED HTF-200 FOAM**

SPECIMEN NO.	TENSILE STRENGTH	
	STERILIZED FOAM (PSI)	UNSTERILIZED FOAM (PSI)
1	35	62*
2	34	48
3	30	45

*ADHESIVE BONDING BETWEEN TENSION GRIPS CAUSED A HIGHER LOAD TO BE DEVELOPED
BEFORE STRUCTURAL FAILURE OF THE FOAM.

TABLE 10.1-2

TRANSDUCER LOCATIONS – COVER PLATE (SIDE
OPPOSITE INSULATION SHOWN)



NOTES

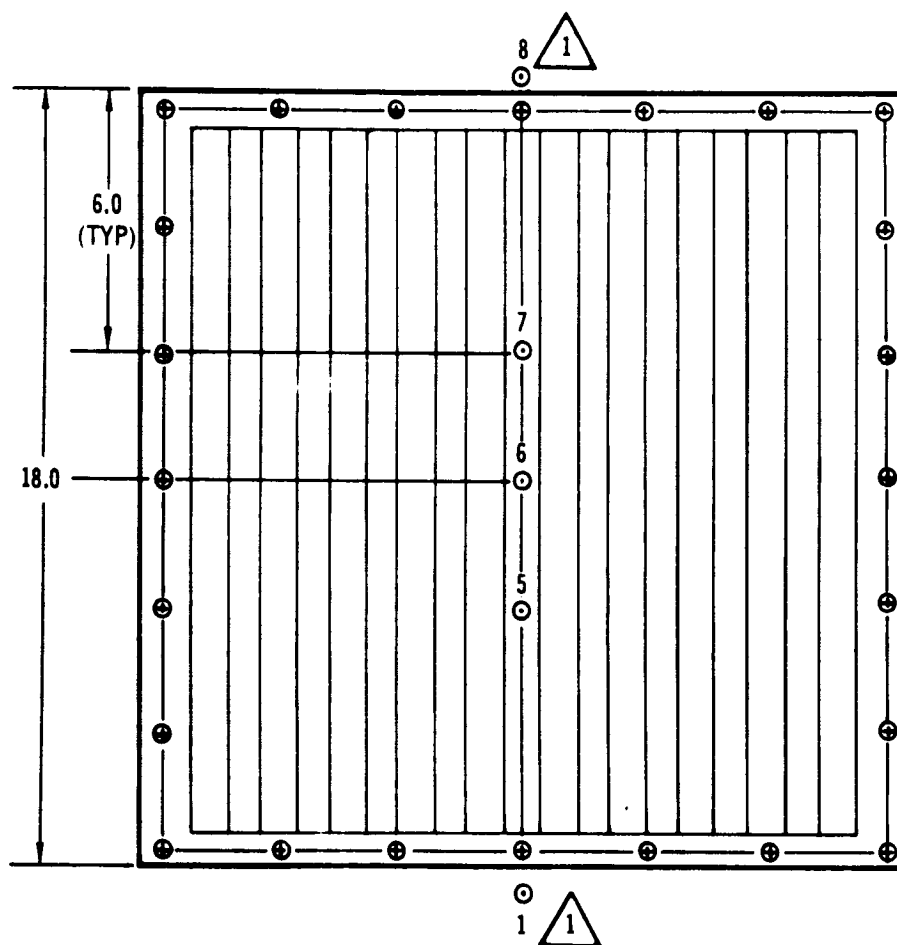
△ ACCELEROMETER

⊙ STRAIN GAGE

- 1 AREA OF LOAD APPLICATION DURING STATIC CALIBRATION.
LOAD DIRECTED OUT OF PAPER.
- 2 SENSITIVE AXIS OF ALL STRAIN GAGES PARALLEL TO CORRUGATIONS
ON COVER PLATE.

FIGURE 10.2-1

TRANSDUCER LOCATIONS FOR SHOCK TESTS - PLASTIC LAMINATE
CASING (SIDE OPPOSITE INSULATION SHOWN)



NOTES:

- ⊙ ACCELEROMETER
- △ 1 INPUT ACCELEROMETERS LOCATED ON TEST FIXTURE CLAMP RING

FIGURE 10.2-2



frequency was varied at a logarithmic rate from 5 to 2000 Hz in 10 minutes. The vibration levels were 0.1 inch double amplitude from 5 to 14 Hz and 1 g from 14 to 2000 Hz. Upon completion of the response survey, the panel was subjected to a shock environment. Half sine pulse were applied normal to the panel starting at an acceleration level of 90 g and proceeding in incremental increases of 30 g until the limit of the Hyge machine was reached at 250 g's. A visual inspection for external structural damage of the ISM was made after each shock.

10.2.4 Test Results - The results of the strain gauge static calibration are shown in Table 10.2-1. Strain gauge 5 gave erroneous readings and hence no data was recorded. Because of symmetry, however, strain gauge 3 provided the same information as 5. The vibration response testing provided transmissibility data plots (ratio of response acceleration to input acceleration). Data for accelerometer 3 location is shown in Figure 10.2-3. From the curve, the primary cover plate frequencies were found at 105 and 150 Hz.

The results of the shock test, Table 10.2-2 include peak strain data, peak acceleration, and pulse duration. No structural damage was observed during or after any shock test.

10.2.5 Conclusions - Based on visual examination of the ISM after shock testing, it was concluded that the panel tested was more than adequate for the dynamic environments defined for this program. Within constraints imposed by manufacturing and minimum gage limitations, it appears possible to reduce weight by using thinner gages and still satisfy the imposed dynamic environments. Potential ISM weight reductions are discussed in Section 11.

ISM COVER PLATE STATIC LOAD TEST SUMMARY

APPLIED LOAD (LBS)	DEFLECTION MEASURED AT STRAIN GAGES (INCHES)			STRAIN VALUES (MICRO-INCHES/INCH)				
	STRAIN GAGE NUMBER 			STRAIN GAGE NUMBER 				
	1	2	4	1	2	3	4	5
9.00	0.050	0.040	0.038	230	20	0	20	-
20.00	0.100	0.070	0.068	425	20	62	40	-
33.25	0.150	0.098	0.094	595	62	95	95	-
51.75	0.200	0.125	0.120	765	95	103	95	-
76.25	0.250	0.150	0.150	965	124	145	125	-
0.00	0.000	0.000	0.000	0	0	0	0	-

 SEE FIGURE 10.2-1 FOR STRAIN GAGE LOCATIONS

TABLE 10.2-1

ACCELERATION TRANSMISSIBILITY – CENTER OF ALUMINUM COVER

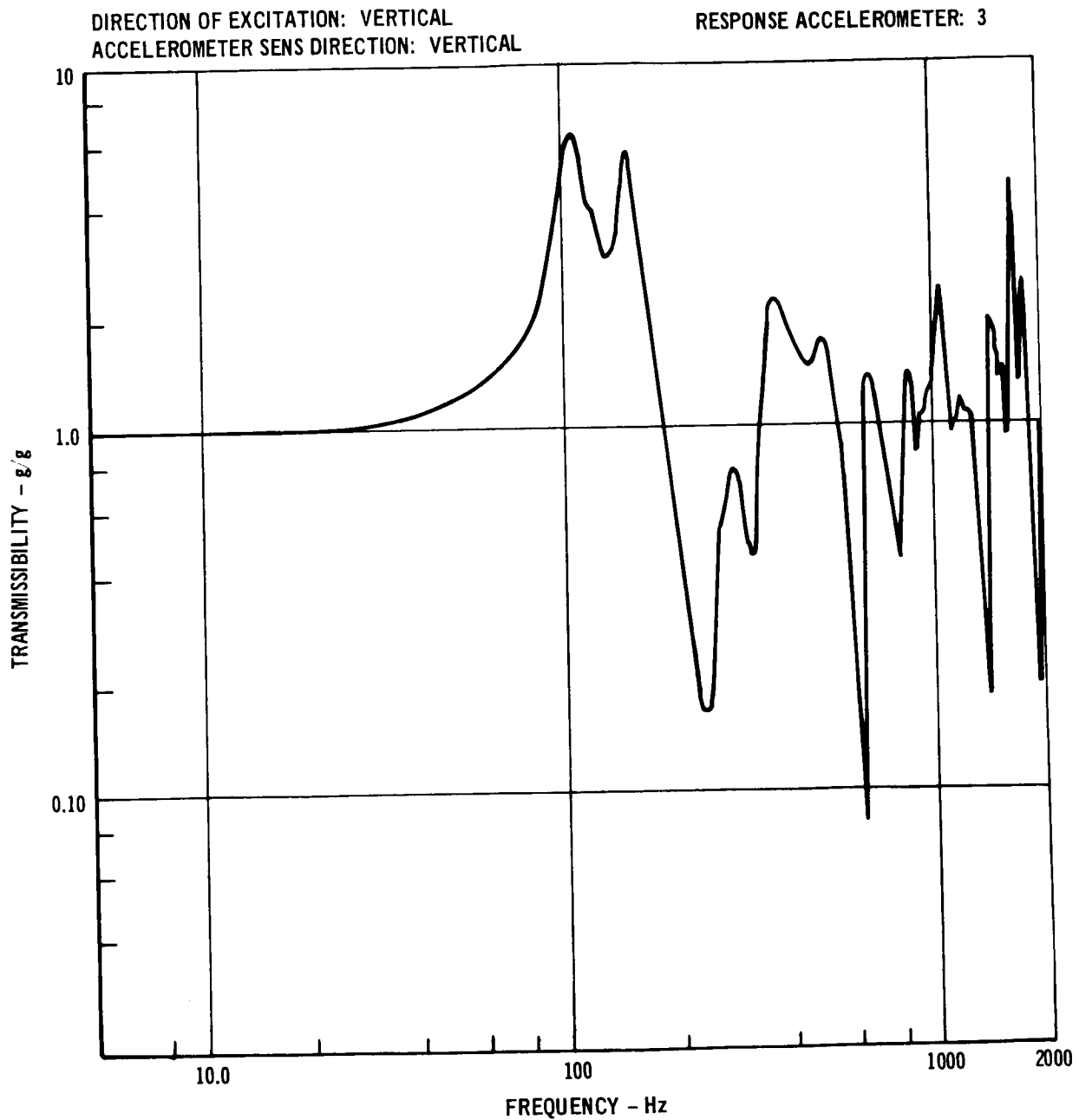


FIGURE 10.2-3

INCREMENTAL SHOCK TEST SUMMARY



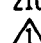



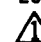
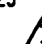
SHOCK NUMBER	ACCELEROMETER			STRAIN GAGE DATA	
	ACCELEROMETER NUMBER	TIME DURATION OF INPUT ACCELERATION PULSES (MILLISECONDS)	MAXIMUM LEVEL OF ACCELERATION (g)	STRAIN GAGE NUMBER	MAXIMUM STRAIN (MICRO-IN./IN.)
1	1 (INPUT)	15.2	89	1	805
	2		△	2	192
	3		200	3	192
	4		160	4	202
	5		180	5	△
	6		200		
	7		160		
	8 (INPUT)	15.2	88		
2	1 (INPUT)	13.3	120	1	970
	2		△	2	255
	3		204	3	234
	4		162	4	255
	5		210	5	△
	6		247		
	7		192		
	8 (INPUT)	13.3	118		
3	1 (INPUT)	12.5	150	1	1080
	2		△	2	300
	3		260	3	288
	4		185	4	308
	5		298	5	△
	6		322		
	7		260		
	8 (INPUT)	12.5	147		
4	1 (INPUT)	11.2	178	1	1160
	2		△	2	318
	3		300	3	308
	4		240	4	361
	5		365	5	△
	6		390		
	7		320		
	8 (INPUT)	11.2	173		

△ ERRONEOUS DATA

(CONTINUED)

TABLE 10.2-2

INCREMENTAL SHOCK TEST SUMMARY (Continued)

SHOCK NUMBER	ACCELEROMETER		STRAIN GAGE DATA		
	ACCELEROMETER NUMBER	TIME DURATION OF INPUT ACCELERATION PULSES (MILLISECONDS)	MAXIMUM LEVEL OF ACCELERATION (g)	STRAIN GAGE NUMBER	MAXIMUM STRAIN (MICRO-IN./IN.)
5	1 (INPUT)	11.0	186	1	1180
	2			2	320
	3		318	3	308
	4		252	4	365
	5		415	5	
	6	11.0	440		
	7		365		
	8 (INPUT)		174		
6	1 (INPUT)	10.5	210	1	1220
	2			2	330
	3		334	3	318
	4		272	4	367
	5		463	5	
	6	10.5	520		
	7		410		
	8 (INPUT)		208		
7	1 (INPUT)	10.0	246	1	1305
	2			2	362
	3		410	3	330
	4		334	4	393
	5		557	5	
	6	10.0	587		
	7		500		
	8 (INPUT)		242		
8	1 (INPUT)	9.4	254	1	1330
	2			2	382
	3		453	3	352
	4		392	4	425
	5		680	5	
	6	9.4	762		
	7		605		
	8 (INPUT)		250		

NOTES:

 ERRONEOUS DATA

TABLE 10.2-2 CONTD.

11. COMPARISONS OF TEST DATA

The thermal test data obtained during the Thermal Diffusivity and Thermal Conductivity Tests are compared in this Section with the available literature values. The test data appears to have good internal consistency and compares well with similar literature data. In addition estimated reductions in ISM weight are developed, based on further evaluations and the successful incremental shock testing described in Section 10.2. Because the ISM survived shock loads well in excess of those required, the data indicates that appreciable weight reduction can be achieved.

11.1 COMPARISON OF THERMAL TEST DATA - The data obtained in the Thermal Diffusivity Tests and the Thermal Conductivity test can be compared with available literature values at one atmosphere and at vacuum. At 20 mb pressure the test data can be compared only with literature values in air. For the Thermal Diffusivity Test these comparisons indicate good agreement for the Mars atmosphere (20 mb) data and the one atmosphere air data, with less agreement of the vacuum data. The Thermal Diffusivity data was thus valid for this study since the primary condition for material selection was the 20 mb Mars atmosphere data.

11.1.1 Thermal Diffusivity Test Comparisons - Comparison data for this test, Table 11.1-1 indicates agreement with literature data to within about 20% for fiberglass materials at one atmosphere pressure in air. Agreement for the foam and powder materials was not as good, with the test data in most cases resulting in higher thermal conductivity than that from the literature. Roughly the same comparative results occurred for the fiberglass material at 20 mb pressure, where the test gas composition was the LRC maximum model mixture.

In vacuum the thermal diffusivity test data was a factor of 2 to 4 higher than available literature values. It is probable that at this condition the thermal conductivity of the materials becomes sufficiently small that heat absorbed by the heater becomes significant compared to that transferred through the insulation. This effect would result in higher computed conductivity values. Since the vacuum data was not considered in the materials selections, no further attempts were made to refine the vacuum results.

11.1.2 Thermal Conductivity Test Data - The data from this test cannot be compared directly with any literature results since measurements in the Martian atmospheric conditions have not been previously reported. Comparison with one atmosphere data in air, and with results obtained in the Thermal Diffusivity Test are shown in Figure 11.1-1. The agreement of the six test points with each other appears consistent, as does the comparison with the other available test data. These results verify the basic design adequacy of the test apparatus.

THERMAL DIFFUSIVITY TEST DATA COMPARISONS

MATERIAL CLASS	DENSITY LB/FT ³		K VACUUM BTU/HR-FT-°F		K, 20 MB BTU/HR-FT-°F		K, 1 ATM BTU/HR-FT-°F	
	TEST	LITERATURE	TEST	LITERATURE	TEST	LITERATURE	TEST	LITERATURE
FIBERS								
UNBONDED "AA"	1.2	1.2	.0052	.0027	.018	.016	.022	.018
UNBONDED "AAA"	1.2	1.2	.0052	.0022	.018	.016	.021	.019
UNBONDED "AAAA"	0.7	0.7	.013	.0033	.021	.018	.024	.020
UNBONDED "AAAA"	2.2	2.2	.0046	.0016	.017	.013	.020	.018
SILICONE BONDED "AA"	1.08	1.2	.0050	-	.018	-	.020	.020
FOAMS								
UPJOHN HTF-200	2.04	-	.010	-	.015	-	.017	.011
GE PPO	2.45	2.50	.010	-	.023	-	.026	.034
DIAMOND SHAMROCK G-302	2.35	2.0	.012	-	.018	-	.020	.017
POWDERS								
COLLOIDA SILICA	3.15	2.26	.0063	-	.013	-	.022	.010

TABLE 11.1-1

TEST DATA COMPARISON SILICONE BONDED "AA" FIBERGLASS

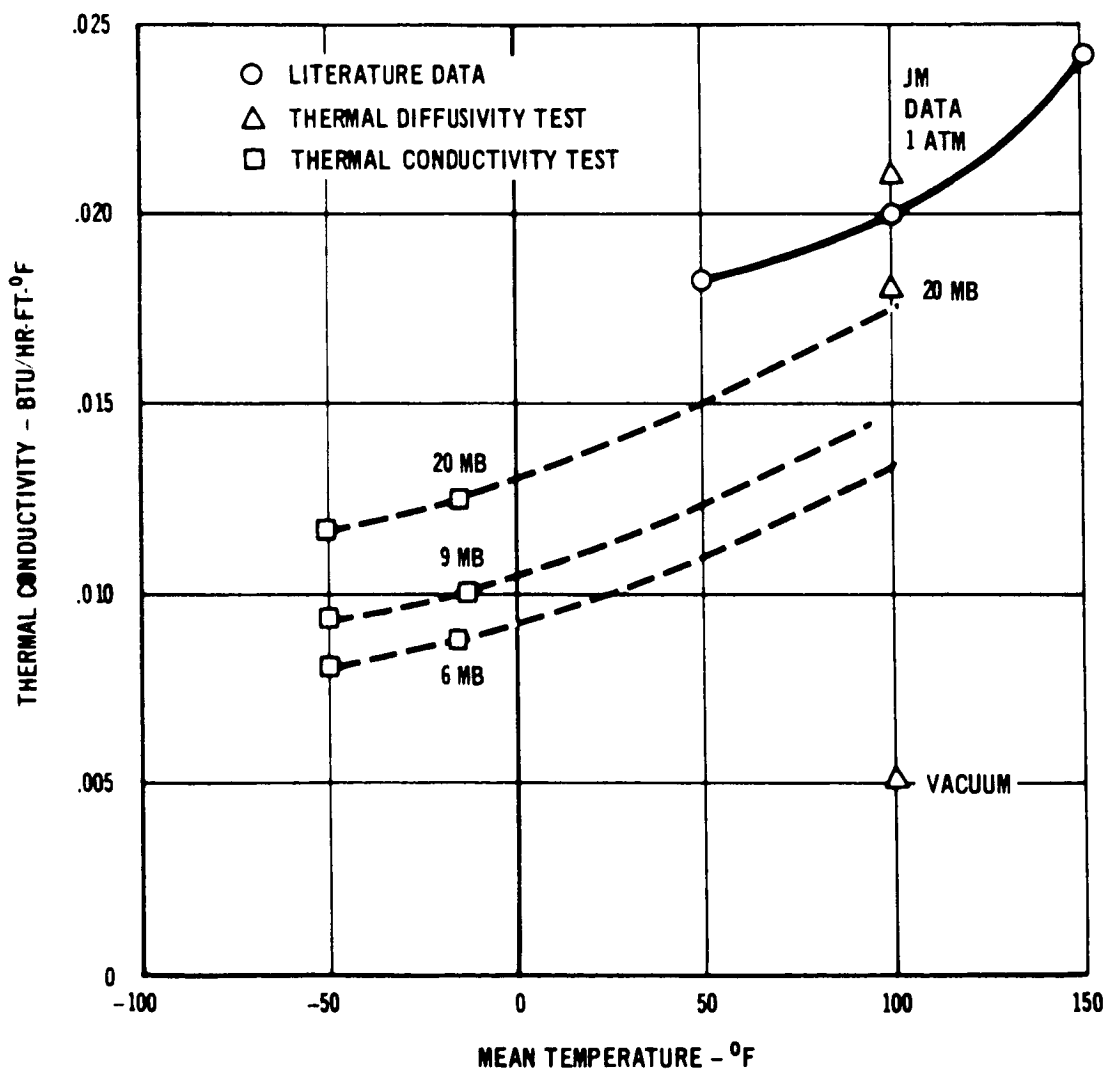


FIGURE 11.1-1

COMPARISON OF MINIMUM WEIGHT DESIGNS
(3 INCH THICKNESS)

PANEL TYPE	MINIMUM PREDICTED WEIGHT LB	COMPARABLE PRESENT DESIGN WEIGHT LB
FOAM INSULATION		
CASE (FIBERGLASS)	0.20	0.59
COVER (ALUMINUM)	0.39	0.38
ADHESIVE	-	0.66
FOAM INSULATION (2.0 PCT)	0.88	* 0.88
	1.47	2.51
FIBROUS INSULATION		
CASE (FIBERGLASS)	0.65	1.28
COVER (ALUMINUM)	1.04	1.05
SCREEN (STAINLESS)	0.06	0.07
BONDING	0.03	0.03
FIBROUS INSULATION (1.2 PCF)	0.53	0.50
	2.31	2.93

* ADHESIVE WEIGHT BETWEEN LAYERS DELETED

TABLE 11.2-1

11.2 EXTRAPOLATION OF ISM WEIGHTS - It is anticipated that structural weight can be reduced on any future ISM designs, based on the successful shock testing of a fiberglass filled ISM to a level of 250 g (Section 10.2). These data have allowed the prediction of design configurations and weights recommended for any subsequent evaluation.

11.2.1 Improved Panel Design - Lower weights are achievable by reducing the number of fiberglass plies in the casing, reducing the thickness of each ply, and using thinner aluminum for the cover. Weights of ISM panels shown in Table 11.2-1 were obtained by changing only the number of fiberglass plies. It was assumed that for the foam design, the number of plies could be reduced from 3 to 1, while in the fiberglass ISM design the number of plies could be changed from 4 to 2. Local reinforcing at stress concentration points was included also, and use of foam-in-place techniques was assumed for the improved foam design.

Comparable weights for the current design are also shown in the table for a constant panel thickness of 3 inches. Thus, these new designs indicate a potential weight savings of 1.04 lb per panel for foam, and 0.62 lb per panel for fiberglass, and a weight advantage of 0.84 lb/panel for the foam over the fiberglass (for ISM panels of equal thickness).

Comparing the ISM designs at constant heat loss the difference between the foam and fiberglass concepts would be increased since the fiberglass material requires 3.72 in thickness for heat loss equal to that from 3.0 inches of foam (Table 8.1-1). For these thicknesses the predicted panel weights would be 1.47 lb for foam and 2.52 lb for fiberglass, for a weight savings of 1.05 lb/panel. These weights are essentially for minimum gage material. They also contain less conservative design margins and hence should be shock tested prior to any other testing.

11.2.2 Effect on Lander Weight - A typical Martian lander would use the equivalent of about 20 of the ISM panels tested in this study. Thus, the total predicted insulation system weights (minimum weight design) would be 29.4 lb for foam and 50.4 lb for fiberglass. The weight difference of 21.0 lb is significant in that it is about half of the total weight for science equipment and when appropriate weight ratios are applied, a difference in flight vehicle weight of about 92 lb, would be necessary, thereby accounting for a major portion of the allowable weight contingency available.

These comparisons can be extended to examine the weight difference between the present fiberglass ISM design, and the minimum weight foam design. The comparable present design weights for the lander would be 50.2 lb for foam (3 inches thick) and 66.8 lb for fiberglass (3.72 inches thick). Comparing the present design weight for fiberglass (66.8 lb) with the minimum predicted weight for foam (29.4 lb) gives a lander weight difference of 37.4 lb, which, translated to change in flight vehicle weight, results in 164 lb difference between the current fiberglass design, and the predicted foam design. From these comparisons it is clear that even though the initial evaluation with the foam panel was unsuccessful, considerable gains are projected if this concept were explored further.

12. CONCLUSIONS AND RECOMMENDATIONS

The major result of the study was identification and demonstration of the applicability of the silicone bonded "AA" fiberglass system to successfully withstand the significant mission environments with no structural degradation or change in performance. The foam system shows promise of being a lighter weight installation and it is unfortunate that program constraints would not enable demonstration of all aspects of its inherent qualities.

The reason for failure of the foam ISM has not been identified. Several approaches to avoiding the problem are apparent, such as simply venting the panel, even though both analysis and testing indicate this is not necessary. The potential lander weight savings predicted for the foam (Section 11.2), continues to indicate that it should be a high value candidate.

Should the fiberglass material be selected for use on the Viking lander, the detailed thermal conductivity measurements will aid in design of the Lander insulation, however, an appreciable range of uncertainty in the actual thermal conductivity remains due to sensitivity of this material to the current uncertainty range of Martian atmospheric temperature pressure and gas composition.

This study also demonstrated means by which two high value insulation materials can be rapidly selected from numerous possible candidates, how the materials can be integrated into structural configurations and successfully tested as an insulation system.

As a direct result of this study and parallel Mars lander studies, several areas of additional effort have been identified and are recommended for the period prior to development of a thermal control test model.

- o Pursue Development of Foam Materials - In light of the predicted effectiveness of the foam materials, additional ISM type panels should be fabricated, using foam-in-place techniques to reduce bonding weight and assure adherence to the ISM structure. These panels should be subjected to the same environments of heat sterilization, launch venting and vibration, and landing shock with thermal performance tests used to determine degradation.
- o Determine the Sensitivity of Foam Material Performance to Interstitial Gas Pressure - The best foam materials considered in this study are nominally of the closed cell type requiring long periods for the interstitial gas to diffuse out of the cells after launch, and then to diffuse Martian atmosphere back into the cells after landing. The time necessary for these phenomena to occur is important since the presence of the gas will significantly affect thermal conductivity. It is conceivable, and cursory analysis verifies that even for a 90 day mission, the Martian atmospheric gas would only begin to diffuse back into the cells and the foam would continue to exhibit low conductivity as if it were still in the interplanetary vacuum. Conversely if the gas diffused back into the cells within

a few days, the lander thermal control system would require sufficient flexibility to accommodate the changes in insulation heat loss as the performance changed. A combination of tests using Thermal Diffusivity and guarded hot plate approaches would resolve these uncertainties.

- o Investigate Several New Materials Not Available For This Study - Materials which either were not available or were too costly for this study should be investigated (See Appendix A.3). These include polyimide foam (high temperature compatibility), hollow fiberglass fibers (reduced density), and phenolic fibers (reduced solid conduction). Each of these materials could be rapidly screened using the Thermal Diffusivity technique.
- o Develop Means of Rapidly Determining Sterilization Compatibility of Materials - Our sterilization screening tests were an attempt to determine sterilization compatibility by accelerating any changes which might occur over the normal heat sterilization period of 384 hours. The screening test exposed the samples to a peak temperature of 235°C, which is 100°C above the normal heat sterilization temperature. The technique allowed identification of two polyurethane foam materials which would not endure heat sterilization, but did not detect two other materials which were considered to have failed heat sterilization (one, a polyurethane foam, shrank, and the other, the multilayer layer material, suffered loss of crinkle stiffness). It appears that sterilization compatibility testing should include in addition to TGA, DTA and EGA evaluations, dimensional checks, and determination of other physical characteristics such as tensile strength. Development of a rapid means of making these tests on various materials to gain confidence in ultimate sterilization compatibility should significantly reduce total cost of sterilization verification by early elimination of questionable materials.
- o Investigate means of simulating the Martian Surface Environment for Thermal Model Tests - In addition to the problem of simulating a moving sun and surrounding terrain a cold sink representing the sky must be provided for adequate thermal balance tests of the lander thermal control system. The cold sink, usually liquid nitrogen, creates one of the test problems since the Martian atmospheric gases will condense at liquid nitrogen temperature. Adequate means of simulating the Martian environment in this temperature range is thus necessary, possible with a replacement gas which would have the same influence on the major heat transfer modes, but would not condense. Identification of this gas and the proper test conditions to obtain the same performance as the Martian gas could be obtained using the Thermal Diffusivity test approach.

- o Investigate Multilayer Insulation Configurations which are More Applicable to the Viking Lander - These materials are primarily applicable to areas which must be insulated during the flight (vacuum) phases of the mission. Since most of these areas are rather small, minimum sensitivity to edge losses is necessary, in addition to heat sterilization compatibility. These requirements suggest that a multilayer configuration with flat reflecting foils and spacer material would be appropriate since this would eliminate the crinkle relaxation problem during heat sterilization, and the spacer material would reduce radiation and conduction losses to edges.

APPENDIX A: VENDOR SURVEY

The survey letter sent to 51 insulation vendors is reproduced in this section. Following the letter is the list of addressees, and synopsis of additional materials information obtained during the course of the study.

A.1 VENDOR SURVEY LETTER
(COPY)

REPORT NO. MDC E0018
15 SEPTEMBER 1969

MCDONNELL DOUGLAS



13 November 1968
Ref: PS-E457-002

Attn: Sales Manager

Gentlemen:

McDonnell Douglas Astronautics has recently been awarded a contract by Jet Propulsion Laboratory to study thermal insulation systems for planetary probes and lander vehicles. As partial fulfillment of this contract, we are requested to undertake a vendor survey in an effort to locate materials that show potential as useful insulation materials.

To assist you in recommending applicable materials, the following requirements should be considered:

1. The prime requirement is for a material with as low a density and thermal conductivity product as possible.
2. The material should have a low and reproducible thermal conductivity. Data where available should include specific heat, and show the effect of material density and ambient gas pressure upon thermal conductivity.
3. Candidate materials should be unaffected by a gas composition that can vary from 100 percent CO₂ to a varying percentage mixture of CO₂, Argon and Nitrogen over the temperature range specified in paragraph 4 for a time period extending up to three months.
4. The material should be useful through the temperature operating range of a maximum of 125°F and a minimum of -190°F.
5. The insulation should be sufficiently permeable to remain intact, maintaining its original dimensions when rapidly evacuated.

6. The material should be capable of heat sterilization consisting of six cycles of 92 hours each at 275°F.
7. The material should be capable of withstanding a landing shock load of 2500 "g" peak for a one-two millisecond duration.
8. The insulation should be capable of withstanding the vibration spectra associated with a Titan III-C launch vehicle (refer to Figure 1).
9. The material should have low moisture absorption and entrapment characteristics under a 75 percent relative humidity condition at 75°F.
10. The percentage of organic binder and/or other volatile materials must be known. Since the insulation will be exposed to deep space vacuum for six-eight months, outgassing may be harmful; therefore, its effects must be known so that an accurate assessment on the overall thermal performance can be made.
11. It is desirable that the candidate materials be rigid enough to be self supporting although this is not a requirement.
12. Other information on your materials that would be helpful to know include; maximum material dimensions available (length, width, and thickness), as well as approximate cost and lead time necessary for procurement.

It should be emphasized that we are predominantly interested in materials that will be commercially available within the very near future. We would, however, also be interested in materials which your organization has that are still in the research and development stage.

Due to the urgency involved, your immediate response to the above is solicited. Information or data on any materials that show promise for utilization under this program should be received by the undersigned by November 29, 1968. Should it prove more expedient for you to make personal contact, the undersigned can be reached at the following telephone number: Area Code 314, 232-7449/7043.

Joseph C. Conti, Sr. Engineer
Material & Process Development
McDonnell Douglas Astronautics Company
Eastern Division

LAUNCH VIBRATION SPECTRUM

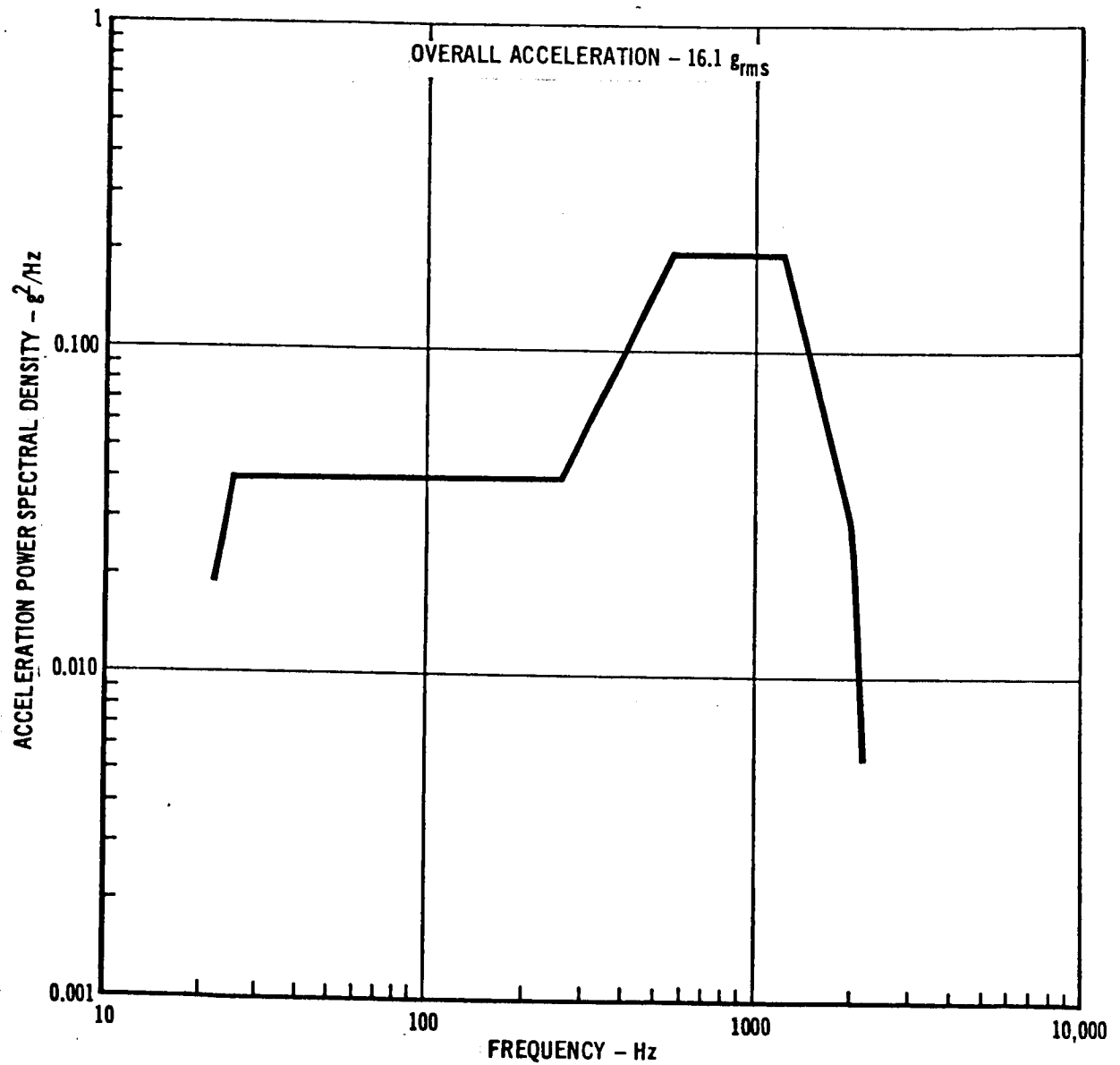


FIGURE (11)

A.2 VENDOR LIST

1. Carborundum Co.
P.O. Box 337
Niagara Falls
New York 14302
2. Hitco
1600 W. 135 St.
Gardena
California 90249
CC: John Veil
3. Super - Temp. Co.
11120 S. Norwalk Blvd.
Santa Fe Springs
California 90670
4. Thermo - Kinetic Fibers
General Technologies
136 Washington Ave.
Nutley, N. J. 07110
5. P.P.G. Industries
Fiber Glass Div.
One Gateway Center
Pittsburgh, Pa. 15222
6. Johns - Manville
22 E. 40 St.
New York, New York 10016
CC: Leonard Johnson
7. Bausch & Lomb. Inc.
98467 Bausch St.
Rochester, New York 14602
8. Micro Beads Div.
Cataphate Corp.
P.O. Box 2369
Jackson, Mississippi 39205
9. Babcock & Wilcox Co.
Refractories Div.
Old Savannah Road
August, Ga. 30903
10. FMC Corp.
American Viscose Div.
1617 Kennedy Blvd.
Philadelphia, Pa. 19103
11. Armstrong Cork Co.
Industry Products Div.
West Liberty St.
Lancaster, Penna. 17604
12. CPR Division, Upjohn Co.
555 Alaska Avenue
Torrance, Calif. 90503
13. General Tire & Rubber Co.
Chemical/Plastics
1708 Englewood Avenue
Akron, Ohio 44309
14. B.F. Goodrich Industrial
Products Co.
500 S. Main St.
Akron, Ohio 44318
15. Olin Mathieson Chemical Corp.
Polytron Dept.
661 S. 10th Street
Richmond, California 94804
16. National Metallizing Division
Standard Packaging Corp.
Cranbury, N. Jersey 08512
17. Alfred E. Wechsler
Arthur D. Little Inc.
Acron Park
Cambridge, Mass. 02140
18. Heath Plastics Division
Heath Tecna Corp.
19819 84th St., South
Kent, Washington 98031
19. Hi-Temp. Insulation Inc.
7404 Fulton Avenue
N. Hollywood, California
20. National Research Corp.
70 Memorial Drive
Cambridge, Mass. 02140

VENDOR LIST (cont)

- | | |
|------------------------------------------------------------------------------------------------------------------|---------------------------------------------------------------------------------------------|
| 21. Linde Company
Cryogenic Products Dep.
East Park Dr. & Woodward
Tonawonda, N. Y. 14150 | 33. Godfrey L. Cabot Inc.
White Pigments Division
Boston 10, Mass. |
| 22. AGC Incorporated
106 Evansville Ave.
Meriden, Conn. | 34. Atomic Laboratories Inc.
3086 Claremont Ave.
Berkeley, California |
| 23. Emerson & Cuming Inc.
59 Walpole Street
Conton, Mass. | 35. Thermo-Sound Products
714 W. Olympic Blvd.
Los Angeles, California |
| 24. Owens - Corning Fiberglass Corp.
Pacific Coast Division
Santa Clara, California | 36. Pittsburgh Coke & Chemical Co.
Grant Building
Pittsburgh, Pa. |
| 25. Balsa Ecudor Lumber Corp.
500 Fifth Avenue
New York, New York 10036 | 37. Union Carbide Corp.
Development Department
P.O. Box 324
Tuxedo, New York 10987 |
| 26. Unarco Industries, Inc.
Chemical and Asbestos Division
1111 West Perry Street
Bloomington, Illinois | 38. Dow Chemical Co.
Midland, Michigan 48641 |
| 27. E. I. DuPont de Nemours & Co.
Film Department
Willington, Delaware 19898 | 39. CIBA Products Co.
Div. CIBA Corp.
Summit, N. J. |
| 28. General Electric Company
Chemical Development Operation
1285 Baston Ave.
Bridgeton, Conn. 06602 | 40. Donray Products Co.
Cleveland, Ohio |
| 29. G. T. Schjeldahl Co.
Northfield, Minn. | 41. Firestone Plastics Co.
Div. Firestone Tire & Rubber Co.
Pottstown, Pa. |
| 30. Dow Corning Corporation
Midland, Michigan | 42. Cell-Foam Inc.
Fort Worth, Texas |
| 31. Pittsburgh - Corning
One Gateway Center
Pittsburgh, Pa. 15222 | 43. Firestone Rubber &
Latex Products
Fall River, Mass. |
| 32. Floridin Company
Tallahassee, Florida | 44. International Foam Corp.
Chicago, Ill. |
| | 45. Nopco Chemical Co.
Newark, N.J. |

VENDOR LIST (cont)

- | | |
|-----------------------------------------------------------------------------------------------|-------------------------------------------------------------------------------------------------------------|
| 46. Monsanto Chemical Co.
Inorganic Sales
800 N. Lindbergh Blvd.
St. Louis, Missouri | 49. Narmco Materials Division
Telecomputing Corp.
9229 Sunset Boulevard
Los Angeles 69, California |
| 47. Silbrico Corporation
5901 W. 66th Street
Chicago 38, Illinois | 50. Minnesota Mining & Mfg. Co.
New Products Division
2501 Hudson Road
St. Paul 19, Minn. |
| 48. W. R. Grace Corp.
Davison Chemical Div.
101 N. Charles St.
Baltimore, Md. | 51. Union Carbide Corp.
Plastics Division
122 N. Kirkwood Dr.
St. Louis, Missouri 63122 |

A.3 ADDITIONAL MATERIALS DATA

Backup data obtained during the course of the program indicated several materials considerations which should be incorporated into any future investigations.

- o Contact with personnel in the research laboratories of Pittsburgh Plate Glass (PPG) revealed that it would be possible to produce a fiberglass insulation material having a "kp" product of about one half that of conventional fiberglass materials. This could be accomplished by drawing hollow fibers instead of the solid fibers now used as insulation batt. PPG studies on "G" size and larger fibers show that the "kp" can indeed be reduced by one half. Problems at present however, involve fabrication of hollow fibers with diameters equal to the smaller "AA" or "B" size fibers presently used. Hollow fibers of the larger sizes are now being drawn and are in use as a lightweight reinforcing media.
- o Dr. Sam Steingiser from Monsanto Research Company, Dayton, Ohio, reported that his company was working on:
 - A. Isocyanurate foam
 - B. Foamed polyimide
 - C. Syntactic polyimide foam

All three of these materials appeared promising for the present study but their costs were greater than the program budget would allow. The isocyanurate foam is different from urethane (isocyanate) foam. The maximum temperature capability of isocyanurate foam is reported to be between that of urethane and polyimide foam. (approx. 350 - 400°F). Density of isocyanurate is close to the 2 pcf density urethanes. According to Monsanto, HTF-200 foam from the CPR Division of the UpJohn Company is a commercially available product very similar in chemistry to the Monsanto isocyanurate. This material (UpJohn HTF-200) was selected to represent the isocyanurate material class.

Monsanto is also developing polyimide foam by two processes, (a) chemically blown and (b) syntactic. Densities of the syntactic foam composed of polyimide spheres fused together can be made to approach the 2 pcf urethane foams. At the time of the initial contact Monsanto had no data on thermal properties, cost or availability of these materials.

- o Initial effort at MDAC-ED in attempting to die crinkle the JPL supplied goldized Kapton led to samples that had a significant portion of the gold smeared or removed. Contact was made with National Metallizing to determine if they had done any work on the deposition of SiO coatings over gold to increase its wear resistance. According to their records, it was found that the JPL supplied material was some of the first made and although it had the best adhesion available at the time of its manufacture, it was now possible to supply material that had increased rub-off resistance. It was the belief of National Metallizing that deposition of SiO over gold was valid but that extensive work would be required to obtain the optimum thickness of SiO necessary to reduce rub-off yet maintain a low effective emittance.
- o As part of MDAC-ED continuing effort to keep abreast of new material developments, information regarding Kynol, a new material developed by the Carborundum Company was obtained late in this study. The material does appear promising and is worthy of additional comment. Kynol is an organic fiber having properties unlike the normal organic materials. It is a nonmelting/char forming material with reported excellent long term vacuum compatibility. Specific gravity is 1.25 (approximately one half that of glass) so that for an equivalent fiber diameter, Kynol will yield lower densities than fiberglass. Kynol is resistant to chemicals and is also much more temperature resistant than polyimide type materials. Company funded testing of this material was not completed in time for test results to be included in this report.

REFERENCES

- 4-1) Mars Engineering Model Parameters for Mission and Design Studies (Preliminary Draft), Langley Research Center, May 1968.
- 4-2) JPL Letter 626-CP:db, 7 January 1969.
- 7-1) Carslaw, H.S., and Jaeger, J.C., "Conduction of Heat in Solids, Oxford Press; 1947.
- 7-2) Coston, R. M., "A Study on High-Performance Insulation Thermal Design Criteria," Vol. 1, Contract NAS 8-20353, LMSC-A847882, 25 June 1967.
- 7-3) Sparrow, E. M., "Radiant Emission, Absorption, and Transmission Characteristics of Cavities and Passages," Symposium on Thermal Radiation of Solids, March 4-6, 1964, NASA SP-55 (1965).